

# **SYNTHESIS AND BIOLOGICAL EVALUATION OF SOME BENZOTHAZOLE AND BENZOTHAZINE DERIVATIVES**

Thesis Submitted for the Award of the Degree of

**DOCTOR OF PHILOSOPHY**

**in**

**Chemistry**

**By**

**Andleeb Amin**

**Registration Number: 11919389**

**Supervised By**

**Dr. Praveen Kumar Sharma (14155)**

**Chemistry (Professor)**

**Lovely Professional University,**

**Phagwara, Punjab-144411**

**Co-Supervised by**

**Dr. Khalid Z Masoodi**

**Biotechnology (Associate Professor)**

**SKUAST-Shalimar,**

**Srinagar, J&K-190025**



**L** OVELY  
**P** ROFESSIONAL  
**U** NIVERSITY

*Transforming Education Transforming India*

**LOVELY PROFESSIONAL UNIVERSITY, PUNJAB**

**2024**

## **Dedication**

This thesis is dedicated to my *parents*

(for never giving up on me)

## DECLARATION

I, hereby declared that the presented work in the thesis entitled “Synthesis and Biological Evaluation of Some Benzothiazole and Benzothiazine Derivatives” in fulfilment of degree of **Doctor of Philosophy (Ph. D.)** is outcome of research work carried out by me under the supervision of Dr. Praveen Kumar Sharma, working as Professor in the Department of Chemistry, School of Chemical Engineering and Physical Sciences, Lovely Professional University, Punjab, India. In keeping with general practice of reporting scientific observations, due acknowledgements have been made whenever work described here has been based on findings of other investigator. This work has not been submitted in part or full to any other University or Institute for the award of any degree.



**18.10.2024**

**(Signature of Scholar)**

Name of the scholar: Andleeb Amin

Registration No.: 11919389

Department of Chemistry

School of Chemical Engineering and Physical Sciences

Lovely Professional University,

Punjab, India

## CERTIFICATE

This is to certify that the work reported in the Ph.D. thesis entitled “Synthesis and Biological Evaluation of Some Benzothiazole and Benzothiazine Derivatives” submitted in fulfillment of the requirement for the reward of degree of **Doctor of Philosophy (Ph.D.)** in the Department of Chemistry, School of Chemical Engineering and Physical Sciences, Lovely Professional University, is a research work carried out by Andleeb Amin, 11919389, is bonafide record of her original work carried out under my supervision and that no part of thesis has been submitted for any other degree, diploma or equivalent course.



19.10.2024

**(Signature of Supervisor)**

Dr. Praveen Kumar Sharma

Professor

Department of Chemistry,

School of Chemical Engineering and

Physical Sciences,

Lovely Professional University, Punjab India



16.10.2024

**(Signature of Co-supervisor)**

Dr. Khalid Z Masoodi

Assistant Professor

Division of Plant Biotechnology,

Faculty of Horticulture

SKUAST-Kashmir

J&K, India

## **ABSTRACT**

Heterocyclic chemistry stands as a pivotal branch within organic chemistry, contributing significantly to the extensive realm of known organic compounds. Its impact extends across both medical and industrial domains, with a profound influence on the development of society. A substantial proportion of pharmaceuticals, dyes, cosmetics, polymers, agrochemicals, and more are comprised of heterocyclic structures. The paramount importance of heterocyclic ring systems in industry is evident, as these compounds often serve as fundamental templates for synthesizing diverse industrially valuable substances. They play a crucial role in the synthesis of pharmaceuticals, natural products, vitamins, biomolecules, dyes, agrochemicals, and other essential compounds. Some heterocycles also exhibit biochemiluminescence and photochromic properties, adding to their versatility. Additionally, heterocycles play roles as semiconductors, organic conductors, light-emitting diodes, photovoltaic cells, light-harvesting systems, and liquid crystalline compounds. The synthetic utility of heterocycles extends to their use as catalysts, protecting groups, and metal ligands in inorganic synthesis.

Given these multifaceted applications, heterocycles warrant substantial attention in organic chemistry. The continuous exploration and development of efficient methods for creating new heterocycles represent a significant area of focus within the discipline. Common heterocycles typically consist of 5 or 6-membered rings containing nitrogen, oxygen, or sulfur, emphasizing their prevalence and importance in organic chemistry. In this regard, benzothiazole and benzothiazine ring systems are of utmost significance. The pharmaceutical and biological activities of benzothiazines (4H-1,4-benzothiazines) have been acknowledged due to their structural flexibility, facilitated by folding along the N-S axis. The extent of folding is significantly influenced by the arrangement and nature of substituents. Benzothiazoles hold a prominent position in research, particularly within synthetic and medicinal chemistry, owing to their noteworthy pharmaceutical properties. This crucial class of derivatives exhibits a diverse array of biological activities, encompassing anti-inflammatory, antidiabetic, anticancer, anticonvulsant, antibacterial, antiviral, antioxidant, antituberculosis, enzyme inhibition, and more. Consequently, numerous methodologies have been developed to synthesize benzothiazole compounds, emphasizing considerations such as purity, yield, and selectivity of the final products.

The present study is divided into five main chapters focusing on developing new synthetic routes and demonstrating anti-cancer activity of various substituted benzothiazole and benzothiazine derivatives. The first chapter deals with the general introduction of

heterocycles with focus on structural and biological applicability. The second chapter specifically deals with the recent advancements in the synthesis of benzothiazole and benzothiazine containing core structures involving diverse methods such as microwave-assisted techniques, nanocatalysis, environmentally friendly (green) synthesis, click reactions, and multicomponent routes. The diverse range of therapeutic benefits linked to medications containing benzothiazole and benzothiazine has inspired medicinal chemists to not only develop a multitude of innovative therapeutic agents but also to explore additional methods for synthesizing their derivatives.

In the third chapter, green unconventional route involving oxidative cycloaddition of 2-amino benzenethiol and 1,3-dicarbonyls employing a catalytic amount of ceric ammonium nitrate has been devised for the synthesis of 2,3-disubstituted-1,4 benzothiazines. CAN, like several other oxidizing agents, has the capability to transform thiols into sulfenyl radicals, leading to the formation of disulfides and various subsequent oxidation products such as sulfoxides, sulfones, and other derivatives. To establish the role of CAN, experiments were conducted where thiols were oxidized with an equivalent amount of CAN in presence of oxygen at room temperature. All the molecules were characterized by spectral analysis and tested for anticancer activity against various cancer cell lines using various functional assays, thereby, exhibiting maximal activity against A-549 lung cancer cell line. Further *in silico* screening of **Propyl 3-methyl-3,4-dihydro-2H-benzo[b][1,4]thiazine-2-carboxylate** against six crucial inflammatory molecular targets such as I11- $\alpha$  (PDB ID: 5UC6), I11- $\beta$  (PDB ID: 6Y8I), I16 (PDB ID: 1P9M), Vimentin (PDB ID: 3TRT), COX-2 (PDB ID: 5KIR), I18 (PDB ID: 5D14) and TNF- $\alpha$  (PDB ID: 2AZ5), was done using AutoDock tool.

Fourth chapter includes synthesis of new analogs based on benzothiazole-piperazine conjugates which were investigated for their anticancer properties using *in vitro* and *in silico* techniques. The compounds were tested against various cancer cells, and the results revealed that all the compounds displayed significant anticancer potency against C4-2 cells. Among all, **2-(4-(pyrimidin-2-yl) piperazin-1-yl) benzo[d]thiazole** demonstrated the most significant activity in the cell viability assay conducted on the C4-2 cell line. Molecular docking results also revealed that all the compounds exhibited good energy binding score against the androgen receptor (AR) with a maximum binding energy of **-9.87** kcal/mol followed by other compounds. Docking results were further supported by MD simulation studies, which confirmed that the ligand+protein complex was in stable conformation throughout the simulation time of 100 nanoseconds.

Fifth chapter, specifically, deals with benzothiazole derivatives incorporating various phenyl/heterocyclic moieties with an imine linkage have exhibited promising anti-cancer properties across various stages of cancer development. Notably, a synthesized derivative, **(E)-1-(4-(1H-indol-2-yl)phenyl)-N-(6-nitrobenzo[d]thiazol-2-yl)methanimine**, has demonstrated remarkable efficacy against the C4-2 cancer cell line, fueling enthusiasm for the exploration of small molecules in cancer therapy. In the computational realm, analyses have identified compound **(E)-1-(4-(1H-indol-2-yl)phenyl)-N-(6-nitrobenzo[d]thiazol-2-yl)methanimine** as exhibiting the highest binding affinity for the AR protein, marking such molecules as potential lead candidates with favorable pharmacokinetic properties.

## ACKNOWLEDGEMENTS

I would like to express my deepest gratitude to my supervisor, **Dr. Praveen Kumar Sharma**, for their invaluable guidance, unwavering support, and continuous encouragement throughout the research process. His expertise, patience, and constructive feedback have been instrumental in shaping this thesis. Having the chance to work under him, a teacher of unparalleled excellence, has truly been a privilege for me.

I am also immensely thankful to my co-supervisor, **Dr. Khalid Z Masoodi** for his insightful comments and suggestions that have significantly enhanced the quality of this work. I will always be grateful to him for believing in the value of my work and, most significantly, for his genuine care and support during my doctoral research. Special appreciation goes to SKUAST- Shalimar, J&K, and NIT Srinagar for providing the necessary resources and facilities for conducting this research.

I extend my sincere gratitude to **Dr. Kailash Chandra Juglaan**, Head of School of Chemical Engineering and Physical Sciences at Lovely Professional University, Punjab, for granting me the opportunity to be a scholar in this esteemed department and for providing the necessary resources for my research.

I would like to convey my heartfelt appreciation to **Dr. Gurpinder Singh** and **Dr. Harpreet Kaur** for their invaluable mentorship and support throughout my research journey. Their expertise, insightful guidance, and constructive feedback have significantly influenced the direction and quality of my work. Their commitment to nurturing intellectual growth and sharing their knowledge has been invaluable to my academic progress.

I extend my heartfelt thanks to my family for their unconditional love, understanding, and encouragement. Their unwavering support has been my source of strength throughout this journey. I am grateful to my friends and colleagues for their moral support and for being a constant source of inspiration.

Lastly, I would like to acknowledge the participants of this study for their willingness to contribute valuable insights, without whom this research would not have been possible.

*Andleeb Amin*  
20-04-2024



## TABLE OF CONTENTS

1	Title	i
2	Dedication	ii
3	Declaration	iii
4	Certificate	iv
5	Abstract	v-vii
6	Acknowledgements	viii
7	Table of Contents	ix-xv
8	List of Tables	xv
9	List of Figures	xv-xvii
10	List of Schemes	xvii-xviii
11	List of Abbreviations	xix-xx

# TABLE OF CONTENTS

## **Chapter no. 1: Review of Heterocyclic Compounds**

<b>1.1</b>	<b>Introduction</b>	2
<b>1.2</b>	<b>Classification of heterocyclic compounds</b>	2-6
<b>1.3</b>	<b>N-containing heterocycles</b>	6-15
1.3.1	Pyrrole and its benzo derivatives	6-8
1.3.2	Azoles and their derivatives	8-10
1.3.3	Quinolines and isoquinolines	10-11
1.3.4	Quinazolines	11
1.3.5	Quinoxalines	12
1.3.6	Benzazepines	12-13
1.3.7	Benzoxapines	13
1.3.8	Benzothiazepines	13-14
1.3.9	Benzodiazepines	14
1.3.10	Pteridines	14-15
1.3.11	Triazine and its derivatives	15
<b>1.4</b>	<b>Oxygen-containing heterocycles</b>	16-21
1.4.1	Furans and Benzofurans	16-17
1.4.2	Coumarins	17-18
1.4.3	Chromans/chromenes	18-19
1.4.4	Flavonoids	19
1.4.5	Xanthenes and Xanthonenes	20-21
<b>1.5</b>	<b>Sulfur heterocycles</b>	21-24
1.5.1	Thiophenes and benzothiophenes	22
1.5.2	Thiochromenes	23
1.5.3	Thioxanthenes	23-24
<b>1.6</b>	<b>Heterocyclic compounds with more than a single heteroatom</b>	24-28
1.6.1	Oxazoles	24-25
1.6.2	Isoxazoles	25-26
1.6.3	Thiazoles	26
1.6.4	Thiadiazoles	27
1.6.5	Oxadiazoles	27-28
1.6.6	Oxazolidinones	28
<b>1.7</b>	<b>Conclusion</b>	29

## Chapter no. 2: Synthesis and Importance of Benzothiazole and Benzothiazine

### Nucleus

<b>2.1</b>	<b>Benzothiazoles</b>	31-46
<b>2.1.1</b>	<b>Introduction</b>	31
<b>2.1.2</b>	<b>Synthetic routes of Benzothiazoles</b>	31-40
2.1.2.1	Synthesis of Benzothiazoles via condensation reaction	32-37
2.1.2.2	Synthesis of Benzothiazoles Via cyclization	37-40
<b>2.1.3</b>	<b>Pharmacological Significance of Benzothiazole derivatives</b>	40-46
2.1.3.1	Anti-cancer and cytotoxic effects	40-41
2.1.3.2	Anti-microbial activity	41-44
2.1.3.3	Anti-inflammatory activity	44-45
2.1.3.4	Anti-diabetic activity	45-46
<b>2.2</b>	<b>Benzothiazines</b>	46
<b>2.2.1</b>	<b>Introduction</b>	46
<b>2.2.2</b>	<b>Synthesis</b>	46-51
2.2.2.1	From condensation with $\alpha$ -halo Ketones, esters and acids	46-47
2.2.2.2	Through oxidative cyclization involving 1,3-dicarbonyl compounds	47
2.2.2.3	From condensation with $\alpha,\beta$ -unsaturated acetylinic acids	48-49
2.2.2.4	From substituted amines	49
2.2.2.5	From 2,2'-dithiodianiline	49-50
2.2.2.6	From ring expansion of Benzothiazoline	50-51
<b>2.2.3</b>	<b>Pharmacological significance of benzothiazine derivatives</b>	51-56
2.2.3.1	Anti-cancer activity	51-53
2.2.3.2	Anti-microbial activity	53-54
2.2.3.3	Anti-convulsant activity	54-55
2.2.3.4	Miscellaneous Biological Activities	55
<b>2.3</b>	<b>Conclusion</b>	55-56

**Chapter no. 3: Synthesis, Characterization, Biological evaluation and  
Molecular Docking Analysis of 1,4-benzothiazine derivatives**

<b>3.1</b>	<b>Introduction</b>	58-59
<b>3.2</b>	<b>Materials &amp; Methods</b>	59-65
3.2.1	Instruments	59
3.2.2	Synthetic procedure	59-62
3.2.2.1	<i>General synthetic procedure for 2-alkoxy carbonyl-3-methyl-4H-1,4-benzothiazines (3a-3h)</i>	59-60
3.2.2.1.1	<i>Methyl 3-methyl-4H-benzo[b][1,4]thiazine-2 carboxylate(3a)</i>	60
3.2.2.1.2	<i>Ethyl 3-methyl-4H-benzo[b][1,4]thiazine-2-carboxylate(3b)</i>	60
3.2.2.1.3	<i>Propyl 3-methyl-4H-benzo[b][1,4]thiazine-2-carboxylate(3c)</i>	60-61
3.2.2.1.4	<i>Methyl 6-chloro-3-methyl-4H-benzo[b][1,4]thiazine-2 carboxylate(3d)</i>	61
3.2.2.1.5	<i>Ethyl 6-chloro-3-methyl-4H-benzo[b][1,4]thiazine-2-carboxylate (3e)</i>	61
3.2.2.1.6	<i>Propyl 6-chloro-3-methyl-4H-benzo[b][1,4]thiazine-2-carboxylate (3f)</i>	61
3.2.2.1.7	<i>Isobutyl 3-methyl-4H-benzo[b][1,4]thiazine-2-carboxylate (3g)</i>	61-62
3.2.2.1.8	<i>Isobutyl 6-chloro-3-methyl-4H-benzo[b][1,4]thiazine-2-carboxylate (3h)</i>	62
3.2.3	<b>Biological Assay</b>	62-65
3.2.3.1	MTT Assay	62-63
3.2.3.2	Colony formation unit (CFU) Assay	63
3.2.3.3	In vitro scratch Assay/Wound Healing Assay	63-64
3.2.3.4	RNA Isolation, PCR amplification, and quantitative RT-PCR	64
3.2.3.5	Molecular Docking	64-65
3.2.3.6	ADMET Analysis	65
3.2.3.7	Statistical Analysis	65
<b>3.3</b>	<b>Results &amp; discussions</b>	65-78
3.3.1	Chemistry	65-67
3.3.2	Bioassay	67-
3.3.2.1	MTT assay reveals significant cytotoxic effects of the synthesized derivatives against C4-2 cell line	67-69
3.3.2.2	CFU illustrates a dose-dependent inhibition of Cell growth in vitro	69-70
3.3.2.3	Compound 3c inhibits cell migration/wound healing in vitro	70-71
3.3.2.4	Compound 3c reduces expression of pro-inflammatory genes	71-73
3.3.2.5	Molecular Docking Analysis	73-77
3.3.2.6	ADME and drug likeness properties	77-78
<b>3.4</b>	<b>Conclusion</b>	79q
	Representative Spectra	80-87

**Chapter no. 4: Benzothiazole-piperazine Hybrids: Synthesis, Characterization, Cytotoxic and Computational Studies**

<b>4.1</b>	<b>Introduction</b>	89-91
<b>4.2</b>	<b>Materials &amp; Methods</b>	91-98
4.2.1	Chemistry	91-92
4.2.2	<i>General Procedure for the Synthesis of 2-(Piperazin-1-yl)Benzothiazole derivatives</i>	92-94
4.2.2.1	<i>2-(4-ethylpiperazin-1-yl) benzothiazole (3a')</i>	92
4.2.2.2	<i>2-(4-methyl piperazine-1-yl) benzo[d]thiazole (3b')</i>	93
4.2.2.3	<i>tert-butyl 4-(benzo[d]thiazol-2-yl) piperazine -1- carboxylate (3c')</i>	93
4.2.2.4	<i>2-(4-(benzo[d]thiazol-2-yl) piperazin-1-yl) ethan-1-amine (3d')</i>	93
4.2.2.5	<i>2-(4-(benzo[d]thiazol-2-yl) piperazin-1-yl) ethan-1-ol (3e')</i>	93
4.2.2.6	<i>2-(4-(o-tolyl) piperazin-1-yl) benzo[d]thiazole (3f')</i>	94
4.2.2.7	<i>2-(4-(pyrimidin-2-yl) piperazin-1-yl) benzo[d]thiazole (3g')</i>	94
4.2.2.8	<i>2-(4-(2-methoxyphenyl) piperazin-1-yl) benzo[d]thiazole (3h')</i>	94
4.2.2.9	<i>2-(4-phenylpiperazin-1-yl) benzo[d]thiazole (3i')</i>	94
4.2.2.10	<i>2-(4-(4-nitrophenyl) piperazin-1-yl) benzo[d]thiazole (3j')</i>	94
4.2.3	Biological Assay	94-98
4.2.3.1	MTT Assay	95
4.2.3.2	Colony formation unit (CFU) Assay	95
4.2.3.3	In vitro scratch Assay/Wound Healing Assay	95-96
4.2.3.4	RNA Isolation, PCR amplification, and quantitative RT-PCR	96
4.2.4	Molecular Docking Analysis	96-97
4.2.5	Molecular Dynamics Simulation	97
4.2.6	Binding Free Energy Examination	98
4.2.7	ADMET Analysis	98
<b>4.3</b>	<b>Results &amp; discussions</b>	99-114
4.3.1	Chemistry	99-100
4.3.2	Bioassay	100-
4.3.2.1	MTT assay reveals significant cytotoxic effects of the synthesized derivatives against the C4-2 cell line	100-101
4.3.2.2	CFU assay indicated the suppression of cellular growth in vitro dose-dependently	101-102
4.3.2.3	Compound 3g suppresses wound healing/cell migration in vitro	102-103
4.3.2.4	Compound 3g reduces the expression of genes that respond to androgens	104-105
4.3.2.5	Molecular Docking Study	105-108
4.3.2.6	Molecular Dynamics Simulation	109-110
4.3.2.7	MM-GBSA calculations	111
4.3.2.8	Free Energy Landscape (FEL) and PCA Analysis	111-113
4.3.2.9	ADMET and Drug likeness properties	113-114
<b>4.4</b>	<b>Conclusion</b>	115
	Representative Spectra	116-123

**Chapter no. 5: Design, Synthesis, *In vitro* anti-tumor activity, and**  
**Computational study of Benzothiazole derived Schiff bases**

<b>5.1</b>	<b>Introduction</b>	125-126
<b>5.2</b>	<b>Materials &amp; Methods</b>	126-133
5.2.1	Instruments	126
5.2.2	Synthetic Procedure	126-130
5.2.2.1	Synthetic Procedure 2-Amino-6-nitro Benzothiazole	127
5.2.2.1.1	2-Amino-6-Nitro Benzothiazole	127
5.2.2.2	General Procedure for the synthesis of (6-nitrobenzo[5]thiazol-2-yl)-1-phenylmethanimine derivatives	127-130
5.2.2.2.1	( <i>E</i> )- <i>N</i> -(6-nitrobenzo[5]thiazol-2-yl)-1-(4-nitrophenyl)methanimine (5a)	127
5.2.2.2.2	( <i>E</i> )-1-(4-chlorophenyl)- <i>N</i> -(6-nitrobenzo[5]thiazol-2-yl)methanimine (5b)	128
5.2.2.2.3	( <i>E</i> )-4-(((6-nitrobenzo[5]thiazol-2-yl)imino)methyl)phenol(5c)	128
5.2.2.2.4	( <i>E</i> )- <i>N</i> -(6-nitrobenzo[5]thiazol-2-yl)-1-(3 nitrophenyl)methanimine(5d)	128
5.2.2.2.5	( <i>E</i> )- <i>N</i> -(6-nitrobenzo[5]thiazol-2-yl)-1-phenylmethanimine (5e)	128
5.2.2.2.6	2-methoxy-4-(((6-nitrobenzo[5]thiazol-2-yl)imino)methyl)phenol (5f)	128-129
5.2.2.2.7	2-methoxy-6-(((6-nitrobenzo[5]thiazol-2-yl)imino)methyl)phenol (5g)	129
5.2.2.2.8	( <i>E</i> )-1-([1,1'-biphenyl]-4-yl)- <i>N</i> -(6-nitrobenzo[5]thiazol-2-yl)methanimine (5h)	129
5.2.2.2.9	( <i>E</i> )-1-(4-(1 <i>H</i> -indol-2-yl)phenyl)- <i>N</i> -(6-nitrobenzo[5]thiazol-2-yl)methanimine(5i)	129
5.2.2.2.10	( <i>E</i> )- <i>N</i> -(6-nitrobenzo[5]thiazol-2-yl)-1-( <i>p</i> -tolyl)methanimine (5j)	130
5.2.3	Biological Assay	130-133
5.2.3.1	MTT Assay	130-131
5.2.3.2	Colony formation unit (CFU) Assay	131
5.2.3.3	In vitro scratch Assay/Wound Healing Assay	131-132
5.2.3.4	RNA Isolation, PCR amplification, and quantitative RT-PCR	132
5.2.3.5	Molecular Docking	132-133
5.2.3.6	ADMET Analysis	133
5.2.3.7	Statistical Analysis	133
<b>5.3</b>	<b>Results &amp; discussions</b>	133-146
5.3.1	Synthesis & Characterization	133-135
5.3.1.1	Reaction Mechanism	136
5.3.2	MTT Assay demonstrates pronounced cytotoxic effects of the synthesized compounds on various cell lines	136-138
5.3.3	The Colony Formation Unit assay reveals a dose dependent reduction in cellular growth in vitro	138-139
5.3.4	Compound 5i suppresses wound healing/cell migration in vitro	139-140
5.3.5	Compound 5i reduces expression of androgen responsive genes	140-141
5.3.6	Analysis of Molecular Docking	141-145
5.3.7	ADME and drug-alikeness analysis	146

<b>5.4</b>	<b>Conclusion</b>	147
	Representative Spectra	148-153

## **Chapter no. 6: Future Scope**

<b>6.1</b>	<b>Introduction</b>	155-156
<b>6.2</b>	<b>Development of metal complexes containing thiazole/thiazines as chelating agents</b>	156-157
<b>6.3</b>	<b>Development of versatile nanoparticles of thiazole/thiazines as drug delivery systems</b>	157-158

## **Chapter no. 7: Summary & Conclusion** 159-163

<b>REFERENCES</b>	<b>164-186</b>
<b>LIST OF PUBLICATIONS</b>	<b>187</b>
<b>LIST OF CONFERENCES</b>	<b>188</b>

### **LIST OF TABLES**

<b>Table no.</b>	<b>Description</b>	<b>Page no.</b>
3.1	2D & 3D interaction of compound 3c with respective amino acid residues	<b>75-77</b>
3.2	Evaluation of drug like properties of the screened compounds using Lipinski's rule	<b>78</b>
4.1	Energy binding score of compounds (3a'-3j') against AR protein target	<b>108</b>
4.2	Binding free energy components for the 2PNU+3g calculated from MM-GBSA	<b>111</b>
4.3	ADMET and drug-likeness properties of the screened molecules	<b>114</b>
5.1	List of synthesized benzothiazole-schiff bases	<b>135</b>
5.2	Energy binding score of the compound 5i (Kcal/mol) against various protein targets.	<b>142</b>
5.3	ADME characteristics and drug alikeness properties of the screened molecules	<b>146</b>
7.1	The inhibition rates for A-549 and C4-2 in vitro (3a-3g)	<b>161</b>

7.2	The inhibition rates for A-549 and C4-2 in vitro (3a'-3j')	<b>162</b>
7.3	The inhibition rates for C4-2 and A-549 cell lines in vitro (5a-5i)	<b>163</b>

### **LIST OF FIGURES**

<b>Figure no.</b>	<b>Description</b>	<b>Page no.</b>
1.1	Examples of aliphatic heterocyclic compounds	<b>2</b>
1.2	Examples of aromatic heterocyclic compounds	<b>3</b>
1.3	Five membered heterocycles with one hetero-atom	<b>3</b>
1.4	Five membered heterocyclic compounds with more than one heteroatom	<b>3</b>
1.5	Six membered heterocyclic compounds with one heteroatom	<b>4</b>
1.6	Six-membered heterocycles with more than one heteroatom	<b>4</b>
1.7	Fused heterocyclic compounds	<b>4</b>
1.8	Isomers of triazine	<b>15</b>
3.1	Cytotoxicity test of compounds (3a-3g) by MTT assay	<b>68</b>
3.2	Illustrates the dose-dependent inhibition of colony formation by compound 3c in A549 lung cancer cells	<b>69</b>
3.3	The time-dependent inhibition of cellular migration or wound healing in A549 lung cancer cells treated with compound 3c	<b>71</b>
3.4	The real-time gene expression analysis of pro-inflammatory genes was conducted after treatment with compound 3c and using DMSO as the vehicle control. The data was normalized to GAPDH expression. Each data point represents an experiment with a single sample mean value obtained from three replicates. Significance was determined with *P < 0.0001 using GraphPad Prism 7.0 software.	<b>72-73</b>
3.5	Energy binding score of the compound <b>3c</b> (kcal/mol) against various protein targets	<b>74</b>
4.1	FDA approved anti-cancer drugs containing benzothiazole as core scaffold	<b>91</b>
4.2	Evaluation of compound cytotoxicity (3a-3j) using MTT assay	<b>101</b>
4.3	. Inhibition of C4-2 cancer cell colony formation by compound 3g	<b>102</b>
4.4	Time-dependent wound healing inhibition in C4-2 cancer cells by compound 3g	<b>103</b>
4.5	Real-time gene expression of androgen-responsive genes after intervention with compound <b>3g</b> compared to DMSO as vehicle control.	<b>104</b>
4.6	2D representation of the binding interactions between the AR protein binding site and compounds 3a-3j	<b>105-107</b>
4.7	M.D. simulation analysis of 100 ns trajectories of the protein and ligand (AR protein and 3g)	<b>109-110</b>
4.8	Free energy decomposition of individual residues of protein during ligand binding	<b>111</b>
4.9	PCA-analysis performed on the eigenvalues of 1000 frame cartesian coordinates extracted from the MD trajectory of the	<b>112-113</b>



	ligand-protein complex over a period of 100 nanoseconds. Free energy breakdown of isolated residues of protein during binding with the ligand	
5.1	Cytotoxicity test of 5i by MTT assay against HEK293T cell line	137
5.2	Inhibition of colony formation by compound 5i in a dose dependent manner	139
5.3	Inhibition of cellular migration in C4-2 cancer cells treated with compound 5i in a time dependent manner	140
5.4	Realtime gene expression of AR responsive genes following treatment with 5i (16.50 $\mu$ M) and DMSO as vehicle control	141
5.5	2D representation of the binding interactions between AR protein binding site and compounds <b>5a-5j</b>	143-145
6.1	An overview of diverse pharmacological properties of thiazole ring	155

### LIST OF SCHEMES

Scheme no.	Description	Page no.
2.1	Condensation between 2-amino thiophenol and 5-aldehyde bis thiophene compounds	32
2.2	Condensation of 2-amino thiophenol with benzaldehyde derivatives	33
2.3	Visible light mediated condensation of 2-amino thiophenol with aldehydes	33
2.4	Microwave irradiation driven condensation between aldehydes and 2-amino thiophenol	34
2.5	Condensation between 2-amino thiophenol and aryl ketones	34
2.6	Condensation of 2-aminothiophenol and diketones	34
2.7	Condensation of 2-aminothiophenol and aryl methyl ketones	35
2.8	Condensation between 2- amino thiophenol and various benzoic acid compounds	35
2.9	Condensation of 2-aminothiophenol with fatty acids under microwave irradiation	36
2.10	Condensation between carboxylic acids and 2-amino thiophenol	36
2.11	Condensation between various acid chlorides and 2-aminothiophenol	36
2.12	Condensation of 2-amino-3-mercaptobenzoic acid with p-nitro benzoyl chloride	37
2.13	Condensation of 2-aminothiophenol with chloro acetylchloride	37
2.14	Cyclization of sulfamide substrates to benzothiazole derivatives	38
2.15	Cyclization of benzamides at room temperature	38
2.16	Cyclization of substituted thioformanildes	38
2.17	Cyclization of thioamide derivatives	39
2.18	Cyclization of 2-aminobenzenethios with hydrosilane and CO <sub>2</sub> at 0.5 Mpa	39
2.19	Cyclization of 2- aminobenzenethios and CO <sub>2</sub> at 0.1 Mpa	40

2.20	Synthesis of 1,4-benzothiazines through condensation with 2-bromoalkanoates	<b>47</b>
2.21	Synthesis of 1,4-benzothiazines through the condensation process involving 2-bromo-1- phenyl ethanones	<b>48</b>
2.22	Efficient synthesis of 1,4-Bs from condensation with 1,3-dicarbonyls	<b>48</b>
2.23	Synthesis of 1,4-Bs from condensation with unsaturated acids	<b>49</b>
2.24	Synthesis of 1,4-B's from substituted amines	<b>49</b>
2.25	Synthesis of 1,4-B's from 2,2'-dithiodianiline	<b>50</b>
2.26	Synthesis of 1,4-Bs from ring expansion of benzothiazolines	<b>50</b>
2.27	Synthesis of 1,4-Bs from ring expansion of benzothiazolines using Meldrum's acid	<b>51</b>
3.1	Synthesis of benzothiazine derivatives using CAN	<b>67</b>
4.1	Cross-coupling of 2-chlorobenzothiazole with several piperazine derivatives	<b>100</b>
5.1	Synthesis of benzothiazole fused schiff bases (5a-5j)	<b>134</b>
5.2	Mechanism of benzothiazole schiff base (5a-5j) formation	<b>136</b>
6.1	Synthesis of complexes of 4-(pyridin-4-yl)-2-(2-(pyridin-2-ylmethylene) hydrazinyl) thiazole	<b>157</b>
6.2	Synthetic Procedure for Zn-thiazole nanoparticle	<b>158</b>

## LIST OF ABBREVIATIONS

<b>ABBREVIATION</b>	<b>DESCRIPTION</b>
DCM	Dichloromethane
PBMC	Peripheral blood mononuclear cell
Pet ether	Petroleum ether
SEM	Standard error of mean
TLC	Thin layer chromatography
IR	Infra-red
CDKs	Cyclin dependent kinase
PUD	Peptic ulcer disease
GERD	Gastroesophageal Reflux Disease
AMPA acid	$\alpha$ -amino-3-hydroxy-5-methyl-4-isoxazolepropionic
PPAR	Peroxisome proliferator activated receptor
MRSA	Methicillin resistant Staphylococcus aureus
VRE	Vancomycin resistant Enterococcus
TEMPO	2,2,6,6-tetramethyl-1-piperidinyloxy
MIC	Minimum inhibitory concentration
PHA	Polyhydroxyalkanoate
IL-1	Interleukin-1
IL-1 $\beta$	Interleukin-1 beta
TNF- $\alpha$	Tumor Necrosis Factor alpha
COX-2	Cyclooxygenase-2
PGE-2	Prostaglandin E(2)
NSCLC	Non-small cell lung cancer
IL-6	Interleukin-6
IL-8	Interleukin-8
EMT	Epithelial Mesenchymal Transition
TGF- $\beta$	Transforming Growth Factor beta
CAN	Ceric ammonium nitrate
DMSO	Dimethyl sulfoxide
PBS	Phosphate-buffered saline

RPMI	Roswell Park Memorial Institute
MMLV	Moloney Murine Leukemia Virus
RT-PCR	Reverse Transcription-Polymerase Chain Reaction
GAPDH	Glyceraldehyde-3-phosphate dehydrogenase
MCF-7	Michigan Cancer Foundation-7
EC-9706	Esophageal Carcinoma-9706
ELL2	ELL Associated Factor 2
EAF2	Elongation Factor For RNA Polymerase 2
PSA	Prostate-specific antigen
CALR	Calreticulin gene
AR	Androgen Responsive
ADT	Androgen Deprivation Therapy
CRPC	Castration resistant prostate cancer
RPMI	Roswell Park Memorial Institute
GAPDH	Glyceraldehyde-3-phosphate dehydrogenase
MMLV	Moloney Murine Leukemia Virus
HePG2	Hepatoma G2
Rg	Radius of gyration
RMSF	Root Mean Square Fluctuations
SASA	Solvent Accessible Surface Area
RMSD	Root Mean Square Deviation

*Chapter 1*

***Review of Heterocyclic Compounds***

## 1.1 Introduction

Heterocyclic compounds refer to the cyclic structures that are formed by introducing one or more heteroatoms (atoms other than carbon) into a carbocyclic system. The most commonly encountered heteroatoms, either individually or in combination, in a cyclic system, are nitrogen, sulfur, and oxygen. Though heterocycles containing heteroatoms like Te, Pb, B, etc., are documented, they are not very prevalent. Heterocycles consisting of five and six members are prevalent both as independent structures and as components of integrated ring systems in both synthetic/natural compounds [1]. Heterocyclic compounds can be primarily categorized into three classes based on their saturation level: completely saturated, partially saturated, and completely unsaturated. Saturated heterocycles, like aliphatic amines, exhibit similar behavior. In saturated heterocycles, all the carbon and heteroatoms are  $sp^3$  hybridized, and a lone electron pair is found in a non-bonded hybridized orbital. In contrast, un-saturated heterocycles consist of atoms that are  $sp^2$  hybridized. These electrons contribute to a pi-electron sextet, which imparts aromatic characteristics to the unsaturated heterocycles [2]. Completely un-saturated conjugated heterocycles involve all carbons being  $sp^2$  hybridized. The p orbital, perpendicular to the hybrid orbital, actively participates in the creation of  $\pi$  bonds. These heterocycles exhibit aromatic characteristics as they satisfy the criteria of having  $4n+2\pi$  electrons [3].

## 1.2 Classification of heterocyclic compounds

Heterocycles are classified into two categories based on their structural and electronic configuration: aliphatic and aromatic heterocycles and aromatic. Aliphatic heterocyclic compounds include cyclic ethers /thioethers or amines (**Figure 1.1**).

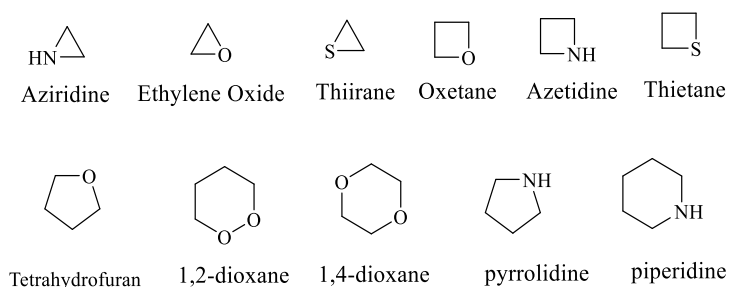


Fig. 1.1 Examples of aliphatic heterocyclic compounds

Aromatic heterocyclic compounds, similar to benzene, exhibit characteristics governed by Huckel's rule. They can be considered analogs of benzene in terms of their structure and electronic properties [4] (**Figure 1.2**)

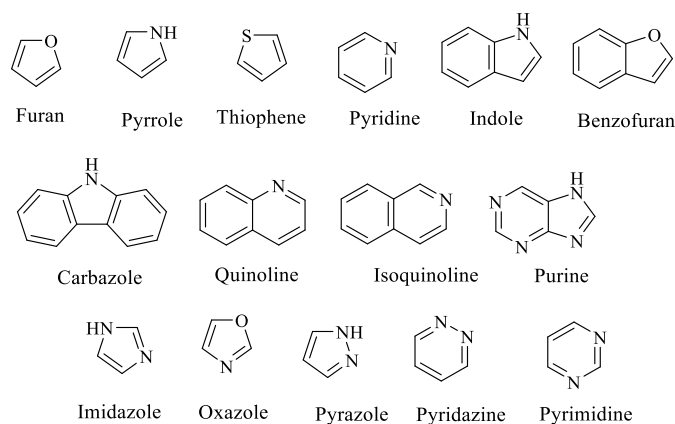


Fig. 1.2. Examples of aromatic heterocyclic compounds

Based on the structural diversity, heterocyclic compounds can be classified into three groups.

1. 5-membered heterocycles: These compounds can be obtained from benzene by substituting one C=C bond with a heteroatom possessing a lone pair of electrons. Based on the number of heteroatoms that are present in the cyclic ring, this category can be further divided into the following subcategories:

a) Heterocycles with one hetero-atom: Examples of this group include furan, thiophene, and pyrrole (**Figure 1.3**)

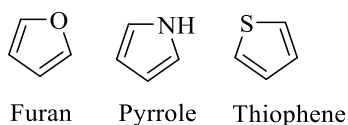


Fig. 1.3. Five membered heterocycles with 1 hetero-atom

b) Heterocycles with more than a single heteroatom: These heteroatoms can be either the same or different. Examples include pyrazole, imidazole, thiazole, oxazole, triazole, etc. (**Figure 1.4**)

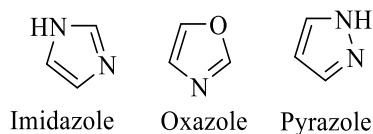


Fig. 1.4. Five membered heterocyclic compounds with more than one heteroatom

2. 6-membered heterocycles: This category of compounds can be obtained by replacing a C-atom in benzene with an iso-electronic atom. Comparable to 5-membered heterocycles, 6-membered heterocyclic compounds can also be further divided into subcategories.

a) Heterocyclic compounds with a single heteroatom: Examples of this group include pyridine, pyran, and thiopyran (**Figure 1.5**)

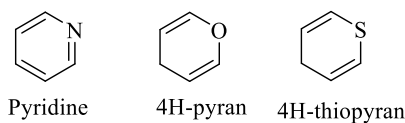


Fig. 1.5. Six membered heterocyclic compounds with one heteroatom

b) Heterocycles having more than one hetero atom: Examples of this group of compounds are pyridazine, pyrazine, pyrimidine etc. (**Figure 1.6**)

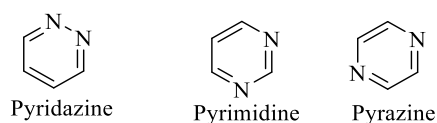


Fig. 1.6. Six-membered heterocycles with more than one heteroatom

3. Fused heterocycles belong to a class of compounds that contain two or more rings that are fused. These fused rings can be a combination of carbocyclic (containing carbon atoms) and heterocyclic (containing heteroatoms) rings. Examples of such compounds include indole, quinoline, isoquinoline, and carbazole. Alternatively, the fused rings can be entirely heterocyclic, as seen in compounds like purine and pteridine [5] (**Figure 1.7**)

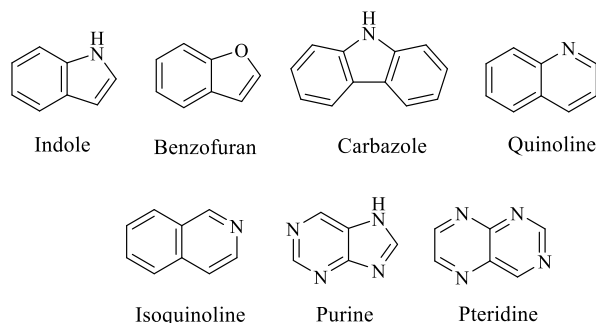


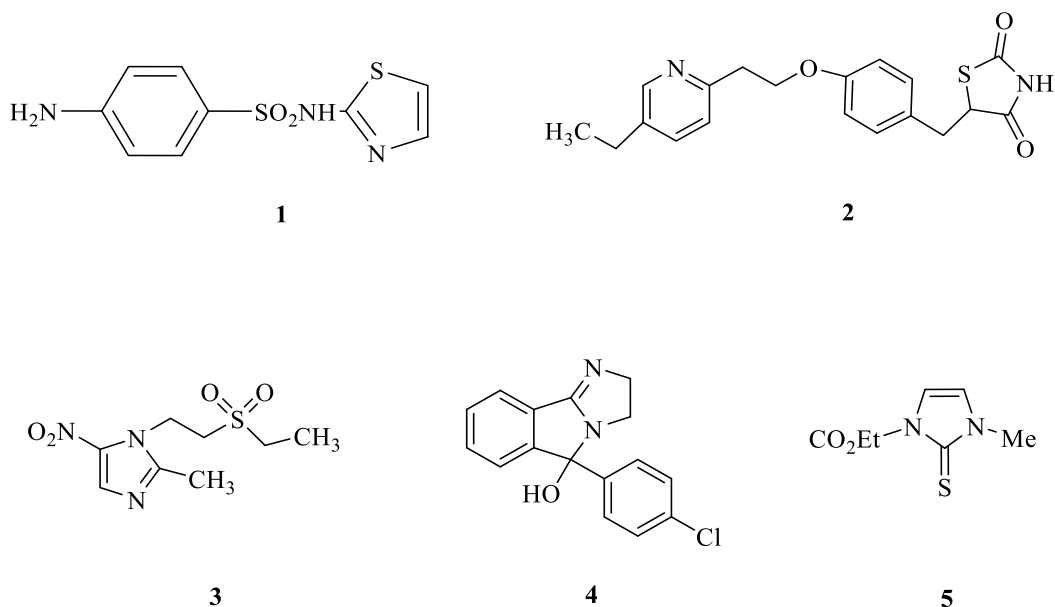
Fig. 1.7. Fused heterocyclic compounds

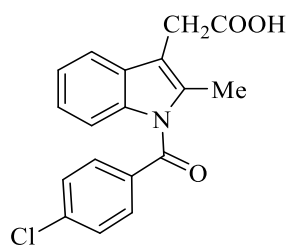
Heterocyclic compounds, prized for their ability to mimic biological structures and serve as reactive pharmacophores, play a crucial role in both natural pharmaceuticals and synthesized substances, offering extensive opportunities for uncovering novel lead compounds and understanding activity correlations with biological targets. Their distinctive characteristics, including hydrogen bond donors/acceptors within a partially rigid framework, make them highly attractive in drug discovery, garnering considerable focus in research efforts [6]. The adaptability of heterocycles arises from their capability to integrate compact and rigid molecular structures while maintaining a high level of molecular heterogeneity [7].



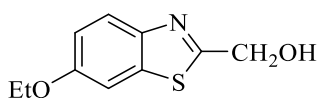
Heterocyclic nuclei are prevalent in various crucial components within living cells. Examples encompass the purine and pyrimidine bases within the genetic material DNA, vital amino-acids as well as essential substances such as coenzyme precursors and vitamins [8]. Heterocyclic nuclei are present in the B<sub>12</sub> and E vitamin families, chlorophyll, haemoglobin, and its degradation by-products, bile pigments, as well as various hormones such as kinetin, heteroauxin, serotonin, and histamine. Furthermore, several sugars include diverse heterocyclic nuclei [9].

A broad spectrum of natural compounds, encompassing antibiotics like penicillin, cephalosporins, along with alkaloids such as vinblastine, morphine, and reserpine, feature heterocyclic components. Heterocyclic structures are also evident in cyclo-peptides, macrolides, poly-ketides, steroids, glycosides etc. By examining the structures of various marketed drugs currently used in therapy, we can appreciate the presence of heterocyclic moieties. Instances include tubercidin, aminoglycosidal antibiotics like streptomycin and sulfa drugs like Sulphathiazole **1**, the anti-diabetic medication Pioglitazone **2**, the anti-protozoal medication Tinidazole **3**, the C.N.S stimulant Mazindaol **4**, the anti-thyroid agent Carbimazole **5**, the anti-inflammatory medication Indomethacin **6**, diuretic like Ethoxzolamide **7**, and the anti-histamine Trimeprazine **8**. All of the mentioned compounds feature varied heterocyclic moieties [10].

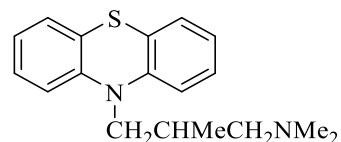




6



7



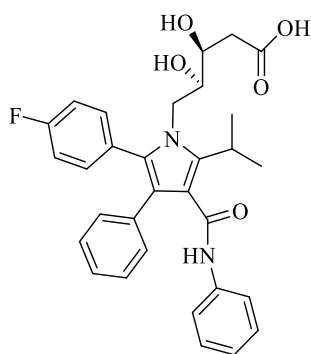
8

### 1.3 N-containing heterocycles

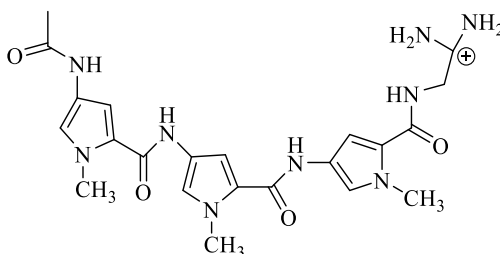
Nitrogen-possessing heterocycles are widely distributed in the natural world and hold a pivotal role in numerous biological processes. They serve as indispensable structural elements present in a myriad of natural products, encompassing vitamins, hormones, antibiotics, alkaloids, herbicides, dyes, and pharmaceuticals [11].

#### 1.3.1 Pyrrole and its benzo derivatives

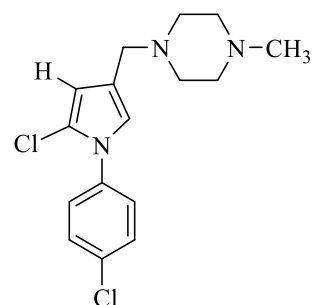
Pyrrole and its benzo derivatives, like indole, are crucial nitrogen-containing heterocycles that serve as fundamental building blocks for naturally occurring porphyrins, essential in biological processes such as heme synthesis. Their diverse derivatives display a spectrum of physiological activities, with 1,2,3,5-tetrasubstituted pyrrole derivatives particularly noted for their antibacterial, antiviral, anti-cancer, and antioxidant properties, as well as their potential in treating cytokine-mediated diseases and hypertension. For instance, Atorvastatin **9** is used for treating cardiovascular disorders, Bisdistamycin **10** exhibits anti-HIV activity, and BM 212 **11** shows efficacy against multi-drug-resistant tuberculosis [12].



9

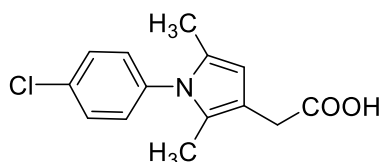


10



11

Most of the NSAIDs (Nonsteroidal anti-inflammatory drugs) contain a benzene ring as the aromatic nucleus. These drugs often have a propionic acid attached to the 2<sup>nd</sup> position in the benzene entity, which serves as the side chain. An example of such a compound is Clopirac **12**.



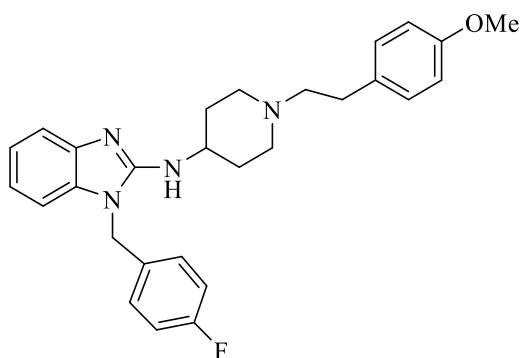
**12**

Indole and its derivatives, benzopyrroles, are pivotal in drug discovery due to their pharmaceutical activities, serving as essential structural elements for potential drug candidates. Their presence in alkaloids and the recognition of tryptophan's significance in human nutrition have spurred extensive research, leading to the development of diverse therapeutic agents. Indole-based compounds exhibit multifaceted pharmacological effects, including anti-inflammatory actions, phosphodiesterase inhibition, modulation of 5-hydroxytryptamine and cannabinoid receptors, and HMG-CoA reductase inhibition. Leveraging the conserved binding pocket in G-protein associated receptors (GPCRs), indole scaffolds are widely utilized in medications such as indomethacin, ergotamine, ondansetron, among others [13].

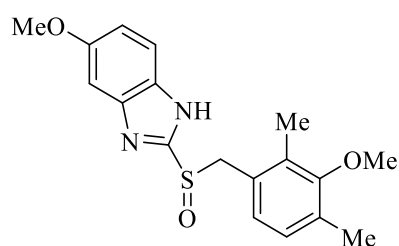
Indole is a widely recognized structure in heterocyclic compounds that plays a crucial role in various natural products and medicinal agents. Compounds featuring the indole moiety have demonstrated antibacterial, antifungal, antiviral, and anti-estrogenic characteristics. Many natural products with the indole ring have been discovered, including Nortopsentins **13**, known for their antitumoral effects, Martefragin A **14**, a potent inhibitor of lipid peroxidation, Indololactum V **15**, a protein kinase C activator, and Fumitre morgan **16**, a distinct counteracting agent for the protein resistant to breast cancer. Indole serves as a key component in medications like Indomethacin for inflammation and selective factor Xa inhibitors, showcasing its diverse pharmacological properties. Its versatile structure makes it valuable in drug development, with related heterocycles like indolizines showing antiarrhythmic effects, oxindoles with anti-rheumatic properties and inhibition of mandelo-nitrile Lyase, and derivatized indolines known for their potency and selectivity as 5-HT<sub>3</sub> receptor antagonists [14].



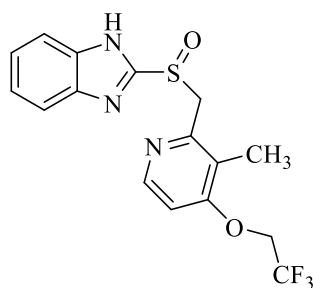
Benzimidazoles are a class of compounds that consist of an imidazole ring fused to a benzene ring. They have been found to possess significant physiological and pharmacological activity. Compounds derived from benzimidazole have been employed in addressing various health conditions such as epilepsy, and diabetes, and as agents with antimicrobial and anticancer properties. Notable examples of benzimidazole compounds with clinical relevance include the antihistamine Astemizole **22** and proton pump inhibitors such as Omeprazole **23**, Lansoprazole **24**, and Pantoprazole **25** [16].



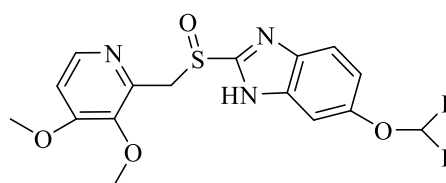
**22**



**23**

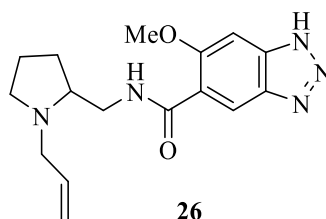


**24**



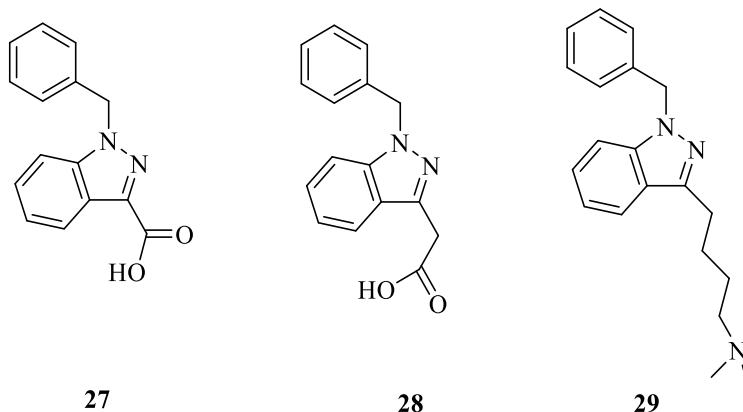
**25**

Benzotriazole derivatives, which feature a benzene ring fused with a nitrogen-containing ring, represent a unique class of bioactive compounds. These compounds have been employed as antiemetics, with Alizapride **26** being a notable benzo-triazole derivatives utilised in the management of adverse effects associated with cisplatin chemotherapy [17].



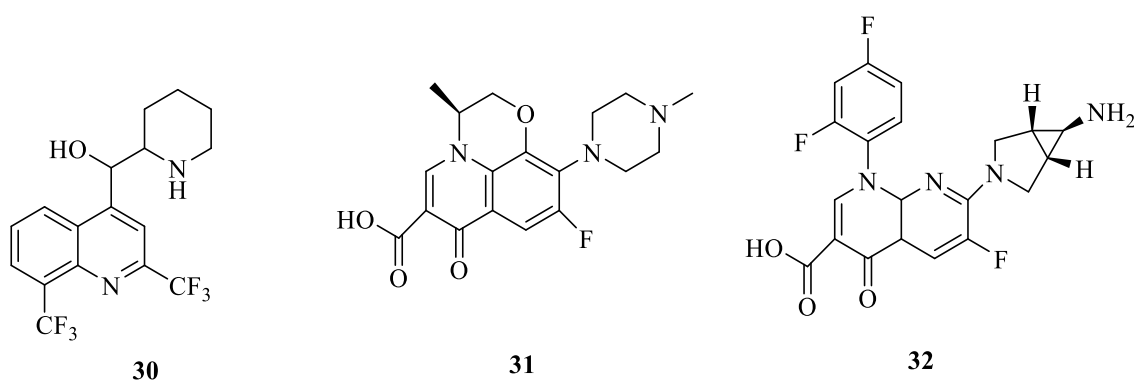
**26**

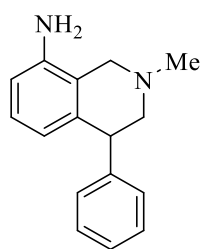
The indazole nucleus is a crucial component in numerous drug compounds, exhibiting diverse pharmacological activities including antitumor, antimicrobial, and antiplatelet effects. Lonidamide **27**, which contains an indazole moiety, demonstrates anticancer activity. Similarly, Bendazac **28** and Benzydamine **29** are examples of indazole-containing drugs marketed for their anti-inflammatory properties [18].



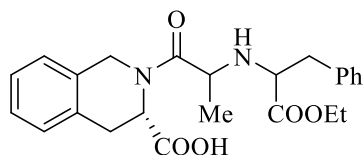
### 1.3.3 Quinolines and isoquinolines

Quinolines and isoquinolines, along with their tetrahydroderivatives, are widely present in both natural and synthetic compounds with prominent biological activity. For instance, Mefloquine **30**, an antimalarial drug, Levofloxacin **31**, Trovafloxacin **32**, which are broad-spectrum antibacterial agents, Ciprofloxacin, which can also treat anthrax, Nomifensine **33**, an antidepressant drug, and Quinapril **34**, an inhibitor of angiotensin-converting enzyme. Chloroquine **35**, a widely recognized medication for treating malaria, also incorporates a quinoline core. Furthermore, these heterocycles have demonstrated their ability to act as ligands for the human glucocorticoid receptor [19, 20]

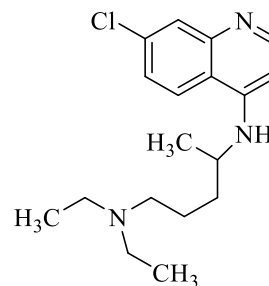




33



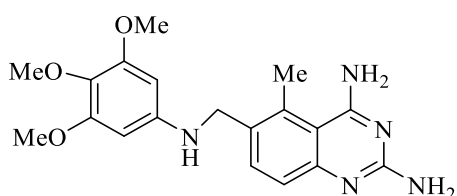
34



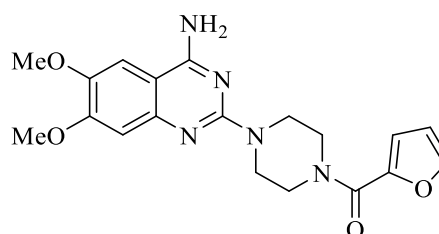
35

### 1.3.4 Quinazoline

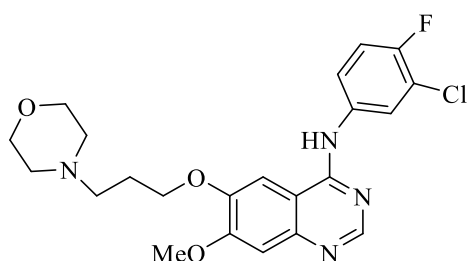
Quinazoline, also known as benzopyrimidine, and its derivatives serve as fundamental building blocks for approximately 150 naturally occurring alkaloids found in various plant families, microorganisms, and animals. This heterocyclic arrangement is present in Trimetrexate **36**, a medication utilized for pneumonia induced by *Pneumocystis carinii*, as well as in Prazosin **37**, employed for managing BPH, and the antihypertensive medication ketanserin. Quinazoline derivatives demonstrate diverse biological properties, encompassing antitumor effects **38**, robust non-nucleoside reverse transcriptase inhibition of HIV- 1, and anti-microbial activity **39**, antagonism of the human adenosine A(3) receptor and anti-inflammatory, anti-asthmatic, and anti-ischemic activities [21].



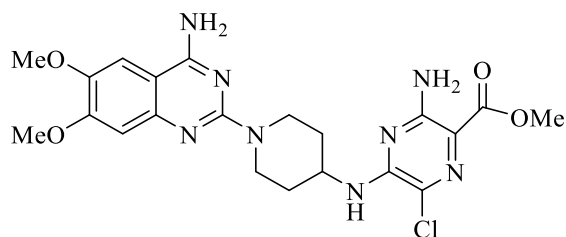
36



37



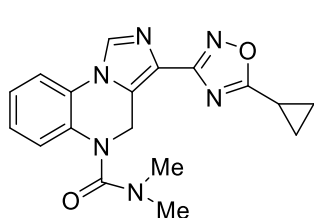
38



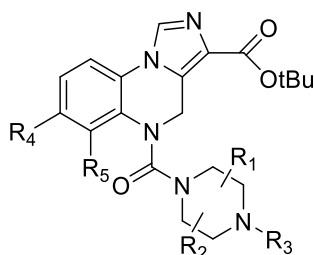
39

### 1.3.5 Quinoxaline

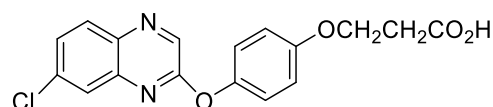
Quinoxaline is a type of nitrogen-containing compound. One specific derivative, quinoxaline di-N-oxide **40**, has been known to demonstrate anti-trypanosomal activity in laboratory tests against *Trypanosoma cruzi*. Certain analogs of imidazo[1,5-a]quinoxaline **41** have demonstrated anxiolytic properties by effectively binding to GABA receptor. Chloro derivative of quinoxaliniyl with a phenoxy along with propionic acid group **42** (known as XK 469), has shown broad effectiveness against mammary adeno-carcinoma. Numerous quinoxaline compounds have been identified as having angiotensin II receptor antagonist activity as well as adenosine receptor antagonistic activity [22].



**40**



**41**

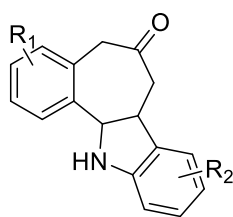


**42**

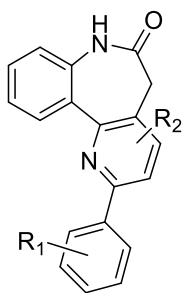
### 1.3.6 Benzazepines

Benzazepines are the group of heterocyclic systems featuring a nitrogen atom within a seven-member ring structure. In a study by Link et al. in 1998, a group of derivatives called 7, 12-dihydro-indolo-[3, 2-d][1]benzazepin-6 (5H)-one **43** and similar heterocycles **44** were found to have the ability to inhibit cyclin-dependent kinases (CDKs). These compounds have also demonstrated biological activity as selective inhibitors of acetylcholinesterase in the central nervous system. Additionally, some compounds containing this structural motif have shown effects as vasopressin receptor antagonists and specific agents for treating bradycardia [23, 24]. One example of such a compound is Zatebradine **45**.

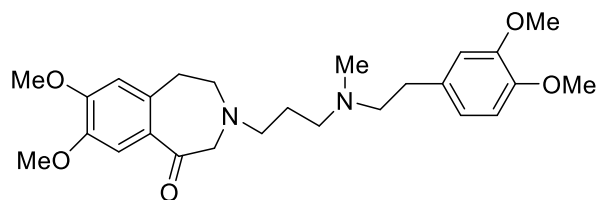




43



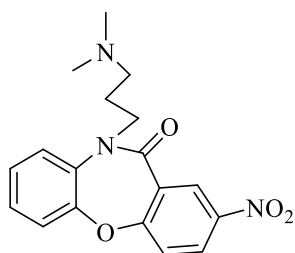
44



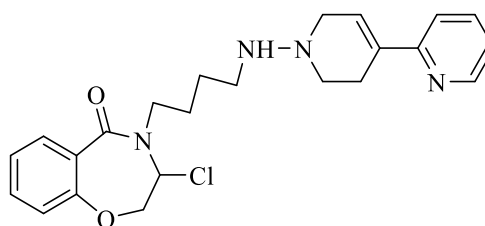
45

### 1.3.7 Benzoxapines

Benzoxapines are a class of compounds that feature a benzoxazepine ring system. Among these compounds, nitroxazepine **46** and related derivatives have been found to possess significant antidepressant activity. Additionally, a novel class of derivatives called 1,4-benzoxazepines (BZO) **47** has been identified as effective and selective 5-HT<sub>1A</sub> agonists, demonstrating potent antiischemic effects [25].



46



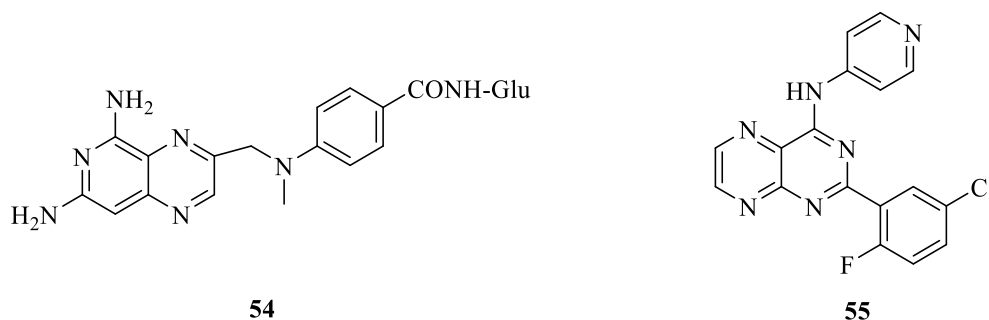
47

### 1.3.8 Benzothiazepines

Benzothiazepines are a class of compounds that share a structural resemblance to benzodiazepines. They consist of bicyclic heterocycles comprised of a benzene unit attached to a thiazepine moiety. The most commonly encountered structural isomers for these heterocyclic frameworks are 1,4-benzothiazepines and 1,5-benzothiazepines. Diltiazem **48**, a renowned 1,5-benzothiazepine-4-one, stands as one of the extensively employed medications for managing cardiovascular disorders, primarily owing to its function as a calcium channel blocker. Certain others **49**, **50** are selective and potent bradykinin antagonists [26].



been noted for their interactions with biological entities like alkyltransferase, adenosine kinase, xanthine oxidase, and neuronal NO synthase [29].



### 1.3.11 Triazine and its derivatives

Triazines and their benzoderivatives are the compounds bearing a resemblance to the benzene structure, with nitrogen atoms replacing the carbon atoms. The three distinct isomers of triazine can be identified by the arrangement of their nitrogen atoms (**Figure 1.8**).

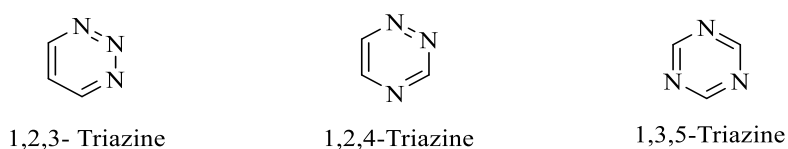
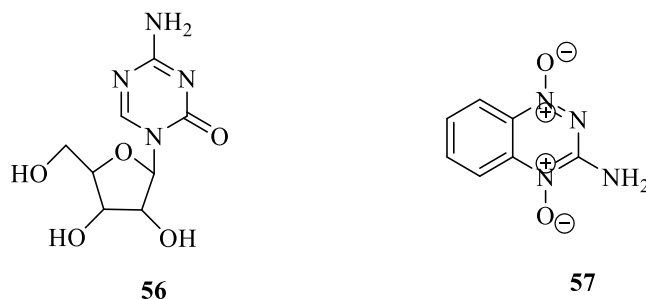


Figure 1.8. Isomers of triazine

Many man-made compounds featuring the triazine ring display notable biological activity and find applications as pharmaceutical agents [30]. 5-azacytidine 4-amino-D-ribofuranosyl derivative of triazine **56**, is a man-made analog of the naturally occurring cystidine, displaying potent anti-leukemic properties. Tirapazamine **57** (TPZ 1, 2, 4- benzotriazin-3- amine 1,4-dioxide) represents a highly advanced bioreductive drug that selectively targets hypoxic cells. Additionally, specific phenyl substituted triazines have been employed for therapeutic purposes, acting as antimalarial, antifungal, and antiparasitic agents [31].

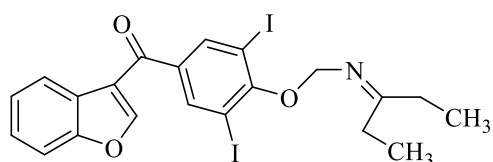


## ***1.4 Oxygen-containing heterocycles***

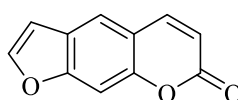
Oxygen-containing heterocyclic compounds are extensively distributed and can be identified in a multitude of natural products. They are also present in diverse synthetic compounds. They have demonstrated capabilities in anticoagulant, antipsoriasis, viral protease inhibition, antibacterial, antitumoral, antioxidant, antiproliferative, and central nervous system altering activities [32]. The category of oxo-heterocyclic compounds encompasses the following varieties:

### ***1.4.1 Furans and Benzofurans***

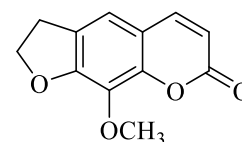
Furan and its analogs is an important category of compounds found in nature that have attracted attention due to their biological activity and their role in defense systems. They are utilized as oxidants, antioxidants, and brightening agents, and have relevance in the development of drugs. One prominent example is amiodarone **58**, which is a lipophilic benzofuran derivative containing iodine. It is widely employed for the treatment of ventricular tachyarrhythmia. Naturally prevalent furocoumarins, including Psoralen **59** and Methoxalen **60**, contain benzofuran structures. These compounds are derived from the seeds of *Ammi majus* L and are utilized in the cure for psoriasis and other skin diseases [32]. Psoralen also finds application in phototherapy, where it can undergo photoaddition reactions with thymine units in DNA [33]. Usnic acid **61**, which contains a benzofuran moiety, is a commonly found and abundant metabolite in lichens. It is renowned for its antibiotic properties and exhibits other intriguing pharmacological effects such as antimicrobial activity and the ability to regulate tumor proliferation [34]. Nitrofurantoin **62** and Nitroxyzone **63**, both containing a furan nucleus, function as antibacterial agents, with Nitroxyzone being a hydrophilic congener. Dantrolene **64** is a muscle relaxant which operates by interfering with contraction-excitation coupling in muscle cells through its interaction with the ryanodine receptor. It is extensively employed as an efficacious remedy for hyperthermia [35]. Ranitidine **65** is a histamine H<sub>2</sub>-receptor antagonist that operates by suppressing the generation of stomach acid. It is frequently recommended for managing PUD and GERD [36].



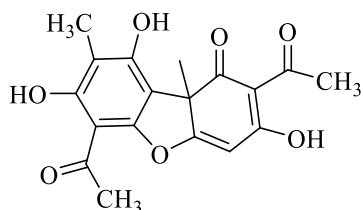
58



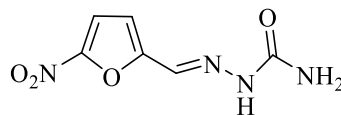
59



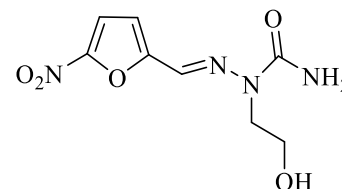
60



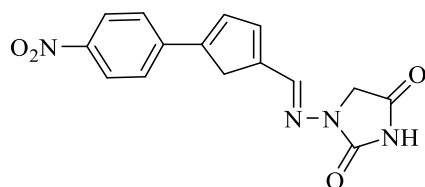
61



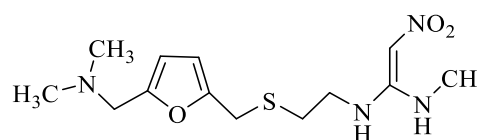
62



63



64

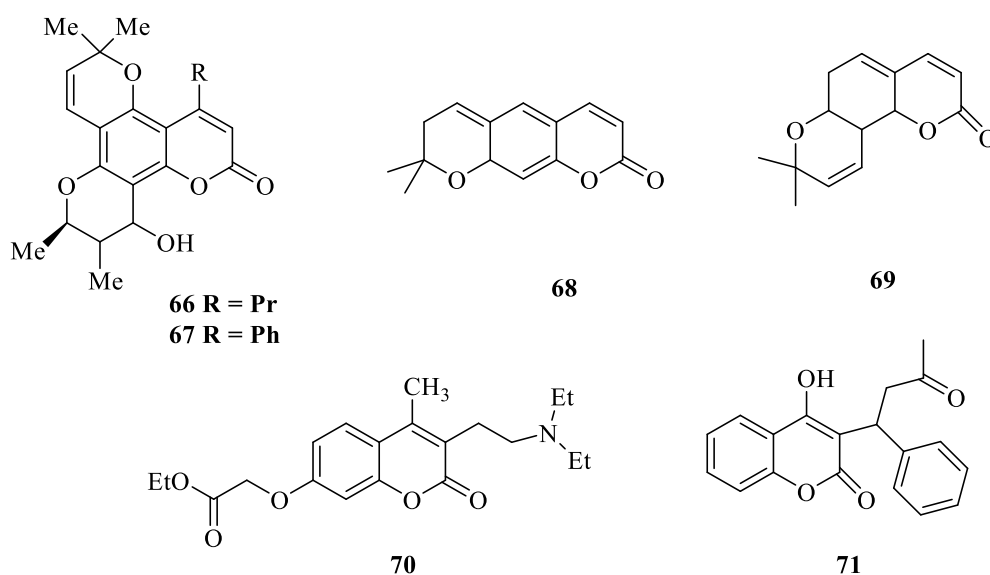


65

### 1.4.2 Coumarins

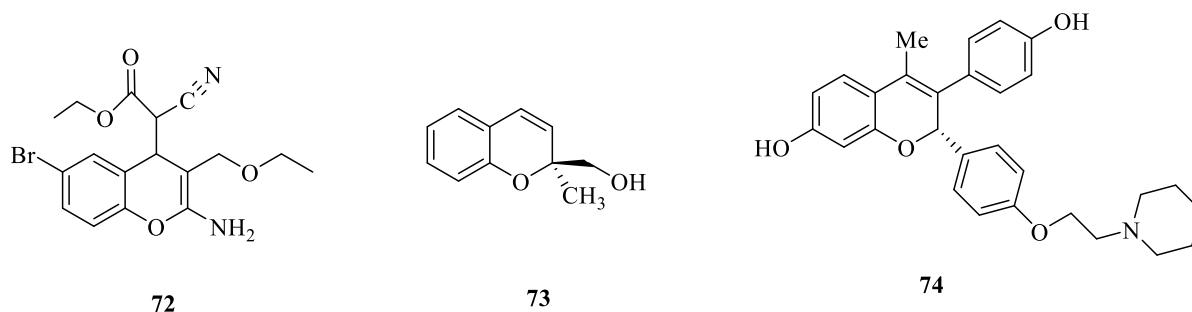
Coumarins, whether derived naturally or synthesized as 2-benzopyranone derivatives, are part of a group of compounds exhibiting a range of pharmaceutical properties. Coumarin derivatives have been found to exhibit anticoagulant, antioxidant, antiproliferative, and estrogen-agonist effects [37]. These derivatives have the potential to be employed as therapeutic substances to mitigate the onset of negative effects linked to menopause, for example; osteoporosis, atherosclerosis, and cognitive impairment [38]. Significantly, specific derivatives of coumarin, such as Calanolide **66** and Inophyllum **67**, extracted from the Calophyllum genus (Guttiferae), have demonstrated potent activity against human HIV-I [39].

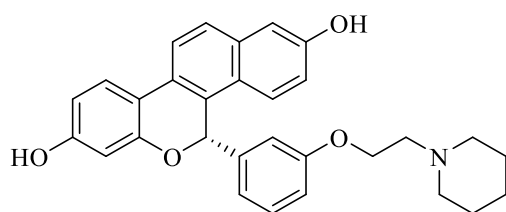
Two pyranocoumarin derivatives found in nature, specifically Xanthyletin **68** and Seselin **69**, have demonstrated a variety of effects, including antimicrobial, insecticidal, antitumor, and anti-HIV activity. Seselin is additionally utilized as a photosensitive drug for treating skin disorders [40]. Carbochromen **70**, a highly effective and selective coronary vasodilator, has been employed for an extended period in the treating angina pectoris. Warfarin **71**, a different derivative of coumarin, exhibits robust anticoagulant activity and favorable pharmacokinetic attributes [41].



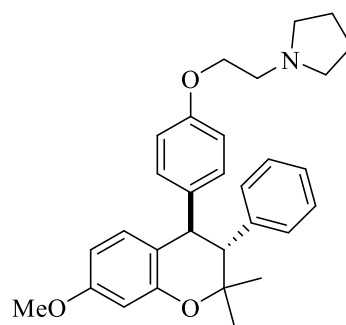
### 1.4.3 Chromans/ chromenes

Chromans/es, notable for their O-containing heterocyclic structures, exhibit varied biological activities, including spasmolytic, anticoagulant, and cognitive enhancement properties. Explored for treating neurodegenerative conditions like Alzheimer's and Parkinson's diseases, they also show potential in addressing AIDS-associated dementia, Down's syndrome, schizophrenia, and myoclonus [42]. Chromenes are also examined as antagonists for anti-apoptotic Bcl-2 proteins to address drug resistance in cancer **72** [43]. Additionally, a specific chromene derivative called Quercinol **73** has been investigated for its anti-inflammatory properties. Significantly, a variety of derivatives of chromene and chroman have surfaced as a new category of medications recognized as selective estrogen receptor modulators (SERMs) **74,75,76** [44].





75

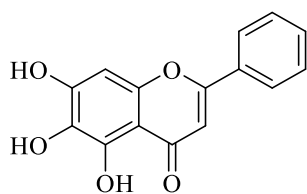


76

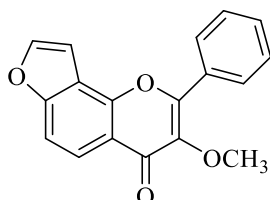
#### 1.4.4 Flavonoids

Flavonoids constitute an extensive category of compounds found naturally, characterized by aryl-substituted chromonones or pyrones, sharing a unified 3-ring scaffold. These compounds were identified to possess diverse advantageous properties. They exhibit antitumoral, anti-atherosclerotic, cardioprotective, anti-inflammatory, antioxidant, antiosteoporotic, antimicrobial, and antiviral characteristics, as indicated by various studies [45,46]

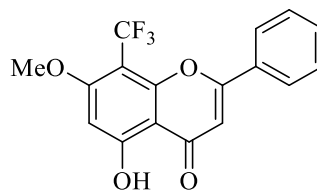
The antioxidant activity of flavonoids is one of the extensively researched health benefits. Flavonoids can scavenge free radicals and protect cells from oxidative damage. In the realm of anticancer investigation, flavonoids have demonstrated the ability to impede the cellular metabolic activity of the carcinogen benzopyrene. Additionally, they amplify the cytotoxicity of TNF- $\alpha$ . Furthermore, flavonoids display inhibitory activity against tyrosinase, moderate aromatase inhibitory activity, and the capacity to hinder estradiol-induced DNA synthesis [47]. Particular flavonoids, like Baicalein, have been recognized as strong inhibitors of platelet 12-human lipoxygenase [48]. Karanjin **77** exhibits hypoglycemic properties, whereas derivatives **78** and **79** display anti-cancer activity [49].



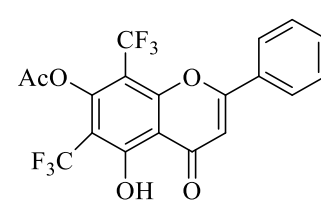
77



78



79

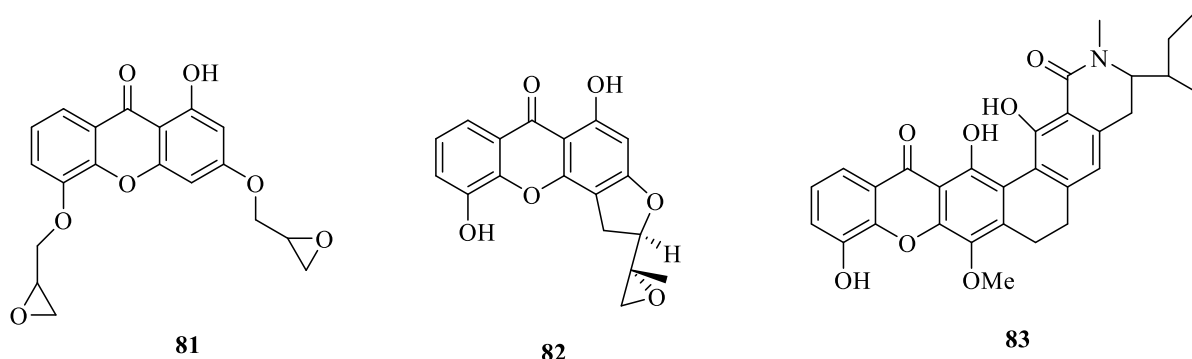


80

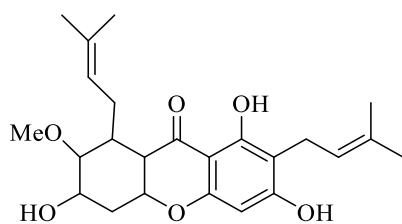
### 1.4.5 Xanthenes and Xanthones

The distinct structural features and biomedical property of xanthenes have inspired researchers to discover or create novel derivatives with the potential for drug development. Xanthenes exhibit a wide range of biological activities based on their molecular structures. Research, exemplified by the investigation carried out by Sanugul et al. in 2005, has underscored the varied attributes of xanthenes, encompassing anti-hypertensive, anti-oxidative, anti-thrombotic, and anticancer properties. Whether synthesized or obtained from natural sources, polyoxygenated xanthenes have exhibited inhibitory effects against diverse cancer cells. Psorospermin **81**, for instance, derived from the African plant *Psorospermum febrifugum*, has displayed promising anti-cancer effects on both human and murine cancer cell lines [50].

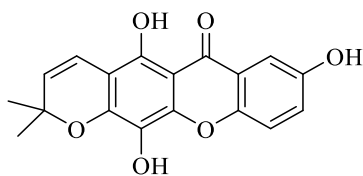
Certain derivatives of xanthenes have displayed distinct activities and roles. Mangiferin, categorized as a xanthone glucoside, functions as a robust  $\alpha$ -glycoside inhibitor. Sch-56036 **82** has showcased potent antifungal capabilities.  $\alpha$ -Mangostin **83**, another xanthone derivative **84**, serves as a competitive antagonist for the histamine H1 receptor, inhibits both topoisomerases I and II, demonstrates antibacterial effects against *H. pylori*, possesses anti-inflammatory properties, and can inhibit oxidative damage to human low-density lipoprotein [51]. Astroviridin **85** is a recently extracted tetracyclic poly-hydroxylated xanthone from the stem bark of *G. atroviridis*. It has traditionally been used for ear ache and is currently being studied for its potential pharmacological properties. These examples illustrate the diverse biological activities exhibited by xanthenes and highlight their potential as sources for developing new drugs [52].







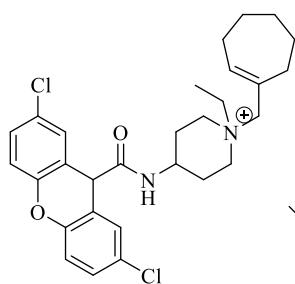
84



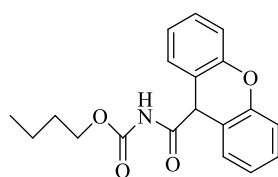
85

Xanthenes are a group of alkaloids derived from xanthine that are commonly utilized for their mild stimulant properties and as bronchodilators, particularly in the treatment of asthma symptoms. Instances of xanthene derivatives with methyl groups comprise caffeine, aminophylline, IBMX, paraxanthine, theobromine, and theophylline etc. [53]

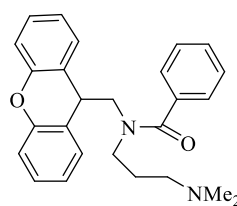
Xanthene derivatives display a diverse array of medicinal characteristics, encompassing antifungal, and anti-inflammatory properties. For instance, a novel CCR1 receptor agonist **86** is an example of a biologically active xanthene that has specific effects on the CCR1 receptor. Additionally, certain xanthene derivatives have been identified as chemosensitizers **87**, **88**, **89** enhancing the effectiveness of treatment against chloroquine-resistant *Plasmodium falciparum*, a malaria-causing parasite. The diverse applications of xanthene derivatives extend beyond their biological activities. They are also utilized in various fields due to their functionalities. For instance, xanthene derivatives are used as dyes and find applications in laser technology. Additionally, they can serve as fluorescent materials sensitive to pH changes, enabling the visualization of biomolecular assemblies [54].



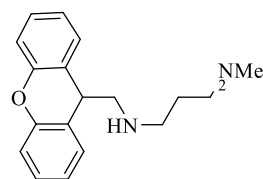
86



87



88



89

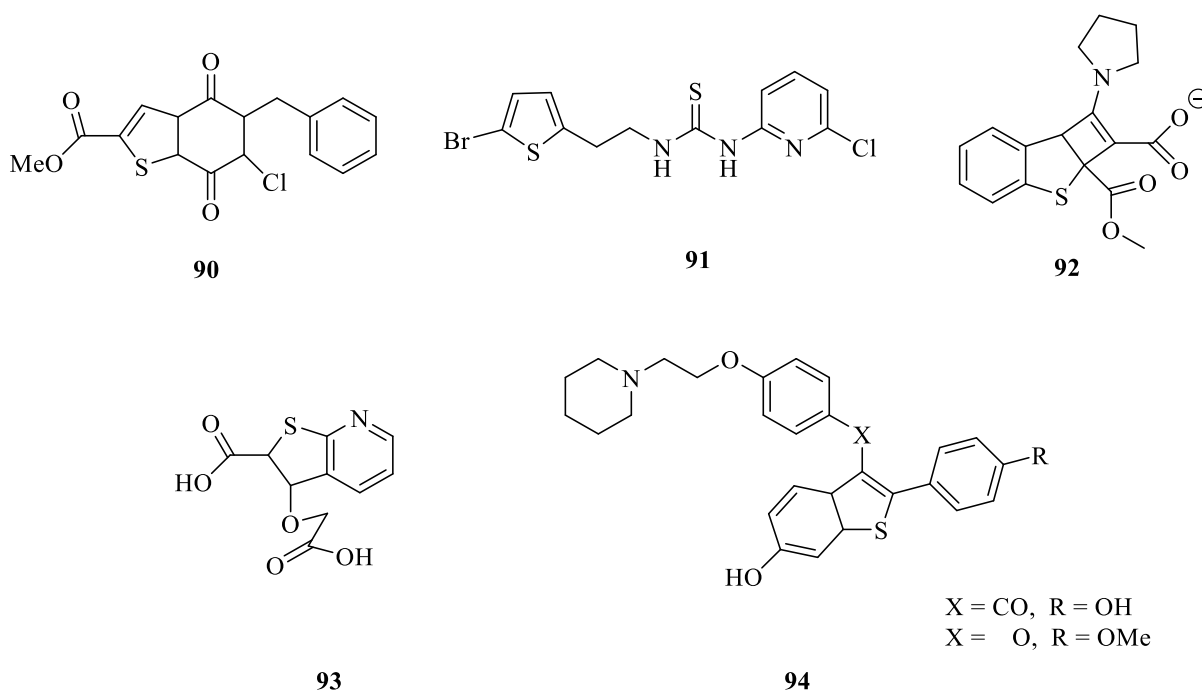
### 1.5 Sulfur heterocycles

Heterocyclic compounds possessing sulfur occur in a variety of biologically active substances, demonstrated by the identification of various medications like sulphonamides and sulfones. These drugs have demonstrated significant activities against malaria, mycobacterial infections,

bacteria, fungi, and other pathogens. Several drug molecules containing a sulfur heterocyclic ring system have been developed for specific therapeutic purposes. As an example, Raloxifene, incorporating a benzothiophene core, is employed for osteoporosis treatment. Chlorprothixene, containing a thioxanthene structure, is employed as a psychotropic drug. Additionally, drugs derived from thiadiazole, such as Cezopram, have been utilized as antibiotics [55].

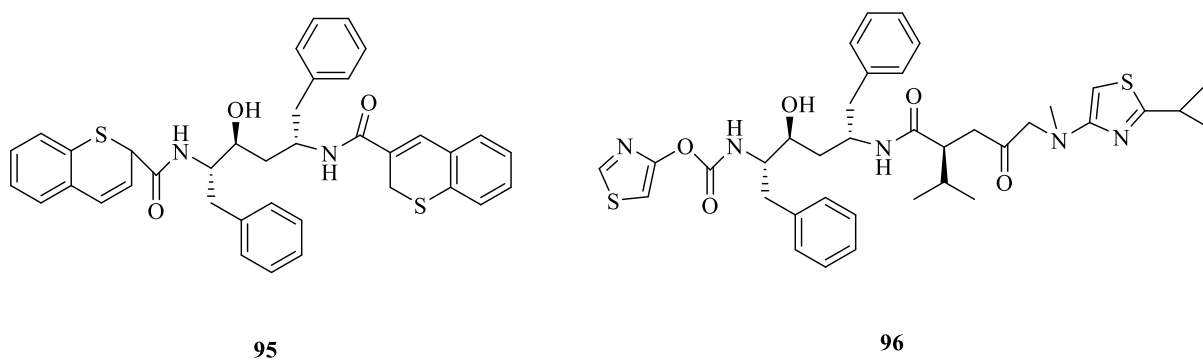
### 1.5.1 Thiophenes and benzothiophenes

Thiophenes and benzothiophenes are widely found in nature and exhibit diverse biological activities. They are extensively used as functional materials in various applications including dyes, liquid crystal moieties, and organic polymers. Certain derivatives of 4,7-dioxobenzo(b)thiophene **90**, **91** have demonstrated antifungal properties. Additionally, compounds like DDE934 **92** and NSC-380292 **93** have been utilized as anti-HIV agents and have shown greater potency than Nevirapine. Benzothiophenes have gained significance as crucial pharmacophores in the field of medicinal chemistry [56]. Significantly, Raloxifene and Arzoxifene **94** have been effectively formulated as inhibitors of bone resorption and are part of an innovative category known as selective estrogen receptor modulators (SERMs). These examples highlight the significant role of thiophenes and benzothiophenes in the development of biologically active compounds with therapeutic potential [57].



### 1.5.2 Thiochromenes

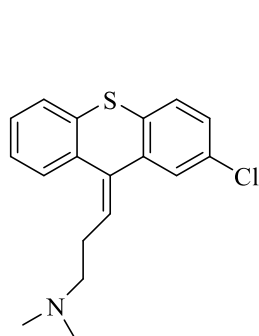
Thiochromenes, specifically those belonging to the 2H-1-benzothiopyran group, are integral in the synthesis of pharmaceuticals. Derivatives of thiochromenes **95** have been found to possess interesting biological properties, including their ability to modulate estrogen receptors and inhibit cyclooxygenase-2 (COX-2), an enzyme involved in inflammation [58]. What makes thiochromene derivatives particularly noteworthy is their greater biological efficacy in comparison to their oxygen equivalent, the benzopyran moiety, when it comes to drug development. For example, a thiochromene analog of Ritonavir **96** has been recognized as a potent inhibitor of HIV-I protease, demonstrating greater efficacy than the original Ritonavir compound. These findings emphasize the significance of thiochromenes and their derivatives in the development of pharmaceutical compounds with notable biological effects [59].



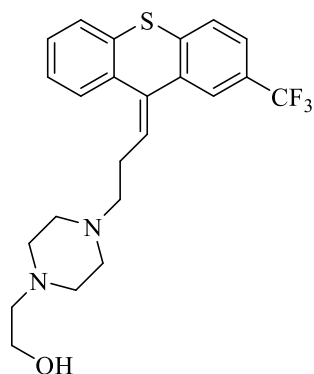
### 1.5.3 Thioxanthenes

This group of compounds constitutes an important classification of drugs regarded as tricyclic pharmaceuticals, which have been extensively studied and widely used in the treatment of various mental and physical disorders. These compounds have demonstrated effectiveness in various conditions, including depression, Parkinson's disease, and diverse types of allergies. Several drugs belonging to this category are presently employed in clinical settings. For instance, Chlorprothixene **97** is a psychotropic drug, Flupenthixol **98** is an antimicrobial drug, and Clopenthixol **99** is a neuroprotector [60]. However, these drugs also possess additional clinical properties, including being anti-tumor agents, positive allosteric modulators of mGlu receptors, ligands for the  $\sigma$ 1 receptor, anti-emetic and anti-nausea agents, antihistamines, and enhancers of the sedative and general anesthetic effects of analgesics. Overall, these tricyclic

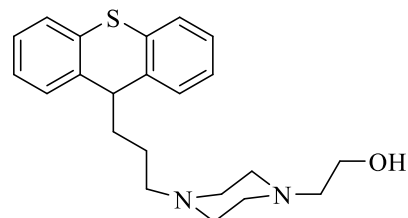
pharmaceuticals exhibit a wide range of clinical benefits and diverse pharmacological effects, making them versatile compounds in the field of medicine [61].



97



98

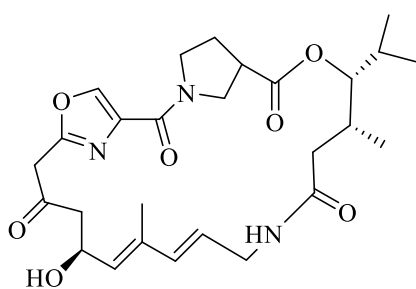


99

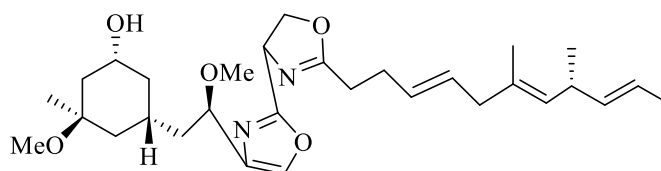
## 1.6 Heterocyclic compounds with more than a single hetero atom

### 1.6.1 Oxazoles

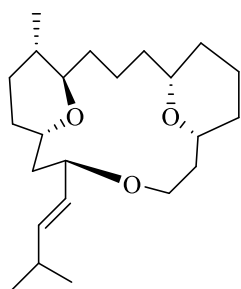
Oxazoles, characterized by a 5-membered heterocyclic ring containing both nitrogen and oxygen atoms, serve as essential components in the synthesis of natural products and synthetic intermediates. The substituted oxazole motif, prevalent in numerous natural compounds, showcases diverse biological activities across various therapeutic domains, with particular attention drawn to polyoxazole-containing molecules identified over the last two decades for their distinctive biological properties. For instance, Telomestatin and Ulapualide A are natural products featuring polyoxazole moieties and have been noted for their diverse biological activities. Virginiamycin M2 **100** serves as an antibiotic, Hennoxazole A **101** displays antiviral properties, and Leucascandrolide A **102** acts as an antifungal agent. Moreover, BMS-337197 **103** has been recognized as an inhibitor of IMPDH, demonstrating anti-proliferative activity [62].



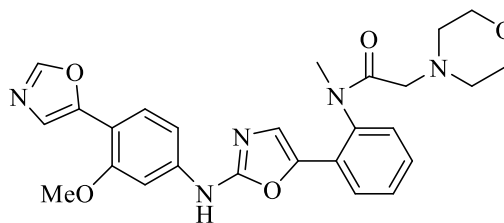
100



101



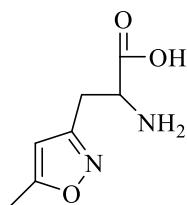
102



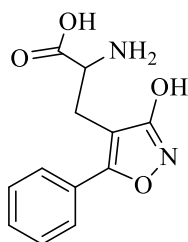
103

### 1.6.2 Isoxazoles

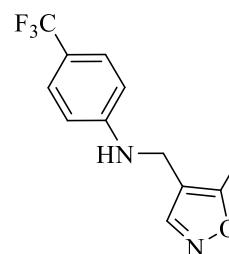
Isoxazoles are widely acknowledged as versatile building blocks in organic synthetic chemistry. They have undergone extensive investigation for their pharmaceutical attributes, encompassing hypoglycemic, analgesic, anticancer, and antibacterial activities. Hydroxy substituted isoxazoles, in particular, have been employed in formulating drugs for the central nervous system (CNS), such as AMPA **104** and APPA **105**. In these instances, the 3-hydroxy oxazole unit acts as a conformationally restricted substitute for the 7-carboxylic part of glutamate, a primary neurotransmitter [63]. Recent research has concentrated on creating and assessing various isoxazole derivatives for their anti-HIV, anti-thrombotic, and inhibitory activities against 5-HT. Leflunomide **106** serves a modifying anti-inflammatory orally administered agent employed in treating advanced rheumatoid arthritis. Another potent compound, XU065 **107**, has shown antiplatelet effects. Furthermore, ki-6425 **108** has been identified as an antagonist for lysophosphatidic acid (LPA) [64].



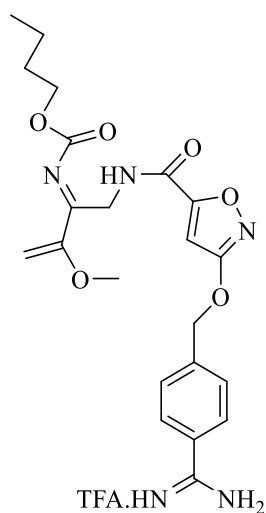
104



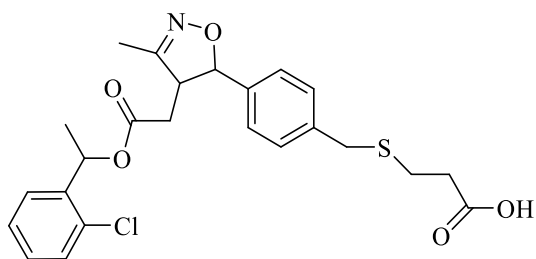
105



106



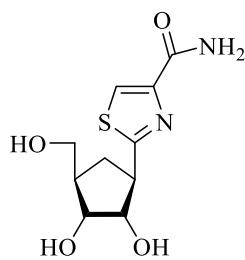
107



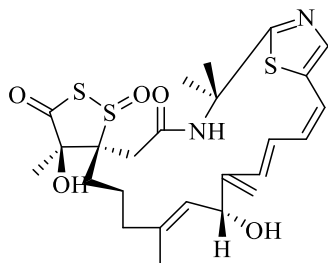
108

### 1.6.3 Thiazoles

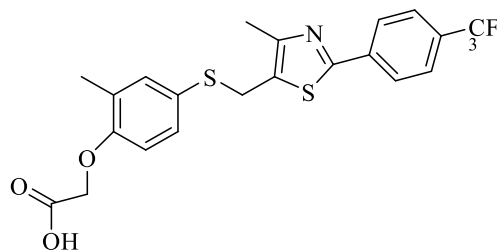
Thiazoles are a class of heterocycles consisting of a five-membered ring containing both nitrogen and sulfur atoms. They play a crucial role in natural processes, where the thiazole component is a part of thiamine, a coenzyme vital for the oxidative decarboxylation of  $\alpha$  keto acids. The tetrahydrothiazole structure is evident in the core structure of penicillin, one of the earliest and most significant broad-spectrum antibiotics [65]. Over the years, numerous thiazole derivatives have garnered considerable interest due to their diverse biological activities. Aminothiazoles, for example, have been identified as ligands for estrogen receptors and novel adenosine receptor antagonists. Several noteworthy thiazole-based drugs include Tiazofurin **109**, used for inhibiting the enzyme inosin5"-monophosphate (IMP) that plays a vital role in cell progression. Leinamycin **110** causes DNA damage with strong antimicrobial properties. GW501516 **111** has been identified as the most powerful and selective agonist for PPAR [66].



109



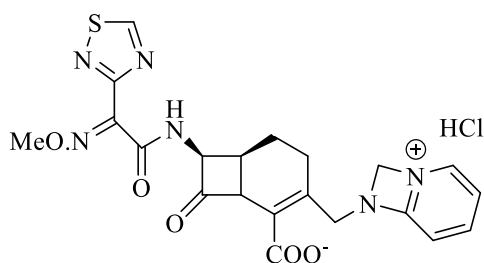
110



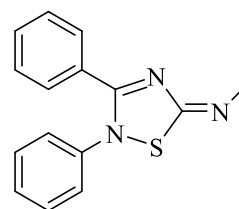
111

### 1.6.4 Thiadiazoles

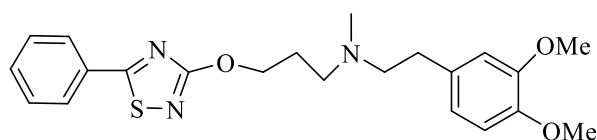
The 1,2,4-thiadiazole ring system has demonstrated fascinating therapeutic applications, with numerous synthetic compounds displaying a diverse array of biological effects. As an illustration, cefozopram possesses antibiotic attributes, whereas SCH-202676 **112** exhibits potential as an allosteric modulator for G-protein clubbed receptors. KC-12291 **113** acts as a cardioprotective agent. In recent years, the thiadiazolidinone derivative TDZD-8 **114** has been identified as the first non-ATP competitive inhibitor of glycogen synthase-3 $\beta$ , showcasing its potential in medicinal chemistry. Researchers have also synthesized various derivatives of thiadiazoles **115** to enhance the pharmacological characteristics of these primary compounds [67].



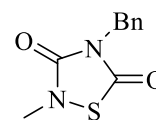
**112**



**113**



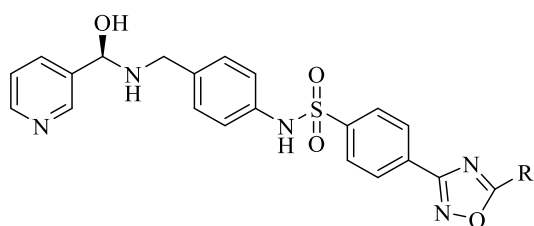
**114**



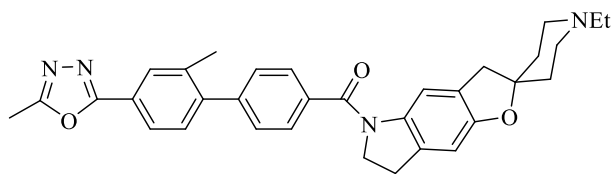
**115**

### 1.6.5 Oxadiazoles

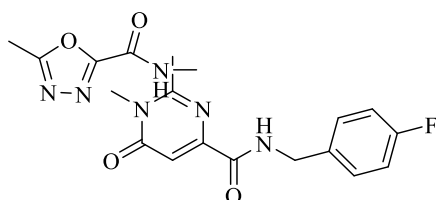
1, 2, 4-oxadiazoles are of substantial interest in the medicinal field as heterocyclic amide and ester isoesters. These have found widespread application in the development of diverse pharmacologically significant compounds, ranging from muscarinic agonists, tyrosine kinase inhibitors, histamine H-3 antagonists, and cytotoxic agents, to monoamine oxidase inhibitors. Recent investigations have revealed that oxadiazole substituted benzene sulphonamide **116** functions as an adrenergic receptor agonist, **117** demonstrates higher affinity, selectivity, and inverse agonist tendency at the human 5-HT<sub>1B</sub> receptor **118**, showcases robust anti-HIV properties, and **119** exhibits tryptase inhibitor activity [68].



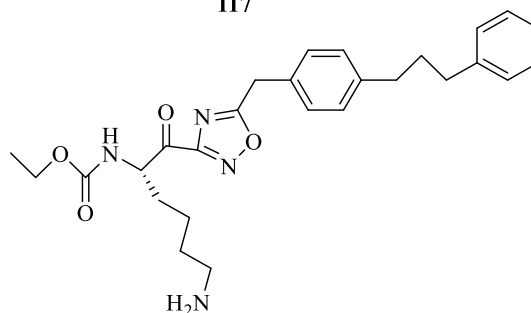
116



117



118

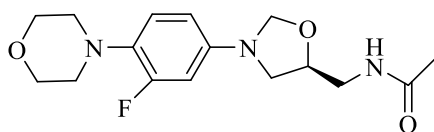


119

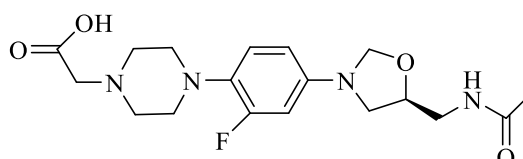
### 1.6.6 Oxazolidinones

Oxazolidinones represent a notable category of heterocyclic compounds extensively employed as intermediates in organic synthetic procedures. Chiral 2-oxazolidinones are known for their remarkable efficacy in the stereoselective creation of numerous natural products, antibiotics, and medically significant compounds [69]. The identification of oxazolidinones as a novel group of synthetic antibacterials has introduced promising avenues in antibiotic research, particularly given their effectiveness against drug-resistant Gram-positive organisms such as MRSA and VRE [70].

Linezolid **120**, the inaugural oxazolidinone to attain regulatory approval, has emerged as a crucial therapeutic choice for severe infections caused by Gram-positive bacteria [71]. It has demonstrated efficacy against multidrug-resistant pathogens, including MRSA and VRE. Additionally, other oxazolidinones such as the piperazine analog epezolid **121** have advanced into clinical trials [72].



120



121



## ***1.7 Conclusion***

Heterocyclic compounds stand as the largest and most diverse category within organic compounds. Among these, aromatic heterocyclic compounds serve as fundamental structural patterns present in numerous biologically active natural and synthetic compounds, as well as in agrochemicals and pharmaceuticals. These compounds also play a crucial role in the creation of dyes and significant polymeric materials. In the realm of organic synthesis, aromatic heterocyclic compounds are frequently employed as transitional stages. While various effective methods have been previously documented for constructing aromatic heterocyclic compounds and their derivatives, the pursuit of new techniques remains constant. Particularly, there is a continuous demand for innovative synthetic approaches towards heterocyclic compounds, aiming to achieve higher levels of molecular intricacy and enhanced compatibility with functional groups. These methods should ideally be resourceful, environmentally friendly, and capable of utilizing readily accessible raw materials under normal conditions. This pursuit stands as a significant focal point within the field of synthetic organic chemistry.

## *Chapter 2*

# *Synthesis and Importance of Benzothiazole and Benzothiazine nucleus*

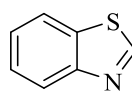
## 2.1 Benzothiazoles

### 2.1.1 Introduction

Thiazole **1** is a well-known group of heterocyclic compounds characterised by a planar, aromatic 5-membered ring that contains both sulphur and nitrogen atoms. Thiazoles exhibit greater aromaticity compared to their corresponding oxazoles due to the delocalization of  $\pi$ -electrons. These compounds can be found in various natural substances from both terrestrial and marine sources, and they possess diverse biological activities. Thiazoles serve as fundamental structures that have a natural affinity for different biological receptors, making them highly interesting for therapeutic purposes. When substituted, thiazoles exhibit distinct properties such as easy metabolism, improved solubility in lipids, and enhanced stability [73, 74]. Benzothiazole **2** is a class of sulfur and nitrogen possessing heterocyclic compounds that consist a thiazole ring bridged with benzene ring. This unique benzothiazole structure is commonly found in natural compounds and has various applications in phytohormones, antioxidants, electroluminescent devices, vulcanization processes, and enzyme inhibition [75]. Importantly, benzothiazole possesses a crucial role in pharmaceutical chemistry by providing a wide range of compounds with significant properties such as antibacterial [4], antiviral [5], antimicrobial [76], anticancer [77], antioxidant, anti-inflammatory [78], antituberculosis [79], antiparkinson's [80], muscle relaxants [81], and enzyme inhibition [82]. Because of its various applications in the bio-medicinal and industrial fields, the synthesis and modification of benzothiazole structures are highly important.



**1**



**2**

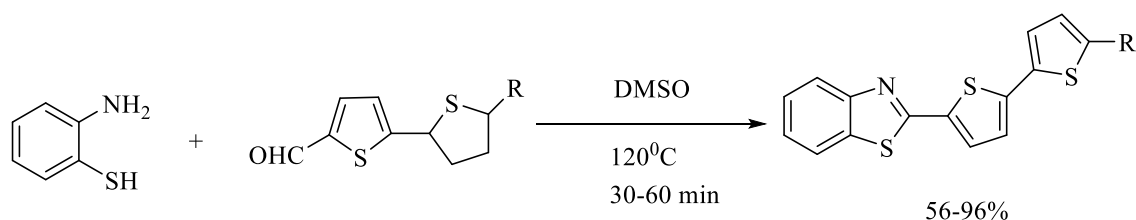
### 2.1.2 Synthetic routes for benzothiazoles

Various synthetic routes have been developed for synthesis of benzothiazole containing derivatives. The most commonly employed method involves the condensation of 2-aminobenzenethiol with cyano or carbonyl compounds [83]. Riadi and colleagues demonstrated that benzothiazoles can be synthesized by condensing 2-aminobenzenethiol with aromatic aldehydes [84]. Another approach reported in the literature is the condensation of benzo-thiols and nitriles, which enables the formation of 2-substituted benzothiazoles [85]. Furthermore, researchers have discovered that benzothiazoles can be prepared from aniline

through reactions with compounds such as carbon disulfide, piperidine, and isothiocyanate [86]. However, all these traditional methods suffer from drawbacks such as lesser productivity, restricted specificity, rigorous reaction conditions, or the use of hazardous reagents. In contrast, proponents of green chemistry promote the use of methods that eliminate or/and minimize the use and production of substances that can have a negative impact on the environment. Over the last ten years, several environmentally friendly approaches have been developed to produce benzothiazoles.

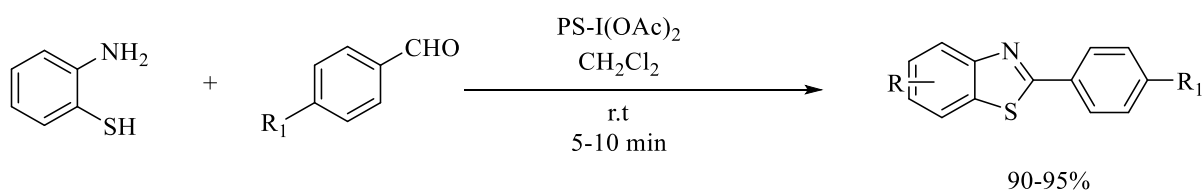
### 2.1.2.1 Synthesis of benzothiazole via condensation reaction

Batista and colleagues (**Scheme 2.1**) discovered a method to synthesize products containing 2-bisthiophene substituted benzothiazole by condensing 2-amino benzenethiol with 5- aldehyde bisthiophene compounds using DMSO subjected to refluxing for 1 hour [87]. The researchers then evaluated the fluorescence properties of these products and found that they exhibited robust fluorescence in the 450-600 nm range, along with higher quantum yield and significant stokes shift. The vigorous fluorescence exhibited by these compounds suggests that they could have potential applications as fluorescent markers.



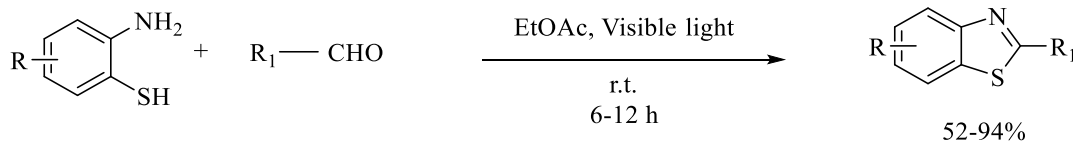
**Scheme 2.1.** Condensation between 2-amino thiophenol and 5-aldehyde bis thiophene compounds

Kumar et al. (**Scheme 2.2**) made an interesting discovery regarding the condensation of 2-amino benzenethiol and benzaldehyde compounds to prepare benzothiazole derivatives. They discovered that polystyrene based polymer catalysts, which were attached with Iodine acetate, effectively promoted this condensation reaction in dichloromethane [88]. The catalyst was prepared using a promising synthetic process and utilized in combinatorial synthetic protocol of benzimidazoles. This approach offered the advantages of solid- phase support and preserved diversity in the libraries, which was not the case in previous reports. Subsequent to the process, the catalyst underwent conversion to polymer-supported iodo benzene, that could be conveniently recovered through filtration. It was then transformed into poly[4-diacetoxyiodo] styrene (PDAIS) for subsequent reuse. Notably, the catalyst retained its activity even after multiple cycles of reuse, indicating its high durability.



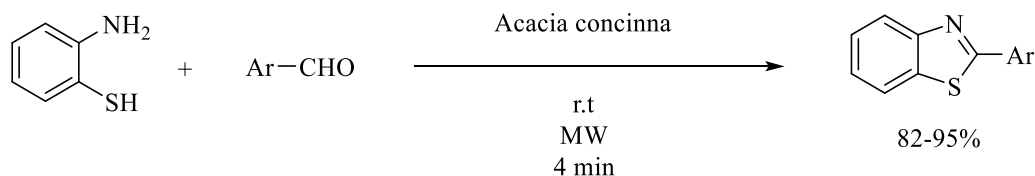
**Scheme 2.2.** Condensation of 2-amino thiophenol with benzaldehyde derivatives

Ye and colleagues (**Scheme 2.3**) have proposed a distinct method for the visible light driven synthetic protocol of benzothiazoles using 2-amino thiophenols and aldehydes. In this approach, the reaction mixture was subjected to irradiation using a 12W blue LED for a duration of 6 hours under normal atmospheric conditions. The researchers aimed to investigate the versatility of the reaction procedure for various substrates, and thus, a range of aldehyde containing compounds was examined [89]. The results demonstrated that aromatic, hetero-aromatic, and aliphatic aldehydes could all undergo conversion successfully. This discovery provides an efficient and convenient synthetic route to benzothiazoles, without the need for transition-metal catalysts or additional additives.



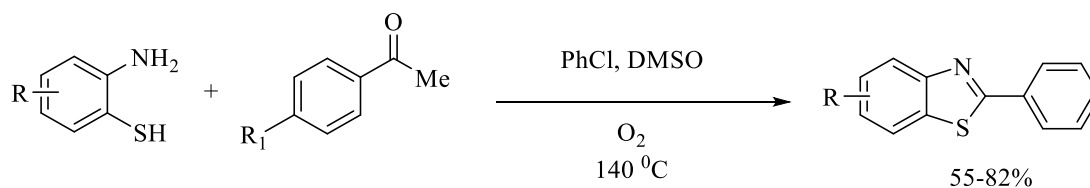
**Scheme 2.3.** Visible light mediated condensation of 2-amino thiophenol with aldehydes

Bhat and colleagues (**Scheme 2.4**) investigated a rapid method for synthesizing 2-arylbenzoxa/(thia)zoles by condensing 2-amino thiophenol with various aryl aldehydes using *acacia concinna* as a biocatalyst exposed to microwave irradiation exposure [90]. The researchers compared this microwave irradiation technique with the conventional method and observed that it offered a significantly lesser reaction time while achieving increased yield of the desired derivatives. Additionally, this reaction approach demonstrated eco-friendliness as it eliminated the need for solvents.



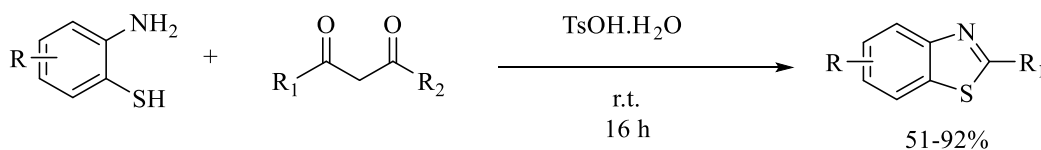
**Scheme 2.4.** Microwave irradiation driven condensation between aldehydes and 2-amino thiophenol

Deng and colleagues (**Scheme 2.5**) have presented an effective method for synthesizing 2-arylbenzothiazoles from aryl-ketones and 2-amino thiophenol, using molecular Oxygen as an oxidising agent, without the need for metal catalysts or iodine [91]. The authors conducted a comparative study using various solvents, including DMF, DMSO, toluene/ DMSO, chlorobenzene/ DMSO etc. among others. Among these solvents, chlorobenzene/DMSO was found to be the most favourable as far yield is concerned. Additionally, this procedure allowed for the synthesis of benzothiazoles under iodine and metal free conditions, demonstrating its versatility with various functional groups. Notably, substrates with methyl, meth-oxy, fluorine, chlorine, nitro etc. substituents were successfully converted into the corresponding products.



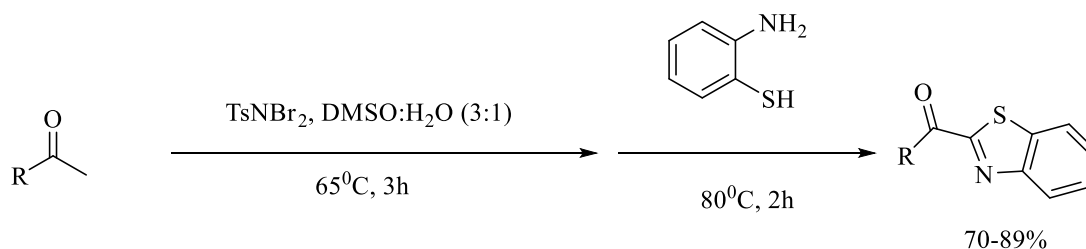
**Scheme 2.5.** Condensation between 2-amino thiophenol and aryl ketones

Bao and collaborators (**Scheme 2.6**) developed an effective procedure for synthesizing of 2-substituted benzothiazoles through the condensation of amino benzenethiol with  $\beta$ -diketone. The catalyst employed was toluene-sulfonic acid (TsOH), and the reaction was conducted under conditions devoid of oxidants, metals, and radiation [92]. The process resulted in the formation of 2-substituted benzenes with satisfactory yields. In the quest for the optimal catalytic system, various acids, such as PhCOOH, CF<sub>3</sub>COOH) and CH<sub>3</sub>COOH), were tested. TsOH•H<sub>2</sub>O emerged as the preferred catalyst for subsequent solvent screening due to its favorable yield outcomes.



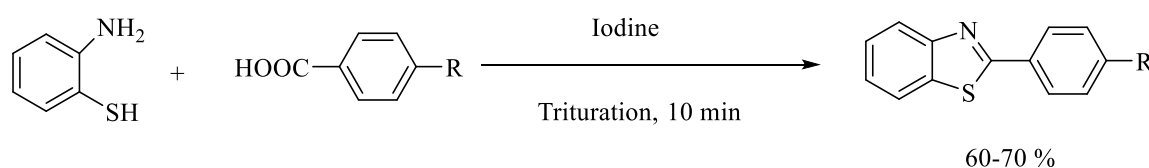
**Scheme 2.6.** Condensation of 2-aminothiophenol and diketones

Loukrakpam and his team have developed a highly effective method for synthesizing derivatives of benzothiazoles from methyl ketones and 2-amino benzenethiol without the need for any metal catalysts. The process involves a one-pot strategy (**Scheme 2.7**). In this mechanism, the aromatic ketones first reacted with TsNBr<sub>2</sub> at 65°C in DMSO for a duration of 3 hours [93]. The resulting crude reaction mixture is then subjected to a sequence of condensation, Michael addition followed with oxidative dehydrogenation with 2-aminobenzenethiol to yield the expected products.



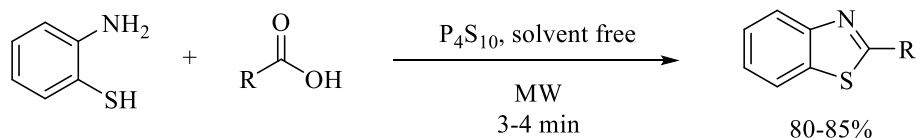
**Scheme 2.7.** Condensation of 2-aminothiophenol and aryl methyl ketones

In a study conducted by Gupta et al., they described a one-pot consolidated, devoid of solvent protocol utilizing molecular iodine. The reaction involved the combination of 2-aminothiophenol with benzoic acid derivatives to produce benzothiazole derivatives with excellent yields in just 10 minutes (**Scheme 2.8**). In comparison to alternative methods such as microwave synthesis catalyzed by polyphosphoric acid and [pmim]-Br, this new approach offers significant cost reduction as it eliminates the need for additional chemicals and reagents during the transformation [94]. The methodology stands out for its economic efficiency, time-saving nature, and absence of solvents.



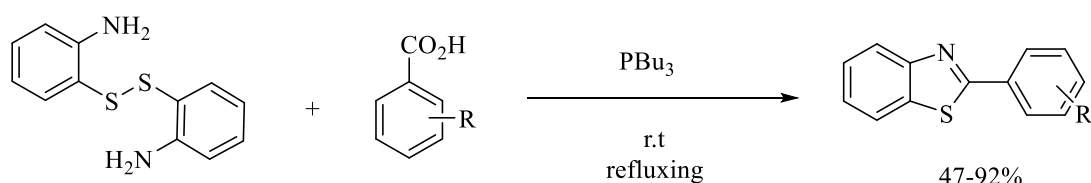
**Scheme 2.8.** Condensation between 2- amino thiophenol and various benzoic acid compounds

Reuf and colleagues have presented a procedure for synthesizing various substituted benzothiazoles through the condensation of *o*-aminothiophenol with different fatty acids. The reaction was carried out under microwave irradiation for a duration of 3 to 4 minutes (**Scheme 2.9**). By employing P<sub>4</sub>S<sub>10</sub> as a catalyst, the reaction yielded the desired products with a high conversion rate [95]. This protocol offers an efficient, rapid, and solvent-free approach for the synthesis of substituted benzothiazoles.



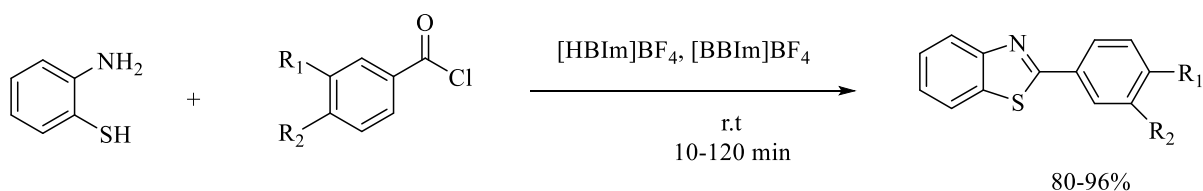
**Scheme 2.9.** Condensation of 2-aminothiophenol with fatty acids under microwave irradiation

Coelho and colleagues have devised an effective general procedure for the synthesizing benzothiazoles. This method involves the condensation reaction between thiophenol disulfides and carboxylic acids, with the assistance of tributyl phosphine, at room temperature (**Scheme 2.10**). The researchers investigated broad applicability of the approach, by employing different 2-amino thiophenol disulfides and various carboxylic acids, including electron withdrawing or donating substituents. The desired benzothiazoles were obtained with average to good yields [96]. The significant benefits of this approach include ambient conditions and the use of non-hazardous reagents.



**Scheme 2.10.** Condensation between carboxylic acids and 2-amino thiophenol

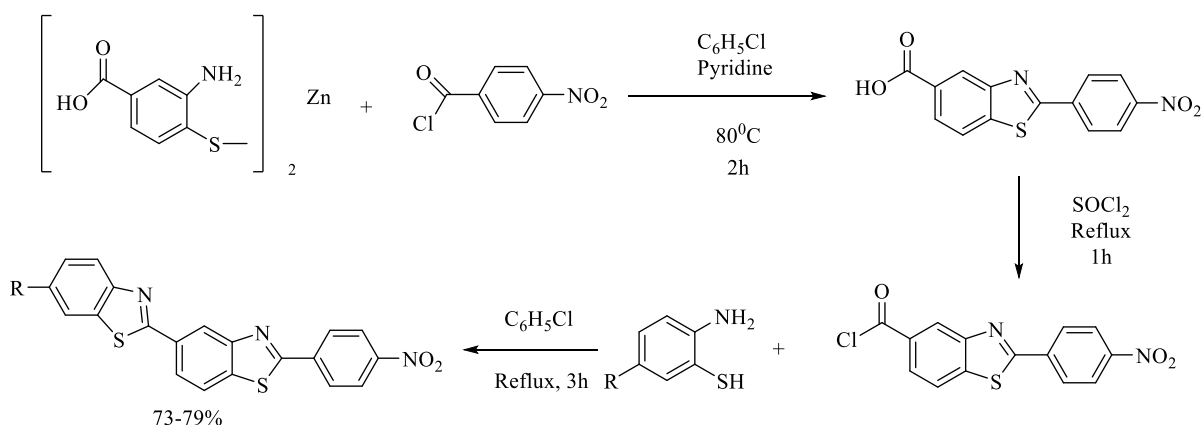
Nadaf and colleagues proposed a highly effective catalyst system consisting of two ionic liquids: 1-butylimidazole tetrafluoro borate and 1,3-dibutylimidazole tetrafluoro borate [97]. This catalyst system enables the formation of substituted benzothiazoles involving the condensation reaction of 2-amino benzenethiol with aromatic acid chloride compounds at normal temperature (**Scheme 2.11**).



**Scheme 2.11.** Condensation between various acid chlorides and 2-aminothiophenol

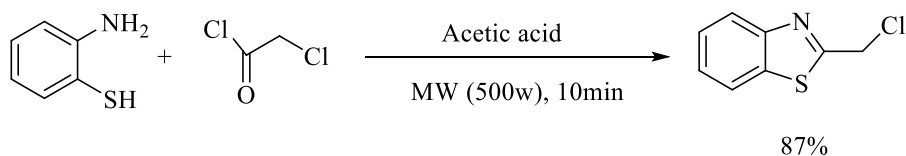


Wu et al. conducted an analysis in which they synthesized novel derivatives of benzothiazole. In their research, they started by suspending the Zn salt of amino mercaptobenzoic acid in pyridine along with  $C_7H_4ClNO_3$ , and the reaction mixture underwent heating at  $80\text{ }^\circ\text{C}$  for one hour [98]. This process resulted in the conversion of the suspension into 4-nitrophenyl-benzothiazole-6-carbonyl chloride through reaction with  $SOCl_2$  (**Scheme 2.12**). Additionally, di-benzothiazole containing compounds were synthesized by introducing substituted aminothiophenols into the system followed by heating and reflux conditions for three hours.



**Scheme 2.12.** Condensation of 2-amino-3-mercaptobenzoic acid with p-nitro benzoyl chloride

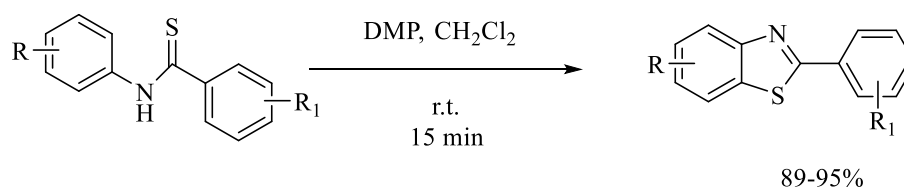
Luo et al. discovered that 2-chloro methylbenzothiazole can be prepared by condensing 2-amino thiophenols with chloro acetyl chloride in  $CH_3COOH$ , utilizing microwave irradiation for a short period of 10 minutes (**Scheme 2.13**). The microwave-assisted method demonstrated superior efficiency and environmental friendliness compared to traditional approaches, as it required less time and yielded high product quantities [99].



**Scheme 2.13.** Condensation of 2-aminothiophenol with chloro acetylchloride

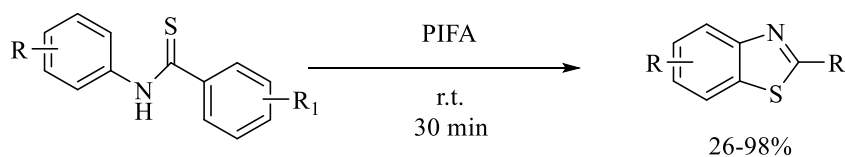
### 2.1.2.2 Synthesis of benzothiazole via cyclization

Bose et al. have created a time-efficient and environmentally friendly method for synthesizing benzothiazoles. This procedure involves the cyclization of sulfamide substrates using Dess-Martin periodinane as a catalyst and DCM as solvent for the reaction [100]. The reaction occurs at ambient temperature and takes only 10-15 minutes to complete (**Scheme 2.14**).



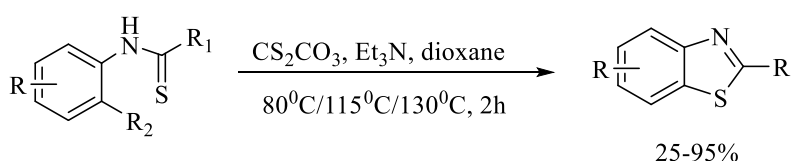
**Scheme 2.14.** Cyclization of sulfamide substrates to benzothiazole derivatives

Downer et al. have explored a universal approach for the intra-molecular cyclization of thiobenzamides into benzothiazoles under mild conditions. This method involves the utilization of aryl cations as reaction intermediates. The researchers employed PIFA in trifluoroethanol or CAN in aqueous acetonitrile to facilitate the cyclization process (**Scheme 2.15**). The reaction was conducted at room temperature and reached completion within 30 minutes, yielding moderate amounts of the desired benzothiazole products [101].



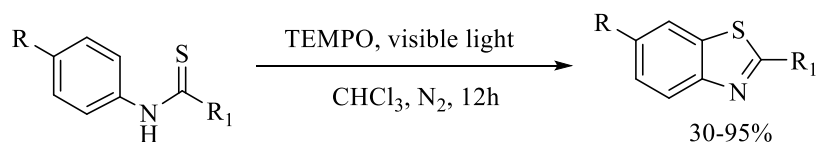
**Scheme 2.15.** Cyclization of benzamides at room temperature

Feng et al. examined the base-promoted preparation of 2-substituted (N, C, O) benzothiazoles from substituted thio-amides/carbamothioates/thioureas via intramolecular C-S bond coupling cyclization in dioxane in the absence of transition metal. Under these conditions, a wide range of functional groups was allowed and desired products were achieved in high yields. This approach has some benefits of transition metal-free, moderate reaction conditions, shorter reaction time, and broad scope of applications [102]. It offers several advantages, including being transition-metal-free, utilizing gentle reaction conditions, having broad range of applications, and shorter reaction times (**Scheme 2.16**).



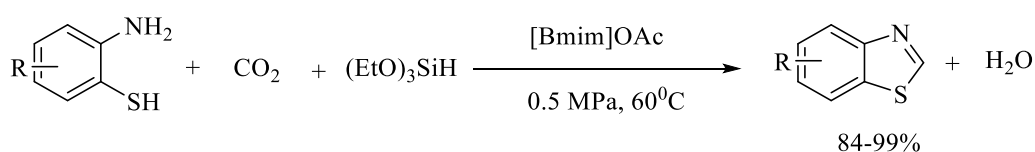
**Scheme 2.16.** Cyclization of substituted thioformanildes

Xu et al. accomplished a simple methodology for intramolecular C-S bond formation of aromatic substrates to produce benzothiazole derivatives in good yields via the cyclization of thioamide derivatives **26** driven by visible-light, in the presence of TEMPO (**Scheme 2.17**). Importantly, this photochemical cyclization does not necessitate the use of an additional photo-redox catalyst, transition-metal catalyst, or base [103].



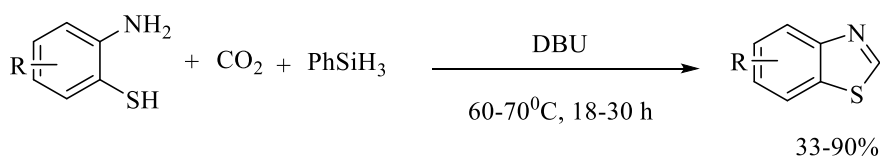
**Scheme 2.17.** Cyclization of thioamide derivatives

Another method involves cyclization of 2-amino benzenethiols with hydrosilane and CO<sub>2</sub>, leading to the synthesis of various benzothiazoles. Importantly, we have developed a mild reaction condition using an ionic liquid as catalyst, resulting in good yield of the desired products (**Scheme 2.18**). Furthermore, we have explored different reaction conditions, including varying catalysts, reaction temperature, and pressure. Among these, the most favorable outcomes were achieved when utilizing ([Bmim][OAc]) as the catalyst at 60 °C and 0.5 Mpa. Additionally, we tested the reusability of [Bmim] [OAc] and found that the yield of benzothiazole remained almost constant even after the ionic liquid was re-used five times. Notably, this pioneering method represents the first procedure for synthesizing benzothiazoles utilising CO<sub>2</sub> as raw material, without the need for metals and under mild conditions.



**Scheme 2.18.** Cyclization of 2-aminobenzenethiols with hydrosilane and CO<sub>2</sub> at 0.5 Mpa

Chun et al. have described a method for synthesizing benzothiazoles from 2-aminobenzenethiols and CO<sub>2</sub> using 1,8-diazabicyclo [5.4.0]undec-7-ene (DBU) as the catalyst. The reaction was conducted at 1 atmosphere of CO<sub>2</sub> and temperatures between 60-70 °C (**Scheme 2.19**). This approach exhibited a wide substrate scope and demonstrated tolerance towards various functional groups [104]. Additionally, the precatalyst salt could be recovered and then re-used multiple times without any decline in activity.

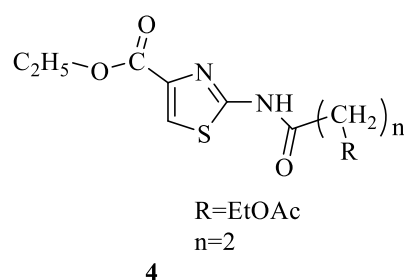
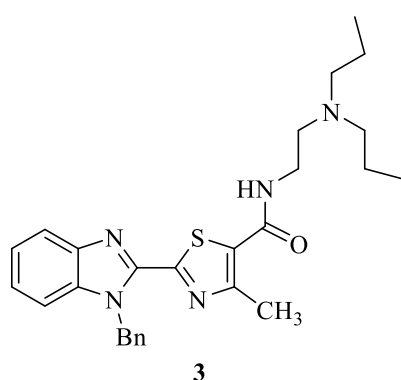


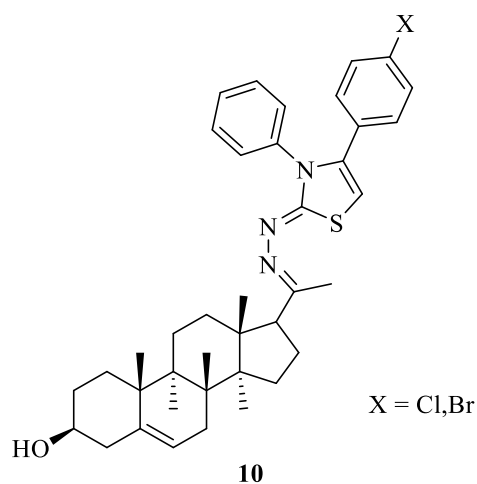
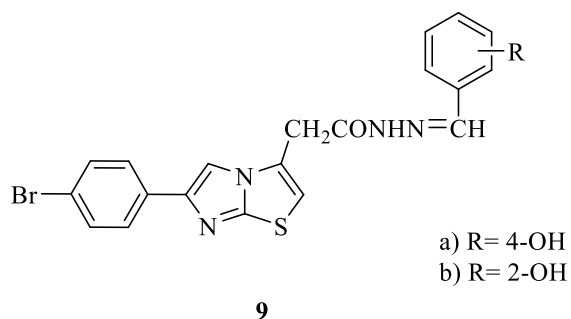
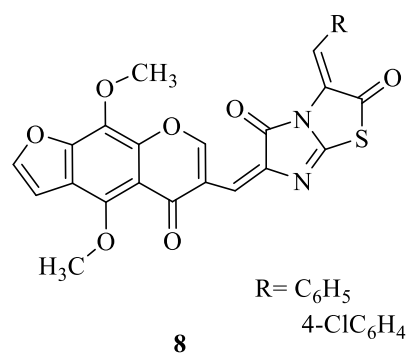
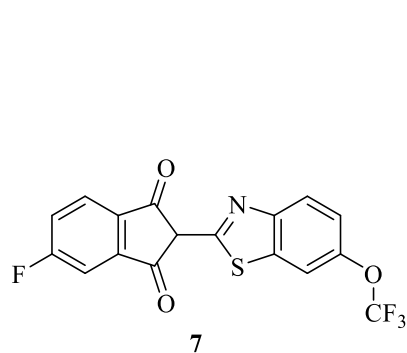
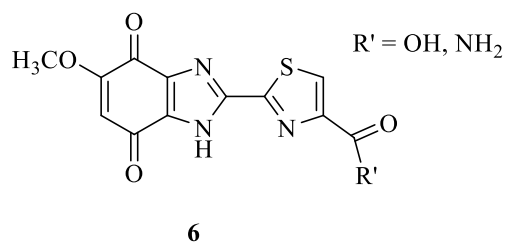
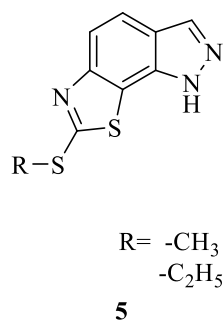
**Scheme 2.19.** Cyclization of 2- aminobenzenethios and CO<sub>2</sub> at 0.1 Mpa

### 2.1.3 Pharmacological significance of thiazole derivatives

#### 2.1.3.1 Anti-cancer and cytotoxic effects

Thiazolyl derivatives **3** were evaluated for their antitumor activity against hepatocarcinoma cells, and most of them exhibited significant effectiveness, with a few displaying exceptional potency. Carboxylate derivative of amino-thiazole **4** showed remarkable anticancer activity. Alkyl-thiazole and alkyl-amine indazole derivatives **5** were synthesized through region-selective cyclization and demonstrated moderate activity against the A549 cell line. Thiazole-containing benzimidazoles **6** exhibited comparable antiproliferative activity to the standard drug doxorubicin. Benzothiazole-phthalimide heterocycles **7** showed substantial cytotoxicity against hepatoma, chronic myelogenous leukemia, and Burkitt lymphoma cell lines. Furochromenyl substituted thiazole derivatives **8** exhibited prominent anti-tumor activity against liver and breast cancer cells. Imidazole-containing thiazole compounds **9** displayed cytotoxic activity, particularly against prostate cancer cells, with hydroxyl group substitution enhancing efficacy. Cytotoxicity screening of pyridine, thiophene, and thiazole derivatives **10** revealed that the thiazole-containing compounds exhibited the highest inhibitory activity against breast adenocarcinoma cells [105, 106].



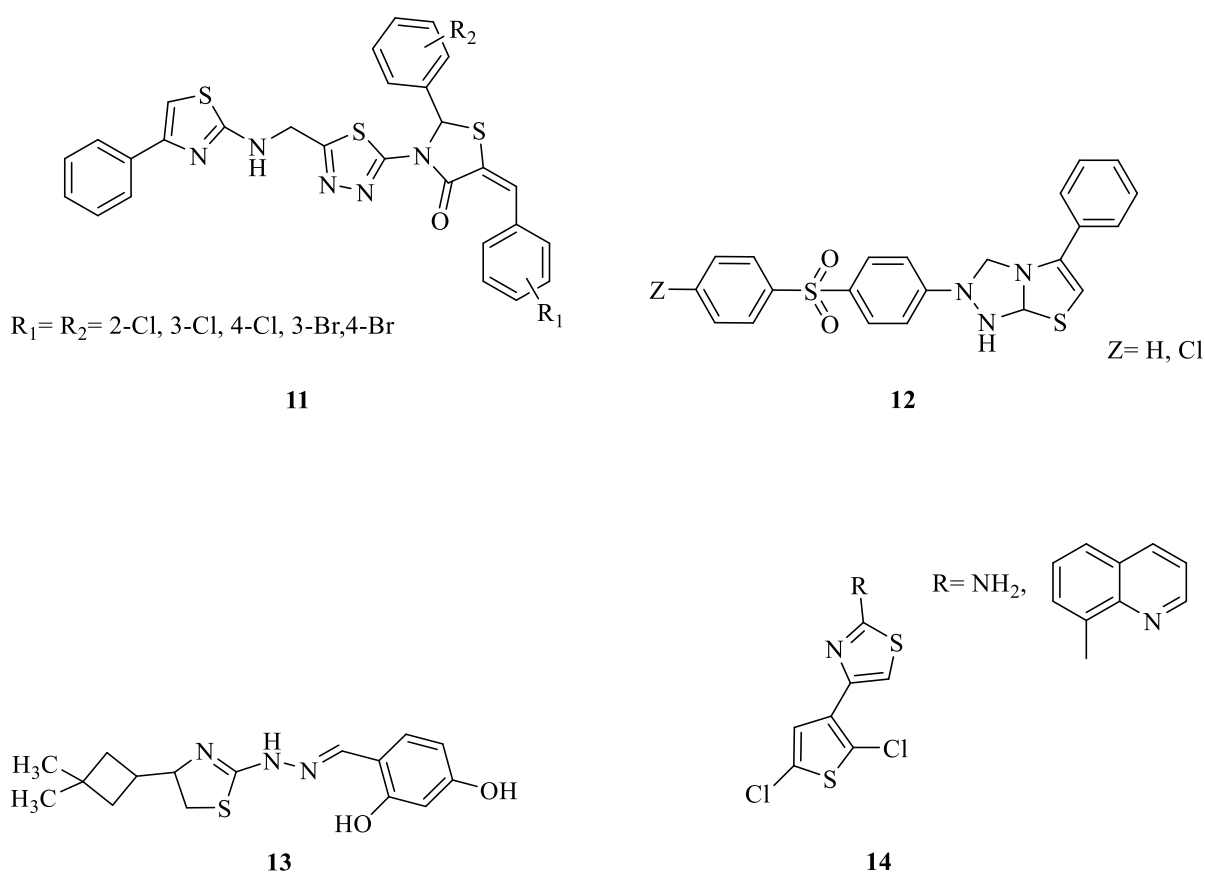


### 2.1.3.2 Anti-microbial activity

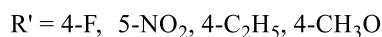
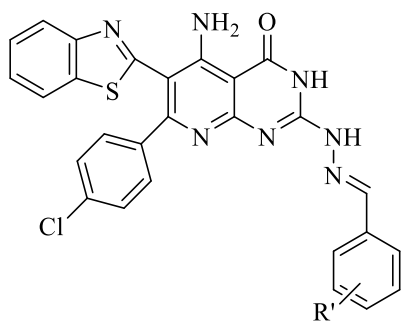
Small heterocyclic compounds with thiazole as a core structure have been extensively investigated for their effectiveness against various microbes. Thiazolidine derivative **11** was studied for its antimicrobial activity against *B. subtilis*, *E. coli*, and *C. albicans*, and it demonstrated promising results. Additionally, a series of thiazole compounds containing a sulfone group **12** were tested for their antibacterial activity against *S. aureus*, *C. freundii*, and others, and they exhibited excellent antibacterial properties [107]. Currently, researchers are

focusing on developing hybrid molecules that combine thiazole with other heterocyclic moieties such as triazole, thiophene, pyridine, indole, and pyrazine. These hybrid compounds have shown significant antimicrobial properties upon biological evaluation. Schiff's bases containing thiazole derivatives **13** have also proven to be effective against microbes like *B. subtilis* and *C. tropicalis*, with an MIC value of 16 $\mu$ g/mol [108].

Furthermore, novel thiazole derivatives **14** formed by the reaction of 2,5-dichloro-3-thienyl ethanone with thiourea were evaluated for their antimicrobial activity. Molecular docking analysis revealed that these compounds exhibited potent efficacy against a broad spectrum of microbes [109].

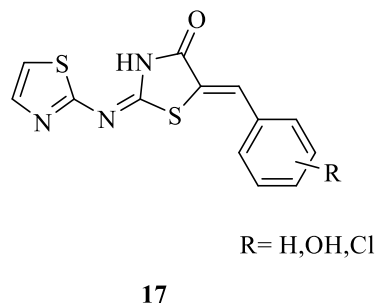
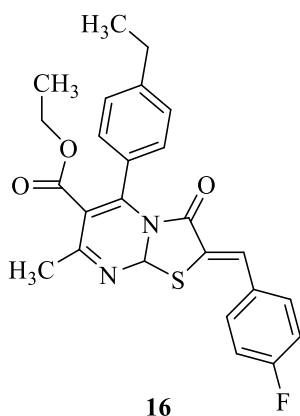


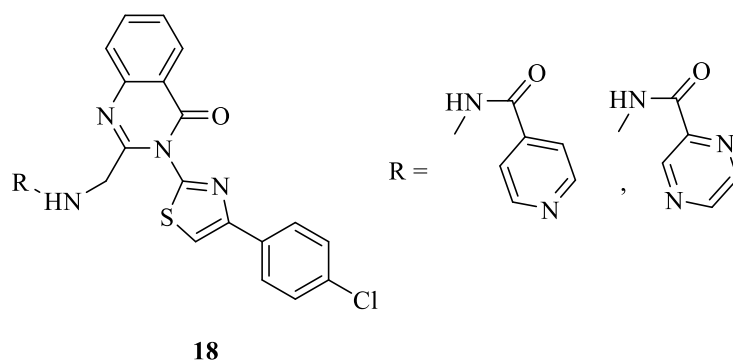
Thiazole pyrimidine derivatives were subjected to evaluation against various microbes, including *Mucor* species. Among these derivatives, the methoxy benzothiazole derivative **15** demonstrated remarkable antimicrobial activity. This finding highlights the potential of thiazoles as promising candidates for the treatment of Mucormycosis, commonly known as Black Fungus, which has led to a surge in research interest in this area [110].



15

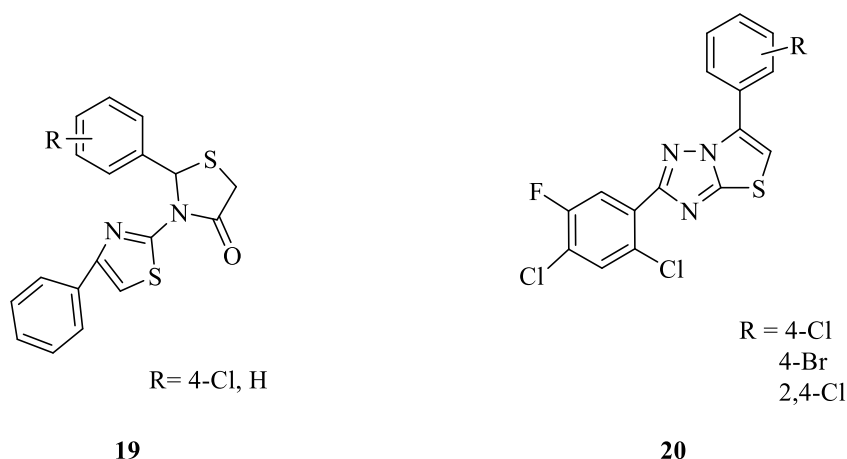
Novel derivatives produced via one-pot synthesis using methyl thiophenyl and dihydropyrimidine as precursors were screened for antifungal and antibacterial activities against *E. coli*, *A. niger*, *S. aureus*, *C. albicans*, etc. Excellent activities were exhibited by the fluoro derivatives. Vicini et al. reported the synthesis of thiazoloimino arylidene derivative **16** via cyclization between substituted aldehydes and 2-amino thiazole [111]. The products were screened for various Gram-positive and Gram-negative bacteria as well as fungi. Miconazole and Ampicillin were used as standards. All synthesized compounds have strong antibacterial action against gram-(+) bacteria. Malipeddi et al. synthesized thiazolidinone **17** through cyclocondensation of thiadiazole with thioglycolic acid [112]. It showed better in vitro activity than the already commercialized drugs. A fused heterosystem containing thiazole and quinazoline moiety **18** was evaluated for its anti-tubercular properties. Streptomycin was used as a baseline. All synthesized compounds can be considered prominent entities for anti-tubercular activity [113].





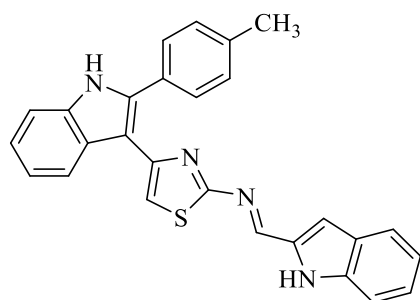
### 2.3.1.3 Anti-inflammatory activity

Derivatives obtained via the reaction between thiazole and various substituted aldehydes were evaluated for anti-inflammatory activities using pentazocine as a standard. Among the synthesized compounds, the phenyl derivative of 1,3-thiazolidinone **19** showed remarkable anti-inflammatory activity. Fluorine containing triazole **20** derivative showed good analgesic and anti-inflammatory activity that was further enhanced by the presence of electron-withdrawing groups [114].

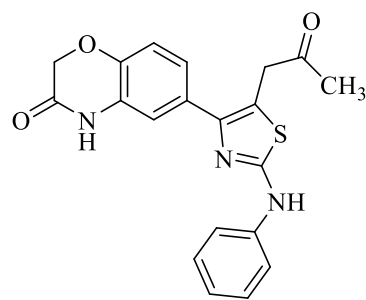


A group of formazyliindoles **21** was assessed for their anti-inflammatory properties using a carrageenan-induced edema model in albino rats. The results demonstrated a substantial inhibition of edema and a lower likelihood of causing ulceration, indicating promising anti-inflammatory efficacy [115]. In a separate study, specific compounds **22**, **23** were synthesized through Friedel Crafts acylation between benzoxazine derivatives and substituted thiazoles. These compounds were then investigated for their potential as inhibitors of COX-2. The inhibitory activity was assessed using a chromogenic assay, and one compound from the series **24** showed potent COX-2 inhibitory activity [116, 117].

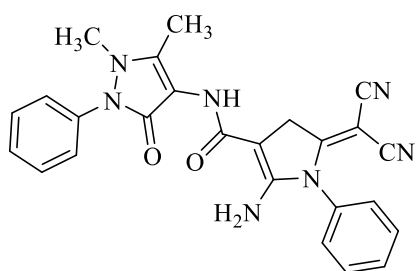




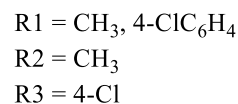
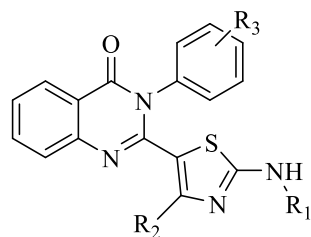
21



22



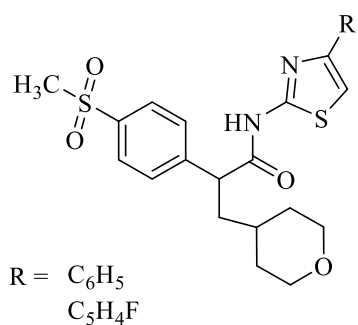
23



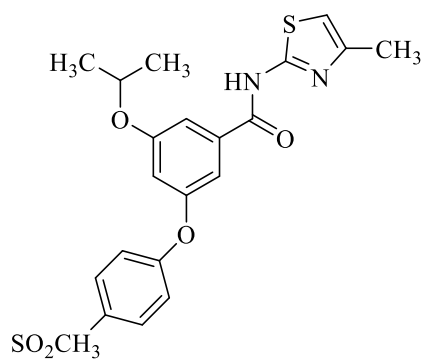
24

#### 2.3.1.4 Anti-diabetic activity

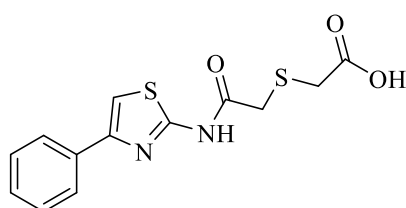
Methylsulfonyl derivatives of thiazole **25** have proved to be potent glucokinase activators and promising candidates for treating diabetes. Iino et al. synthesized aminobenzamide derivatives incorporating thiazole **26** as a substituent, which acts as a glucokinase activator. The structure-activity relationship showed that incorporation of a phenoxy or alkoxy group increases the oral bioavailability of the compound. Recent studies have demonstrated the role of lipid carriers on metabolic disorders related to diabetes (Type 2) as well as atherosclerosis. In this regard, thiazole and indole-based derivative, after being synthesized, were screened for their inhibition activity against TNF- $\alpha$ . A series of novel substituted thiazoles were tested for their antihyperglycemic activity against several enzymes, including  $\alpha$ -amylase, in which (Indol-3-yl) pyrazole **27**, **28** derivative of thiazole showed maximum activity [118, 119].



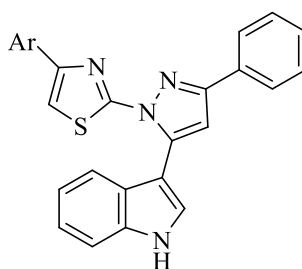
25



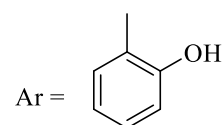
26



27



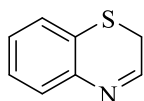
28



## 2.2 Benzothiazines

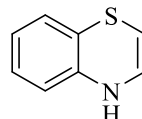
### 2.2.1 Introduction

The compound 1,4-benzothiazine, which contains sulfur and nitrogen atoms in its structure, has garnered continuous attention and holds significant importance in the creation of novel drug candidates. This compound serves as a crucial foundation for constructing new drugs [120]. The term "1,4-benzothiazine" is used for both variations of the molecule: the 2H-isomer **29** and the 4H-isomer **30**. The 4H-1,4-benzothiazine (4H-1,4-B) analogs have been extensively investigated over many years. A highly valuable characteristic of the 1,4-benzothiazine structure that contributes to its versatile range of activities that exist because of a fold along the N-S axis.



2H-1,4-benzothiazine

29



4H-1,4-benzothiazine

30

### 2.2.2 Synthesis

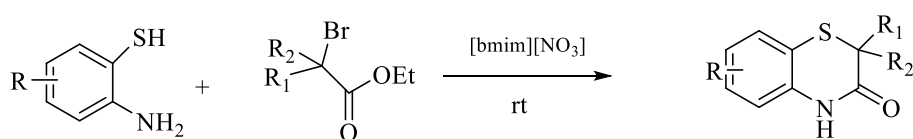
To make the reactions more convenient and to improve the feasibility of the process, various synthetic methods have been employed in different studies [121]. These methods primarily encompass two approaches:

(a) The first approach involves the cyclization of the ring, achieved by reacting 2-aminothiophenol and its derivatives with a range of compounds such as haloacyl systems,  $\alpha$ -haloketones,  $\alpha$ -haloacids,  $\alpha$ -haloacyl chlorides,  $\alpha$ -haloesters,  $\alpha,\beta$ -unsaturated acids and esters, maleic anhydride,  $\alpha$ -cyano  $\alpha$ -alkoxy carbonyl epoxides, and alkynes.

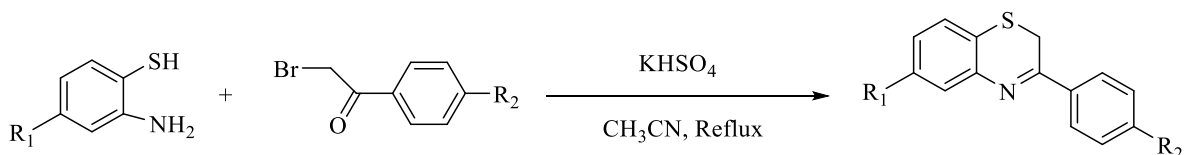
(b) The second approach entails the expansion of the benzothiazoline ring. This involves strategies where the ring structure is modified and expanded.

### 2.2.2.1 From Condensation with $\alpha$ - halo Ketones, Esters and Acids

In alignment with the use of  $\alpha$ -haloesters, Sharifi et al. introduced an environmentally friendly method for the synthesis of benzothiazin-3-ones at room temperature, devoid of any base or additives [122]. This synthesis method entails the reaction of 2- aminothiophenols with 2-bromoalkanoates within an ionic liquid environment, specifically [bmim] [NO<sub>3</sub>]. The outcome of this procedure is the production of benzothiazin-3-ones with remarkable yield rates (**Scheme 2.20**). In a study conducted by Baghernejad and colleagues [123], a one-pot procedure was executed for the synthesis of 3-aryl-2H-benzo[1,4]thiazines (**Scheme 2.21**). This synthesis involved the condensation of 2- amino benzenethiols and 2-bromo-1-phenyl ethanones in acetonitrile, utilizing a catalytic quantity of KHSO<sub>4</sub>. The results of this reaction yielded the desired products, 3-aryl-2H-benzo[1,4]thiazines, in satisfactory yields.



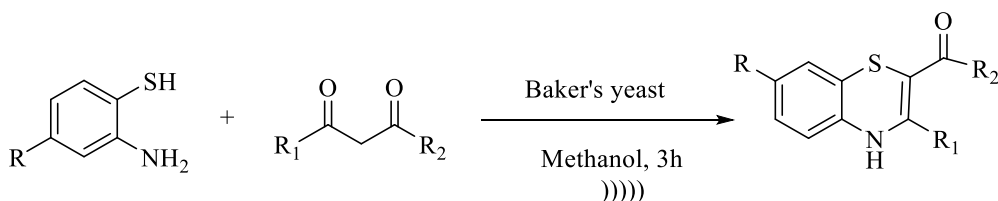
**Scheme 2.20.** Synthesis of 1,4-benzothiazines through condensation with 2-bromoalkanoates.



**Scheme 2.21.** Synthesis of 1,4-benzothiazines through the condensation process involving 2-bromo-1-phenyl ethanones.

### 2.2.2.2 Through Oxidative Cyclization Involving 1,3-dicarbonyl Compounds

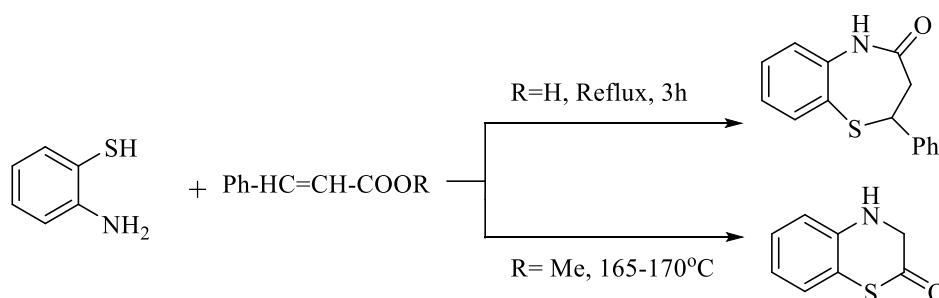
Taking into account the limitations of the conventional approach for synthesizing 1,4-benzothiazines and the aim to examine the potential of biocatalyst in the cyclocondensation process, Pratap et al. introduced an effective pathway utilizing an economical bio-catalyst, namely baker's yeast (**Scheme 2.22**). In this chemical transformation, a streamlined one-pot synthesis strategy was utilized, facilitating the merging of 2-aminothiophenols and 1,3-dicarbonyls [124]. Additionally, to accelerate the reaction rate of the condensation process, an alternative technique involving ultrasonication could be implemented within a similar framework.



**Scheme 2.22.** Efficient synthesis of 1,4-Bs from condensation with 1,3- dicarbonyls

### 2.2.2.3 From Condensation with $\alpha,\beta$ -unsaturated Acetylinic Acids

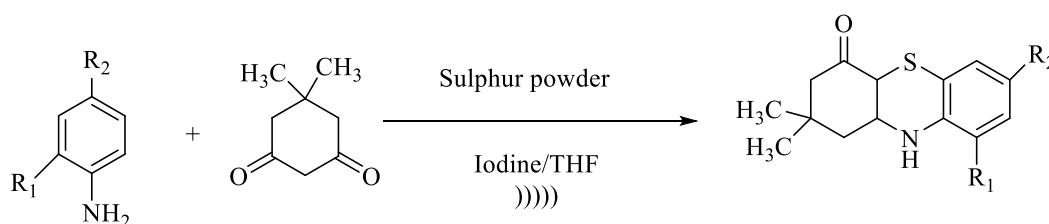
In a study conducted by Heravi et al., a method for producing 1,4- benzothiazines was detailed. This approach is characterized by its user-friendly, swift, and green procedure, resulting in a substantial yield. The synthesis entails combining dialkyl acetylenedicarboxylate with 2-aminothiophenol through microwave irradiation within a solvent-free environment (**Scheme 2.23**) [125].



**Scheme 2.23.** Synthesis of 1,4-Bs from condensation with unsaturated acids

#### 2.2.2.4 From substituted amines

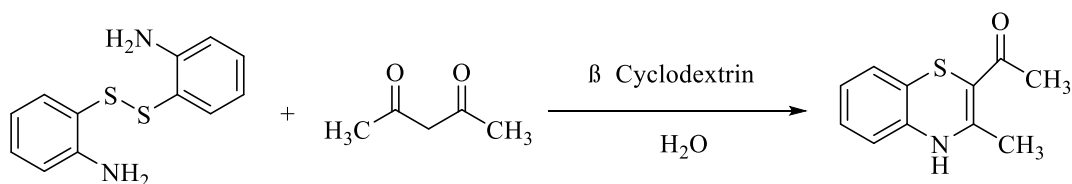
Another method that demonstrated the synthesis of 1,4-benzothiazines with remarkable efficiency, achieving impressive yields through a straightforward and expeditious ultrasonication technique. In order to generate the desired products, equivalent quantities of substituted amines and dimidone are combined with sulfur powder and iodine within tetrahydrofuran, and the resulting mixture is then exposed to ultrasonication (**Scheme 2.24**) [126].



**Scheme 2.24.** Synthesis of 1,4-B's from substituted amines

#### 2.2.2.5 From 2,2'-dithiodianiline

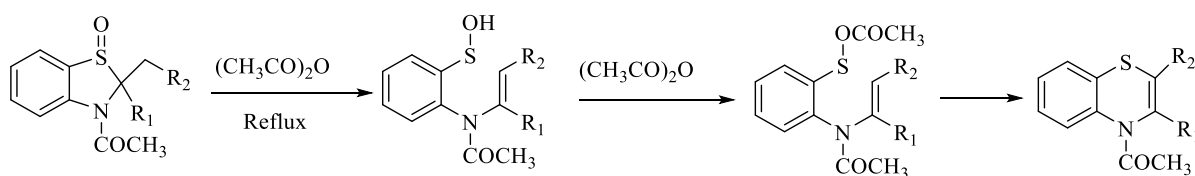
Londhe et al. introduced an ingenious and environmentally conscious one-step cyclization procedure, yielding 2,3-disubstituted 1,4-benzothiazines in impressive quantities. This method involves the cyclo-condensation of dicarbonyl compounds with 2-(2-(2-aminophenyl)disulfanyl)benzenamines, employing a supra-molecular catalyst called  $\beta$ -Cyclodextrin ( $\beta$ -CD), all within a water-based system with a neutral pH (**Scheme 2.25**). Additionally, the utilization of  $\beta$ -CD in this process has been validated as it enhances the speed of the cyclocondensation reaction. This biomimetic catalytic approach stands out for its simplicity, efficiency, rapidity, eco-friendliness, and cost-effectiveness [127].



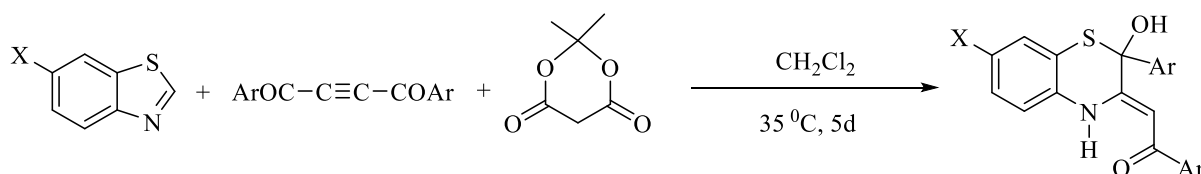
**Scheme 2.25.** Synthesis of 1,4-B's from 2,2'-dithiodianiline

### 2.2.2.6 From ring expansion of Benzothiazoline

Hori et al. introduced a method involving the ring expansion of 3-acetylbenzothiazolin-1-oxide to form 4-acetylbenzothiazines. This conversion was achieved by refluxing the compound in the presence of acetic anhydride (**Scheme 2.26**) [128]. On the other hand, Adib et al. developed a novel and well-structured approach for the ring expansion of benzothiazoles into 1,4-benzothiazines. In this process, benzothiazoles were combined with diacylacetylenes to produce reactive 1:1 zwitterionic intermediates. These intermediates were then subjected to Meldrum's acid under normal conditions, leading to the formation of 2-[2-hydroxy-1,4-benzothiazin-3(4H)-yliden] aryl ethanones in good yields (**Scheme 2.27**) [129].



**Scheme 2.26.** Synthesis of 1,4-Bs from ring expansion of benzothiazolines



**Scheme 2.27.** Synthesis of 1,4-Bs from ring expansion of benzothiazolines using Meldrum's acid

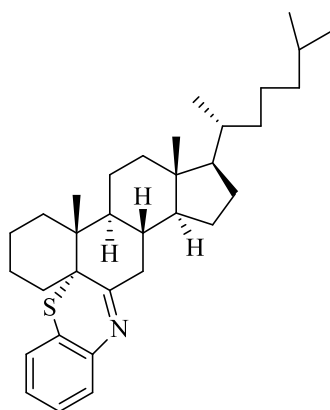
### 2.2.3 Pharmacological significance of benzothiazine derivatives

Heterocyclic compounds originating from the 1,4-benzothiazine (1,4-B) ring structure demonstrates a pivotal role in the domain of biomedical sciences because of their immense therapeutic properties. The relatively untapped reservoir of heterocyclic compounds derived from the 1,4-B ring offers a diverse range of pharmacological benefits. These compounds exhibit a spectrum of medical activities, encompassing antitumor, antipsychotic, and cardiovascular effects. Simultaneously, they hold significant importance in combatting pathogens, displaying antibacterial, antifungal, antiviral, antitubercular, and antiprotozoal activities.

#### 2.2.3.1 Anti-cancer activity

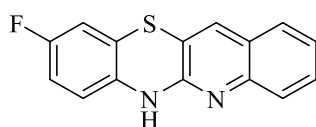
Shamsuzzaman and his colleagues conducted an *in vitro* assessment of the anticancer properties of a range of derivatives based on 5 $\alpha$ -cholestano[5,6-b]benzothiazine. They evaluated these derivatives against various human cancer cell lines, including A-549 (lung carcinoma), SW480 (colon adenocarcinoma), HeLa (cervical cancer), and HepG2 (hepatic carcinoma), utilizing the MTT assay.

In their research, one specific compound **31**, demonstrated a significant enhancement in its potential to inhibit cancer growth. Notably, it exhibited a 50% growth inhibition (IC<sub>50</sub>) value of 13.73  $\mu\text{mol/L}$  against HeLa cells, showcasing heightened effectiveness when compared to doxorubicin, a well-known anticancer drug. Compound 2 also exhibited IC<sub>50</sub> values of 15.83  $\mu\text{mol/L}$  and 16.89  $\mu\text{mol/L}$  against HepG-2 and A549 cells, respectively [130].



31

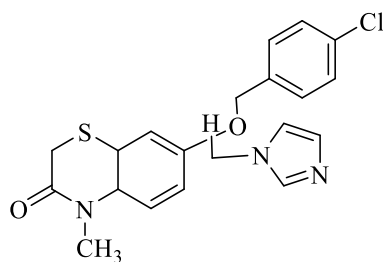
Jelen and his colleagues in their study [131] discovered several derivatives of tetracyclic azaphenothiazines, specifically within the quino benzo-1,4-thiazines ring structure **32**. These derivatives were found to possess confirmed effectiveness in inducing cytotoxicity. This effectiveness was observed through their impact on the PHA induced proliferative response of human PBMC and TNF- $\alpha$  response triggered via lipopolysaccharide (LPS). Among these derivatives, compound 3 displayed the highest level of activity. It exhibited anticancer properties against various cancer cell lines, especially colon cancer cells, A-341 cells, and leukemia L-1210 cells. Remarkably, its anticancer efficacy was found to be comparable to that of cisplatin.



32

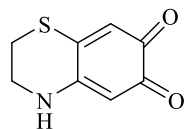
Marchetti and their research team, as mentioned in reference [132], conducted investigations into the neurotoxic and cytotoxic effects of 1,4-benzothiazine (1,4-B) derivatives, both *in vitro* and *in vivo*. They aimed to elucidate the mechanisms responsible for the cytotoxicity induced by 1,4-B compounds and screened these compounds for their potential apoptotic effects. To do so, they used a susceptible cell population of mouse thymocytes to trigger apoptosis. Several analogs of 1,4-B were found to activate apoptosis in thymocytes *in vitro* and lead to thymus cell loss *in vivo*. Notably, among the series of analogs, compound **33**, also known as 6FS5, emerged as one of the most potent and active compounds.





33

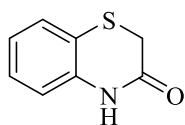
Hasegawa and team conducted research that emphasized the significance of dihydro-1,4-benzothiazine-6,7-dione (BQ) **34** as an exceptionally harmful metabolite derived from 4-S-CAP and 4-S-CAC. Their study focused on assessing the melanocytotoxic effects of these compounds [133].



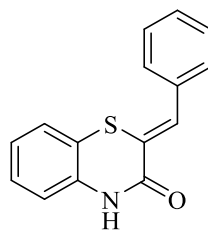
34

### 2.2.3.2 *Anti-microbial activity*

Sebbar and their colleagues conducted a study in which they assessed the *in vitro* biological properties of 1,4-benzothiazinones combined with triazole and oxazolidinone. They found that these compounds exhibited significant antibacterial effects against various microorganisms. Conversely, when a benzylidene group was included at position-2 of compound **35**, it resulted in compound **36**, which displayed increased MIC values against all bacterial strains including *S. fasciens*, *S. aureus*, *E. coli*, and *P. aeruginosa*. When compounds **35** and **36** were alkylated with propargyl chloride and bis(2-chloroethyl)amine hydrochloride, their inhibitory activity was further enhanced [134].

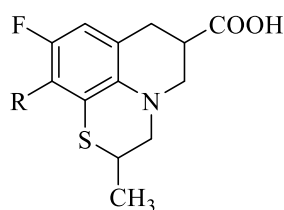


35



36

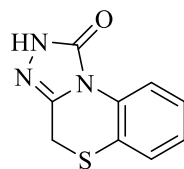
Cecchetti and their team conducted an initial assessment of the in vitro antibacterial properties of a range of 2- substituted-7-oxo-7H-pyrido benzothiazine-6-carboxylic acid derivative. In their study, they identified that compound **37** exhibited the highest level of antibacterial activity. This compound was readily absorbed and led to sustained levels in both plasma and urine [135].



37

### 2.2.3.2 *Anti-convulsant activity*

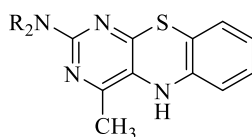
Junnarkar and colleagues discussed the neuro-psychopharmacological effects of a novel skeletal muscle relaxant referred to as [1,2,4] triazolo [3,4-c][1,4]-benzothiazinone **38**. They compared the effects of IDPH-791 with those of mephenesin, a well-established centrally acting muscle relaxant. The results of their study revealed that IDPH-791 is notably safer and has an extended period of effectiveness in comparison to mephenesin. Moreover, IDPH- 791 demonstrated nearly twice the potency in terms of anticonvulsant activity when contrasted with mephenesin. Additionally, IDPH- 791 was twice as effective in inhibition of various spinal poly-synaptic reflexes, including linguomandibular reflexes, crossed extensor reflexes, and flexor reflexes. Similar to mephenesin, IDPH-791 lacked sedative properties, but it differed from mephenesin in that it did not exhibit hemolytic activity [136]. In summary, IDPH-791 proved to be an effective and safe muscle relaxant and anticonvulsant with a long time of action than mephenesin.



38

### 2.2.3.3 Miscellaneous Biological Activities

Bakavoli and their team conducted a screening process to assess the enzyme inhibition property of a series of 2-substituted pyrimido derivative of benzothiazines **39** on 15-lipoxygenase. Among the compounds examined, two, namely compound, exhibited significant potential in inhibiting 15-lipoxygenase. This is significant as 15-lipoxygenase is linked to cardiovascular complications due to its involvement in the oxidative modification of low-density lipoproteins (LDL), which is a contributing factor to the development and progression of atherosclerosis [137].



39

## 2.3 Conclusion

Benzothiazole and benzothiazine scaffolds are extensively utilized in diverse therapeutic applications around the world. These compounds, along with their derivatives, constitute an important category of substances with a wide range of biomedical effects. Recent advancements in the synthesis of heterocyclic compounds containing these as core structures involve diverse methods such as microwave-assisted techniques, nanocatalysis, environmentally friendly (green) synthesis, click reactions, and multicomponent routes. The diverse range of therapeutic benefits linked to medications containing benzothiazole has inspired medicinal chemists to not only develop a multitude of innovative therapeutic agents but also to explore additional methods for synthesizing derivatives of benzothiazole and benzothiazine. Various analogs that incorporate the benzothiazole/benzothiazine ring system

have demonstrated significant activities such as antitubercular, anti-tumor, antimicrobial, antidiabetic, antiasthmatic, anti-inflammatory, anticonvulsant, antiviral, antioxidant, antimalarial, etc.

## *Chapter 3*

# ***Synthesis, Characterization, Biological Evaluation and Molecular Docking Analysis of 1,4-benzothiazine Derivatives***

### 3.1 Introduction

Thiazine is a critical foundational structure found in many medically important compounds, characterized by a unique 6-membered heterocyclic pattern containing both nitrogen and sulfur atoms. Benzothiazines are structurally similar to phenothiazines, offering comparable flexibility and specificity [138, 139]. The specific arrangement of nitrogen and sulfur atoms in phenothiazines and 4H-1,4-benzothiazines plays a crucial role in their biological activities, making both series relevant not only structurally but also pharmacologically and industrially [140-144]. Thiazine-based heterocycles are widely present in bioactive compounds, showcasing remarkable functional diversity and a closer alignment with biological systems. Additionally, the exploration of traditional synthetic methods for nitrogen and sulfur-containing heterocycles has spurred interest in environmentally friendly approaches for their synthesis. Benzothiazine derivatives have gained a prominent status in the scientific community, particularly in the fields of synthetic and medicinal chemistry, due to their significant pharmacological properties [145-151]. These important derivatives possess a diverse range of biological effects, including antibacterial [152], anticancer [153], anti-inflammatory [154], analgesic [155], antioxidant [156], anticonvulsant [157], antidiabetic [158] etc. The therapeutic benefits of small molecules based on thiazine can be attributed to their ability to target multiple therapeutic pathways, ultimately inhibiting the progression, proliferation, and vascularization of cancer cells [159-161].

Synthetic chemists have developed numerous methods to synthesize biologically active 1,4-benzothiazines, recognizing their significant biological relevance. Some of the widely adopted approaches include oxidative cyclocondensations involving 2-thiolphenols and 1,3-dicarbonyls/diketones, with techniques such as using DMSO/ $\text{Al}_2\text{O}_3$ , employing microwave irradiation, utilizing baker's yeast as a catalyst, etc. However, the existing methods involve the use of expensive and hazardous organic solvents, as well as inorganic/organic bases and harsh oxidants, which can be improved for faster reactions [162-168]. Hence, it is essential to create a more efficient, succinct, and expeditious synthetic pathway for this significant group of compounds using readily available solvents and catalysts. Cerium ammonium nitrate (CAN), among other types of oxidants, is known for its capability to convert thiol into sulfenyl radicals, ultimately resulting in the formation of disulfides or/and other oxidation products like sulfones, sulfoxides etc. CAN is stable in various solvents and easily obtainable commercially, making it one of the most attractive oxidants in most organic synthetic procedures. Its use in a variety of reactions involving the formation of C-S, C-N, C-Cl, etc., has been extensively investigated

[169-172].

Building on our previous research, we established a straightforward and effective method for synthesizing heterocycles. Our approach involved creating a catalytic pathway and exploring the use of various organic catalysts in cyclocondensations. Additionally, we recognized the imperative to develop novel pharmaceuticals for lung cancer that minimize off-target effects while promoting patient recovery and extending life expectancy. In our current study, we synthesized substituted 1,4-benzothiazines through an environmentally friendly process. These compounds were then assessed for their effect on proinflammatory cytokines and subjected to various assays against various cancer cell lines (A549, C4-2).

## **3.2 Materials and Methods**

### **3.2.1 Instruments**

Solvents and chemicals were obtained from Sigma Aldrich and utilised them without further refinement. Melting points were measured in degrees Celsius using an open-end capillary method. For  $^1\text{H}$  and  $^{13}\text{C}$ - NMR analysis, we employed a Bruker 500 (400 MHz) instrument, with TMS serving as the internal standard and  $\text{CDCl}_3$  or  $\text{DMSO-}d_6$  as the solvent. E-Merck aluminum TLC sheets (60 F-254, 20 x 20 cm, 0.2 mm thickness) precoated with silica gel and containing a charring agent (ceric ammonium sulfate) were used for monitoring chemical reactions. Spot detection was done using a UV chamber at 366 and 254 nm wavelengths. Additionally, column chromatography was conducted using Merck silica gel (60-120 mesh). For our cell culture experiments, we sourced RPMI-1640 medium (Catalogue no. 11875-093), fetal bovine serum (FBS), L-glutamine (Catalogue no. 25030081), PenStrep (Catalogue no. 15240062), and trypsin (Catalogue no. 25200056) from Gibco/Life Technology. A-549 and normal cell line (HEK293T) was procured from NCCS Pune. C4-2 cells were obtained from Professor Zhou Wang at the University of Pittsburgh, USA, under a Material Transfer Agreement (MTA) with M.D. Anderson Cancer Centre, Texas, USA.

### **3.2.2 Synthetic Procedure**

Unless specified otherwise, we used reagents and solvents in their original state as obtained from commercial suppliers. The yields of the reactions were not fine-tuned or optimized.

#### **3.2.2.1 General synthetic route for 2-alkoxy carbonyl-3-methyl-4H-1,4-benzothiazines (3a-h)**

In a reaction vessel, 2-aminothiophenol **1a** (1 mmol, 125 mg) and 2-amino-4-chlorobenzenethiol **1b** (1 mmol, 160 mg), along with NaHCO<sub>3</sub> (500 mg), were dissolved in anhydrous acetonitrile (15 ml). A solution of ceric ammonium nitrate (1 equiv, 1.096 g) in the same solvent was added dropwise at room temperature while stirring for 10 minutes. Subsequently, 1,3-dicarbonyls (1 mmol) **2(a-d)** were introduced into the reaction mixture, and the mixture was refluxed at 120°C. Monitoring of the progression of the reaction was done using TLC with a pet ether and ethyl acetate in the ratio 8:2 as the eluent. After 15 minutes, the reaction mixture was washed with water and then extracted with ethyl acetate. Following this, the mixture was dried with the help of anhydrous Na<sub>2</sub>SO<sub>4</sub>, the solvent was recovered, and the resulting product was purified by column chromatography, yielding the desired product **3(a-g)** in good yield.

#### **3.2.2.1.1 Methyl 3-methyl-4H-benzo[b][1,4]thiazine-2-carboxylate (3a)**

The title compound was synthesized from compound **1a** (125 mg, 1.0 mmol) and methyl acetoacetate **2a** (107.80 µl, 1.0 mmol) according to the mentioned general procedure. Yield: 88%. mp 209-211 °C. <sup>1</sup>H NMR (400 MHz, CDCl<sub>3</sub>): δ 11.06 (s, 1H, NH), 7.37-7.20 (m, 4H), 4.93 (s, 3H), 2.88 (s, 3H); <sup>13</sup>C NMR (100 MHz, DMSO): δ 164.6 (C=O), 154.5 (C=C-NH), 140.7 (C=C-S), 128.6-122.1 (4C aromatic), 117.2 (2C S-C-C=O, NH-C-CH<sub>3</sub>), 59.98 (O-CH<sub>3</sub>), 14.7 (NH-C-CH<sub>3</sub>). ESI-MS m/z: Calculated for C<sub>11</sub>H<sub>11</sub>NO<sub>2</sub>S [M+H]<sup>+</sup> 221.05; found 221.04.

#### **3.2.2.1.2 Ethyl 3-methyl-4H-benzo[b][1,4]thiazine-2-carboxylate (3b)**

The title compound was synthesized from compound **1a** (125 mg, 1.0 mmol) and ethyl acetoacetate **2b** (127.45 µl, 1.0 mmol) according to the mentioned general procedure. Yield: 93%. mp 141-143 °C. <sup>1</sup>H NMR (400 MHz, DMSO-*d*<sub>6</sub>): δ 8.68 (s, 1H, NH), 6.93-6.59 (m, 4H), 4.05 (q, 2H), 2.20 (s, 3H), 1.19 (t, *J* = 8 Hz, 3H); <sup>13</sup>C NMR (100 MHz, DMSO): δ 163.5 (C=O), 153.5 (C=C-NH), 139.7 (C=C-S), 127.6-120.1 (4C aromatic), 115.2 (2C NH-C-CH<sub>3</sub>, S-C-C=O), 60.1 (-CH<sub>2</sub>-CH<sub>3</sub>), 20.3 (NH-C-CH<sub>3</sub>), 14.7 (-CH<sub>2</sub>-CH<sub>3</sub>). ESI-MS m/z: Calculated for C<sub>12</sub>H<sub>13</sub>NO<sub>2</sub>S [M+H]<sup>+</sup> 235.07; found 235.06.

#### **3.2.2.1.3 Propyl 3-methyl-4H-benzo[b][1,4]thiazine-2-carboxylate (3c)**

The title compound was synthesized from compound **1a** (125 mg, 1.0 mmol) and propyl acetoacetate **2c** (160 µl, 1.0 mmol) according to the mentioned general procedure. Yield: 89%. mp 130-132 °C. <sup>1</sup>H NMR (400 MHz, DMSO-*d*<sub>6</sub>): δ 8.69 (s, 1H, NH), 6.97-6.61 (m, 4H), 4.08 (t, *J* = 8 Hz, 2H), 2.20 (s, 3H), 1.76 (q, 2H), 1.19 (t, *J* = 8 Hz, 3H); <sup>13</sup>C NMR (100 MHz, DMSO): δ 162.6 (C=O), 152.5 (C=C-NH), 138.7 (C=C-S), 126.6-120.1 (4C aromatic), 115.2



(2C NH-C-CH<sub>3</sub>, S-C-C=O), 59.2 (OCH<sub>2</sub>-CH<sub>3</sub>), 19.3 (2C NH-C-CH<sub>3</sub>, CH<sub>2</sub>-CH<sub>2</sub>-CH<sub>3</sub>), 13.7 (-CH<sub>2</sub>-CH<sub>3</sub>). ESI-MS m/z: Calculated for C<sub>13</sub>H<sub>15</sub>NO<sub>2</sub>S [M+H]<sup>+</sup> 249.08; found 249.06.

#### **3.2.2.1.4 Methyl 6-chloro-3-methyl-4H-benzo[b][1,4]thiazine-2-carboxylate (3d)**

The title compound was synthesized from compound **1b** (160 mg, 1.0 mmol) and methyl acetoacetate **2a** (107.80 μl, 1.0 mmol) according to the mentioned general procedure. Yield: 90%. mp 110-112 °C. <sup>1</sup>H NMR (400 MHz, CDCl<sub>3</sub>): δ 11.16 (s, 1H, NH), 7.74 (d, J = 8 Hz, 1H), 7.18 (d, J = 12 Hz, 1H), 6.72 (s, 1H), 4.22 (s, 3H), 2.17 (s, 3H); <sup>13</sup>C NMR (100 MHz, CDCl<sub>3</sub>): δ 164.9 (C=O), 153.0 (C=CH-NH), 138.2 (C-Cl), 135.1 (C=CH-S), 131.0-121.8 (3C aromatic), 118.0 (NH-C-CH<sub>3</sub>), 101.7 (S-C=C), 66.2 (OCH<sub>3</sub>), 21.8 (NH-C-CH<sub>3</sub>). ESI-MS m/z: Calculated for C<sub>11</sub>H<sub>10</sub>ClNO<sub>2</sub>S [M+H]<sup>+</sup> 255.01; found 255.

#### **3.2.2.1.5 Ethyl 6-chloro-3-methyl-4H-benzo[b][1,4]thiazine-2-carboxylate (3e)**

The title compound was synthesized from compound **1b** (160 mg, 1.0 mmol) and ethyl acetoacetate **2b** (127.45 μl, 1.0 mmol) according to the mentioned general procedure. Yield: 85%. mp 191-193 °C. <sup>1</sup>H NMR (400 MHz, CDCl<sub>3</sub>): δ 11.09 (s, 1H, NH), 7.70 (d, J = 12 Hz, 1H), 7.21 (d, J = 12 Hz, 1H), 6.72 (s, 1H), 2.01 (s, 3H), 1.76 (q, J = 8 Hz, 2H), 0.98 (t, J = 8 Hz, 3H); <sup>13</sup>C NMR (100 MHz, CDCl<sub>3</sub>): δ 163.9 (C=O), 152.4 (C=CH-NH), 136.8 (C-Cl), 134.5 (C=CH-S), 130.4-121.2 (3C aromatic), 117.5 (NH-C-CH<sub>3</sub>), 102.1 (S-C=C), 66.5 (OCH<sub>2</sub>CH<sub>3</sub>), 28.7 (OCH<sub>2</sub>-CH<sub>3</sub>), 20.6 (NH-C-CH<sub>3</sub>). ESI-MS m/z: Calculated for C<sub>12</sub>H<sub>12</sub>ClNO<sub>2</sub>S [M+H]<sup>+</sup> 269.03; found 269.02.

#### **3.2.2.1.6 Propyl 6-chloro-3-methyl-4H-benzo[b][1,4]thiazine-2-carboxylate (3f)**

The title compound was prepared from compound **1b** (160 mg, 1.0 mmol) and propyl acetoacetate **2c** (160 μl, 1.0 mmol) according to the mentioned general procedure. Yield: 88%. mp 125-127 °C. <sup>1</sup>H NMR (400 MHz, CDCl<sub>3</sub>): δ 11.16 (s, 1H, NH), 7.72 (d, J = 12 Hz, 2H), 7.18 (d, J = 12 Hz, 2H), 7.67 (s, 1H), 4.22 (t, J = 8 Hz, 2H), 2.22 (s, 3H), 1.30 (q, J = 12 Hz, 2H), 0.98 (t, J = 8 Hz, 3H); <sup>13</sup>C NMR (100 MHz, CDCl<sub>3</sub>): δ 164.0 (C=O), 151.6 (C=CH-NH), 137.0 (C-Cl), 133.6 (C=CH-S), 130.2-120.3 (3C aromatics), 116.7 (NH-C-CH<sub>3</sub>), 101.2 (S-C=C), 65.8 (OCH<sub>2</sub>CH<sub>2</sub>CH<sub>3</sub>), 21.2 (OCH<sub>2</sub>-CH<sub>2</sub>-CH<sub>3</sub>), 20.2 (NH-C-CH<sub>3</sub>), 9.6 (OCH<sub>2</sub>CH<sub>2</sub>-CH<sub>3</sub>). ESI-MS m/z: Calculated for C<sub>13</sub>H<sub>14</sub>ClNO<sub>2</sub>S [M+H]<sup>+</sup> 285.04; found 285.03.

#### **3.2.2.1.7 Isobutyl 3-methyl-4H-benzo[b][1,4]thiazine-2-carboxylate (3g)**

The title compound was synthesized from compound **1a** (125 mg, 1.0 mmol) and isobutyl acetoacetate **2d** (161.22 μl, 1.0 mmol) according to the mentioned general procedure. Yield:

91%. mp 103-101 °C. <sup>1</sup>H NMR (400 MHz, DMSO-*d*<sub>6</sub>): δ 11.69 (s, 1H, NH), 7.70 (d, *J* = 12 Hz, 1H), 7.21 (d, *J* = 12Hz, 1H), 6.72 (s, 1H), 3.98 (d, *J* = 8 Hz, 2H), 2.50 (s, 3H), 1.95-1.90 (m, 1H), 0.98 (d, *J* = 24 Hz, 6H); <sup>13</sup>C NMR (100 MHz, DMSO): δ 164.6 (C=O), 153.5 (C=C-NH), 138.7 (C=C-S), 127.8-121.5 (4C aromatic), 117.5 (NH-C-CH<sub>3</sub>), 112.2 (S-C=C), 61.2 (OCH<sub>2</sub>CH(CH<sub>3</sub>)<sub>2</sub>), 29.8 (OCH<sub>2</sub>CH(CH<sub>3</sub>)<sub>2</sub>), 19.3 (2C OCH<sub>2</sub>CH(CH<sub>3</sub>)<sub>2</sub>), 14.6 (NH-C-CH<sub>3</sub>). ESI-MS *m/z*: Calculated C<sub>14</sub>H<sub>19</sub>NO<sub>2</sub>S [M+H]<sup>+</sup> 265.11; found 265.10.

#### 3.2.2.1.8 Isobutyl 6-chloro-3-methyl-4H-benzo[*b*][1,4]thiazine-2-carboxylate (3h)

The title compound was synthesized from compound **1b** (1.6 mg, 1.0 mmol) and isobutyl acetoacetate **2d** (161.22 μl, 1.0 mmol) according to the mentioned general procedure. Yield: 89%. mp 116-118 °C. <sup>1</sup>H NMR (400 MHz, DMSO-*d*<sub>6</sub>): δ 11.61 (s, 1H, NH), 7.96 (d, *J* = 16 Hz 1H), 7.45 (d, *J* = 24 Hz 1H), 5.77 (s, 1H), 3.98 (d, *J* = 12 Hz, 2H), 3.35 (s, 3H), 2.78-2.46 (m, 1H), 1.08 (s, 6H); <sup>13</sup>C NMR (100 MHz, DMSO): δ 165.1 (C=O), 152.7 (C=C-NH), 138.6 (C-Cl), 129.8 (C=C-S), 126.1-122.7 (3C aromatic), 118.2 (NH-C-CH<sub>3</sub>), 114.3 (S-C=C), 61.2 (OCH<sub>2</sub>CH(CH<sub>3</sub>)<sub>2</sub>), 29.8 (OCH<sub>2</sub>CH(CH<sub>3</sub>)<sub>2</sub>), 19.3 (2C (2C OCH<sub>2</sub>CH(CH<sub>3</sub>)<sub>2</sub>)), 14.6. ESI-MS *m/z*: Calculated C<sub>14</sub>H<sub>18</sub>ClNO<sub>2</sub>S [M+H]<sup>+</sup> 299.07; found 299.06.

#### 3.2.3 Biological Assay

The A-549 cancer cell line and (HEK293T) normal cell line was procured from NCCS Pune and C4-2 cells were obtained from Prof. Zhou Wang at the Pittsburgh University, USA, under a Material Transfer Agreement with MDA Cancer Centre, USA, and both the cell lines were normally retained in RPMI media supplemented with 10% F.B.S, 1% glutamine, and 100g/ml penicillin-streptomycin in 5% carbon dioxide incubated at 37°C.

##### 3.2.3.1 MTT Assay

MTT assay is a colorimetric assay for measuring cellular metabolic activity. MTT method is one of the most widely used methods to analyze cell viability and proliferation. This method was used to assess the effect of compounds (**3a-3h**) on cell viability in both cancer cell lines (A549, C4-2) and the most effective was tested against normal human embryonic kidney cell line (HEK293T). The cells were set up in 96 well plates with a total volume of 100 μl/well to evaluate the compounds. The cells were cultured and incubated for the proper amount of time typically 24-48 hours prior to treatment. Cells were treated with compounds **3a-3h** at various concentrations and incubated for 24hrs. A concluding concentration of 5 mg/ml was reached by adding 10 μl of MTT solution to each well and the MTT-treated cells were incubated at

37°C for 4 hours. To dissolve formazan crystals, 100 µl of solubilization (DMSO) solution was supplied to each well. Using an ELISA reader, the optical density of the tinted solution was gauged at a wavelength of 563 nm. Data was analyzed using Graphpad prism 8.0.

### **3.2.3.2 CFU Assay**

CFU was carried out for *in vitro* quantitative assessment to investigate if a single cell may develop into a big colony through clonal growth in the presence of various concentrations of the compound that produced the most effective results in the MTT experiment. A-549 cells were plated in six-well dishes and given the proper time to grow until they were 70-80% confluent. Confluent cells were treated with different doses of compound **3c** (15, 25, 35, 45, and 55 µM) and DMSO control respectively, and were incubated for about 48 hrs. Equal numbers of cells (hemocytometer was used to count the cells) from both the treated wells and control well were put in 10 cm dishes to develop into colonies for 3 to 5 days. After appropriate colony formation the media was carefully withdrawn from the dishes, 100% methanol covering the cells was added, and the cells were then left to incubate for 20 minutes at room temperature. After the methanol was removed, the cells were gently washed with tap water. The cells were covered with crystal violet solution and was incubated for five minutes at room temperature. To get rid of excess color, the cells were rinsed with water. The plates were then inverted and air-dried overnight on a piece of tissue paper. Then, using ImageJ software, cells were counted. The assay was conducted three times in triplicates, and the P value was confirmed using the t-test and Kruskal-Wallis test in GraphPad prism 8.0. P values below 0.05 were deemed significant.

### **3.2.3.3 In-vitro Scratch Assay/Wound Healing Assay**

A-549 cells were grown in monolayer in 6 well plates. When the monolayer reached 70-80% confluency, the medium was withdrawn, and a sterilized pipette tip with a capacity of 200 µl was utilized to gently scratch the monolayer across its middle (scratches were in line). After washing the isolated cells with PBS, the wells were scratched and then filled with new RPMI media augmented with 10% FBS, 1% PenStrep, and 1% L-glutamine. Before adding compound **3c**, bright field images showing the cellular gap were taken using an LMI inverted microscope. **3c** was then applied to the cells at a dosage of 25 µM, with DMSO serving as the vehicle control. After treatment, 5% CO<sub>2</sub> was used to incubate the well plates at 37 °C, and monitored

for variations in the gap width of the scratch by periodically taking bright field images of the cellular gap after 0, 24, and 48 hours. Using the ImageJ programme, the diameter of the scratch wound was quantitatively assessed. Using GraphPad prism 8.0, the cellular gap distance was quantitatively assessed as the proportion of the wound area.\*P < 0.05 was regarded as significant.

#### ***3.2.3.4 RNA Isolation, PCR amplification, and quantitative Real-Time expression analysis (RT-PCR)***

A-549 cells were cultured in 10 cm dishes for two days. 70-80% confluent cells were treated with 25  $\mu$ M of the compound 3c, and with DMSO respectively, and incubated for 24hrs. This treatment lasted for 24 hours. To isolate total cellular RNA from the A-549 cancer cell line, the Trizol method from Thermo Scientific was employed, following the manufacturer's guidelines. The quality of the isolated RNA was assessed by running it on a gel, and subsequently, cDNA was synthesized using MMLV reverse transcriptase from Gibco. The successful synthesis of cDNA was confirmed using GAPDH primers. For the assessment of relative gene expression, specifically for genes such as Il1- $\alpha$ , Il6, Il1- $\beta$ , Vimentin, COX-2, Il8, and TNF- $\alpha$ , Real-Time PCR (Biorad) was performed. This analysis utilized SYBR qPCR mixture from Kapa, along with specific primers designed for the A-549 cell line, using GAPDH as the control normalizer. The Delta Ct method was used to assess and compare the relative expression outcomes between the treated and untreated samples.

#### ***3.2.3.5 Molecular Docking***

In the present study, Autodock (specific version) was employed, and Autodock tools were utilized for conducting the calculations. An energy-based scoring function was utilized to evaluate the receptor-ligand interactions that were identified. The crystallographic structures of five inflammatory molecular targets, including Il1- $\alpha$  (PDB ID : 5UC6), Il1- $\beta$  (PDB ID : 6Y8I), Il6 (PDB ID : 1P9M), Vimentin (PDB ID : 3TRT), COX-2 (PDB ID : 5KIR), Il8 (PDB ID : 5D14), and TNF- $\alpha$  (PDB ID: 2AZ5), were acquired from the Protein Data Bank (PDB, [www.rcsb.org](http://www.rcsb.org)). To identify potential docking sites for proteins, a grid map was generated using AutoGrid. For all proteins, a grid of dimensions 60 $\times$ 60 $\times$ 60 points was established. AutoGrid was employed to set the spacing between grid points at 0.375, and Gasteiger charges were computed using AutoDock tools. After the docking process was completed, RMSD clustering maps were created by re-clustering with tolerance values of 1, 0.5, and 0.25. This process aimed

to identify the best cluster with the highest population and the lowest energy score. Molecular docking studies were conducted using receptor-ligand interaction tools in Discovery Studio v2.5.

### **3.2.3.6 ADMET Analysis**

Lipinski Rules or the Rule of Five (ROF) serves as a practical guideline for evaluating drug likeness or assessing whether a chemical compound with specific biological or pharmacological activity possesses the characteristics that would make it a potentially effective orally administered drug. The Lipinski rule takes into account various pharmacokinetic drug properties such as absorption, distribution, metabolism and elimination (ADME) on specific physicochemical attributes viz.; molecular weight (MW)  $\leq 500$  Da,  $\log P \leq 5$ , hydrogen bond donor (HBD)  $\leq 5$ , hydrogen bond acceptor (HBA)  $\leq 10$ . The ADME of constituents was carried out by SwissADME software. Constituents were considered active if their oral bioavailability (OB)  $\geq 30$  [173, 174]. Constituents satisfying less than three criteria were deemed inactive.

### **3.2.3.7 Statistical Analysis**

Colony forming unit (CFU) and wound healing assays were conducted, and their measurements were analyzed using Image J software. Graphical and statistical analyses were performed with GraphPad Prism 8.0 software from Graphpad Software, Inc. The data were represented as the mean value SEM, and statistical significance was calculated using either a one-way ANOVA or the student t-test, depending on the applicability. A significance level of  $*P < 0.05$  was considered as statistically significant. ImageJ software was employed for the quantification of both CFU and wound healing assays.

## **3.3 Results and Discussion**

### **3.3.1 Synthetic Procedure**

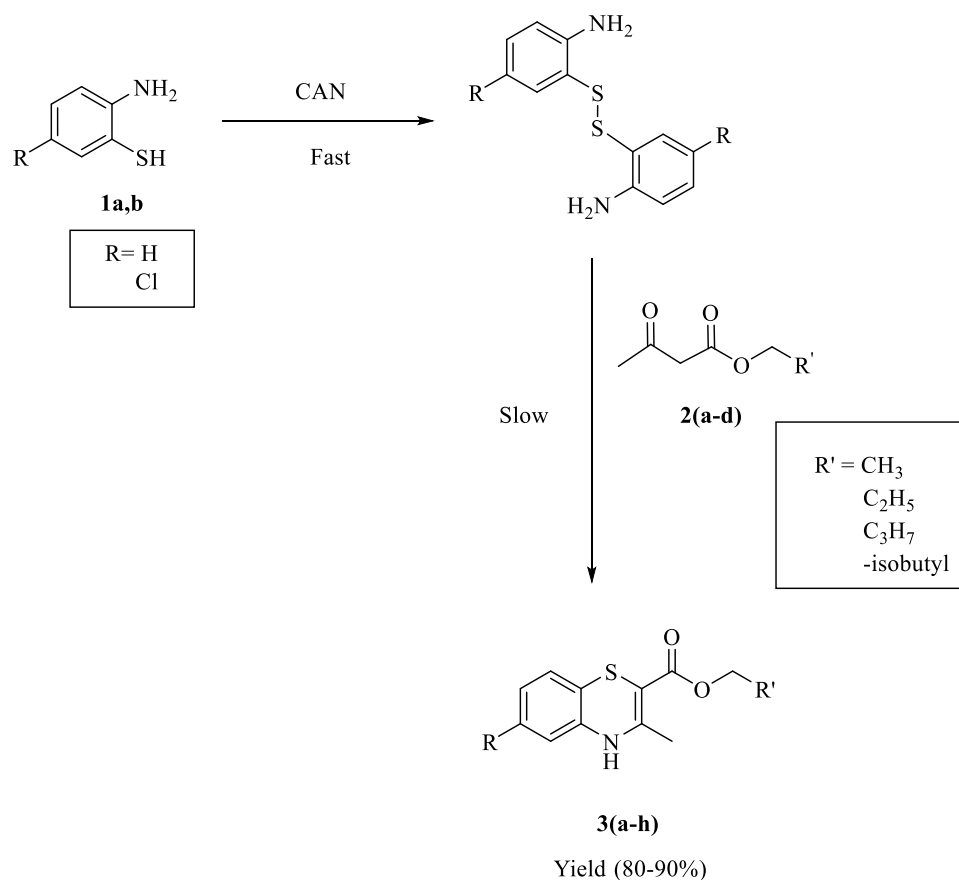
Typically, 1,4-benzothiazines are synthesized by reacting 2-aminobenzenethiols with dicarbonyl compounds in the presence of various oxidizing agents such as DMSO, bromine under phase transfer conditions, sodium perborate, hydrogen peroxide, methoxytributylin- $\text{FeCl}_3$ , among others. A 2-step approach has been proposed for the oxidative cyclocondensation of 2-aminobenzenethiols with 1,3-dicarbonyl compounds. In the first step, 2-aminobenzenethiol is oxidized to disulfide, followed by condensation with 1,3-dicarbonyls to produce the corresponding 1,4-benzothiazine. However, these methods utilize environmentally

unfriendly reagents and yield relatively low product yields (approximately 50-60%), thus requiring enhancement [175].

CAN, like several other oxidizing agents, has the capability to transform thiols into sulfenyl radicals, leading to the formation of disulfides and various subsequent oxidation products such as sulfoxides, sulfones, and other derivatives. To establish the role of CAN, experiments were conducted where thiols were oxidized with an equivalent amount of CAN in the presence of oxygen at room temperature. This resulted in a measurable yield of disulfide, confirming that CAN functions as a catalyst for single-electron transfer in this process [176].

Considering the mechanism of disulfide formation from 2-aminobenzenethiols, we progressed to obtain the corresponding disulfide by treating benzenethiol (1 mmole) and  $\text{NaHCO}_3$  (500 mg) in anhydrous MeCN (10 mL) with a solution of CAN (1 equiv) in the same solvent, that was added dropwise, at room temperature and constant stirring for 10-15 minutes. Then an equimolar quantity of 1,3-dicarbonyl was added to the reaction mixture and refluxed for about 10 minutes to obtain 2,3-disubstituted benzothiazines in good yield (80-85%).

A mechanistic rationale for the reaction would initially involve the oxidation of thiophenol to sulfenyl radical which undergoes dimerization leading to the formation of disulfide followed by cyclocondensation with the 1,3-dicarbonyls to yield the preferred 1,4-benzothiazines. (**Scheme 3.1**)



**Scheme 3.1.** Synthesis of benzothiazine derivatives using CAN

### 3.3.2 Bioassay

#### 3.3.2.1 MTT assay determines high cytotoxic effects for the synthesized compounds against A 549 cell line

For cytotoxicity assay, cancer cell lines A-549 and C4-2 were tested with the series of synthesized substituted benzothiazine derivatives at different concentrations (10, 20, 30, 40, 50  $\mu\text{M}$ ) and DMSO as control. The cytotoxicity results, as illustrated in **Figure 3.1**, demonstrate that all these compounds displayed a notable ability to significantly inhibit the growth of lung cancer cells. Among these, compound 3c demonstrated the most promising cytotoxicity against A 549 cells and was thus selected for further evaluation.

#### 3.3.2.2 Structure-Activity Relationship (SAR) Observations

The SAR analysis from this study provided valuable insights into how different chemical modifications influence the cytotoxicity of thiazine derivatives. This relationship primarily revolves around the electronic nature of the substituents attached to the thiazine core, which

affects the overall reactivity, cellular uptake, and interaction with biological targets. Here's a detailed explanation of the SAR findings:

#### A. Enhancement of Cytotoxicity by Electron-Donating Groups

The presence of electron-donating groups (EDGs), such as methyl (-CH<sub>3</sub>), plays a significant role in increasing the cytotoxic potential of the compounds.

**Methyl Group (-CH<sub>3</sub>):** As seen in compound 3c, the introduction of a methyl group at a specific position on the thiazine core enhances the electron density of the molecule. This increase in electron density leads to stronger interactions with biological targets such as proteins or nucleic acids within the cancer cells. The increased interaction can enhance binding affinity to target enzymes or receptors that regulate cell proliferation, leading to a higher likelihood of inducing apoptosis or cell cycle arrest.

The methyl group also increases the lipophilicity of the compound, which improves its ability to permeate the lipid-rich membranes of cancer cells, facilitating better intracellular uptake. Once inside the cells, the compound can exert its cytotoxic effects more effectively, as demonstrated by the superior performance of compound 3c in the cytotoxicity assay.

#### B. Diminished Cytotoxicity by Electron-Withdrawing Groups

In contrast to electron-donating groups, the presence of electron-withdrawing groups (EWGs), such as chlorine (-Cl), was found to reduce the cytotoxic potential of the thiazine derivatives.

**Chlorine Group (-Cl):** The addition of a chlorine atom to the thiazine core decreases the electron density of the molecule, making it less reactive in interactions with cancer cell targets. The electron-withdrawing nature of chlorine can weaken the binding affinity of the compound to essential biomolecules, such as enzymes or receptors involved in cell division and growth. As a result, compounds with chlorine substituents showed reduced ability to induce cytotoxic effects in the A549 cells compared to their methyl-substituted counterparts.

Furthermore, the chlorine atom may negatively affect the pharmacokinetic properties of the compound, including solubility and membrane permeability. This reduced permeability could hinder the compound's ability to enter the cancer cells in sufficient concentrations to exert its cytotoxic effects, thereby diminishing its overall potency.

#### C. Position of Substituents



The position of the substituents around the thiazine core is another critical factor in determining the compound's cytotoxicity. Even with the same substituent, the exact location on the molecule can influence how it interacts with biological targets.

In compound 3c, the strategic placement of the methyl group likely allowed for an optimal balance between lipophilicity and reactivity, leading to enhanced cytotoxic effects. Conversely, in compounds where the electron-withdrawing chlorine was placed, the negative impact on cytotoxicity was also attributed to its specific position, which may have interfered with key molecular interactions. Similar findings have been reported in studies involving substituted N-(6-methyl-4-phenyl-6H-1,3-thiazin-2-yl) derivatives effective against MCF-7 and EC-9706 cancer cell lines [177].

Furthermore, compound 3c did not show any harmful effect on the HEK293T normal cells. This observation suggests that the compound specifically targets cancerous cells while having no effect on normal cell line. Among these compounds, **3c** was identified as the most potent agent due to its notably high level of cytotoxicity against A549 cancer cells while causing minimal harm to normal cells and therefore, selected for further evaluation.

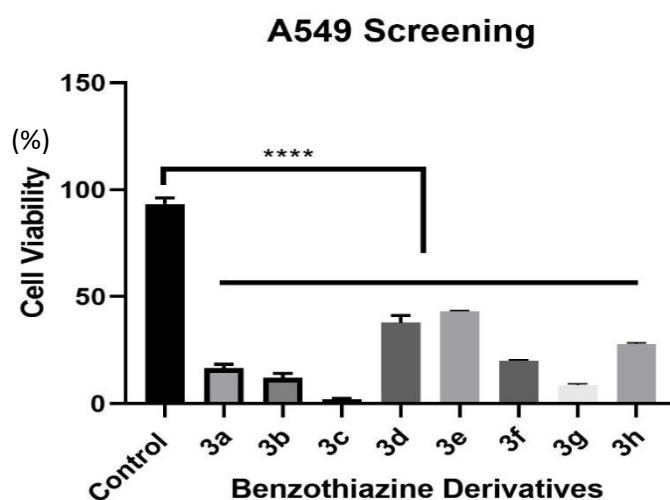


**Fig. 3.1.** Cytotoxicity test of compounds (3a-3g) by MTT assay

### 3.3.2.2 CFU assay illustrates a dose-dependent inhibition of cell growth in vitro

The colony formation study was conducted using five different concentrations (15, 25, 35, 45, 55 $\mu$ M) to investigate the influence of compound 3c on the suppression of growth and progression of lung cancer cells. DMSO was utilised as the vehicle control. The results revealed

a decrease in the ability of lung cancer cells (A-549) dose dependently to form colonies in response to compound 3c, as depicted in **Figure 3.2 (a,b)**. As the concentration of 3c increased, there was a significant reduction in cell proliferation, with a 50% inhibition observed at a dosage of 25  $\mu\text{M}$  in A-549 cells.

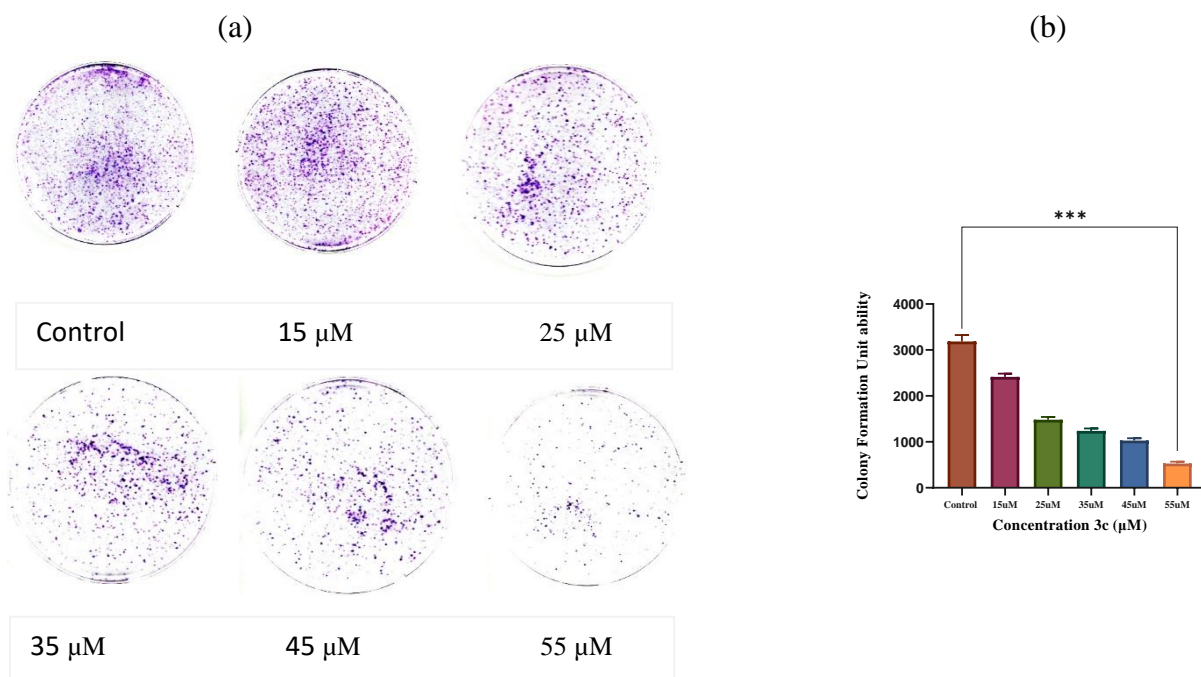


**Fig. 3.2.** Illustrates the dose-dependent inhibition of colony formation by compound 3c in A549 lung cancer cells.

(a) It demonstrates how exposure to different doses of 3c (15, 25, 35, 45, and 55  $\mu\text{M}$ ) impacts the ability of A549 lung cancer cells to form colonies.

(b) The graph visually represents the dose-dependent inhibition of colony formation in A549 cells in vitro. The experiment was conducted in triplicate, and ImageJ software and GraphPad Prism 8.0 were used for both imaging and quantification. Significance was determined with  $*P < 0.0001$ .

### 3.3.2.3. Compound 3c inhibits cellular migration in vitro

By employing a wound healing or scratch assay, we were able to quantify the migration of A-549 cells in response to the presence of compound 3c. The results clearly indicate that the compound led to a substantial and time-dependent reduction in the migration of these cancer cells, as depicted in **Figure 3.3 (a, b, c)**. Gap widths in the cells were measured at 0, 24, and

48 hours after treatment using ImageJ software developed by NIH and were subsequently analyzed using GraphPad Prism 8.0 software.

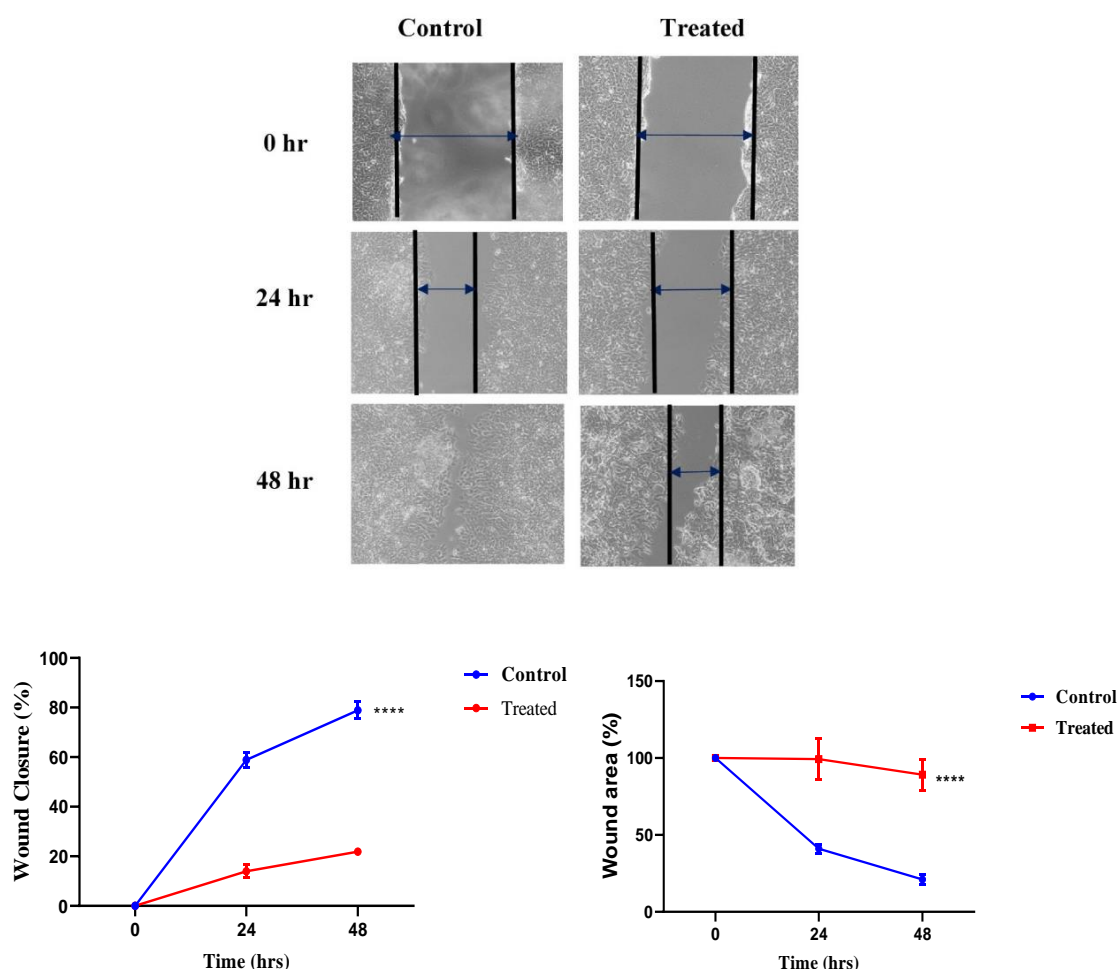


**Fig. 3.3.** The time-dependent suppression of cellular migration or wound healing in A549 cells upon treatment with compound 3c.

(a) Confluent A549 cells were subjected to a treatment of 3c (25  $\mu$ M) after creating wounds in the cell unilayer using a sterilized pipette tip, followed by the evaluation of gap widths at 0, 24, and 48 hours post-treatment.

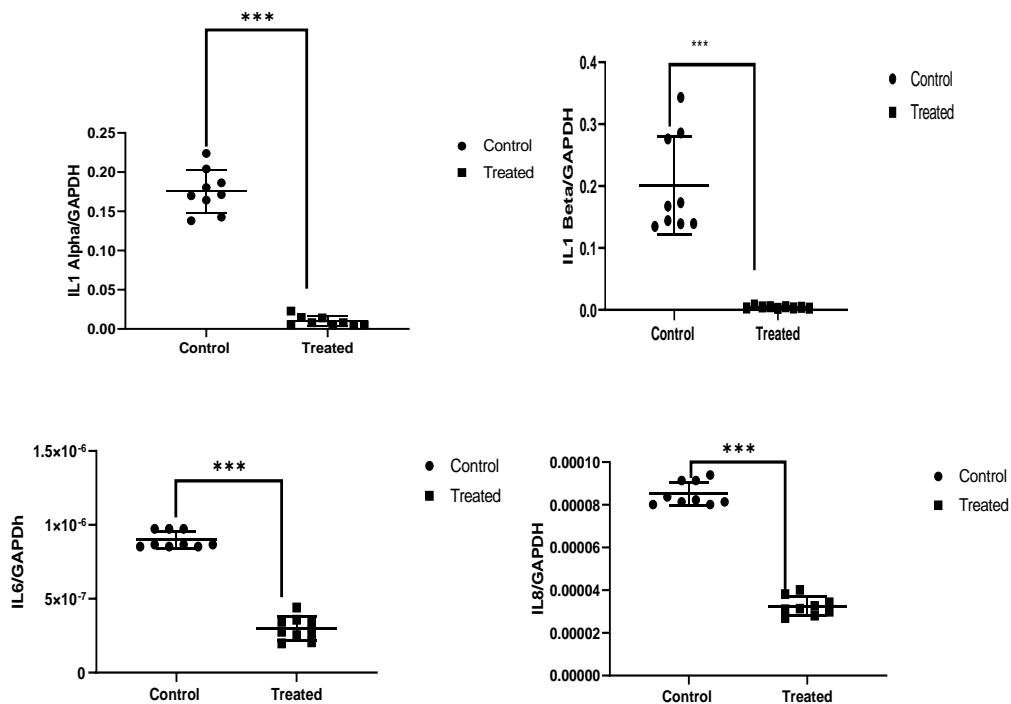
(b) Representative images illustrate the suppression of wound healing in A549 cells upon treatment with 3c, in comparison to control cells treated with DMSO.

(c) A representative image demonstrates the closure of wounds in A549 cells treated with 3c.

Gap closure was assessed using ImageJ software, and the experiment was conducted in triplicates. Quantification was performed utilising Graphpad Prism 8.0 software, with a significance level set at \* $P < 0.0001$ .

#### 3.3.2.4 Compound 3c reduces expression of pro-inflammatory genes

Clinical and epidemiological investigations have established a notable connection between an inflammatory microenvironment, lung cancer, and inflammation. Research has indicated that addressing the inflammatory microenvironment of tumors can decelerate the progression of lung cancer in individuals already afflicted with the disease. The inflammatory response has been associated with cancer cells' distinct capabilities, including rapid proliferation, metastasis, resistance to programmed cell death signals, and the acquisition of resistance to chemotherapy. Existing medications that target individual genes have not yielded successful therapeutic cures, primarily due to the involvement of multiple genes and diverse pathways [178]. The impact of compound 3c on A-549 cell lines, with a focus on proinflammatory genes, demonstrated a noteworthy reduction in the expression of several pro-inflammatory genes (such as IL1- $\alpha$ , IL1- $\beta$ , IL6, IL8, Vimentin, TNF-  $\alpha$ , COX-2) in an in vitro setting, as depicted in **Figure 3.4**. This suggests that compound 3c has the potential to inhibit the baseline activation of proinflammatory genes.



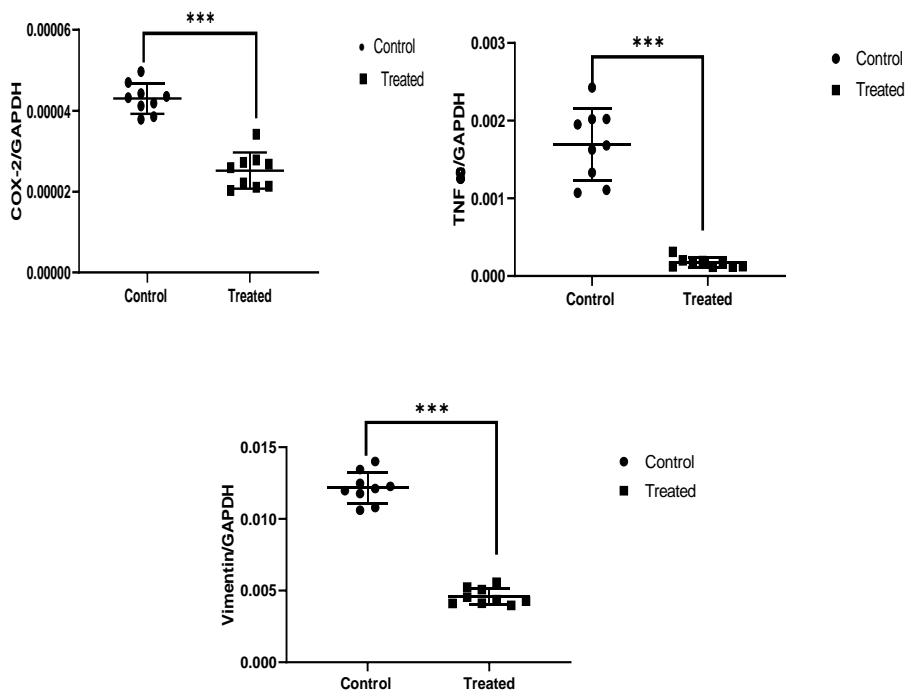
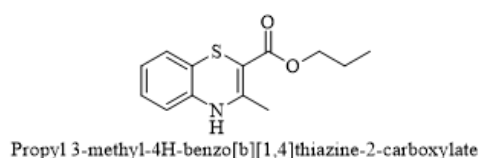


**Fig. 3.4.** The real-time gene expression analysis of pro-inflammatory genes was conducted after treatment with compound 3c (25  $\mu$ M) and using DMSO as the vehicle control. The data was normalized to GAPDH expression. Each data point represents an experiment with a single sample mean value obtained from three replicates. Significance was determined with \*P < 0.0001 using GraphPad Prism 8.0 software.

### 3.3.2.5 Molecular Docking Analysis

The table presents the binding energy scores of the 3c compound when it interacts with the active sites of various protein targets, including IL1- $\alpha$ , IL8, IL1- $\beta$ , IL6, Vimentin, COX-2, and TNF- $\alpha$ , as determined using the AutoDock tool. These interactions were found to be stabilized through the creation of multiple hydrogen bonds and other stacking interactions with important residues within the target proteins. Notably, when 3c interacted with cyclooxygenase-2 (COX-2) and IL-8, it exhibited the strongest binding affinities, with binding energies of -7.06 and -7.54 kcal/mol, respectively (**Figure 3.5**).



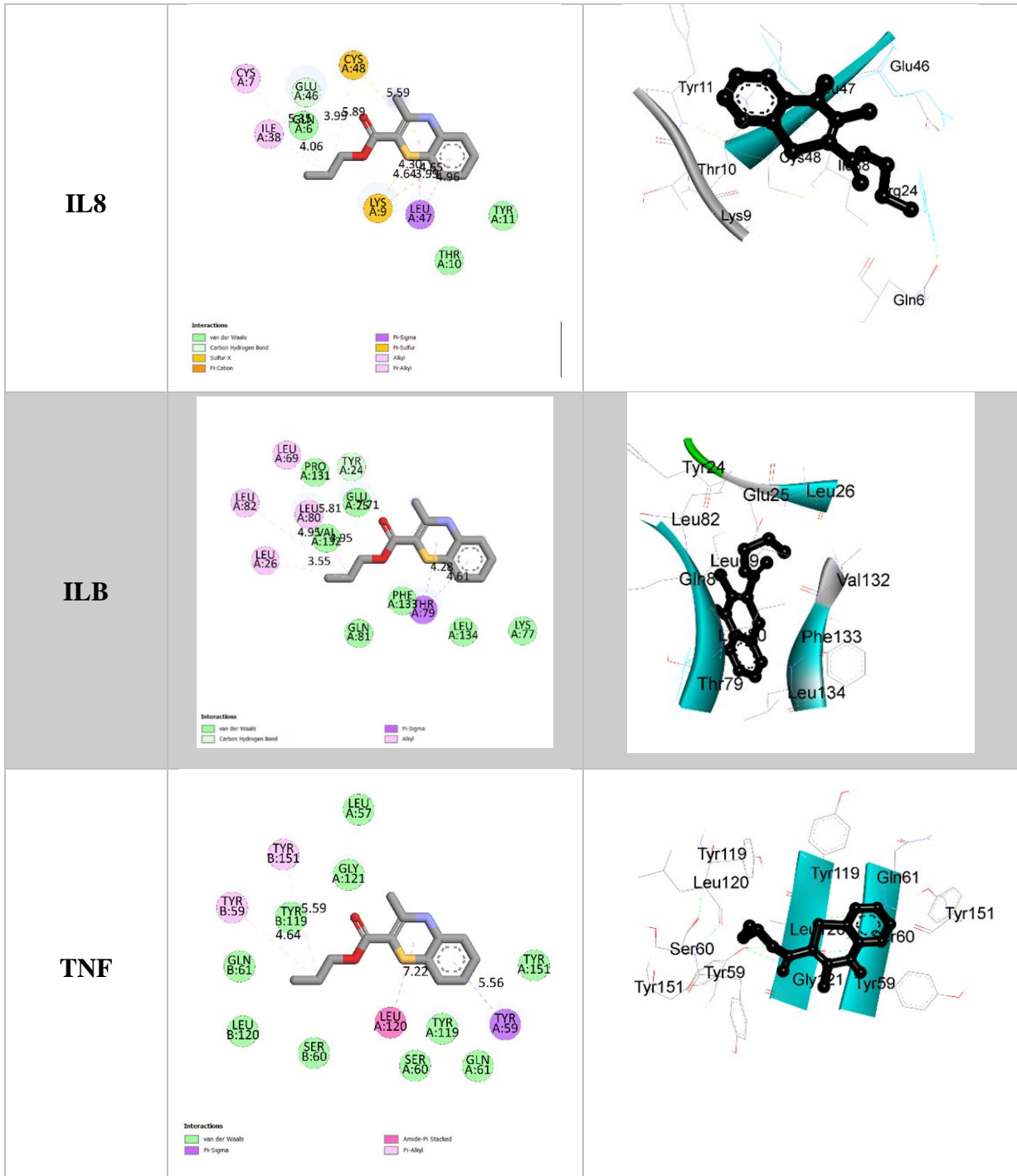
Proteins Involved	Amino acid residues	Energy binding score (kcal/mol)
<b>COX2</b>	LEU(145), GLY(533), ARG(376), HIS(226), GLY(225), GLY(227), VAL(228), ASN(537), GLY(536), TRP(139), VAL(538), PRO (127), TYR(373), GLN(374), PHE(142), ASN(375)	-7.06
<b>IL1</b>	DG(11), ILE(68), TRP(113), DG(13), ILE(18), DG(12), ARG(16), THR(115)	-5.17
<b>IL6</b>	THR(248), TRP(249), ARG(259), SER(260), LYS(252), ILE(232), THR(258), MET(250), ASN(224), LYS(228)	-4.38
<b>IL8</b>	CYS(7), CYS(48), GLU(46), GLN(6), LYS(9), LEU(47), THR(10), TYR(11)	-7.54
<b>ILB</b>	LEU(69), PRO(131), TYR(24), GLU(25), VAL(132), LEU(26), LEU(82), GLN(81), PHE(133), THR(79), LEU(134), LYS(77)	-5.52
<b>TNF</b>	LEU(57), TYR(151), TYR(59), TYR(119), GLY(121), GLN(61), LEU(120), SER(60), LEU(120), TYR(119), TYR(59), SER(60), GLN(61)	-5.36
<b>VIMETIN</b>	SER(299), PHE(295), ALA(296), LYS(292), LEU(298), ALA(302), ALA(301)	-3.81

**Fig. 3.5.** Energy binding score of the compound **3c** (kcal/mol) against various protein targets

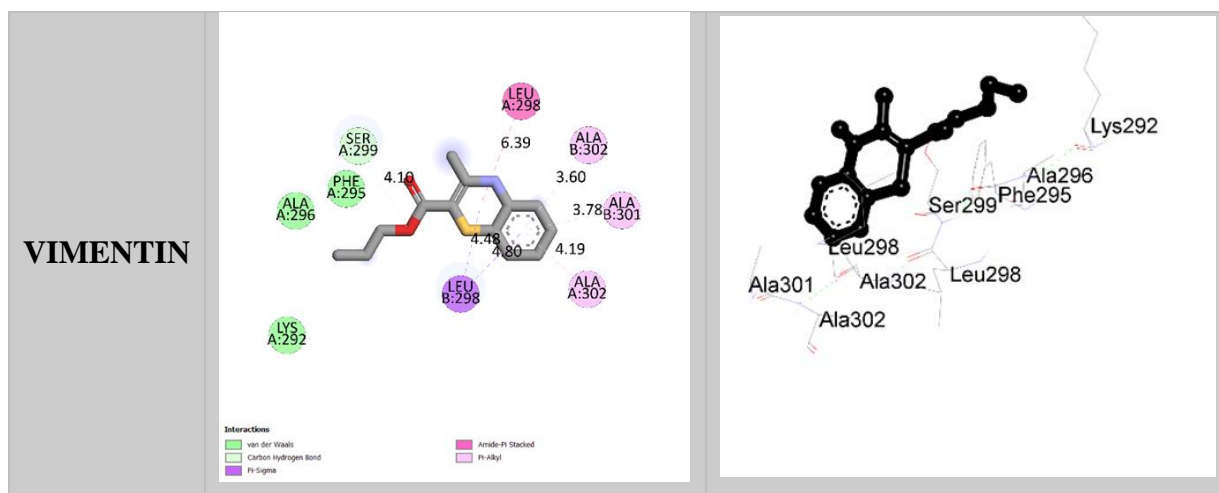
The strong binding affinity of compound **3c** is attributed to its hydrogen bond interactions with specific residues (Val538 and TYR373) of the inflammatory marker enzyme cyclooxygenase (COX-2). Additionally, **3c** forms van der Waals interactions with several other residues (GLY225, GLY227, GLY533, GLY536, LEU145, HIS226, VAL228, GLN374, and ASN375) of COX-2. Furthermore, **3c** demonstrates exceptionally high binding affinity with all three tested cytokine targets, namely TNF- $\alpha$ , IL-1 $\beta$ , and IL-6, as detailed in **Table 3.1**.

Table 3.1. 2D and 3D interaction of compound 3c with respective amino acid residues

PROTEIN	2D INTERACTION	3D INTERACTION
COX2		
IL1		
IL6		







### 3.3.2.6 ADME and drug likeness properties

The pharmacokinetic attributes of the active compounds were analyzed using SwissADME, which predicts certain physicochemical characteristics such as molecular weight (mol MW), solubility (QPlogS and CIQPlogS), as well as the number of hydrogen bonds donated (donorHB) and accepted (accptHB) to water molecules in a medium. These four molecular characteristics collectively form the basis for the Lipinski rule of five, which assesses a molecule's suitability as a drug. To be considered promising, a compound should score higher than 1 and exhibit a specified biological activity of 330. This rule provides insights into how well these compounds may perform in terms of chemical pharmacokinetics within living organisms. The results indicated that all the molecules had the potential to be considered as drug candidates, as they met the criteria set by Lipinski's rule, as shown in Table 3.2.

**Table 3.2. Evaluation of drug-like properties of the screened compounds using Lipinski's rule**

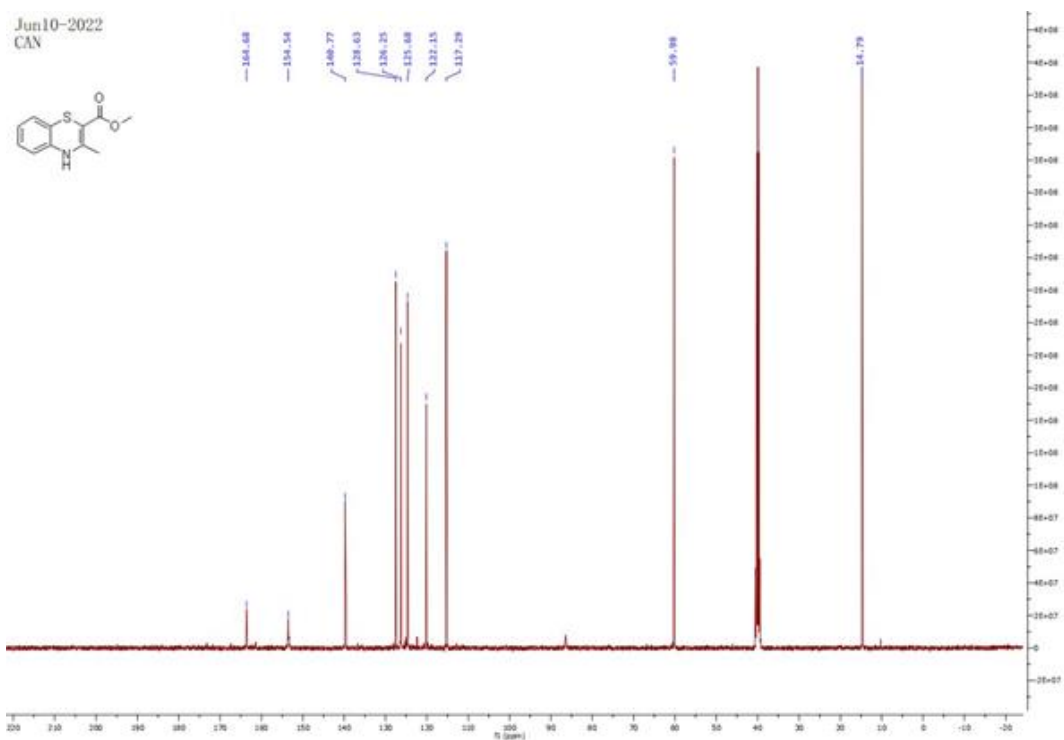
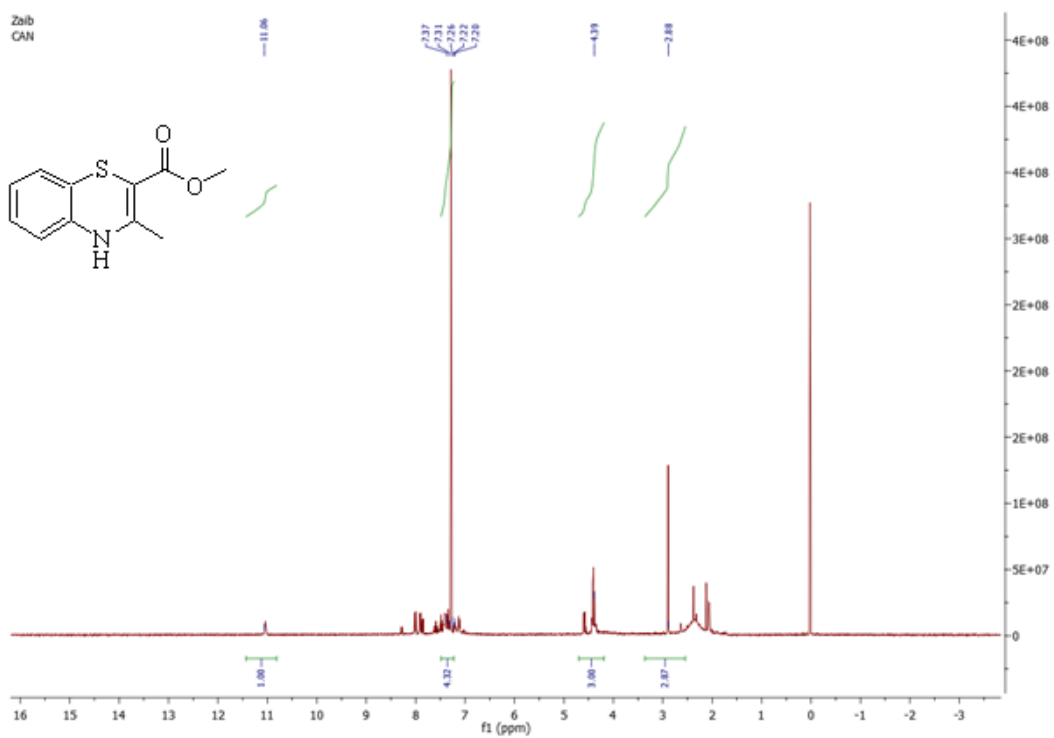
Compound	Canonical SMILES	#Molecular weight	#Rotatable bonds	#H-bond acceptors	#H-bond donors	Lipinski's rule
<b>3a</b>	<chem>COC(=O)C1=C(C)Nc2c(S1)cccc2</chem>	221.28	2	2	1	Yes
<b>3b</b>	<chem>CCOC(=O)C1=C(C)Nc2c(S1)cccc2</chem>	235.30	3	2	1	Yes
<b>3c</b>	<chem>CCCOC(=O)C1=C(C)Nc2c(S1)cccc2</chem>	249.33	4	2	1	Yes
<b>3d</b>	<chem>COC(=O)C1=C(C)Nc2c(S1)ccc(c2)Cl</chem>	255.72	2	2	1	Yes
<b>3e</b>	<chem>CCOC(=O)C1=C(C)Nc2c(S1)ccc(c2)Cl</chem>	269.75	3	2	1	Yes
<b>3f</b>	<chem>CCCOC(=O)C1=C(C)Nc2c(S1)ccc(c2)Cl</chem>	283.77	4	2	1	Yes
<b>3g</b>	<chem>CC(COC(=O)C1=C(C)Nc2c(S1)cccc2)C</chem>	263.36	4	2	1	Yes
<b>3h</b>	<chem>CC(COC(=O)C1=C(C)Nc2c(S1)ccc(c2)Cl)C</chem>	297.80	4	2	1	Yes

### **3.4 Conclusion**

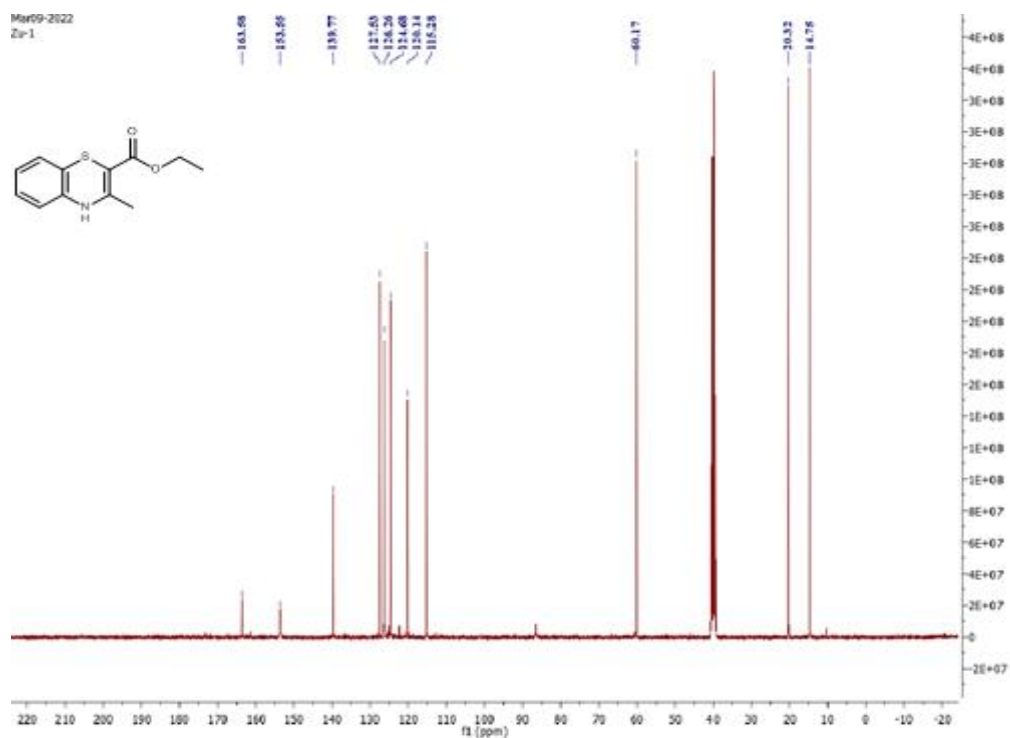
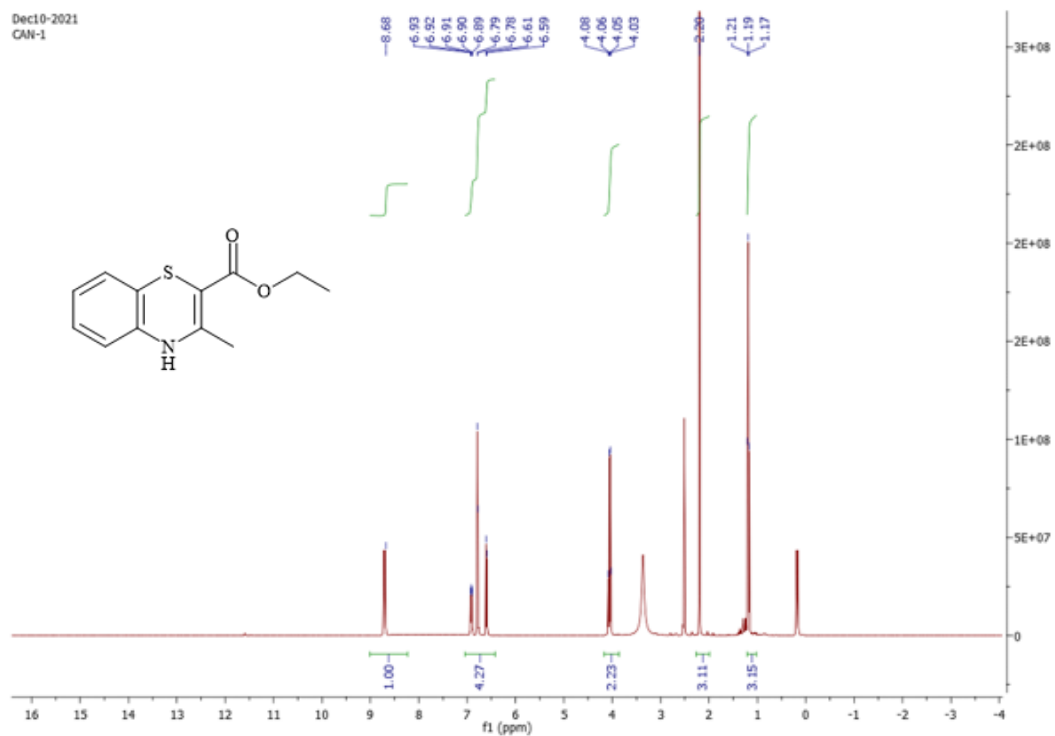
Thiazines are a wide class of synthetic compounds that demonstrated various pharmacological effects. Its derivatives also displayed anticancer activity at various phases of cancer development. In this regard, the synthesized benzothiazine derivative Propyl 3-methyl-benzo[b][1,4]thiazine-2-carboxylate has shown prominent results against A 549 cancer cell line and encouraged the synthesis of small molecules against cancer. Further, it was able to effectively downregulate a number of pro-inflammatory genes in vitro, including IL1- $\alpha$ , IL1- $\beta$ , IL6, Vimentin, COX-2, IL-8, TNF- $\alpha$ . Also, the compound exhibited remarkable binding affinity with various screened cytokines. Drug-likeness analysis also signifies the fact that such molecules can be considered potential candidates for cancer therapy.

## REPRESENTATIVE SPECTRA

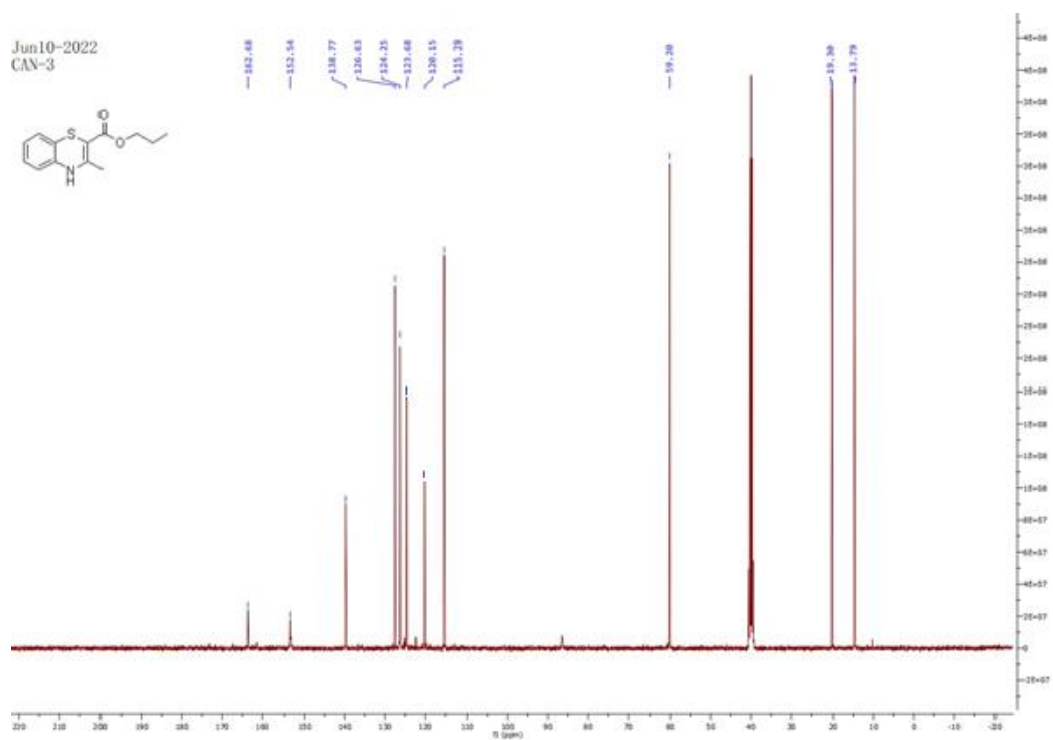
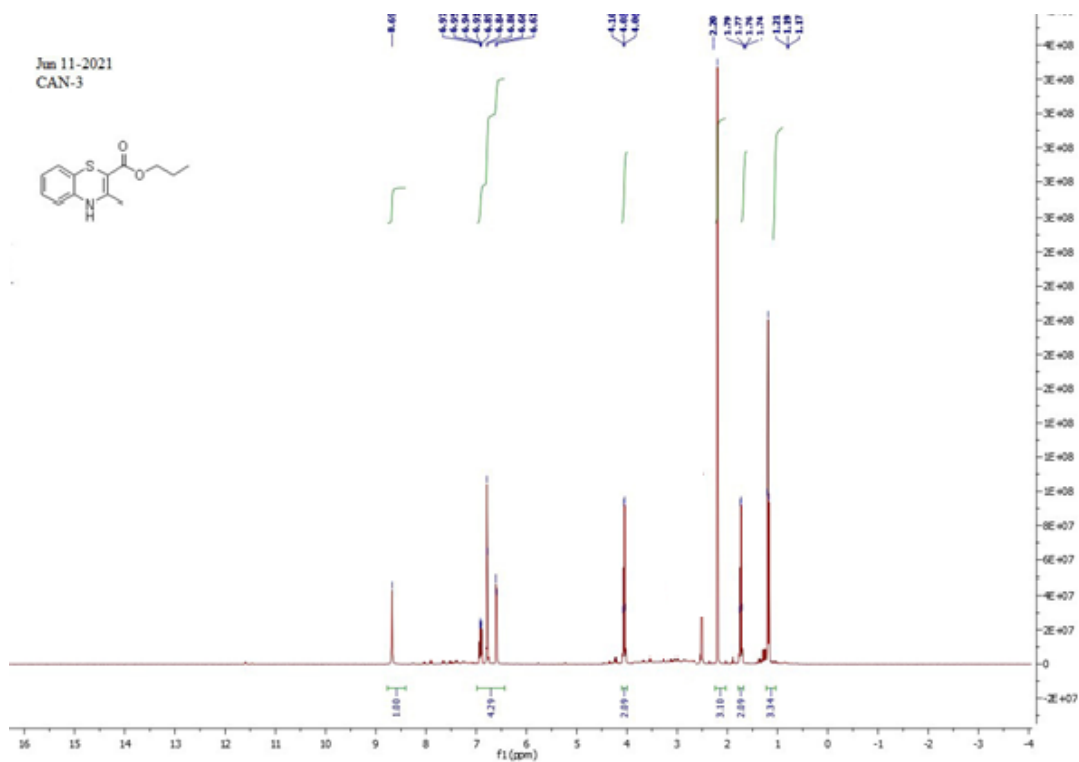
### 3.2.2.1.1 (3a)



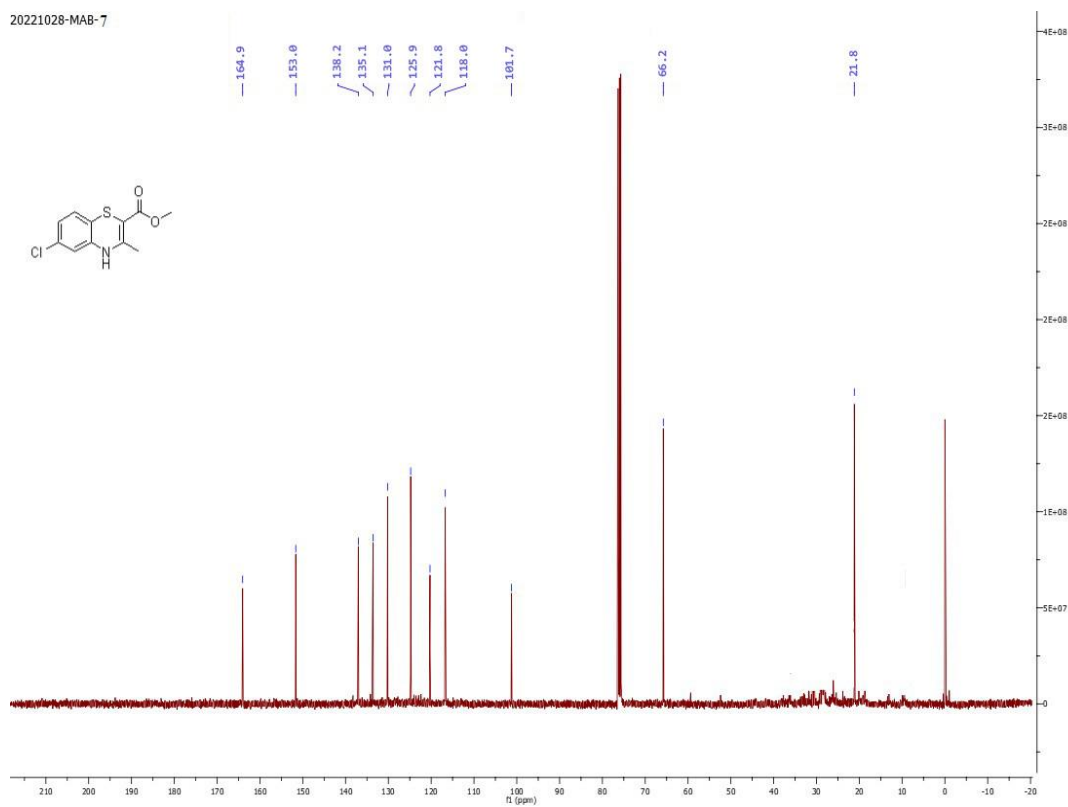
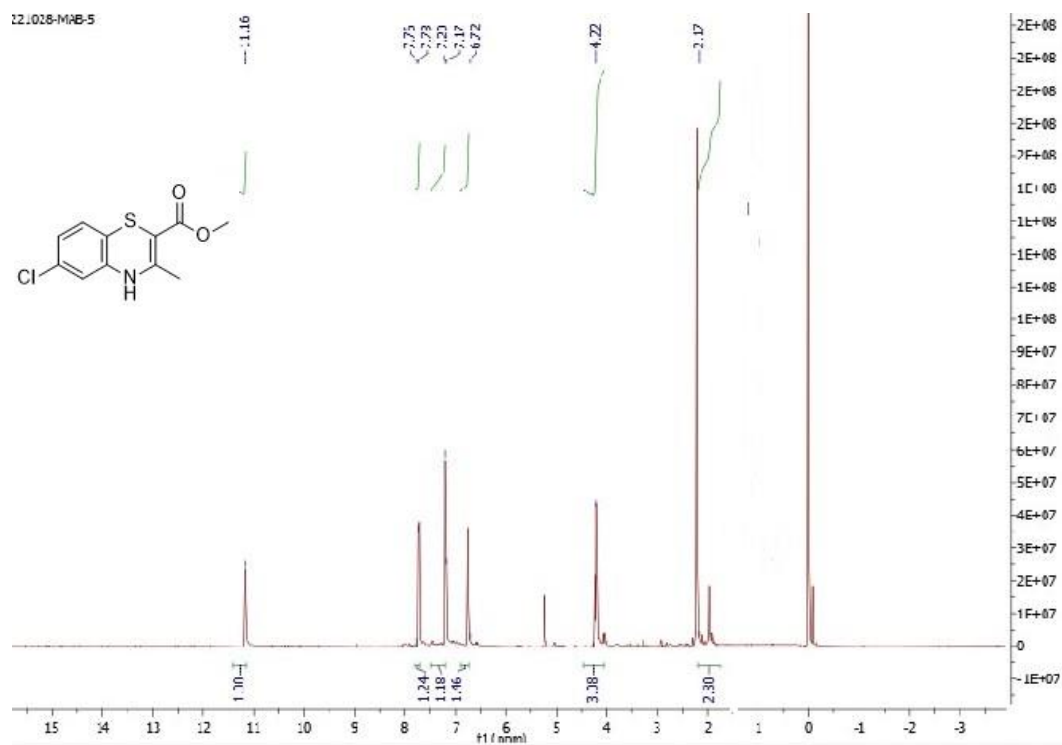
### 3.2.2.1.2 (3b)



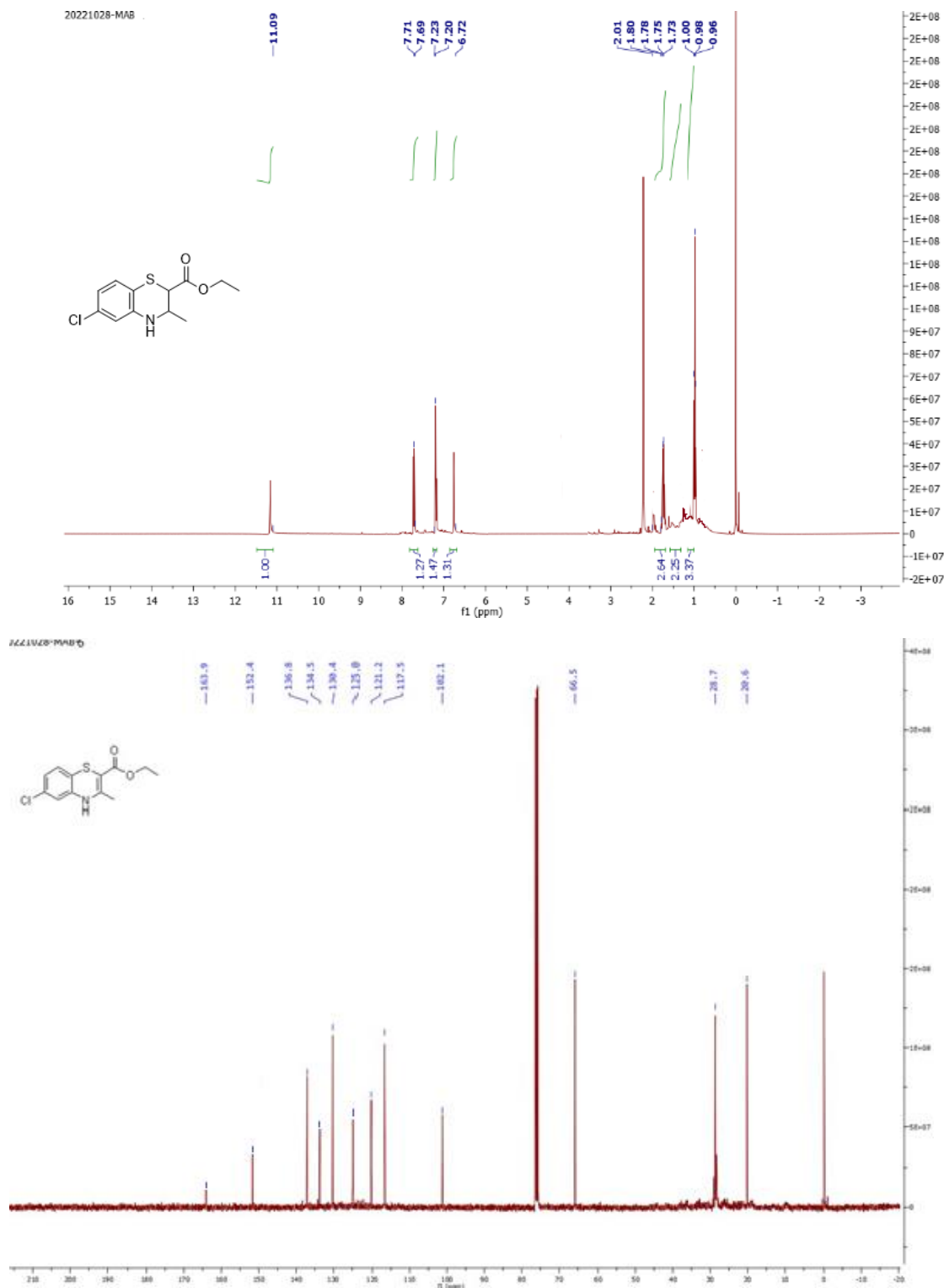
### 3.2.2.1.3 (3c)



### 3.2.2.1.4 (3d)

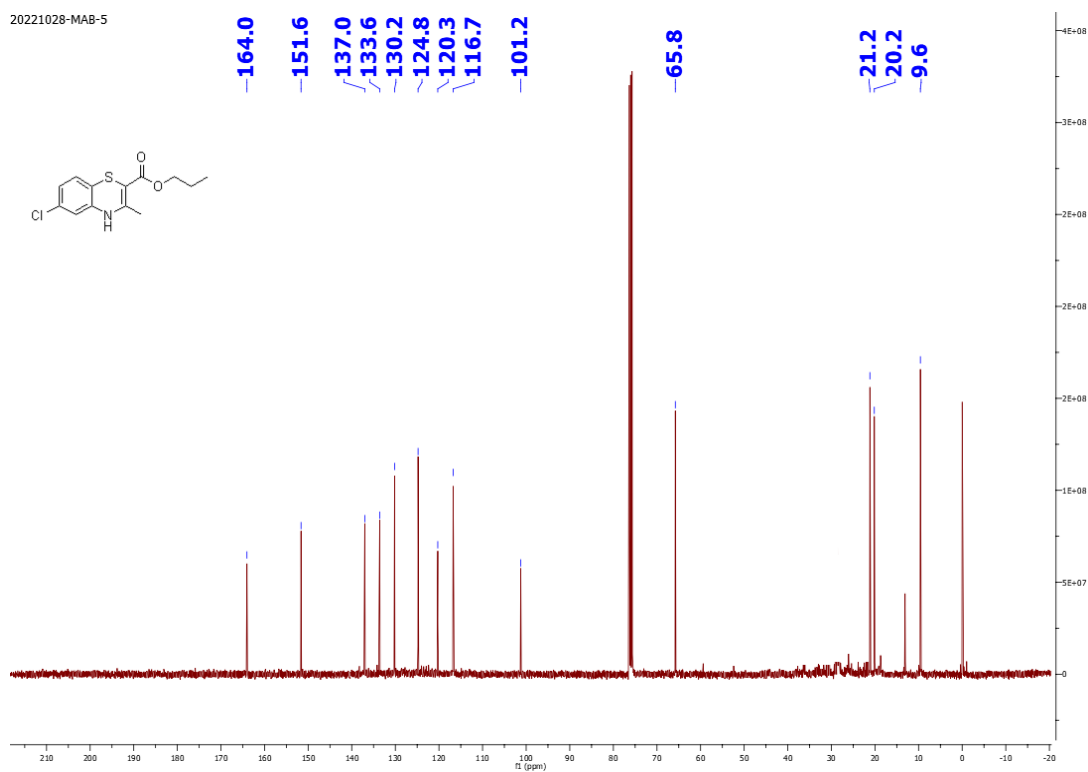
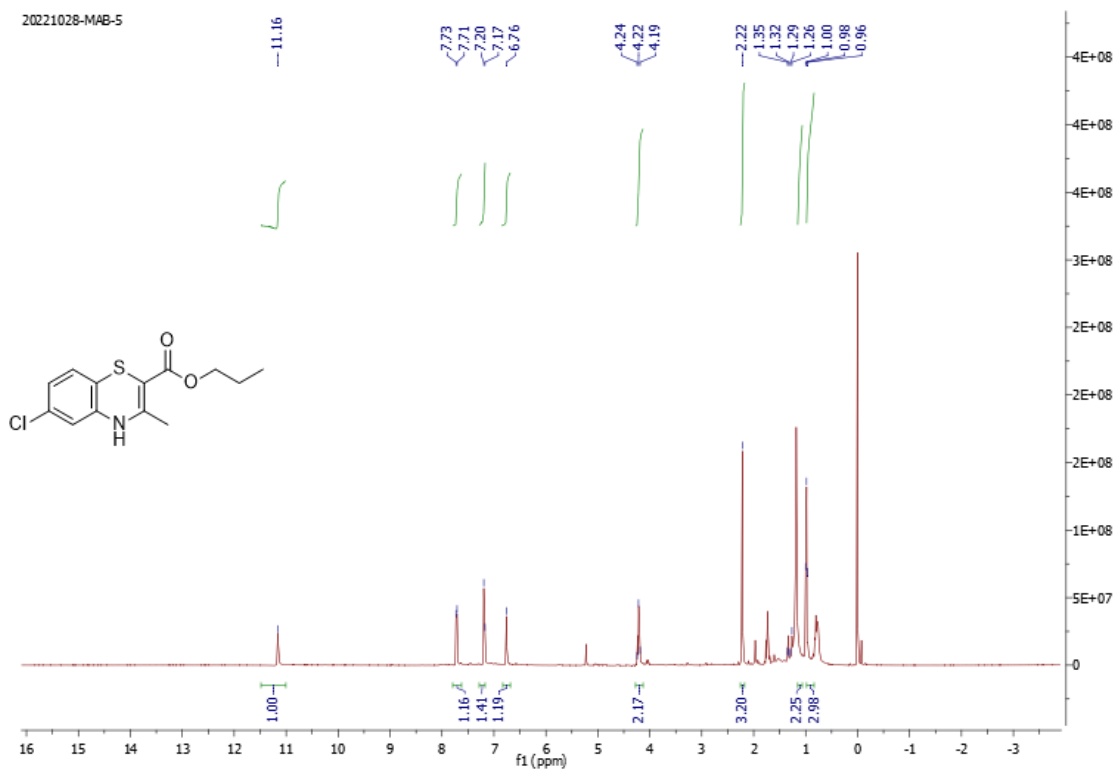


### 3.2.2.1.5 (3e)

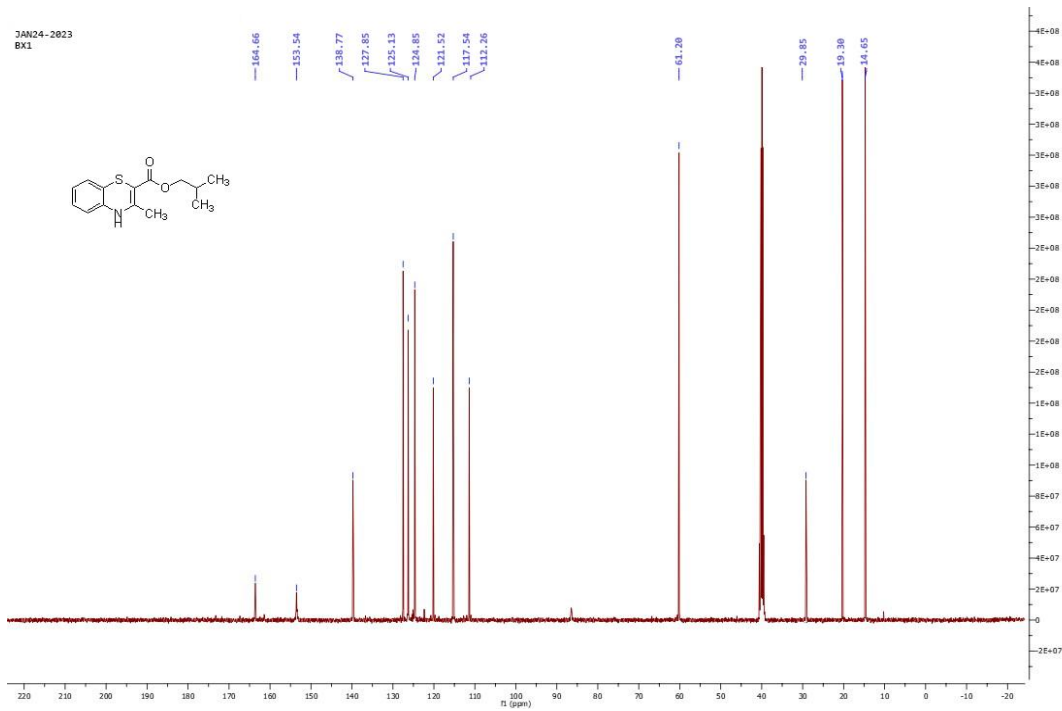
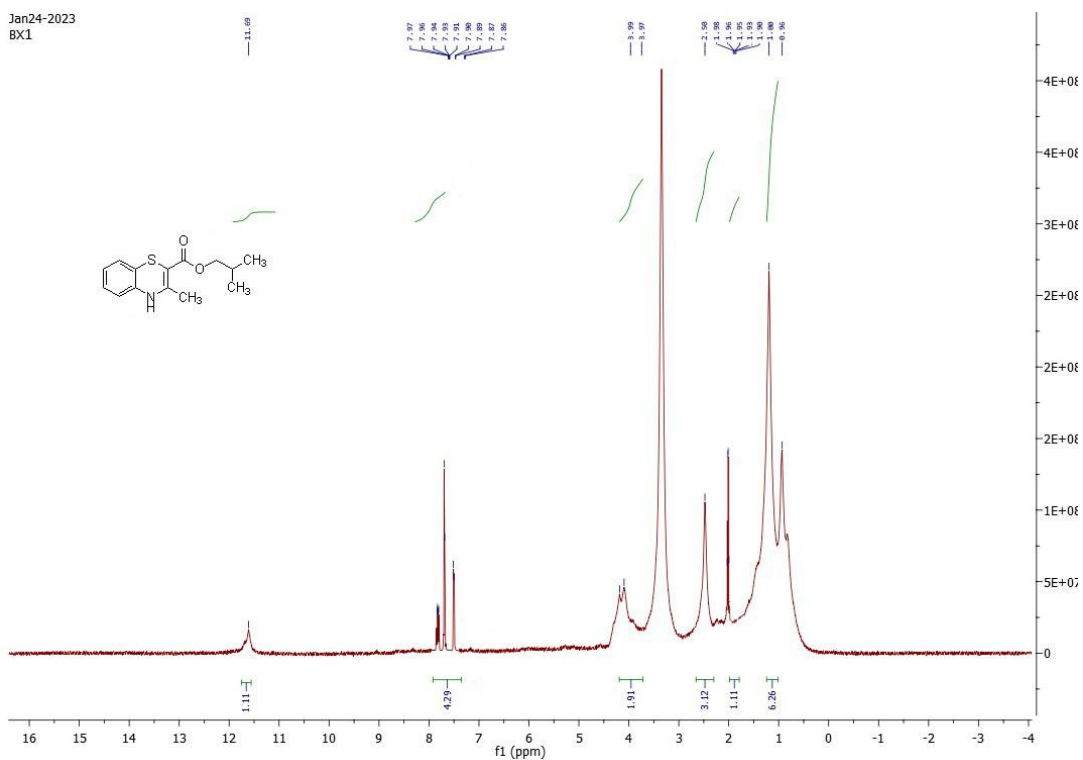




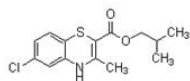
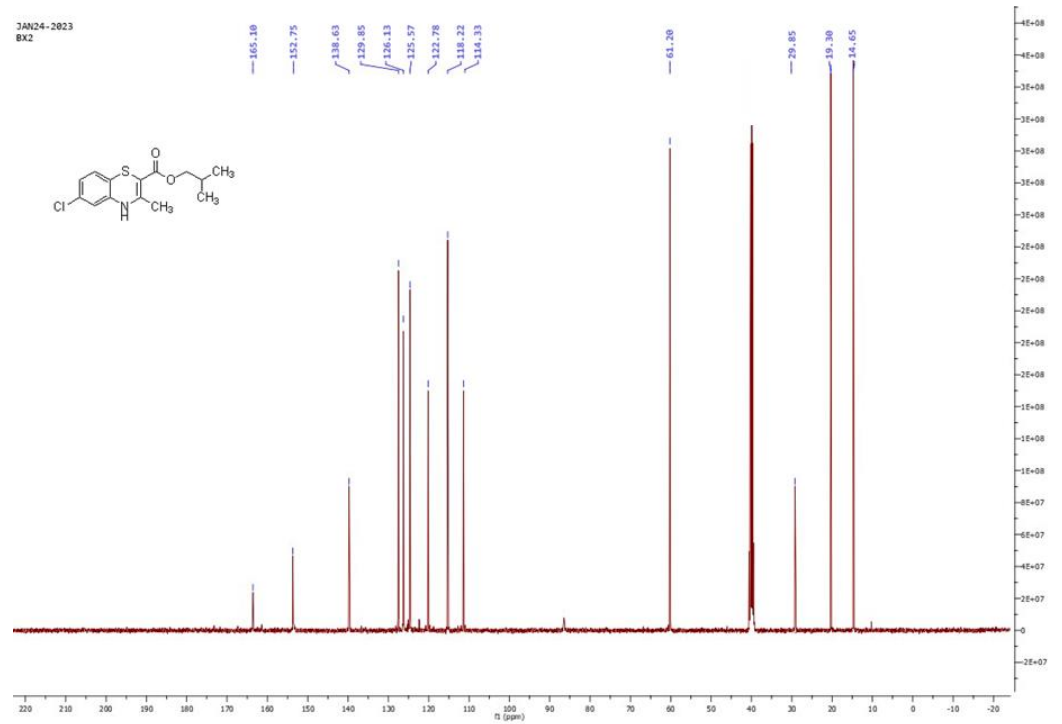
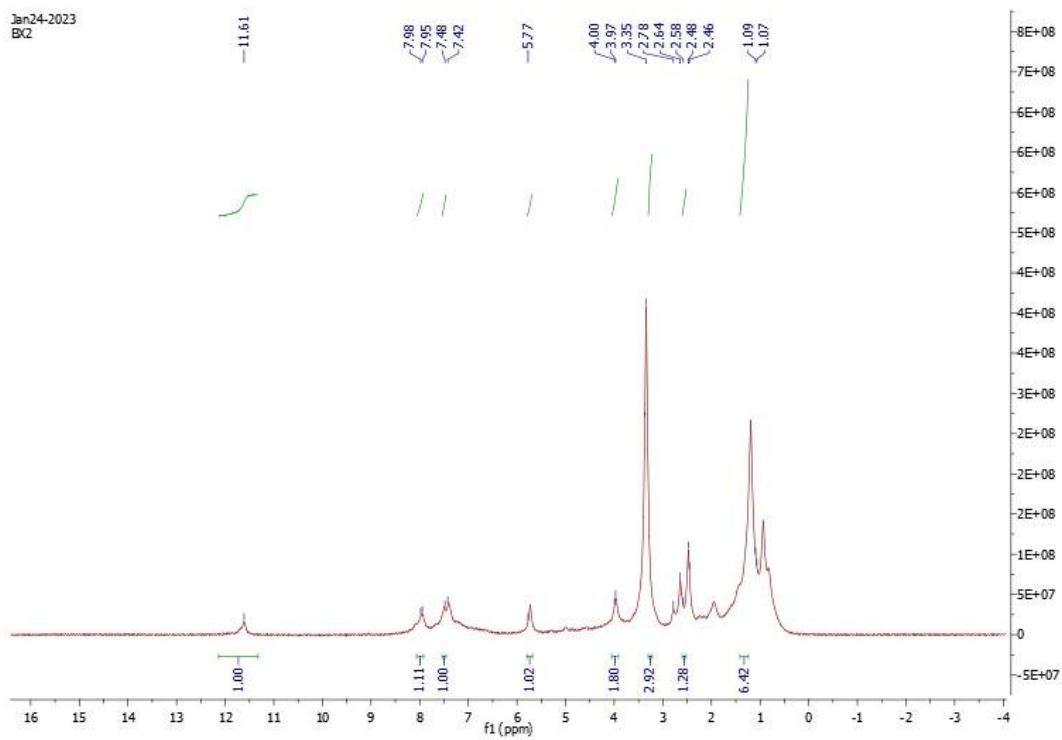
### 3.2.2.1.6 (3f)



### 3.2.2.1.7 (3g)



### 3.2.2.1.8 (3h)



## *Chapter 4*

# ***Benzothiazole-Piperazine Hybrids: Synthesis, Characterization, Cytotoxic and Computational Studies***

## 4.1 Introduction

Benzothiazole is a heterocyclic compound containing both sulfur along with nitrogen atoms in its structure. In recent years, this compound has garnered significant attention due to its favorable biological properties. One of the key features of benzothiazole is its thiazole moiety, which has been proven to be crucial in designing the anticancer drugs. This is evident from the clinical success of various compounds that contain the thiazole ring, such as tiazofurin and its analogs, as well as bleomycins (BLMs) [179, 180]. Researchers are actively engaged in extensive studies over benzothiazole moiety with the aim of discovering primary lead compounds capable of effectively targeting various types of cancer. Recent advancements in this field have been summarized to help understand the potential of benzothiazole derivatives as cancer-fighting agents. This is accomplished by examining the effects resulting from various chemical substitutions. The essential structure of the benzothiazole moiety, which is pivotal for its anti-cancer properties, is depicted in Figure 1 [181-183]. During the process of developing and screening tyrosine kinase inhibitors, researchers have investigated the role and impact of the benzothiazole structure in the field of oncology [184-186]. In 1994, Stevens and his research team synthesized various derivatives of 2-phenylbenzothiazoles that included polyhydroxy groups. These synthesized derivatives were then tested on various cancer cell lines, including those associated with breast cancer, colon cancer, and squamous carcinoma. These specific cell lines were chosen because they were known to exhibit high levels of EGFR. The principal objective of this research was to assess the effectiveness of these derivatives as inhibitors of the tyrosine kinase receptor [187]. Simultaneously, they conducted an assessment of the estrogenic activity of benzothiazole derivatives, considering their structural similarity to 2-phenyl indoles. Interestingly, the synthesized compounds demonstrated prominent and specific toxicity against MCF-7 cell line. This observation led to the conclusion that the compounds' capacity to inhibit tumor growth was not linked to tyrosine kinase receptors [188, 189].

Numerous benzothiazole derivatives that were combined with other biologically relevant heterocyclic systems, such as imidazole and oxazole, demonstrated anticancer properties against various cancer cells. The anticancer effectiveness of these benzothiazole containing derivatives was found to be influenced by the particular heterocyclic substitutions incorporated into their structures [190-192]. Benzothiazole derivatives that featured sulphamide, piperazino-arylsulfonamide, and arylthiol structures were assessed for their potential to inhibit cell proliferation across various cell lines. Specifically, a compound called

4-(benzo[d]thiazol-2-yl)piperazin-1-yl)-2-oxoethyl-4-chloro-benzenesulfonodithiomide exhibited noteworthy activity against the DU-145 cell line. Conversely, another compound, N-(2-(4-(benzo[d]thiazol-2-yl)piperazinyl)-2-oxoethyl)-2,5-dichlorobenzenesulfonodithioamide, displayed strong activity against multiple cell lines derived from human sources [193, 194].

In recent times, molecular hybridization has gained prominence as a valuable approach for altering chemical structures by merging multiple pharmacophores into a unified compound. This innovative technique has emerged as a prominent method in the quest for developing anticancer treatments that may effectively address the pharmacokinetic limitations often encountered with conventional cancer drugs [195, 196]. In the year 2010, scientists employed a hybrid approach to synthesize various derivatives incorporating 2-thiourea-substituted benzothiazoles. These newly created compounds were subsequently evaluated for their potential to combat cancer using MCF-7 and HeLa cell lines as test subjects. The primary objective of this study was to investigate the impact of both the benzothiazole and thiourea components within these compounds on the behavior of DNA topoisomerase enzymes I and II [197, 198]. It is worth highlighting that compounds with alterations involving thiophene and morpholine-substituted thiourea-benzothiazole structures displayed the highest level of effectiveness. This enhanced efficacy was attributed to their ability to induce apoptosis, a regulated cell death process, through the activation of the Caspase-3 pathway [199-201]. In the year mentioned, another research project employing a hybrid methodology was carried out by Havrylyuk and their research team. In this specific study, they developed and synthesized derivatives of 2-aminobenzothiazole that featured substitutions with 4'-thiazolidinyl groups. The inspiration for this design stemmed from a prior investigation led by the same group of researchers, which had a focus on the 4-thiazolidinone moiety [201-203]. The synthesized derivatives were subjected to assessment to determine their efficacy against various cancer cells, including those associated with lung, colon, melanoma, central nervous system (CNS), ovarian, renal, leukemia, and breast cancer. Notably, a compound with the chemical structure (2-(2-[3-(benzothiazol-2-ylamino)-4-oxo-2-thioxothiazolidin-5-ylidenemethyl]-4-chlorophenoxy)-N-(4-methoxyphenyl)-acetamide) demonstrated exceptional potency against all of these tested cancer cell lines [204]. These studies underscored the relevance of utilizing a hybrid-approach in the development of novel benzothiazole derivative molecules with potential applications in cancer therapy.

The inclusion of the piperazine ring offers significant advantages in the development of potential anticancer drugs [205]. Piperzinobenzopyranones have been recognized as notable compounds for the inhibition of the breast cancer resistance protein, a factor that can diminish the efficacy of anticancer drugs [206]. Nucleoside analogs containing the piperazine ring have a tendency to display cytotoxic effects against numerous cancer cells. Consequently, the most potent compounds were subjected to additional research to uncover their mechanism of action. The investigation unveiled that these compounds induced cell death associated with senescence by inhibiting specific kinase proteins [207]. Compounds based on the piperazine-benzothiazole backbone, such as aryl sulphonamides and aryl thiol derivatives, have shown significant cytotoxic effects against numerous cancer cell lines, including MCF-7 and HepG-2 cells [208, 209]. Drawing from these discoveries, we have undertaken the synthesis, separation, purification, and characterization of recently formulated derivatives featuring the piperazine-benzothiazole framework. In order to gauge their efficacy, we conducted assessments of the cytotoxic characteristics of these compounds against the prostate C4-2 cancer cell line through various functional assays.

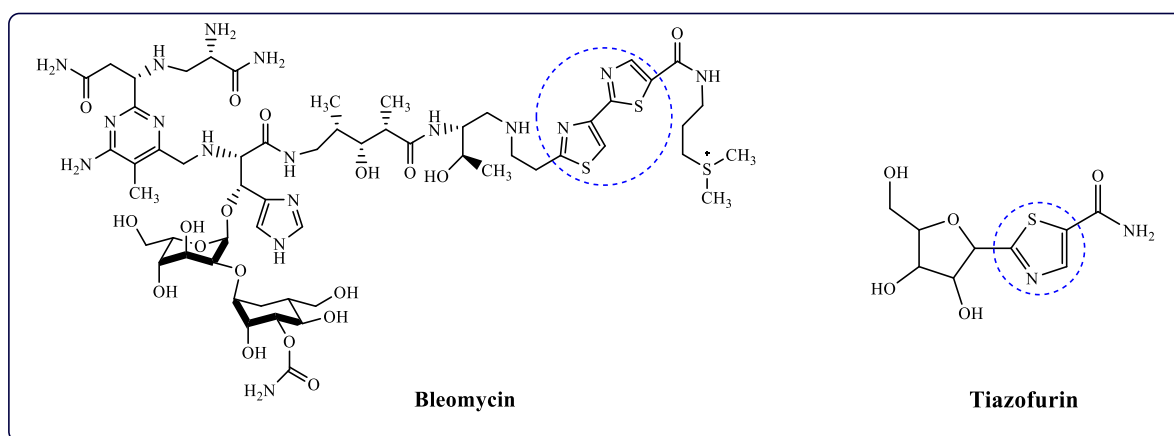


**Fig. 4.1.** FDA approved anti-cancer drugs containing benzothiazole as core scaffold

## 4.2 Materials and Methods

### 4.2.1 Chemistry

Solvents and chemicals were procured from Sigma Aldrich and used without additional refinement. Melting points were identified in degrees Celsius employing the open-end capillary method. NMR analysis was conducted on a Bruker 500 (400 MHz) instrument, referencing to

TMS, and using DMSO/CDCl<sub>3</sub> as the solvent for H<sup>1</sup> and C<sup>13</sup> NMR. Chemical reactions were monitored using E-Merck aluminum TLC sheets (60 F 254, 20 × 20 cm, 0.2 mm thick) coated with silica gel and charring agent (ceric ammonium sulfate). Spot detection was performed under UV light at 366 & 254 nm. Column chromatography utilized Merck silica gel (60-120 mesh). RPMI 1640 medium (catalogue no. 11875-093), FBS, L-glutamine (catalogue no. 25030081), Penstrep (Catalogue no. 15240062), and trypsin (Catalogue no. 25200056) were supplied by Gibco/Life Technology. C4-2 cell line was obtained from the University of Pittsburgh, USA, under a Material Transfer Agreement (MTA) with M.D. Anderson Cancer Centre, USA. Unless otherwise specified, reagents and solvents were used in their original form from commercial suppliers, and the yield was not optimized.

#### ***4.2.2 General Procedure for the Synthesis of 2-(Piperazin-1-yl) Benzothiazole Derivatives:***

The procedure involved conducting the experiment in a 25 mL round-bottom flask equipped with a magnetic stir bar. The flask contained chloro derivative of benzothiazole (1 mmol), an aminating agent (2.0 equivalents), comprising various piperazine derivatives, and water (2 mL). The resultant mixture was gently stirred at normal temperature for a duration varying from 30 minutes to 5 hours, depending on the specific amine utilized. The reaction progression was observed through TLC. Following the culmination of the reaction, ethyl acetate was added to the mixture. The unrefined product underwent purification via column chromatography. The identification and purity of the final product were confirmed through NMR and mass spectrometry techniques.

##### ***4.2.2.1. 2-(4-ethylpiperazin-1-yl) benzthiazole (3a')***

Yield: 82%, mp 100-105°C, <sup>1</sup>H NMR ( 400 MHz, CDCl<sub>3</sub>): δ = 1.03 (t, *J* = 12.0 Hz, 3H), 1.28 (q, *J* = 20.0 Hz, 2H), 2.40 (t, *J* = 8.0 Hz, 4H), 3.59 (t, *J* = 4.0 Hz, 4H), 6.94-7.50 (m, 4H); <sup>13</sup>C NMR ( 100 MHz, CDCl<sub>3</sub>): δ = 10.77, 47.19, 50.91(2C), 51.24 (2C), 118.07, 119.06, 120.40, 124.97, 129.70, 151.08, 167.68 ESI-MS *m/z*: Calculated for C<sub>13</sub>H<sub>17</sub>N<sub>3</sub>S [M+H]<sup>+</sup> 247.11, Found 247.10

##### ***4.2.2.2 2-(4-methyl piperazine-1-yl) benzo[d]thiazole (3b')***



Yield: 82%, mp 100-105°C, <sup>1</sup>H NMR ( 400 MHz, CDCl<sub>3</sub>): δ = 1.03 (t, *J* = 12.0 Hz, 3H), 1.28 (q, *J* = 20.0 Hz, 2H), 2.40 (t, *J* = 8.0 Hz, 4H), 3.59 (t, *J* = 4.0 Hz, 4H), 6.94-7.50 (m, 4H); <sup>13</sup>C NMR ( 100 MHz, CDCl<sub>3</sub>): δ = 10.77, 47.19, 50.91(2C), 51.24 (2C), 118.07, 119.06, 120.40, 124.97, 129.70, 151.08, 167.68 ESI-MS m/z: Calculated for C<sub>13</sub>H<sub>17</sub>N<sub>3</sub>S [M+H]<sup>+</sup> 247.11, Found 247.10

#### 4.2.2.3 *tert*-butyl 4-(benzo[*d*]thiazol-2-yl) piperazine -1- carboxylate (3c')

Yield: 78%, mp 141-145°C, <sup>1</sup>H NMR ( 400 MHz, CDCl<sub>3</sub>): δ = 1.41 (s, 9H), 3.51-3.54 (m, 8H), 6.99-7.54 (m, 4H); <sup>13</sup>C NMR ( 100 MHz, CDCl<sub>3</sub>): δ = 27.36(3C), 28.66, 47.19(2C), 79.39(2C), 118.23, 119.73, 120.66, 125.08, 129.65, 151.49, 153.54, 167.66 ESI-MS m/z: Calculated for C<sub>16</sub>H<sub>21</sub>N<sub>3</sub>O<sub>2</sub>S [M+H]<sup>+</sup> 319.14, Found 319.12

#### 4.2.2.4 2-(4-(benzo[*d*]thiazol-2-yl) piperazin-1-yl) ethan-1-amine (3d')

Yield: 73%, mp 115-118°C, <sup>1</sup>H NMR ( 400 MHz, CDCl<sub>3</sub>): δ = 0.88 (t, *J* = 12.0 Hz, 2H), 1.13 (t, *J* = 24.0 Hz, 2H), 1.62 (t, *J* = 4.0 Hz, 2H), 3.60 (t, *J* = 8.0 Hz, 4H), 3.83 (t, *J* = 12.0 Hz, 4H), 6.98-7.60 (m, 4H); <sup>13</sup>C NMR ( 100 MHz, CDCl<sub>3</sub>): δ = 30.20, 30.56, 47.51(2C), 48.54(2C), 120.66, 121.96, 126.75, 131.19, 149.86, 154.62, 168.83 ESI-MS m/z: Calculated for C<sub>13</sub>H<sub>18</sub>N<sub>4</sub>S [M+H]<sup>+</sup> 262.13, Found 262.12

#### 4.2.2.5 2-(4-(benzo[*d*]thiazol-2-yl) piperazin-1-yl) ethan-1-ol (3e')

Yield: 77%, mp 120-124°C, <sup>1</sup>H NMR ( 400 MHz, CDCl<sub>3</sub>): δ = 1.12 (t, *J* = 24.0 Hz, 2H), 1.97 (t, *J* = 20.0 Hz, 2H), 2.51 (t, *J* = 8 Hz, 2H), 3.59 (t, *J* = 4.0 Hz, 4H), 6.97-7.50 (m, 4H); <sup>13</sup>C NMR ( 100 MHz, CDCl<sub>3</sub>): δ = 21.76, 30.54, 46.84(2C), 50.53(2C), 117.59, 119.32, 120.67, 124.25, 129.48, 151.83, 167.41 ESI-MS m/z: Calculated for C<sub>13</sub>H<sub>17</sub>N<sub>3</sub>OS [M+H]<sup>+</sup> 263.11, Found 263.09

#### 4.2.2.6 2-(4-(*o*-tolyl)piperazin-1-yl)benzo[*d*]thiazole (3f')

Yield: 75%, mp 160-164°C, <sup>1</sup>H NMR ( 400 MHz, CDCl<sub>3</sub>): δ = 2.08 (s, 3H), 3.51 (t, *J* = 8 Hz, 4H), 3.76 (t, *J* = 4 Hz, 4H), 6.98-7.84 (m, 8H); <sup>13</sup>C NMR δ = (100 MHz, CDCl<sub>3</sub>): 18.09, 49.78(2C), 50.21(2C), 113.70, 118.56, 120.66, 121.28, 123.64, 126.11, 128.45, 130.90, 131.44, 140.70, 153.38, 152.90, 168.80 ESI-MS m/z: Calculated for C<sub>18</sub>H<sub>19</sub>N<sub>3</sub>S [M+H]<sup>+</sup> 309.43, Found 309.40

#### 4.2.2.7 2-(4-(pyrimidin-2-yl) piperazin-1-yl) benzo[d]thiazole (3g')

Yield: 78%, mp 165-168°C, <sup>1</sup>H NMR ( 400 MHz, CDCl<sub>3</sub>): δ = 3.63 (t, *J* = 4.0 Hz, 4H), 3.92 (t, *J* = 8.0 Hz, 4H), 7.54–6.42 (m, 5H, aromatic protons), 8.25 (d, *J* = 4 Hz, 2H); <sup>13</sup>C NMR (100 MHz, CDCl<sub>3</sub>): δ = <sup>13</sup>C NMR ( 100 MHz, CDCl<sub>3</sub>): 42.10(2C), 46.83(2C), 109.50,118.19, 119.99, 120.95, 125.40, 129.46, 151.57, 156.55(2C), 159.95, 167.41 ESI-MS m/z: Calculated for C<sub>15</sub>H<sub>15</sub>N<sub>5</sub>S [M+H]<sup>+</sup> 297.10, Found 297.05

#### 4.2.2.8 2-(4-(2-methoxyphenyl) piperazin-1-yl) benzo[d]thiazole (3h')

Yield: 80%, mp 158-161°C, <sup>1</sup>H NMR ( 400 MHz, CDCl<sub>3</sub>): δ = 2.98 (s, 3H), 3.53-3.76 (m, 8H), 6.63-7.45 (m, 8H); <sup>13</sup>C NMR ( 100 MHz, CDCl<sub>3</sub>): δ = 48.73(2C), 50.58(2C), 54.95, 110.86, 118.56, 119.00, 120.35, 121.05, 121.33, 123.64, 126.10, 131.20, 140.69, 152.21, 153.25, 168.84 ESI-MS m/z: Calculated for C<sub>18</sub>H<sub>19</sub>N<sub>3</sub>OS [M+H]<sup>+</sup> 325.12, Found 325.08

#### 4.2.2.9 2-(4-phenylpiperazin-1-yl) benzo[d]thiazole (3i')

Yield: 78%, mp 165-168°C, <sup>1</sup>H NMR ( 400 MHz, CDCl<sub>3</sub>): δ = 2.99 (t, *J* = 4 Hz, 4H) 3.64 (t, *J* = 4 Hz, 4H), 7.48-6.69 (m, 9H, aromatic protons) <sup>13</sup>C NMR ( 100 MHz, CDCl<sub>3</sub>): δ = 48.71(2C), 50.21(2C), 111.49, 118.56, 119.27, 123.64, 126.11(2C), 130.90(2C), 140.79, 152.35, 152.90, 168.84 ESI-MS m/z: Calculated for C<sub>17</sub>H<sub>17</sub>N<sub>3</sub>S [M+H]<sup>+</sup> 295.11, Found 295.07

#### 4.2.2.10 2-(4-(4-nitrophenyl)piperazin-1-yl)benzo[d]thiazole (3j')

Yield: 71%, mp 165-168°C, <sup>1</sup>H NMR ( 400 MHz, CDCl<sub>3</sub>): δ = 3.55 (t, *J* = 12 Hz, 4H), 3.76 (t, *J* = 8 Hz, 4H), 7.98-7.01 (m, 8H); <sup>13</sup>C NMR ( 100 MHz, CDCl<sub>3</sub>): δ = 49.91(2C), 50.89(2C), 114.01, 119.16, 120.29, 121.44, 123.64, 125.32, 126.19, 130.08, 139.95, 141.38, 151.35, 158.90, 168.78 ESI-MS m/z: Calculated for C<sub>17</sub>H<sub>16</sub>N<sub>4</sub>O<sub>2</sub>S [M+H]<sup>+</sup> 340.10, Found 340.10

### 4.2.3 Biological Assay

C4-2 cells were sourced from Professor Zhou Wang at the University of Pittsburgh, Texas, USA, through a Material Transfer Agreement (MTA) with MDA Cancer Centre, USA. A-549 cancer cell line was procured from NCCS Pune. The cells were nurtured in RPMI media, enriched with 10% Fetal bovine serum (FBS), 1% L-glutamine, and 100 µg/ml streptomycin-penicillin. The cell culture was maintained in a 5% CO<sub>2</sub> incubator at a temperature of 37°C.

#### **4.2.3.1 MTT Assay**

The MTT assay is a commonly employed colorimetric method to evaluate cellular metabolic activity, viability, and proliferation. In the assessment of the impact of compounds **3a'**-**3j'**, C4-2 and A-549 cells were grown in a 96-well plate, with each well containing a final volume of 100  $\mu$ l. The cells were allowed to incubate for 24-48 hours prior to treatment with compounds at various concentrations, followed by an additional 24-hour incubation period. To measure cell viability, 10  $\mu$ l of MTT solution was introduced into each well, resulting in a concentration of 5 mg/ml. Subsequently, the cells were placed in an incubator for 4 hours at 37°C. The formazan crystals were dissolved using a solubilization solution (DMSO), and the absorbance of the resulting colored solution was assessed at a wavelength of 563 nm using an ELISA reader. The final data were analyzed using GraphPad Prism 8.0.

#### **4.2.3.2 CFU Assay**

To explore the potential of an individual cell to proliferate and form a substantial colony, an in vitro colony forming unit assay was carried out. C4-2 cells were propagated in six-well plates until they achieved 70-80% confluence. Subsequently, the cells were treated with various doses of compound **3g'** (10, 20, 30, 40, and 50  $\mu$ M) as well as a DMSO control for a duration of 48 hours. Following the treatment, an equal number of cells were evenly distributed in 10 cm dishes, and the colonies were counted using ImageJ software. This experiment was replicated three times, and each group had triplicates. Statistical analysis was performed using a t-test in GraphPad Prism 8.0, with a p-value below 0.05 considered indicative of statistical significance. This assay assessed the compound's efficacy in promoting colony growth.

#### **4.2.3.3 Wound Healing Assay**

To investigate the potential of compound **3g'** in promoting wound healing, an in vitro WHA was conducted. C4-2 cells were cultured in a monolayer within 6-well plates until they achieved 70-80% confluence. An incision was made using a sterilized 200  $\mu$ l pipette tip in the center of the cell unilayer, after which the cells were washed with PBS. Fresh RPMI media supplemented with 1% PenStrep, and 1% L-glutamine, 10% Fetal Bovine Serum was introduced to the wells, and a quantity of 19.45  $\mu$ M compound **3g** was introduced, with DMSO serving as the control. Bright-field images were captured using an LMI microscope to depict

the gap between the cells before the addition of compound 3g'. The plates were then kept in an incubator at 37°C with 5% CO<sub>2</sub>, and images of the incision were taken at 24, 48, 72, and 96 hours to monitor changes in the width of the gap. The ImageJ software was employed to quantify the wound diameter, and Graphpad Prism 8.0 was used to analyze the distance between the cells as a proportion of the wound area. A p-value below 0.05 was deemed to be statistically significant. This assay was conducted to evaluate the impact of compound 3g' on in vitro wound healing.

#### ***4.2.3.4 RNA Isolation, PCR amplification, and quantitative Real-Time expression analysis (RT-PCR)***

C4-2 cells were cultured in 10 cm dishes for two days until they reached 70-80% confluence. Subsequently, these cells were exposed to a dosage of 19.45 µM of compound 3g' and DMSO, respectively, and incubated for 24 hours. To extract total cellular RNA from the C4-2 cancer cell line, the Trizol method (Thermo Scientific) was employed adhering to the manufacturer's guidelines. Isolated RNA was then evaluated for quality by electrophoresis on a gel, and cDNA was synthesized using MMLV reverse transcriptase (Gibco) as per the protocol. The successful synthesis of cDNA was confirmed using GAPDH gene primers. Real-time PCR (Biorad) was utilized to assess the genes' relative expression levels employing SYBR® qPCR mixture (Kapa) and specific primers designed for the C4-2 cell line, with GAPDH serving as the control for normalization.

#### ***4.2.4 Molecular Docking Analysis***

The study involved the examination of the interaction between the synthesized compounds and the protein target, androgen receptor (AR), which was identified using the AutoDock 4 tool [210]. A scoring function based on energy was used to assess the affinity for binding of the ligands towards the molecular target, namely Androgen Receptor (PDB ID: 2PNU), which was sourced from the Protein Data Bank ( [www.rcsb.org](http://www.rcsb.org) ) [211]. AutoGrid was responsible for generating a grid map that represented the docking sites for the proteins. In the case of the protein, a grid measuring 60x60x60 points in each dimension was established. AutoGrid was utilized to define the spacing of grid points (0.375), and Gasteiger charges were calculated using AutoDock tools. After completing the docking protocols, RMSD clustering maps were obtained by re-clustering the data using the tolerances of 0.25, 0.5, and 1.0. This facilitated the identification of the cluster with ideal parameters with the highest number of populations and

the lowest energy score. Molecular docking analysis were then carried out using tools within Discovery Studio v2.5 to examine receptor-ligand interactions.

#### ***4.2.5 Molecular Dynamics Simulation (MDS)***

The molecular docking results of protein and ligand complexes were analyzed using MDS (Molecular Dynamics Simulations) in Desmond version 2020.1 [212] for 100<sup>th</sup> nano-seconds time scale. The initial phase in creating ligand-protein complexes for Molecular Dynamics Simulations (MDS) consisted of conducting docking experiments. In static scenarios, molecular docking studies can predict the binding state of the ligand. MDS commonly utilizes integration to track the motion of atoms over a period. Docking experiments provide a fixed snapshot of how a molecule interacts with a protein's active site. To investigate the dynamic behavior and atom movements over a period, molecular dynamics (MD) simulations are utilized. In these simulations, Newton's classical equation of motion is employed to calculate atom movements, allowing for the prediction of the ligand's binding state in a realistic physiological environment [213, 214]. The ligand-protein complex underwent an initial processing using the protein-preparation wizard, which encompassed minimization and fine-tuning of the complex. Every system was assembled utilizing the system-builder tool. The Solvent Model with an orthorhombic box (SPC) at 3 points, operating at 300K and 1 atm pressure, was employed in conjunction with the Transferable Inter-molecular Interaction Potential (TIIP), and the OPLS 2005 force field was chosen for the simulations [215, 216]. The models were inverted and utilized to replicate physiological conditions, incorporating counter ions and 0.15 M sodium chloride, respectively. The ultimate Molecular Dynamics Simulation (MDS) run was carried out for a duration of 100 nanoseconds. Subsequently, the complexes were examined for their primary components in principal modes ( PC1 and PC2 ) modes utilizing geo measures version 0.8. [217]. The geo measures module records eigen values and represents them in a three-dimensional plot using the Python tool Matplotlib, which is commonly used for statistical computing. The most recent production run was executed at a pace of 100 nano-seconds per unit. Various metrics, including the count of H-bonds, RMSD, RMSF, Rg and SASA were utilized to evaluate the consistency of the Molecular Dynamics Simulations (MDS). The analysis of the 100 nanoseconds simulation was utilized to monitor stability [218].

#### **4.2.6 Binding Free Energy Examination**

The binding free energies of the protein-ligand complexes were determined using the MM GBSA approach, which integrates molecular mechanics calculations with the GBSA method. The Python script "thermal mmgsa.py" was employed to calculate the Primary MM GBSA binding free energy for the ligands. This calculation was performed using the last 50 frames of a simulation trajectory, with a sampling interval of 1 step. The Prime MM GBSA binding free energy, expressed in kcal/mol, was computed by adding up different energy elements, encompassing covalent bonds, coulombic interactions, H-bonds, van der Waals forces, self-contacts, lipophilic interactions, and solvation energies, were considered for protein-ligand complex. This approach follows the principle of additivity, where each energy term contributes to the overall binding free energy ( $\Delta G_{\text{bind}}$ ). The equation for computing  $\Delta G_{\text{bind}}$  is expressed as follows:

$$\Delta G_{\text{bind}} = \Delta G_{\text{Covalent}} + \Delta G_{\text{Hbond}} + \Delta G_{\text{vdW}} + \Delta G_{\text{Lipo}} + \Delta G_{\text{Solv\_GB}}$$

In this equation, each term represents the contribution of a specific energy component to the total binding free energy ( $\Delta G_{\text{bind}}$ ). The MM-GBSA method provides a comprehensive estimation of binding affinity by taking into account multiple energetic factors.

#### **4.2.7 ADMET Analysis**

To confirm the biological results, we assessed the in silico predictions for the ADMET properties of all compounds were generated using the SWISS-ADME software. Evaluating these physicochemical properties is crucial in assessing whether a molecule conforms to Lipinski's rule of five, which is a key factor in determining its suitability as a potential drug candidate [219, 220]. Lipinski's rule of five relies on four essential molecular characteristics to gauge whether a compound possesses desirable drug-like qualities. A compound is considered viable if it attains a score above 1 and demonstrates a specified biological activity of 330 or more. In simpler terms, when a compound's physicochemical properties meet these criteria, it is more likely to be regarded as a potentially active and efficacious molecule for its intended use.

## 4.3 Results and discussion

### 4.3.1 Chemistry

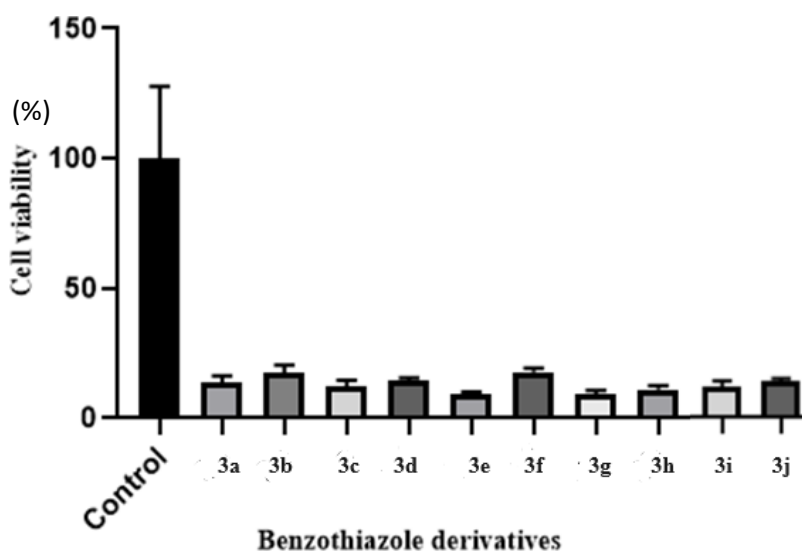
In the past, various techniques have been devised for the synthesis of benzothiazole derivatives containing 2-substituted amines. Typically, these derivatives are prepared by replacing amines with hetero-aryl halides using different combinations of metals and bases like Mn, Cu, Ag, Co, Ni, or Fe. However, some of these methods have drawbacks, including being non-recyclable, toxic, expensive, sensitive to moisture, harmful to the environment, and requiring high reaction temperatures. To address these issues, a new, gentler approach for directly aminating azoles was explored. This method aims to be cost-effective and environmentally friendly. Building upon previous innovative techniques, the current method for synthesizing 2-substituted thiazoles through C-N coupling adheres to the principles of green chemistry.

The initial research focused on aminating 2-chlorobenzothiazole (1mmol) under different reaction conditions, using 2 equivalents of a base in a water-based solvent (2 mL). Among the tested bases, NaOH yielded good results. Interestingly, even without the use of a base, the reaction proceeded and provided satisfactory yields. Increasing the reaction \*t

emperature had minimal impact (**Scheme 4.1**). After a thorough examination of various factors, it can be that the intended cross-coupling product can be achieved by mixing 2-chloro benzothiazole (1mmol) with twice the equivalent amount of a secondary amine at ambient temperature. in a 2 mL water solvent.



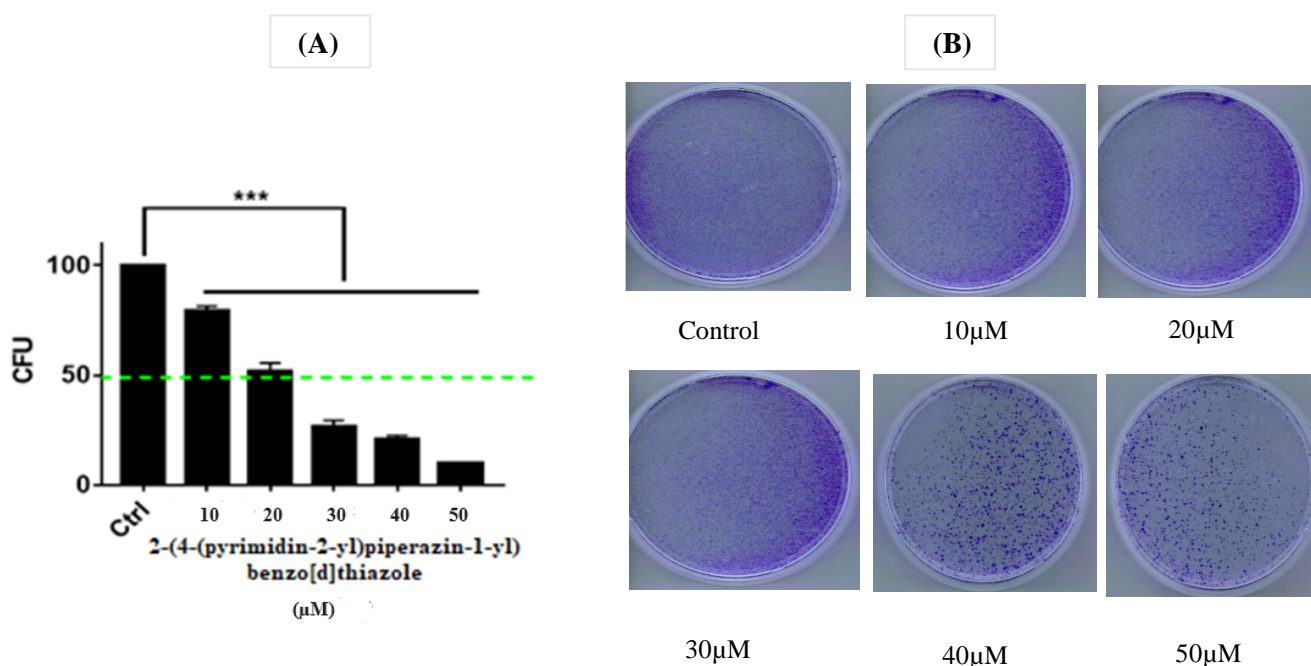




**Fig. 4.2.** Evaluation of compound cytotoxicity (3a'-3j') using MTT assay

#### 4.3.2.2 CFU assay indicated the suppression of cellular growth in vitro dose-dependently

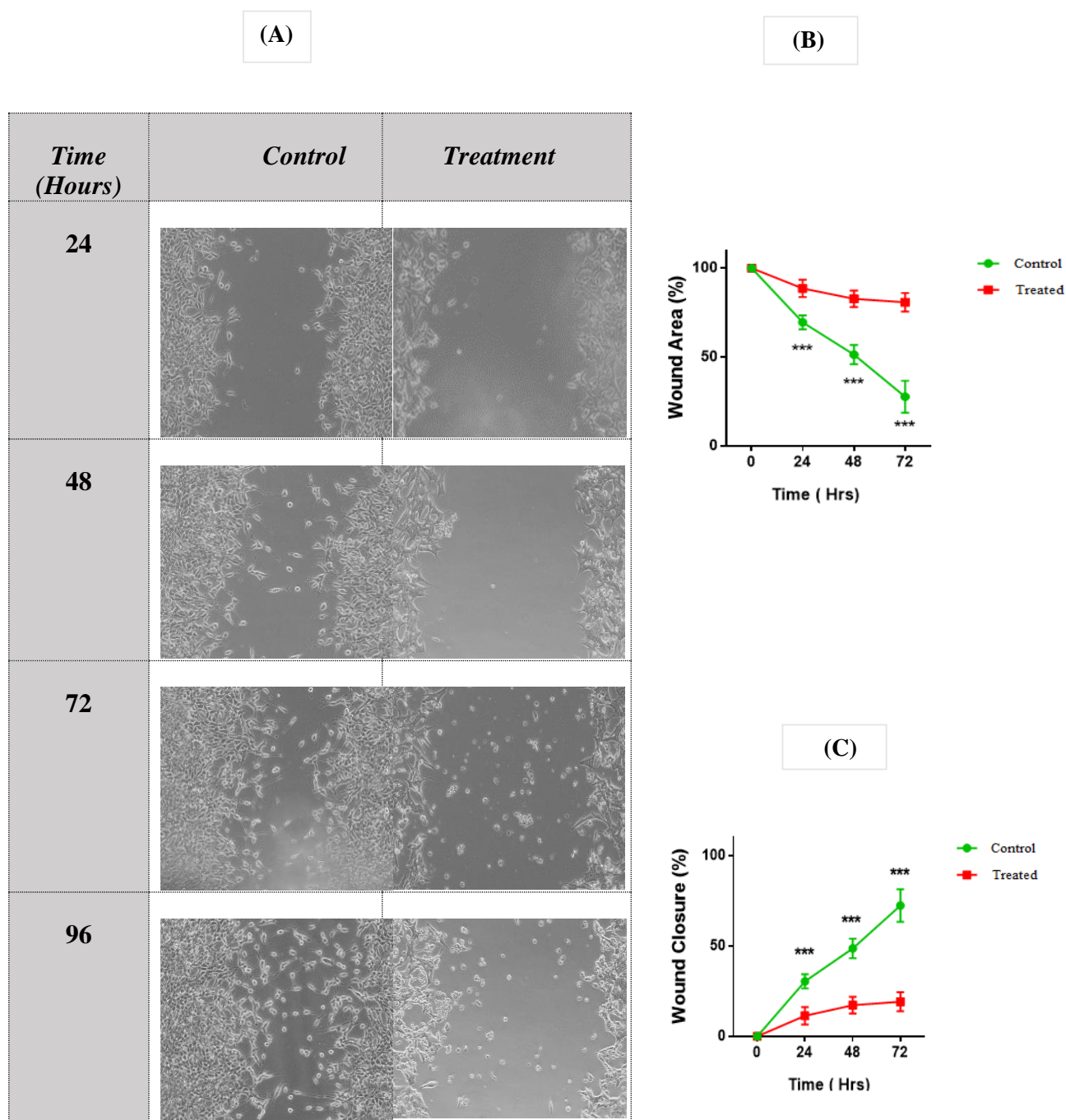
CFU assay was carried out to examine how the growth of prostate cancer cells is influenced by different concentrations of compound 3g'. In this experiment, C4-2 cells were subjected to different concentrations of 3g', varying from 10 to 50 $\mu$ M, while DMSO was used as a control (**Figure 4.3**). The findings indicated that as the concentration of 3g' increased, there was a corresponding decrease in the ability of C4-2 cells to form colonies, showing a dose-dependent response (Fig. 4.3(B)). Precisely, a 50% reduction in cell proliferation was noted at a concentration of 19.45  $\mu$ M in C4-2 cells (Fig. 4.3(A)). This experiment was conducted in triplicate, and both ImageJ software and Graphpad Prism 8.0 were employed for image analysis and quantification. The statistical significance was established at \*P < 0.0001. These results provide an evidence of the suppression of colony formation in C4-2 cells by compound 3g' dose-dependently.



**Fig. 4.3.** Inhibition of C4-2 cancer cell colony formation by compound 3g' (A) Graphical illustration of the dose-dependent suppression of colony formation in C4-2 cells in vitro. (B) Examination of formation of colonies by the C4-2 cancer cell line is influenced by different concentrations of 3g, specifically 10, 20, 30, 40, and 50 μM and DMSO as control.

#### 4.3.2.3 Compound 3g suppresses wound healing/cell migration in vitro

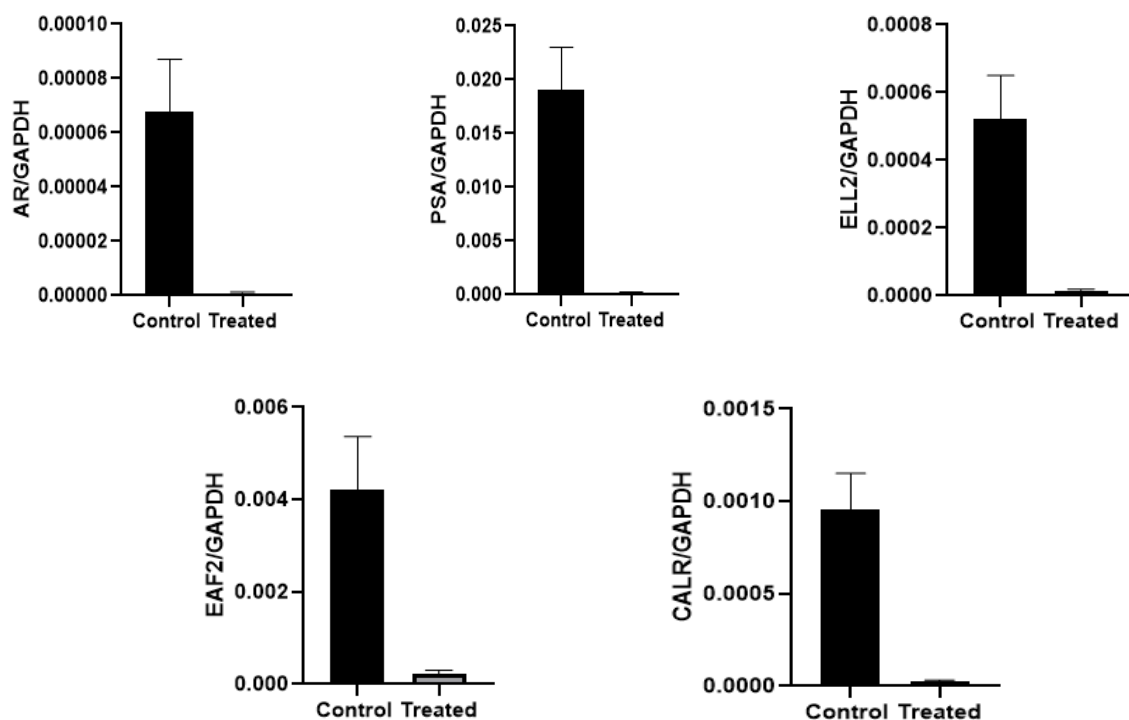
WHA assay results revealed that the derivative 3g' effectively lessened the migration of cancer cells in a time dependent manner. The width of the cell gap was measured at different time points, specifically at 24, 48, 72, and 96 hours after treatment, using ImageJ software (NIH) (Fig. 4.4(A)). The wound area (Fig. 4.4(B)) and the closure of the wound gap (Fig. 4(C)) were quantified using Image J software, and the experiment was carried out in triplicate. Analysis of the data was conducted using Graphpad prism 8.0, and statistical significance was indicated by \*P < 0.0001. These findings indicated a noteworthy inhibitory effect of compound 3g' on the process of wound healing and cellular migration in the C4-2 cell line over time.



**Fig. 4.4.** Time-dependent wound healing inhibition in C4-2 cancer cells by compound 3g' (A) To visually demonstrate the reduction in cell migration in C4-2 cell line treated with compound 3g' in comparison to a control group treated with DMSO. (B) We measured the widths of gaps in the C4-2 cancer cell layer at 24, 48, 72, and 96 hours following treatment to evaluate how compound 3g' affects the inhibition of cell migration over time. (C) A representative image was included to showcase the closure of the wound in C4-2 cells following treatment with compound 3g'.

#### 4.3.2.4 Compound 3g' reduces the expression of genes that respond to androgens

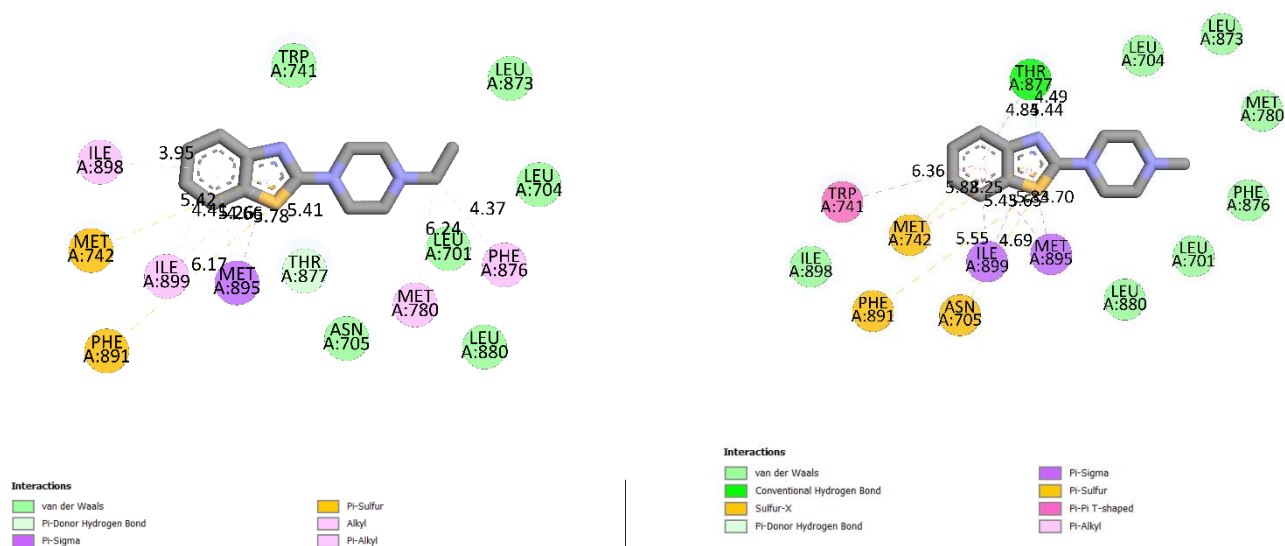
Androgens are recognized for their role in the growth as well as progression of prostate cancer, and the androgen responsive pathway is commonly used as an indicator to monitor the advancement in human prostate cancer. In this examination, the effects of a compound called 2-(4-(pyrimidin-2-yl)piperazinyl)benzo[d]thiazole on the expression of androgen receptor (AR) target genes were investigated in C4-2 cell lines using RT-PCR. The findings of the study showed that this compound effectively reduced the expression of PSA and AR in C4-2 cells when tested in vitro. Additionally, the compound also demonstrated the ability to suppress the expression of ELL2, CALR, and EAF-2, which are genes responsive to AR, in C4-2 cells in vitro (as shown in Fig. 5). Interestingly, it was observed that the compound may additionally have a negative impact on AR negative cells, leading to the suppression of ELL2, a gene known to impede cancer cell proliferation in such cells. These findings suggest that compound 3g' has the potential to suppress the basal transcriptional activity of AR. The gene expression was normalized using GAPDH (glyceraldehyde-3-phosphate dehydrogenase), and statistical analysis was carried out using Graphpad prism 8.0, with significance value indicated as \*P < 0.0001.



**Fig. 4.5.** Real-time gene expression of androgen-responsive genes after intervention with compound **3g'** (**19.45  $\mu$ M**) compared to DMSO as vehicle control.

### 4.3.3 Molecular Docking Study

AutoDock was utilized to assess the binding energy of compound **3g'** within the active site of the AR protein target. The interaction between the protein and **3g'** was stabilized through the formation of multiple H-bonds and other stacking interactions with crucial residues of the protein. The docking analysis implied that the binding affinity between AR and **3g'** was the highest, with a score of -9.87 kcal/mol. 2D representations of the inter-molecular interactions between the docked compounds (**3a-3h**) and the target protein were generated (shown in Fig. 4.6). Notably, amino acid residues such as *Met 749*, *Met 745*, *Gly 708*, *Trp 741*, *Arg 752*, *Met 742*, *Asn 705*, *Leu 880*, *Thr 877*, *Phe 876*, *Phe 891*, *Leu 701*, *Leu 707*, *Phe 764*, *Leu 704*, and *Gln 711* (as listed in Table 4.1) played a significant role in the docking of compound **3g'** to the AR target protein.





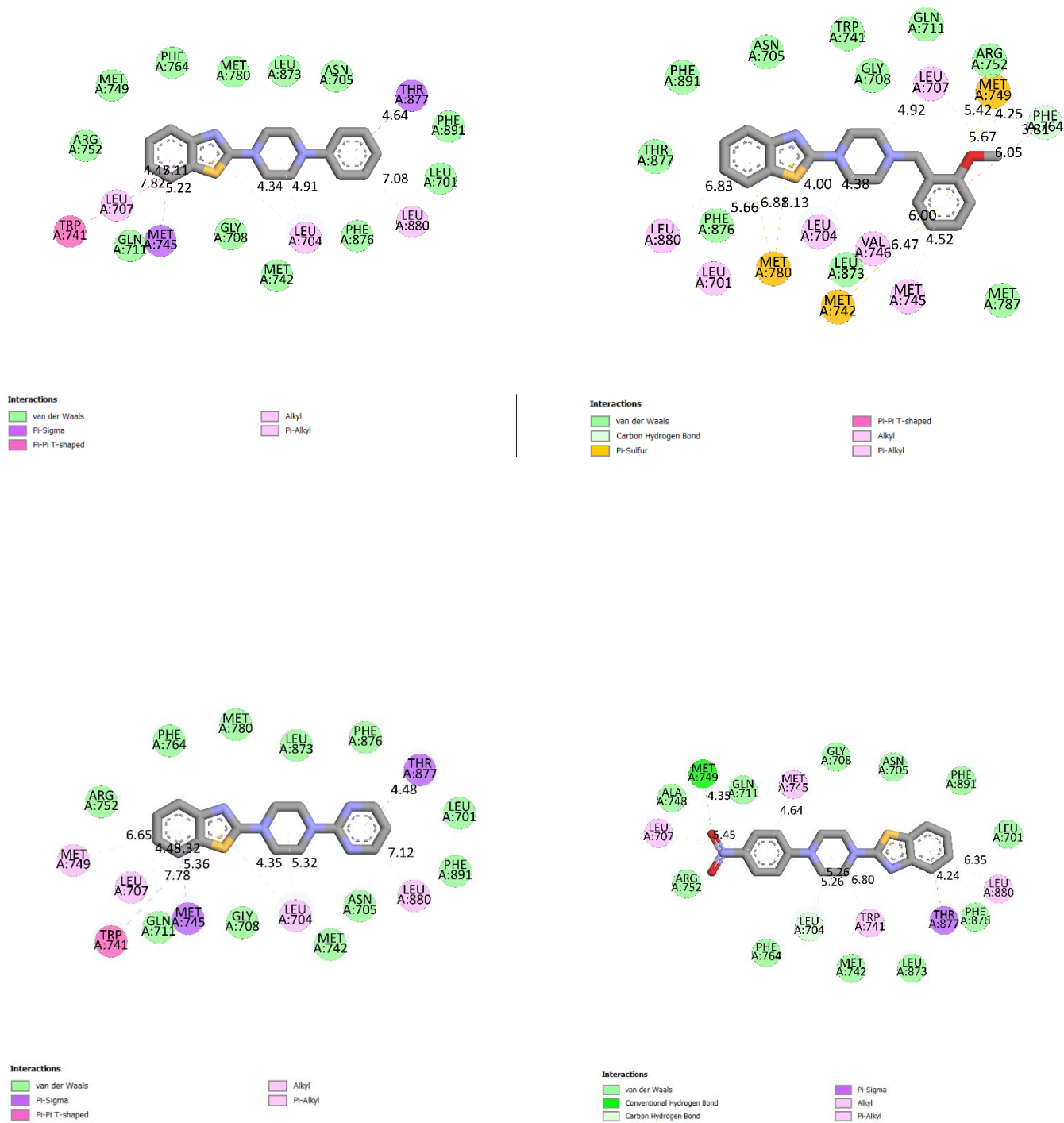


**Fig. 4.6.** 2D representation depicting the binding interactions between the AR protein binding-site and compounds 3a'-3j'

**Table 4.1:** Energy bonding score of compounds (**3a'**-**3j'**) against AR protein target

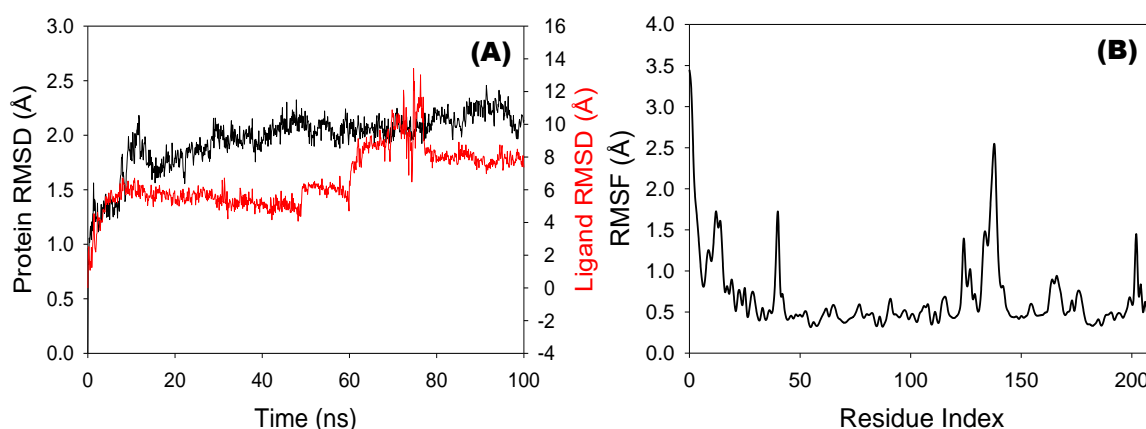
Compound	Amino acid residues	Energy binding score (kcal/mol)
<b>3a'</b>	<i>MET (749), MET (787), MET (742), PHE (876), VAL (746), MET (780), LEU (875), LEU (701), THR (877), LEU (880), PHE (784), LEU (704), LEU (701), MET (745), ASN (705)</i>	7.63 -
<b>3b'</b>	<i>MET (741), MET (742), MET (780), LEU (704), ASN (705), PHE (891), LEU (880), LEU (701), ILE (898), ILE (899), MET (895), PHE (876)</i>	7.26 -
<b>3c'</b>	<i>ARG (752), MET (745), VAL (745), MET (742) LEU (873), MET (780), LEU (880), MET (787), PHE (891), ASN (705), LEU (704), LEU (707), MET (749), THR (877), PHE (876), LEU (701), PHE (764), GLN(711)</i>	9.50 -
<b>3d'</b>	<i>MET (745), ARG (752), MET (787), MET (742), VAL (746), MET (749), LEU (880), PHE (891), MET (780), ASN (705), LEU (704), PHE(764), LEU(873),THR(877), PHE(764), PHE(876), , LEU(701)</i>	7.46 -
<b>3e'</b>	<i>TRP (741), MET (749), GLN (711), MET (745), ARG (752), PHE (764), LEU (707), GLY (708), LEU (704), PHE (875) ASN (705), MET (780), LEU (701), LEU (880), THR (877), PHE (891)</i>	7.64 -
<b>3f'</b>	<i>THR (877), PHE (876), PHE (891), LEU (701),ASN (705), LEU (704),GLY (708), MET (745), ARG (752), VAL (746),MET (749), THR (877), GLN(711), MET (787)</i>	-9.55
<b>3g'</b>	<i>PHE (764), GLN (711), MET (749), MET (745), TRP (741), ARG (752), MET (742), LEU (880), THR (877), PHE (876), PHE (891), LEU (701),ASN (705), LEU (704),GLY (708), LEU (707)</i>	<b>9.87</b> -
<b>3h'</b>	<i>MET (749), MET (787), PHE (764), ARG (752), PHE (876), LEU (880), MET (780), PHE (891), LEU (701), LEU (707), THR(877), ASN (705), TRP (741), LEU (704), MET (742), GLY (708), MET (745), LEU (873), VAL (746)</i>	8.87 -
<b>3i'</b>	<i>ARG (752), MET (745), LEU (707), GLY (708), TRP (741), GLN (711), MET (749), ASN (705), GLN (711), LEU (701), PHE (876), PHE (891), THR (877), LEU (880), PHE (764), LEU (704)</i>	9.37 -
<b>3j'</b>	<i>LEU (880), MET (787), PHE (891), ASN (705), LEU (704), LEU (707), MET (780), LEU (880), MET (787), PHE (891), LEU (704),PHE (764), ASN(705), MET (780), PHE(764)</i>	-8.01



### 4.3.4 Molecular Dynamics Simulation

MD simulation was conducted to assess the convergence including stability of the 2PNU+3g' system over a 100-nanosecond period. The results indicate that the conformation of the system remained relatively stable, which is evident from RMSD analysis. Specifically, the RMSD of the C $\alpha$ -backbone of 2PNU+3g' showed a stable value of 2.0 Å. However, the 3g ligand displayed significant conformational changes, with its RMSD remaining constant until 50 ns, after which it overshot and stabilized at 8 Å (as shown in Fig. 4.7(A)). This behavior indicates that the protein Stromelysin, when bonded to the 3g' ligand, exhibits stable conformations due to a strong affinity with the ligand. RMSF plot revealed notable alterations in the Stromelysin protein bound to the 3g' ligand at specific residues, namely 5-20, 48, 115-125, and 130-148 (as depicted in Fig. 4.7(B)). These fluctuations indicate higher flexibility in these regions, while most of the residues remained relatively stable throughout the entire 100 ns simulation, suggesting that their conformations remained rigid. R<sub>g</sub> was used to measure the compactness of the 2PNU C $\alpha$ -backbone when bound to the 3g' ligand. The R<sub>g</sub> value decreased from 16.9 to 16.54 Å during the simulation, indicating a tendency towards a more compact conformation (as illustrated in Fig. 4.7(C)).

A decrease in R<sub>g</sub> implies that the protein takes on a highly compact structure when it is bound to the ligand. To gauge the strength of interaction and overall stability of the complex, the number of H-bonds formed between the 2PNU protein and the 3g' ligand was monitored. Throughout the 100 ns simulation, the analysis revealed the presence of a few hydrogen bonds on average, as depicted in Fig. 4.7(D).



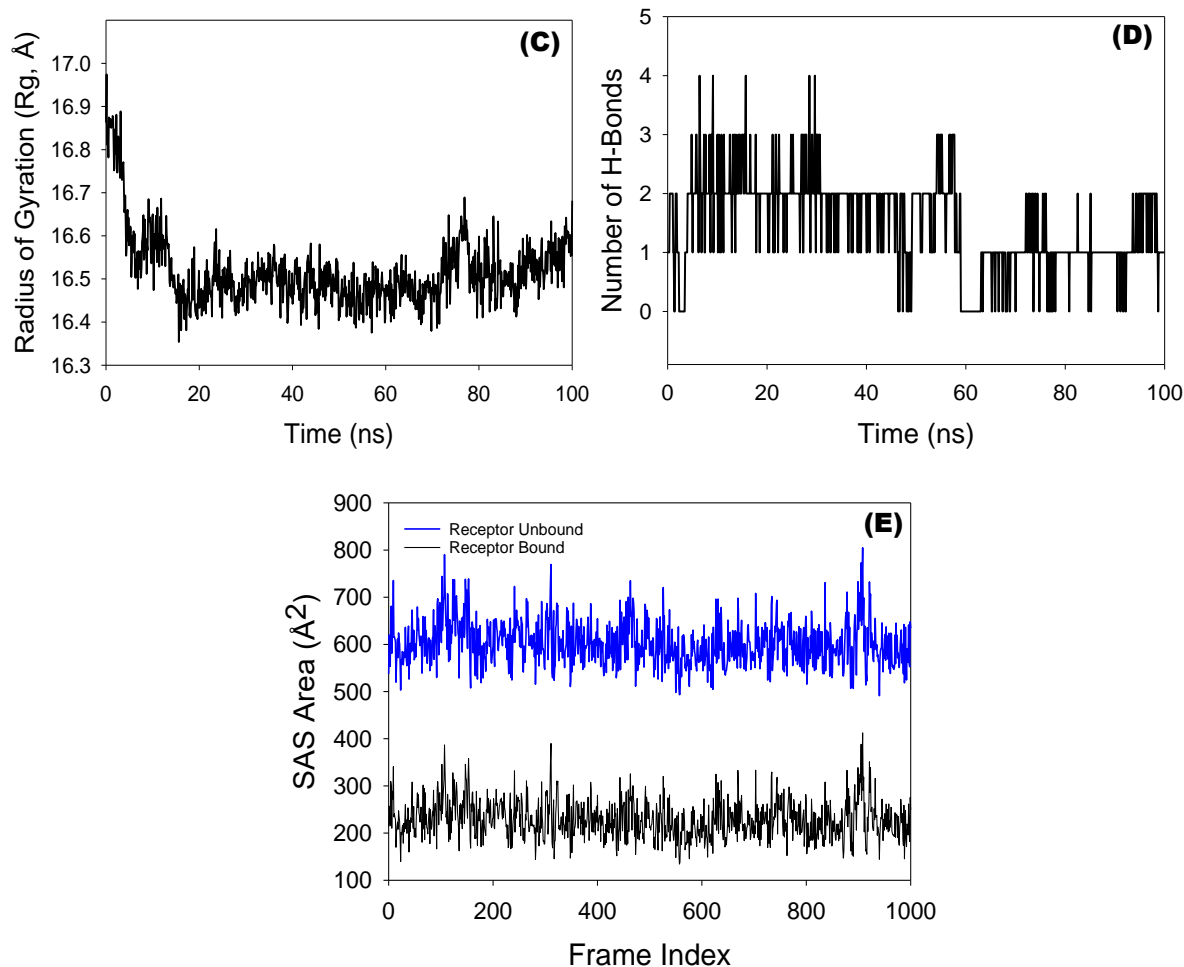


**Fig. 4.7.** M.D. simulation analysis of 100 ns trajectories of the protein and ligand (AR protein and 3g') (A) C $\alpha$  backbone RMSD of 2PNU+3g' (B) RMSF of C $\alpha$  backbone of 2PNU+3g' (C) C $\alpha$  backbone Rg of 2PNU+3g' (D) Formation of H-bonds in 2PNU+3g' (E) Solvent accessible surface area 2PNU+3g'.

Following the analysis of the radius of gyration (Rg), similar trends were observed in the SASA when comparing the unbound and ligand bonded states. As shown in Figure 4.7(E), in the absence of the 3g' ligand and in the unbonded state to the binding protein 2PNU, a large surface area was observed to be exposed to the solvent. However, when the protein formed complexes with the ligands, the SASA values decreased, indicating a reduction in the solvent-accessible surface area. The extent of this reduction in the peak reflects the tightness of the ligand-protein binding. The comprehensive Rg analysis further suggests that ligand binding leads to a higher level of compactness in the respective proteins.

### 4.3.5 MM-GBSA calculations

Using M.D. simulation data, the MM-GBSA approach was employed to calculate the binding free energy and various contributing energies for the complex of 2PNU and the 3g' ligand. The results, presented in Table 4.2, highlight the significant roles played by  $\Delta G_{\text{bindCoulomb}}$ ,  $\Delta G_{\text{bindvdW}}$ , and  $\Delta G_{\text{bindLipo}}$  in enhancing the stability of simulated complexes. Alternatively,  $\Delta G_{\text{bindCovalent}}$  and  $\Delta G_{\text{bindSolvGB}}$  contribute towards the instability of these complexes. Importantly, the 2PNU+3g' complexes displayed notably higher binding free energies. This suggests that the 3g' ligand exhibits a strong binding affinity to the protein, effectively forms stable complexes, and demonstrates efficient binding to the respective protein.

**Table 4.2:** Binding free energy components for the 2PNU+3g' calculated from MM-GBSA.

Energies ( in kcal/mol )	2PNU+3g'
$\Delta G_{\text{bind}}$	- 77.35
$\Delta G_{\text{bindLipo}}$	-10.75
$\Delta G_{\text{bindvdW}}$	-45.60
$\Delta G_{\text{bindCoulomb}}$	-39.68
$\Delta G_{\text{bindHbond}}$	-5.14
$\Delta G_{\text{bindSolvGB}}$	25.56
$\Delta G_{\text{bindCovalent}}$	1.72

### 4.3.6 Free Energy Landscape (FEL) and PCA analysis

PCA was applied to carefully examine the M.D. simulation trajectories of the protein-ligand complex, with the aim of deciphering the stochastic, overall movement of atoms within the amino acid residues. This analysis, as depicted in Fig. 4.8, seeks to unravel the scattered and flexible trajectories observed in the data that can largely be due to the inherent unpredictability and non-correlated global motion intrinsic to structure of the protein. The covariance matrix generated from this analysis captures the temporal variation of internal coordinate mobility qhprojected into 3D space over the course of a 100-nanosecond simulation. This recorded data

enables the interpretation of rational motion within each trajectory through orthogonal sets called Eigen vectors. The M.D. simulation trajectory, specifically focusing on the C- $\alpha$  protein atoms, reveals an unorganized orientation, particularly in principal components (PC1, PC2) modes. Frames are scattered in various directions without forming distinct clusters, as illustrated in Fig. 4.9(A). In contrast, higher principal components like PC2 and PC3 display a more congruent clustering toward the center, as shown in Fig. 4.9(B). Similarly, in higher PC9 and PC10, frames exhibit a greater correlation toward the center due to better alignment of the coordinates, as depicted in Fig. 4.9(C). The last 100 frames of the trajectory are predominantly situated toward positive Eigen values, indicating ordered global motion. This observation suggests that the system has achieved stability and is located at global minima.

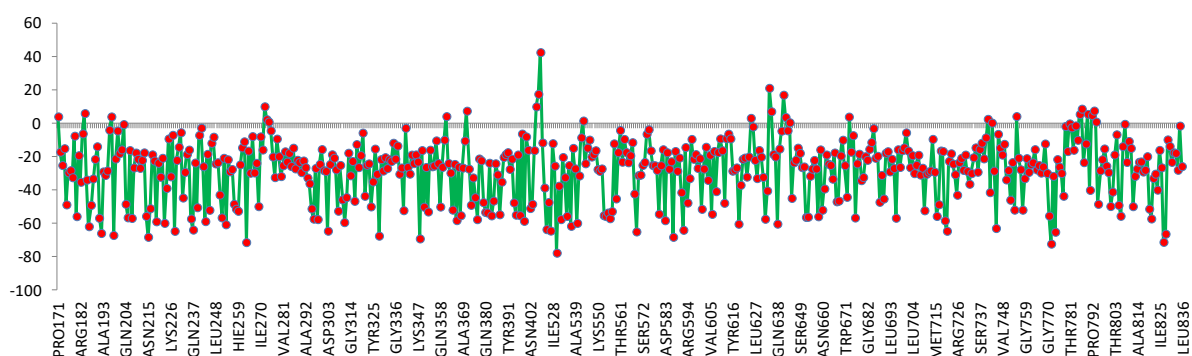


**Fig. 4.8.** Free energy decomposition of individual residues of protein during ligand binding

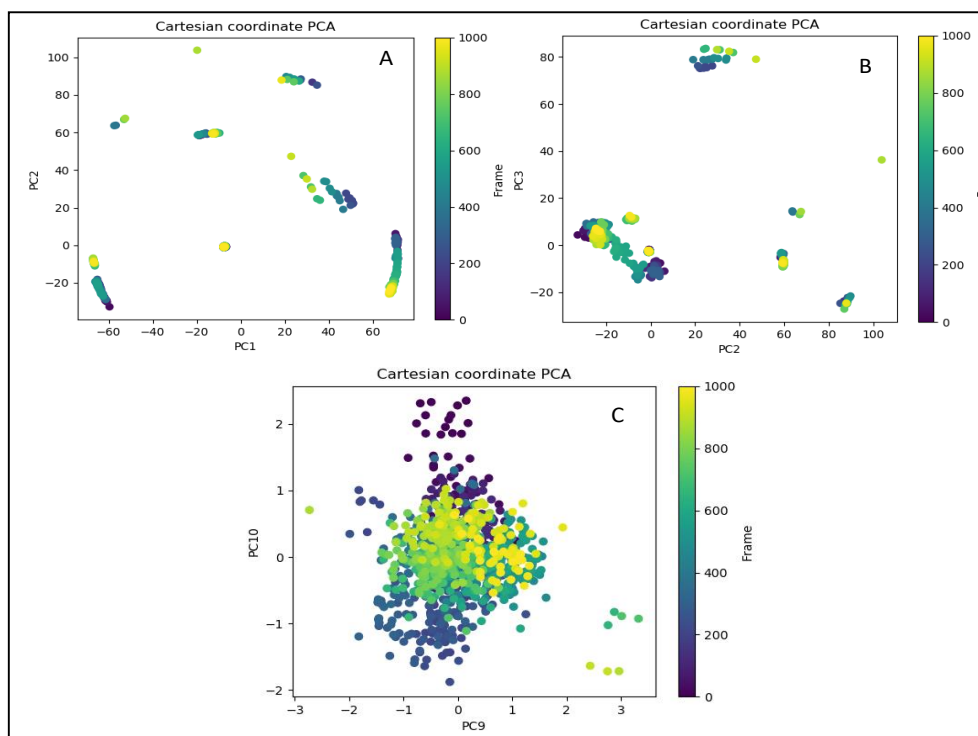


**Fig. 4.9.** PCA-analysis performed on the eigenvalues of 1000 frame cartesian coordinates extracted from the MD trajectory of the ligand-protein complex over a period of 100 nanoseconds. Free energy breakdown of isolated residues of protein during binding with the ligand (A) PC 1 and PC 2, (B) PC 2 and PC 3 (C) PC 9 and PC 10.

#### **4.3.7 ADMET and drug likeness properties**

The compounds chosen for this study have been found to adhere to Lipinski's Rule of Five without any violations, as indicated in Table 4.3. This finding implies that these compounds exhibit favorable drug-like properties, positioning them as promising candidates for further exploration in drug development. Their compliance with Lipinski's Rule of Five suggests a greater probability of successful processes such as absorption, distribution, metabolism, and excretion, all of which are crucial for their potential effectiveness as orally administered drugs.

**Table 4.3.** ADMET and drug-likeness properties of the screened molecules

<b>Derivative</b>	<b>Mol. formula</b>	<b>Mol. weight</b>	<b>No. of rotatable bonds</b>	<b>No. of H-bond acceptors</b>	<b>No. of H-bond donors</b>	<b>Lipinski's rule</b>
3a'	C <sub>13</sub> H <sub>17</sub> N <sub>3</sub> S	247.36	2	2	0	YES
3b'	C <sub>12</sub> H <sub>15</sub> N <sub>3</sub> S	233.33	1	2	0	YES
3c'	C <sub>16</sub> H <sub>21</sub> N <sub>3</sub> O <sub>2</sub> S	319.42	4	3	0	YES
3d'	C <sub>13</sub> H <sub>18</sub> N <sub>4</sub> S	262.37	3	3	1	YES
3e'	C <sub>13</sub> H <sub>17</sub> N <sub>3</sub> OS	263.36	3	3	1	YES
3f'	C <sub>19</sub> H <sub>21</sub> N <sub>3</sub> S	323.46	3	3	1	YES
3g'	C <sub>15</sub> H <sub>15</sub> N <sub>5</sub> S	297.38	2	3	0	YES
3h'	C <sub>19</sub> H <sub>21</sub> N <sub>3</sub> OS	339.45	4	3	0	YES
3i'	C <sub>17</sub> H <sub>17</sub> N <sub>3</sub> S	295.4	2	1	0	YES
3j'	C <sub>17</sub> H <sub>16</sub> N <sub>4</sub> O <sub>2</sub> S	340.40	4	3	1	YES

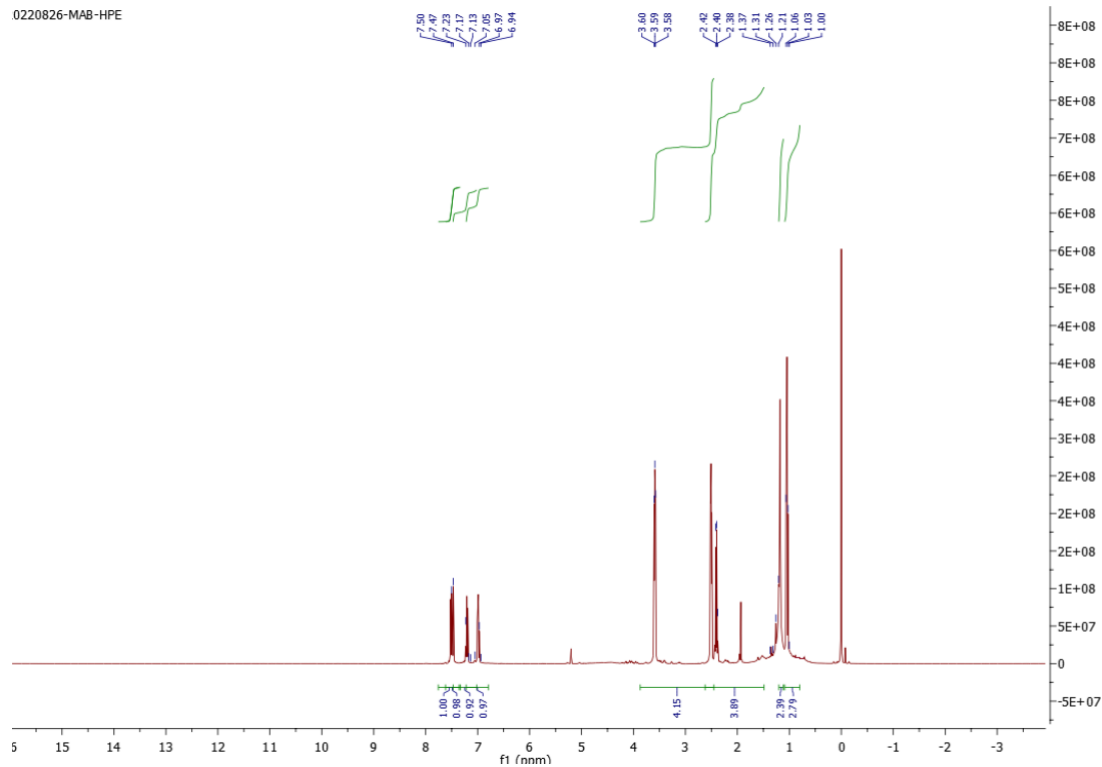
#### 4.4 Conclusion

Benzothiazoles are a diverse group of synthetic compounds with a broad spectrum of pharmacological effects. Some of their derivatives have shown promise in fighting cancer at various stages of its development. Specifically, a synthesized derivative called 2-(4-(pyrimidin-2-yl) piperazin-1-yl) benzo[d]thiazole has displayed impressive effectiveness against the C4-2 cancer cell line. These promising results have inspired the development of small molecules for cancer therapy. Moreover, this derivative has successfully reduced the expression of several genes associated with androgen response, such as AR, EAF2, ELL2, PSA, and CALR, in castration-resistant prostate cancer cells in laboratory settings. Computational analyses have indicated that compound 3g has the highest binding affinity for the AR protein, making it a potential lead candidate with favorable pharmaco-kinetic properties. Molecular dynamics simulations have verified the stability of both the protein and the ligand during interactions. Calculations of binding free energy have shown a significant binding affinity between the ligand and the protein ( $\Delta G$ ) of -77.35 kcal/mol. Principal component analysis has demonstrated a stable and converged structure, suggesting the potential of these compounds as a viable treatment option for prostate cancer.

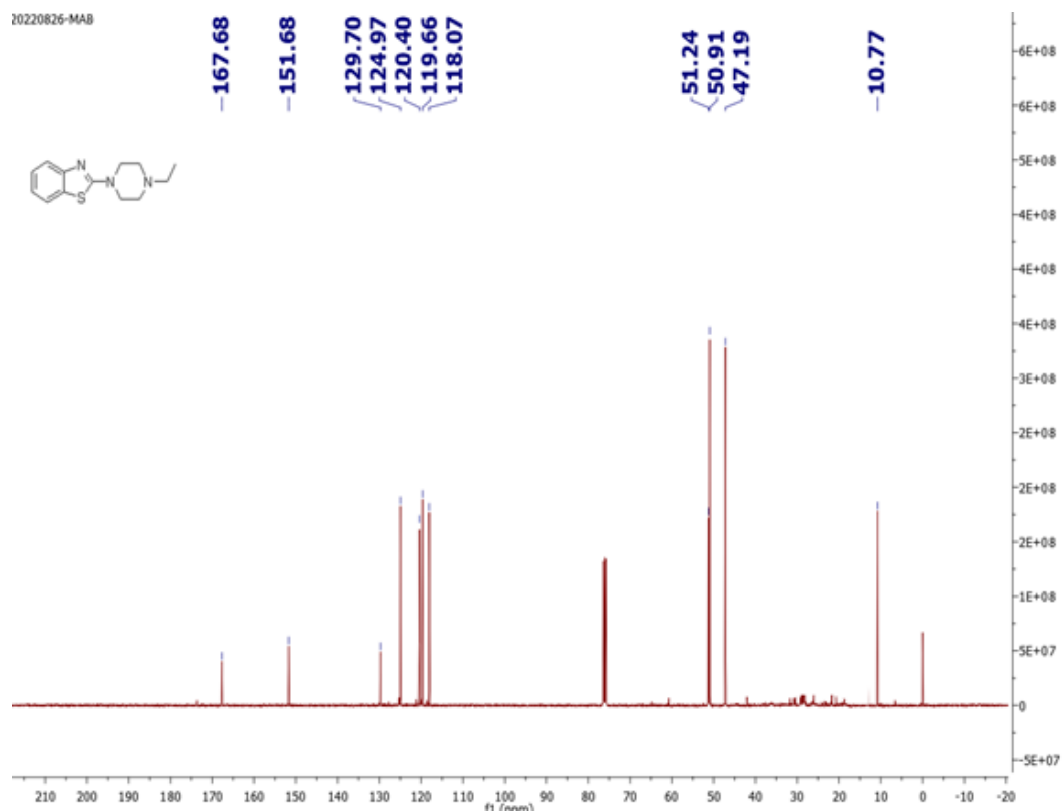
## Representative spectra

### 4.2.2.1 (3a')

0220826-MAB-HPE

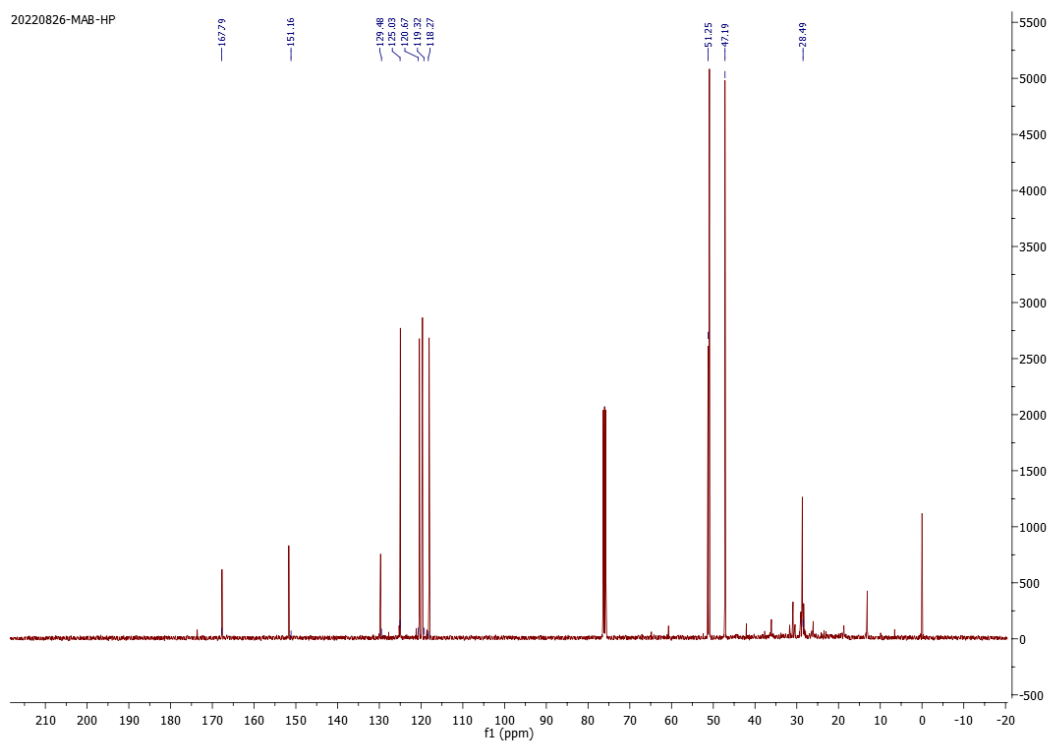
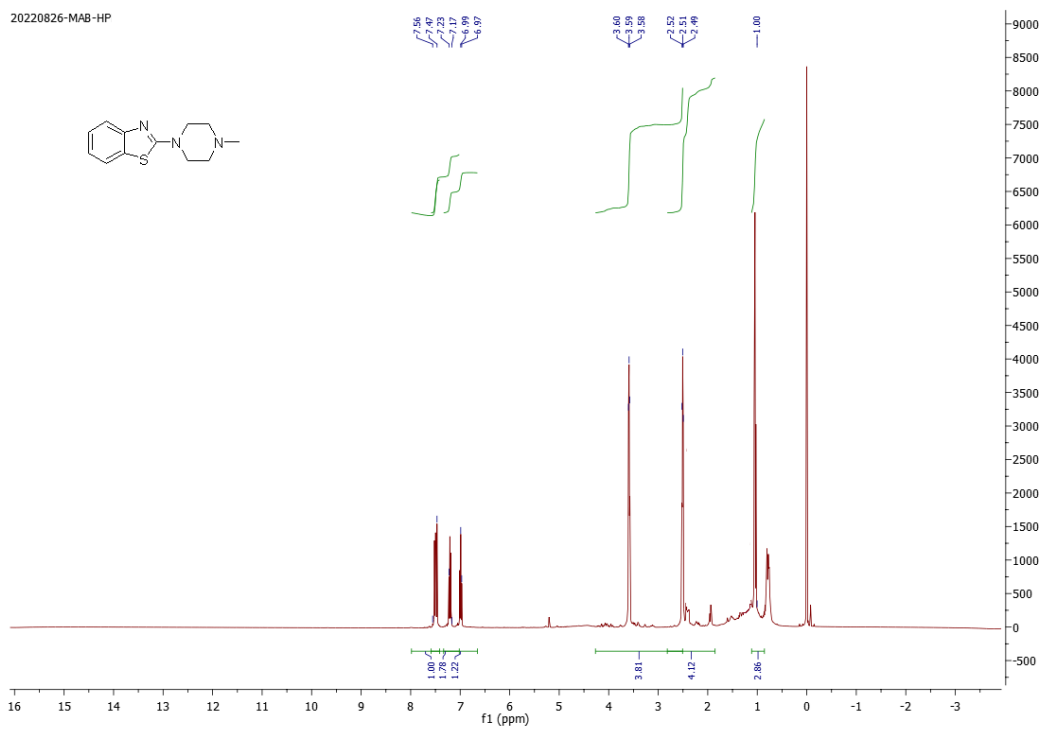


20220826-MAB



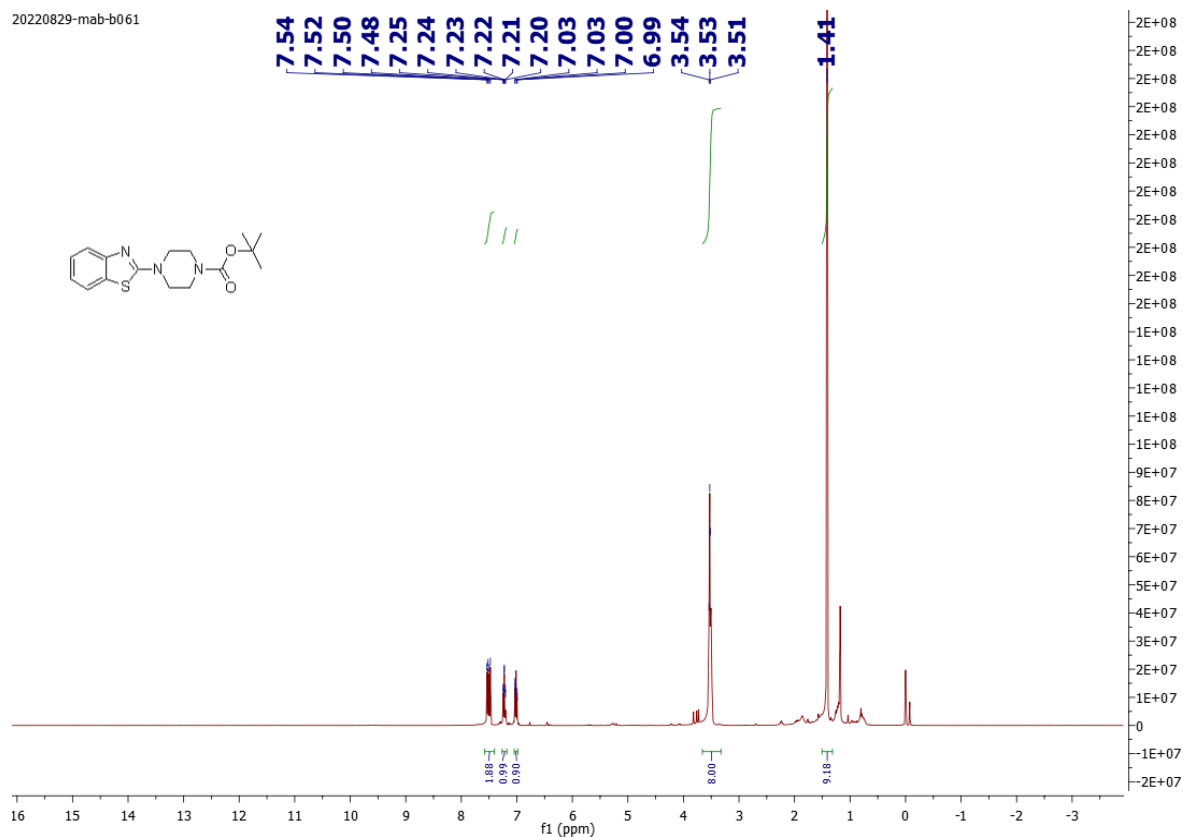


### 4.2.2.2 (3b')

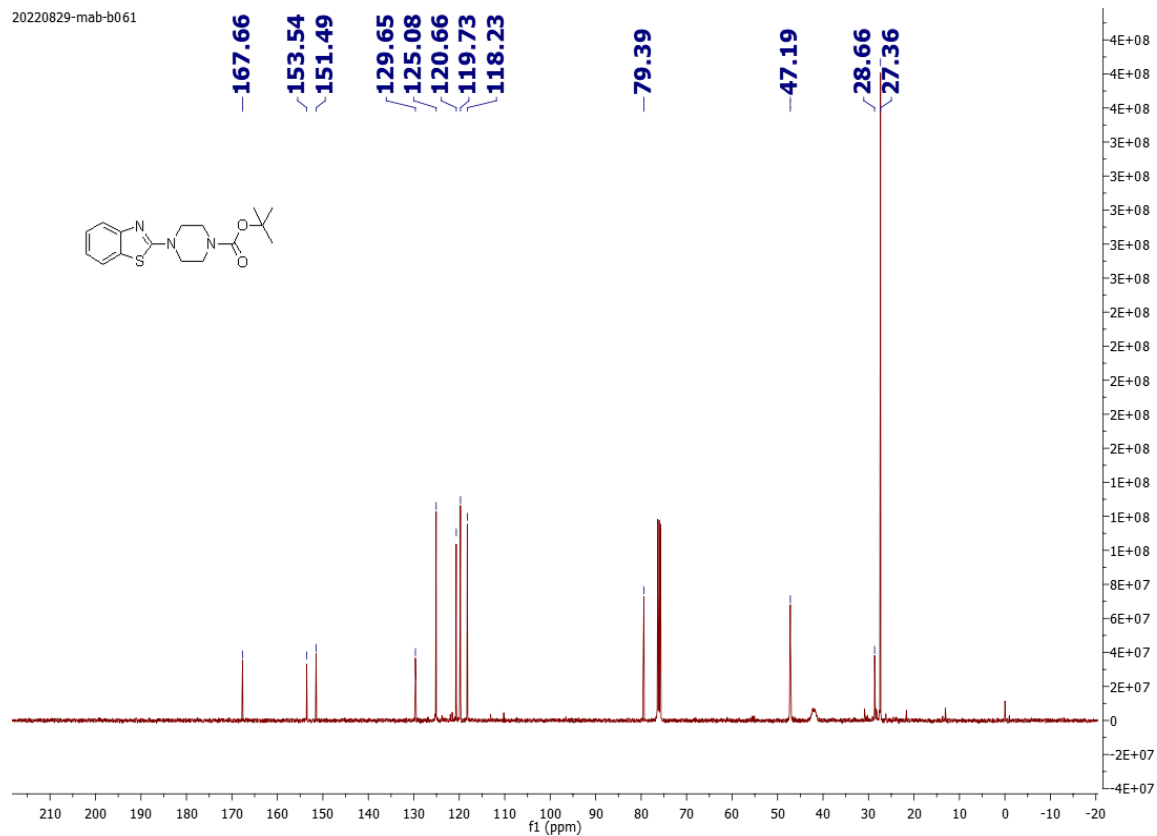


### 4.2.2.3 (3c')

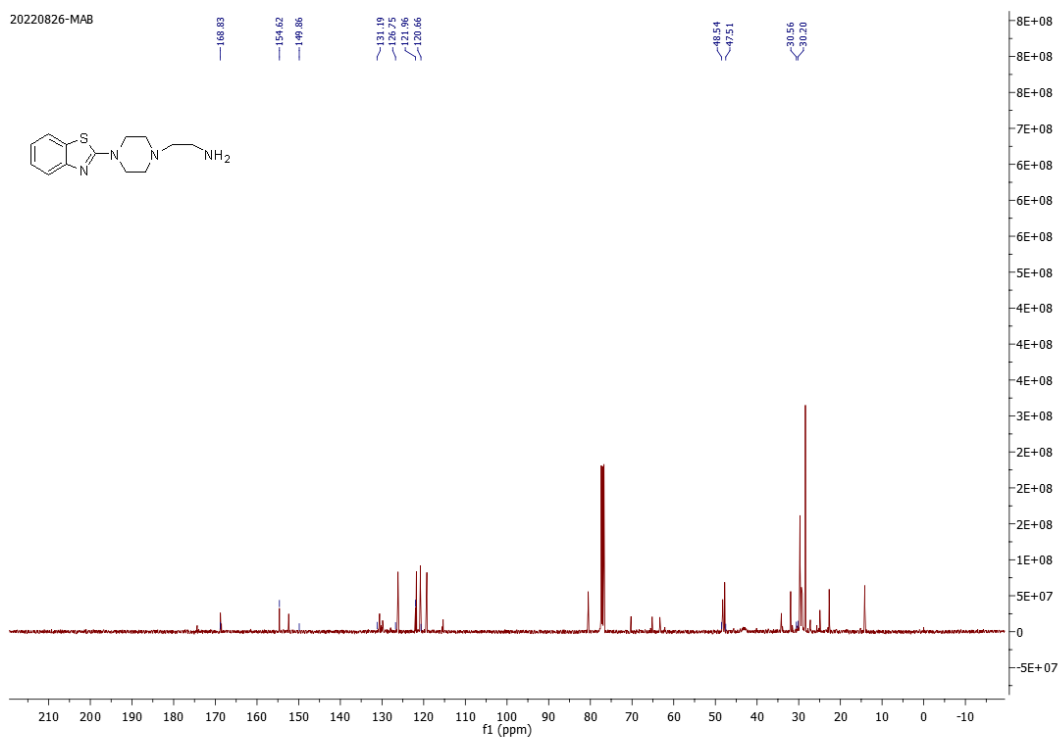
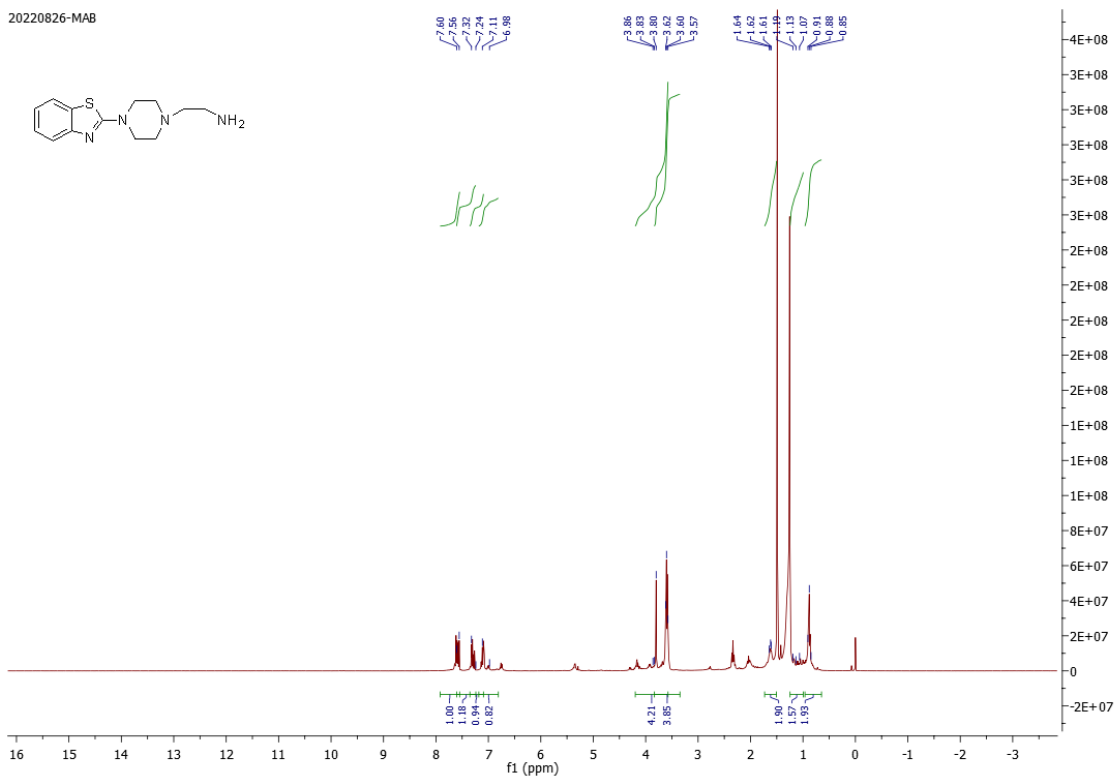
20220829-mab-b061



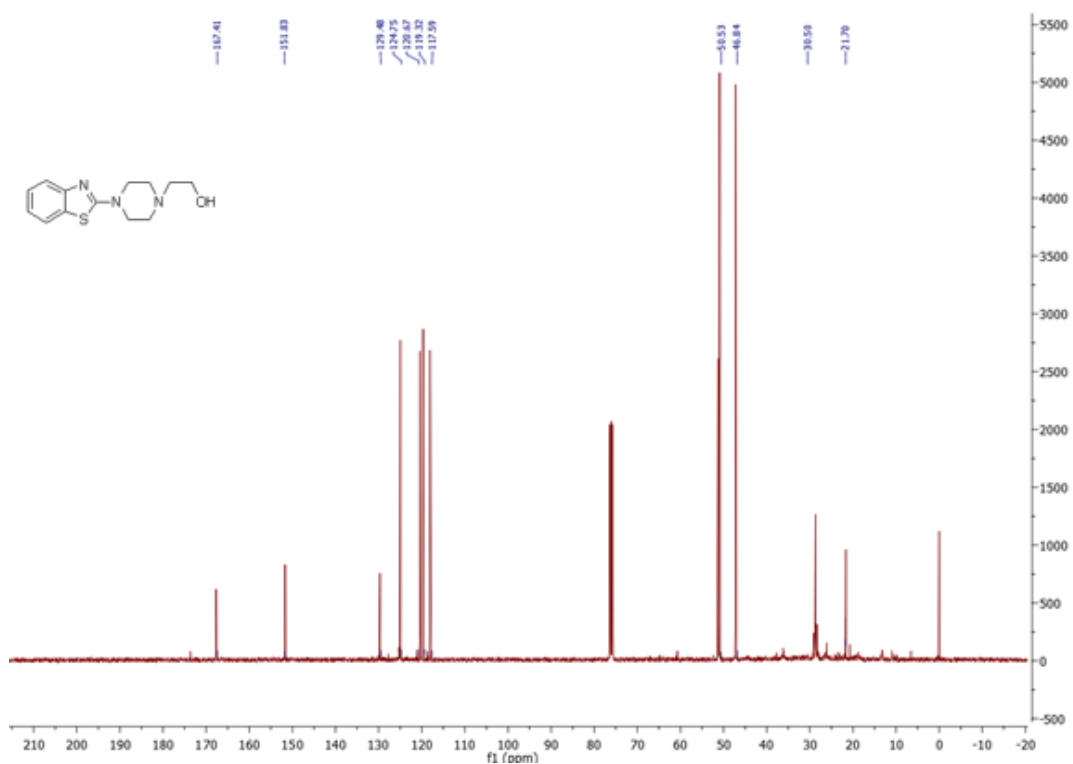
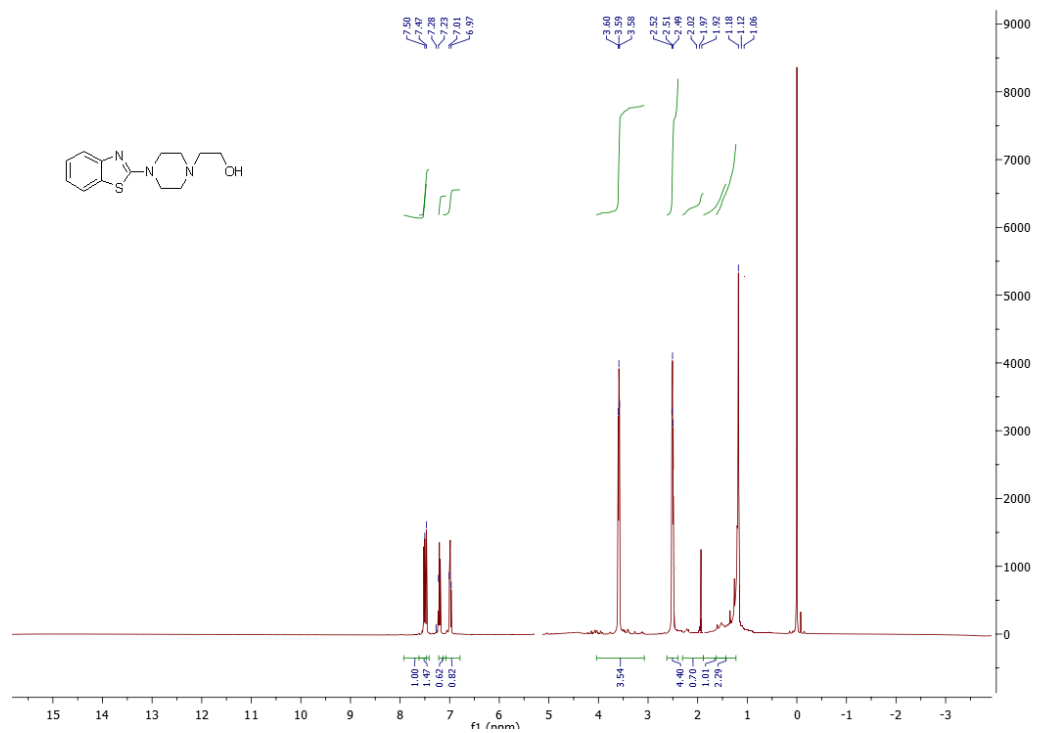
20220829-mab-b061



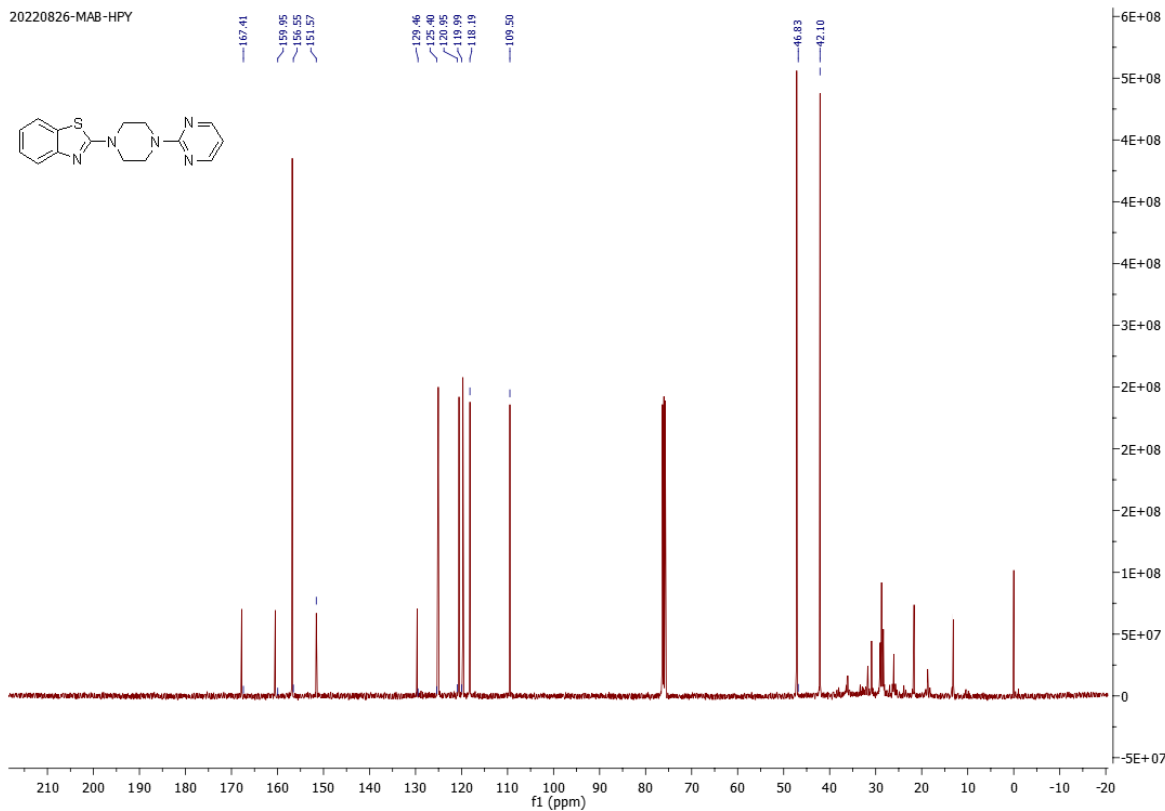
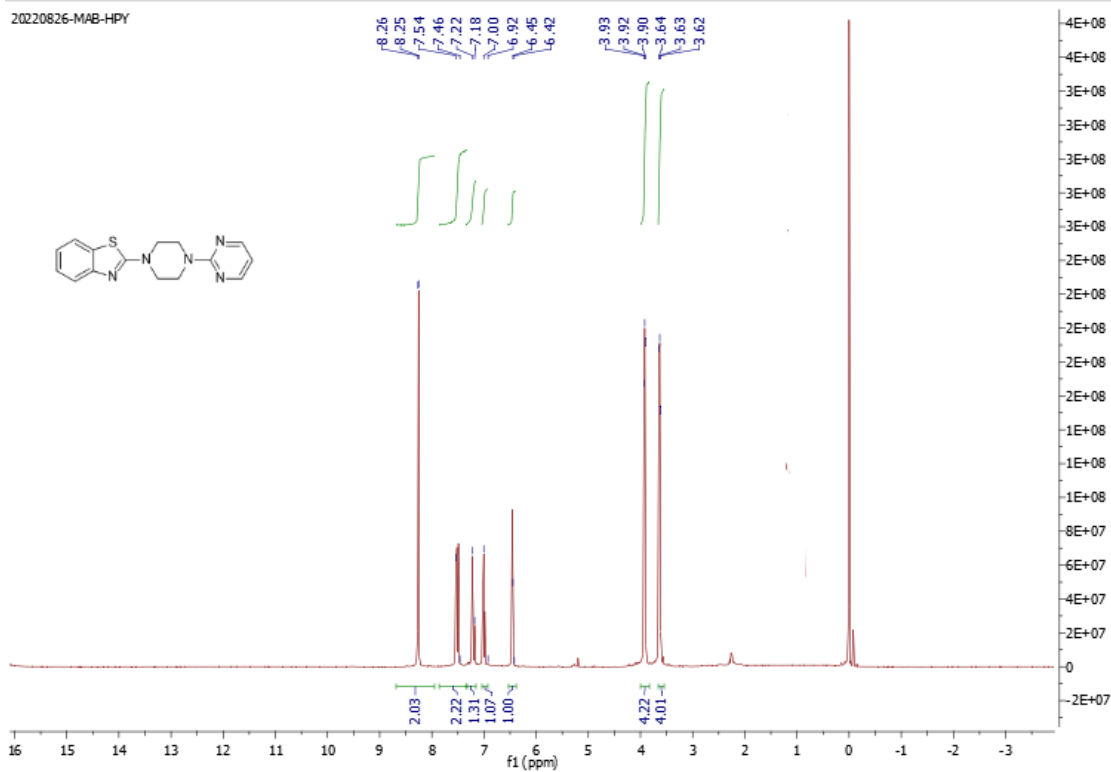
### 4.2.2.4 (3d')



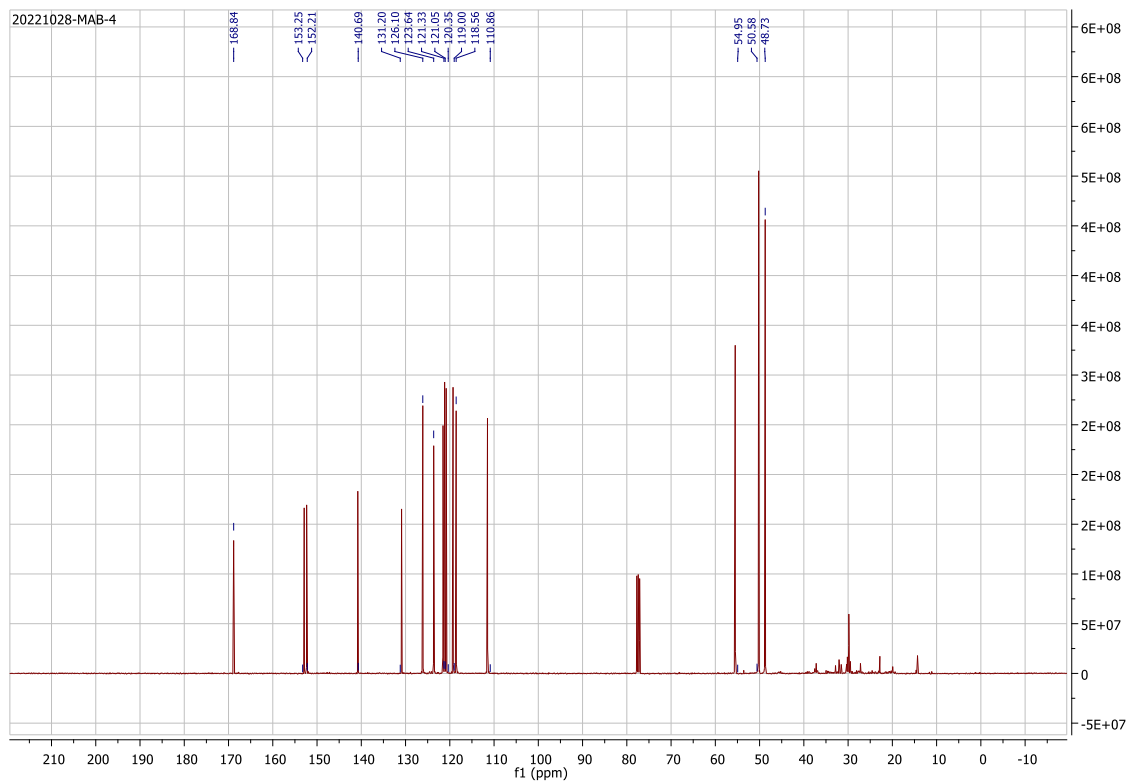
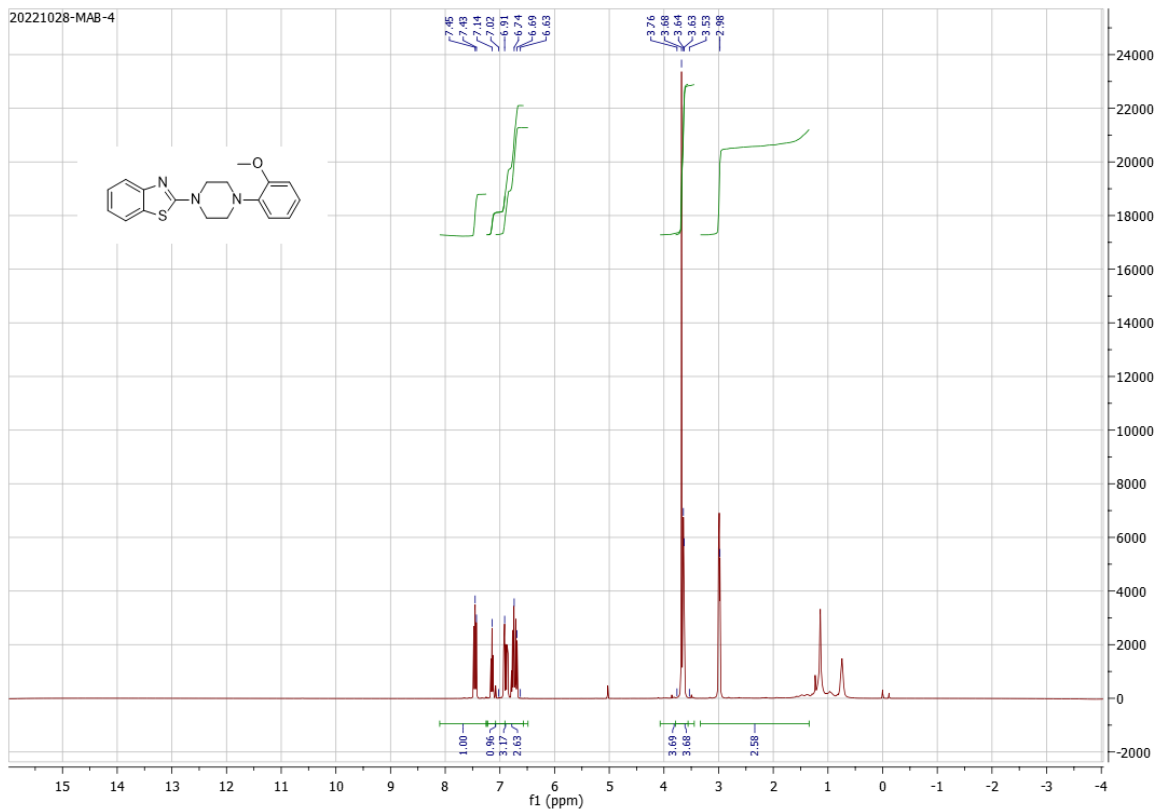
### 4.2.2.5 (3e')



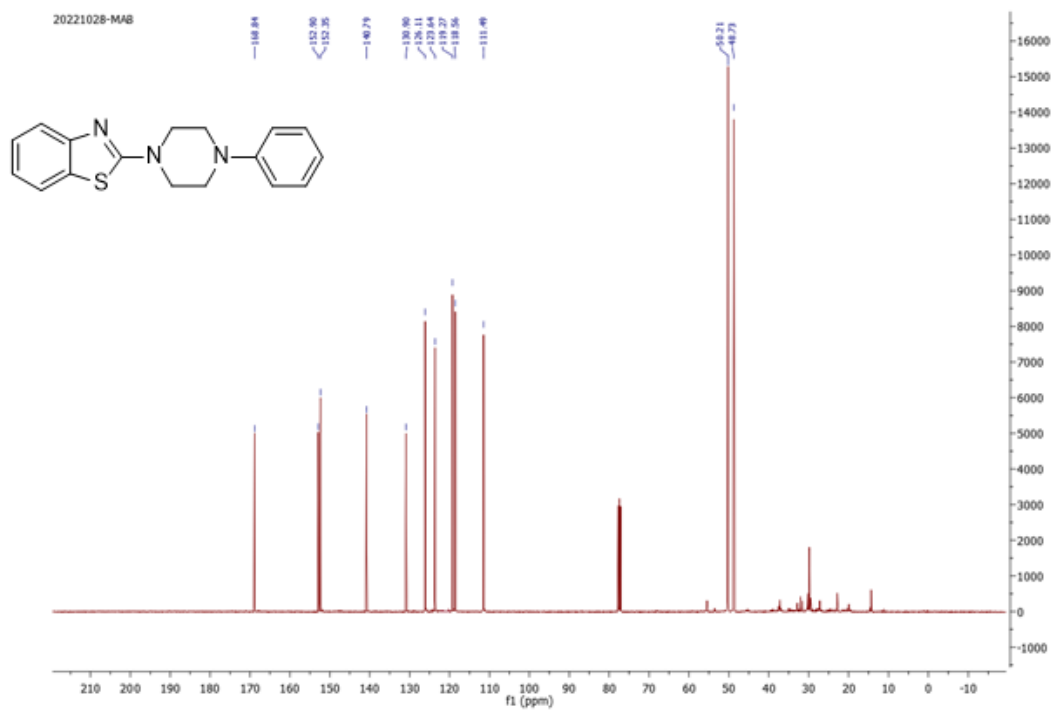
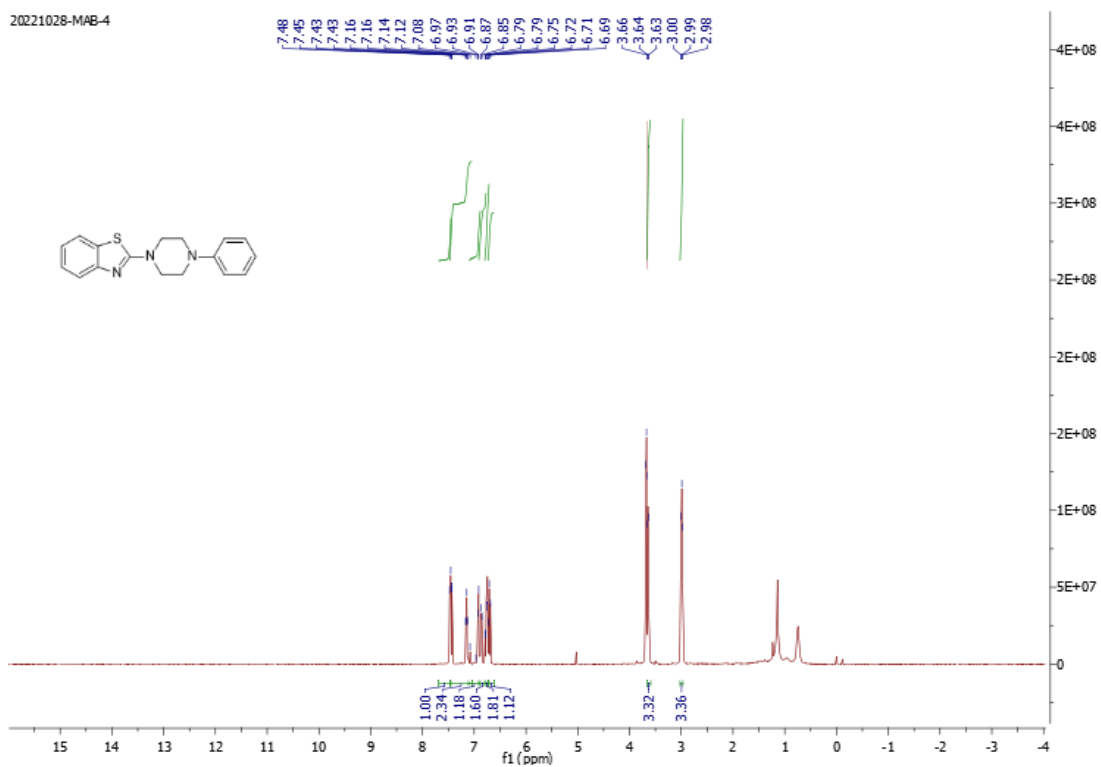
### 4.2.2.7 (3g')



### 4.2.2.8 (3h')



### 4.2.2.9 (3i')



## *Chapter 5*

### ***Design, Synthesis, In-vitro anti-tumor activity, and Computational study of Benzothiazole Derived Schiff Bases***



## 5.1 Introduction

Schiff bases, also referred to as azomethines or imines, structurally mimic ketones or aldehydes, replacing the carbonyl group with an imine or azomethine group [221]. Schiff bases are widely recognized as crucial organic building blocks, playing a significant role in several fields such as pharmacology, biochemistry, inorganic chemistry, and analytical chemistry. They exhibit diverse pharmacological properties, serving as antioxidants, anthelmintics, antitubercular agents, anti-inflammatory substances, anticancer compounds, antimicrobials, anticonvulsants, and more [222-224]. The functional sites within cellular components are believed to engage with the nitrogen atom of azomethine through the formation of hydrogen bonds, disrupting normal cellular processes [225, 226]. This interference leads to the impairment of enzyme functioning in cancer cells, highlighting schiff bases as suitable candidates for the development of anticancer chemotherapeutics [227]. The observed activities can be attributed predominantly to the presence of the azomethine ( $-N=CH-$ ) or imine group [228]. This component plays a pivotal role in understanding the mechanisms of a number reactions within a biological system, particularly those related to transformation reactions [229]. Several research studies have highlighted the significant chemical and biological relevance of the unshared pair of electrons available in the  $sp^2$ -hybridized orbital associated with the N atom within the azomethine group. This lone pair plays a crucial role in disrupting regular cellular functions through the development of hydrogen bonds among the active centers of cellular components and the  $sp^2$ -hybridized nitrogen atom present in the azomethine group [230]. Schiff bases, possessing this distinctive feature, demonstrate diverse applications such as catalysts [231], organic synthesis intermediates [232], dyes [233], pigments [234], polymer stabilizers [235], and corrosion inhibitors [236].

In our recent investigation, our focus was on synthesizing Schiff base derivatives that incorporate a distinct type of heterocycle – benzothiazole. Benzothiazole, a five-membered highly polar aromatic heterocycle, holds significance in both synthetic and natural molecules [237]. Due to its unique electron-rich characteristics, the benzothiazole ring readily forms diverse weak interactions such as coordination, ion-dipole, van der Waals forces, p-p stacking, and hydrophobic interactions [238]. This enables thiazole to bind effectively with various target enzymes in biological systems, showcasing broad bioactivities. Therefore, we opted to use benzothiazole as the initial heterocyclic core for constructing the desired Schiff bases, incorporating an intermediate thiazole entity [239]. This approach serves as a versatile strategy for developing potential anticancer chemotherapeutics [240-242]. Subsequently, various N, S,

and O-based heterocycles were introduced to the Schiff base structure. These heterocyclic compounds are known for playing significant roles as antibacterial agents [243], antivirals [244], antifungals [245], anti-inflammatories [246], and antitumor drugs [247-249].

Heterocycles serve as a prevalent structural motif in many widely-used drugs [250-252]. Therefore, our focus is on developing multiheterocyclic systems for evaluation of their *in vitro* anticancer potential, considering the substantial global impact of cancer on both developed and developing nations [253]. With over 100 types of cancer, causing 8.2 million annual deaths and contributing to approximately 13% of global mortality, there is a pressing need to address this health challenge, especially with an anticipated 70% increase in new cancer cases over the next two decades [254]. In our efforts to identify chemical compounds with potential as leads for novel antitumor agents, we specifically target sulfur and nitrogen containing heterocyclic compounds [255, 256]. Notably, we have observed similar structures in the literature with Schiff bases attached to the 2-aminothiazole nucleus, demonstrating interesting pharmacological effects [257-259]. Consequently, our objective is to synthesize Schiff base derivatives that incorporate diverse heterocyclic building blocks, aiming to produce compounds with significant potential for anticancer effects.

## **5.2 Materials and methods**

### **5.2.1 Instruments**

Solvents and chemicals were procured from Sigma Aldrich and utilized without additional purification. M.P's were measured in degrees Celsius using the open-end capillary method. <sup>1</sup>H and <sup>13</sup>C-NMR analyses were conducted on Bruker 500 (400 MHz) instrument with TMS as a reference standard and DMSO as solvent. Chemical reactions were monitored using E-Merck aluminum TLC sheets (60 F 254, 0.2 mm thick, 20 x 20 cm,) precoated with silica gel and a UV chamber (366 and 254 nm) for spot detection. Column chromatography was conducted employing Merck silica gel with a particle size of 60-120 mesh. Fetal bovine serum (FBS), RPMI 1640 medium (Catalogue no. 11875-093), L-glutamine (Catalogue no. 25030081), PenStrep (Catalogue no. 15240062), and trypsin (Cat no. 25200056) were sourced from Gibco/Life Technology. A-549 and normal cell line (HEK293T) were obtained from NCCS, Pune, India. C4-2 cells were acquired from Professor Zhou Wang at the Pittsburgh University, USA, through a Material Transfer Agreement (MTA) with M.D. Anderson Cancer Centre, Texas, USA.

### **5.2.2 Synthetic Procedure**

Unless specified otherwise, all the chemicals employed were of reagent grade and utilized without any additional purification. The yields were not optimized.

### **5.2.2.1 Synthetic Procedure for 2-Amino-6-nitrobenzothiazole**

Synthesis of 2-amino-substituted benzothiazole was carried out by employing equivalent ratios (1: 1) of substituted *p*-nitro aniline and ammonium thiocyanate (NH<sub>4</sub>SCN) in ethanol. Subsequently, the mixture underwent treatment with bromine in presence of glacial acetic acid. Once the reaction was completed, the mixture was treated with ethyl acetate. Subsequently, the unrefined product underwent purification through column chromatography. The confirmation of the product's identity and purity was checked through the application of NMR and mass spectroscopy techniques.

#### **5.2.2.1.1 2-Amino-6-nitrobenzothiazole (3)**

Yield: 81%, mp 246-249°C, <sup>1</sup>H NMR (400 MHz, DMSO-*d*<sub>6</sub>): δ = 8.66 (s, 1H), 8.23 (s, 1H), 8.09 (d, *J* = 4 Hz, 1H), 7.42 (d, *J* = 8 Hz, 2H); <sup>13</sup>C NMR (100 MHz, DMSO): δ = 172.18, 159.15, 141.15, 132.05, 122.43, 118.12, 117.29 ESI-MS *m/z*: Calculated for C<sub>7</sub>H<sub>5</sub>N<sub>3</sub>O<sub>2</sub>S[M+H]<sup>+</sup> 195.01, Found 195.02.

### **5.2.2.2 General Procedure for the synthesis of (6-nitrobenzo[5]thiazol-2-yl)-1-phenylmethanimine derivatives**

A combination of 2-Amino-6-nitrobenzothiazole (1.0 mmol) and aromatic aldehydes (1.0 mmol) was stirred and refluxed in 15 ml of ethanol for a duration of 3 hours. After the reaction concluded, the mixture was cooled to room temperature and subsequently transferred into 50 ml of chilled water. The resulting product was filtered and subsequently dried.

#### **5.2.2.2.1(E)-N-(6-nitrobenzo[5]thiazol-2-yl)-1-(4-nitrophenyl)methanimine (5a)**

Yield: 85%, mp 175-178°C, FT-IR (KBr) cm<sup>-1</sup>: 3067 (aromatic H-C stretch), 1608 (CH=N stretch, azomethine), 1572 (C-C stretch, aromatic), 1509 (N-C, thiazole), 1147 (N-C), 685 (C-S-C, thiazole ring); <sup>1</sup>H-NMR (400 MHz, DMSO-*d*<sub>6</sub>), δ, ppm: 10.15 (s, 1H), 8.67 (s, 1H), 8.41 (d, 1H, *J* = 8 Hz), 8.16 (d, 1H, *J* = 8 Hz), 8.10 (d, 2H, *J* = 4 Hz), 8.07 (d, 2H, *J* = 4 Hz). <sup>13</sup>C-NMR (100 MHz, DMSO), δ, ppm: 172.25, 159.02, 151.08, 141.14, 140.58, 132.07, 131.10(2C), 124.72(2C), 122.38, 118.08, 117.3.

#### 5.2.2.2.2 (E)-1-(4-chlorophenyl)-N-(6-nitrobenzo[5]thiazol-2-yl)methanimine (5b)

Yield: 88%, mp 188-190°C, FT-IR (KBr)  $\text{cm}^{-1}$ : 3105 (aromatic H-C stretch), 1610 (CH=N stretch, azomethine), 1552 (C-C stretch, aromatic), 1518 (N-C, thiazole), 760 (Cl-C);  $^1\text{H-NMR}$  (400 MHz, DMSO-*d*6),  $\delta$ , ppm: 10.07 (s, 1H), 8.52 (s, 1H), 8.37 (d, 1H,  $J = 4$  Hz), 8.14 (d, 1H,  $J = 8$  Hz), 8.02 (d, 2H,  $J = 8$  Hz), 7.98 (d, 2H,  $J = 4$  Hz).  $^{13}\text{C-NMR}$  (100 MHz, DMSO),  $\delta$ , ppm: 170.26, 158.35, 151.07, 143.74, 140.29, 132.81, 129.17(2C), 126.44(2C), 122.75, 118.73, 116.89.

#### 5.2.2.2.3 (E)-4-(((6-nitrobenzo[5]thiazol-2-yl)imino)methyl)phenol (5c)

Yield: 92%, mp 195-198°C, , FT-IR (KBr)  $\text{cm}^{-1}$ : 3325 (C-OH), 3112 (H-C stretch, aromatic), 1615 (CH=N stretch, azomethine), 1530 (C-C stretch, aromatic), 1511 (N-C, thiazole);  $^1\text{H-NMR}$  (400 MHz, DMSO-*d*6),  $\delta$ , ppm: 10.03 (s, 1H), 9.11 (s, 1H), 8.33 (s, 1H), 8.62 (d, 1H,  $J = 4$  Hz), 8.27 (d, 1H,  $J = 4$  Hz), 8.08 (d, 2H,  $J = 8$  Hz), 7.99 (d, 1H,  $J = 4$  Hz).  $^{13}\text{C-NMR}$  (100 MHz, DMSO),  $\delta$ , ppm: 172.31, 160.05, 159.10, 150.84, 144.27, 140.91, 132.35, 128.50(2C), 126.73(2C), 122.05, 119.24.

#### 5.2.2.2.4 (E)-N-(6-nitrobenzo[5]thiazol-2-yl)-1-(3-nitrophenyl)methanimine (5d)

Yield: 85%, mp 175-178°C, FT-IR (KBr)  $\text{cm}^{-1}$ : 3065 (H-C stretch, aromatic), 1605 (CH=N stretch, azomethine), 1572 (C-C stretch, aromatic), 1510 (N-C, thiazole), 1153 (N-C), 680 (C-S-C, thiazole);  $^1\text{H-NMR}$  (400 MHz, DMSO-*d*6),  $\delta$ , ppm: 10.14 (s, 1H), 8.68 (s, 1H), 8.52 (d, 1H,  $J = 8$  Hz), 8.32 (d, 1H,  $J = 4$  Hz), 8.24 (s, 1H), 8.09 (d, 1H,  $J = 8$  Hz), 7.88 (d, 1H,  $J = 8$  Hz), 7.41 (d, 1H,  $J = 8$  Hz).  $^{13}\text{C-NMR}$  (100 MHz, DMSO),  $\delta$ , ppm: 172.25, 159.02, 148.71, 141.14, 137.61, 135.37, 128.99, 124.48(2C), 122.47, 118.14, 117.32.

#### 5.2.2.2.5 (E)-N-(6-nitrobenzo[5]thiazol-2-yl)-1-phenylmethanimine (5e)

Yield: 80%, mp 190-193°C, 175-178°C, FT-IR (KBr)  $\text{cm}^{-1}$ : 3123 (C-H stretch, aromatic), 1640 (N=CH stretch, azomethine), 1558 (C-C stretch, aromatic), 1510 (N-C, thiazole), 1160 (N-C), 671 (C-S-C, thiazole);  $^1\text{H-NMR}$  (400 MHz, DMSO-*d*6),  $\delta$ , ppm: 9.87 (s, 1H), 8.54 (s, 1H), 8.26 (d, 1H,  $J = 4$  Hz), 8.11 (d, 1H,  $J = 8$  Hz), 7.86-7.50 (m, 5H).  $^{13}\text{C-NMR}$  (100 MHz, DMSO),

$\delta$ , ppm: 170.91, 159.18, 150.70, 143.27, 140.00, 133.52, 127.53(2C), 126.18(2C), 120.08, 120.03.

#### **5.2.2.2.6 2-methoxy-4-(((6-nitrobenzo[5]thiazol-2-yl)imino)methyl)phenol (5f)**

Yield: 85%, mp 198-200°C, FT-IR (KBr)  $\text{cm}^{-1}$ : 3310 (OH stretch), 3100 (H-C stretch, aromatic), 1659 (CH=N stretch, azomethine), 1530 (C-C stretch, aromatic), 1573 (C-N, thiazole), 1170 (N-C), 685 (C-S-C, thiazole);  $^1\text{H-NMR}$  (400 MHz, DMSO-*d*6),  $\delta$ , ppm: 10.43 (s, 1H), 9.77 (s, 1H), 9.04 (s, 1H), 8.27 (d, 1H,  $J = 4$  Hz), 8.00 (d, 1H,  $J = 4$  Hz), 7.59 (d, 1H,  $J = 8$  Hz), 7.38 (d, 1H,  $J = 4$  Hz), 6.98 (s, 1H), 3.89 (s, 1H).  $^{13}\text{C-NMR}$  (100 MHz, DMSO),  $\delta$ , ppm: 177.98, 172.14, 168.76, 159.06, 156.27, 153.58, 148.77, 134.93, 129.18, 122.27, 119.67, 118.12, 117.29, 116.27, 56.05.

#### **5.2.2.2.7 2-methoxy-6-(((6-nitrobenzo[5]thiazol-2-yl)imino)methyl)phenol (5g)**

Yield: 86%, mp 195-198°C, FT-IR (KBr)  $\text{cm}^{-1}$ : 3210 (OH stretch), 3315 (H-C stretch, aromatic), 1701 (CH=N stretch, azomethine), 1548 (C-C stretch, aromatic), 1570 (N-C, thiazole), 1170 (N-C), 780 (C-S-C, thiazole);  $^1\text{H-NMR}$  (400 MHz, DMSO-*d*6),  $\delta$ , ppm: 10.13 (s, 1H), 9.28 (s, 1H), 9.01 (s, 1H), 8.23 (d, 1H,  $J = 4$  Hz), 8.01 (d, 1H,  $J = 4$  Hz), 7.97-6.94 (m, 3H, aromatic protons), 3.77 (s, 3H).  $^{13}\text{C-NMR}$  (100 MHz, DMSO),  $\delta$ , ppm: 170.51, 169.44, 155.07, 149.20, 141.65, 135.53, 126.16, 124.51, 122.36, 121.20, 118.19, 117.24, 114.76, 110.97, 56.01

#### **5.2.2.2.8 (E)-1-([1,1'-biphenyl]-4-yl)-N-(6-nitrobenzo[5]thiazol-2-yl) methanimine (5h)**

Yield: 85%, mp 181-185°C, FT-IR (KBr)  $\text{cm}^{-1}$ : 3115 (H-C stretch, aromatic), 1650 (CH=N stretch, azomethine), 1530 (C-C stretch, aromatic), 1560 (N-C, thiazole), 1159 (N-C), 687 (C-S-C, thiazole);  $^1\text{H-NMR}$  (400 MHz, DMSO-*d*6),  $\delta$ , ppm: 9.95 (s, 1H), 8.75 (d, 1H,  $J = 4$  Hz), 8.68 (d, 1H,  $J = 12$  Hz), 8.23 (s, 1H), 8.09 (d, 2H,  $J = 8$  Hz), 7.99 (d, 2H,  $J = 4$  Hz), 7.81-7.39 (m, 5H, aromatic protons)  $^{13}\text{C-NMR}$  (100 MHz, DMSO),  $\delta$ , ppm: 172.26, 158.99, 157.87, 141.84, 141.10, 138.62, 138.02, 135.85(2C), 132.05, 131.37, 129.41(2C), 122.48(2C), 118.54, 118.15(2C), 117.33, 103.99.

#### 5.2.2.2.9 (E)-1-(4-(1H-indol-2-yl)phenyl)-N-(6-nitrobenzo[5] thiazol-2-yl)methanimine (5i)

Yield: 87%, mp 176-180°C, FT-IR (KBr)  $\text{cm}^{-1}$ : 3381(N-H stretch), 3250 (H-C stretch, aromatic), 1695 (CH=N stretch, azomethine), 1531 (C-C stretch, aromatic), 1564 (N-C, thiazole), 1150 (N-C), 705 (C-S-C, thiazole);  $^1\text{H-NMR}$  (400 MHz, DMSO-*d*<sub>6</sub>),  $\delta$ , ppm: 12.27 (s, 1H), 9.22 (s, 1H), 8.39 (d, 2H, *J* 8Hz), 8.30, (s, 1H), 7.78 (d, 1H, *J* 12Hz), 7.53 (d, 1H, *J* 12Hz), 7.46 (d, 2H, *J* 4Hz), 7.56, 7.37-7.23 (m, 4H, aromatic protons), 6.86 (s, 1H)  $^{13}\text{C-NMR}$  (100 MHz, DMSO),  $\delta$ , ppm: 172.70, 161.56, 151.34, 139.06, 138.03, 133.55, 131.80, 127.21, 126.56, 1254.04, 124.74, 124.16(2C), 122.53(2C), 121.25, 121.06, 119.86, 114.90, 113.02.

#### 5.2.2.2.10 (E)-N-(6-nitrobenzo[5] thiazol-2-yl)-1-(*p*-tolyl)methanimine (5j)

Yield: 79%, mp 110-113°C, FT-IR (KBr)  $\text{cm}^{-1}$ : 3250 (H-C stretch, aromatic), 1681 (CH=N stretch, azomethine), 1530 (C-C stretch, aromatic), 1550 (N-C, thiazole), 1160 (N-C), 750 (C-S-C, thiazole);  $^1\text{H NMR}$  spectrum (400 MHz, DMSO-*d*<sub>6</sub>),  $\delta$ , ppm: 8.92 (s, 1H), 8.75 (s, 1H), 8.67 (d, 2H, *J* = 4 Hz), 8.09 (d, 2H, *J* = 8 Hz), 7.41 (d, 2H, *J* = 4 Hz), 2.51 (s, 3H).  $^{13}\text{C-NMR}$  (100 MHz, DMSO),  $\delta$ , ppm: 172.24, 159.05, 141.14, 132.04, 130.01, 122.43, 119.32, 118.39(2), 118.11, 117.29 (2C), 21.81.

### 5.2.3 Bioassay

The A-549 cancer cell line and the (HEK293T) normal cell line were sourced from NCCS Pune. C4-2 cells were obtained from Prof. Zhou Wang at the University of Pittsburgh, Texas, USA, under a Material Transfer Agreement (MTA) with MDA Cancer Centre, USA. Both cell lines were regularly cultured in RPMI media supplemented with 1% L-glutamine, 10% FBS, and 100g/ml streptomycin-penicillin. The cultures were kept in a 5% CO<sub>2</sub> atmosphere and incubated at 37°C.

#### 5.2.3.1 MTT Assay

The MTT assay serves as a colorimetric technique to gauge cellular metabolic activity, frequently employed for evaluating cell viability and proliferation. In this study, the MTT method was utilized to appraise the influence of compounds (**5a-5j**) on cell viability within both cancer cell lines (A549, C4-2). The most promising compound was subsequently assessed

against the normal human embryonic kidney cell line (HEK293T). The cells were set up in 96-well, each well containing a total volume of 100  $\mu$ l/well to evaluate the compounds. The cells were cultured and incubated for the proper amount of time—typically 24-48 hours prior to treatment. The cells were subjected to treatment with compounds 5a-5j at different concentrations and incubated for 24hrs. Final concentration pertaining to 5 mg/ml was reached by adding 10  $\mu$ l of MTT solution in each well and the MTT-treated cells were placed in an incubator for a duration of 4 hours at 37°C. For the dissolution of formazan crystals, 100  $\mu$ l of solubilization (DMSO) solution was supplied to each well. Using an ELISA reader, the absorbance of the colored solution was measured at a wavelength of 563 nm. Data was analyzed using Graphpad Prism 8.0.

#### **5.2.3.2 CFU assay**

Colony formation assay was employed for quantitative in vitro assessment to explore whether a single cell could give rise to a substantial colony through clonal growth in presence of varying concentrations of the compound that exhibited the most promising results in the MTT experiment. C4-2 cells were seeded in six-well dishes and allowed to grow until reaching 70-80% confluence. Upon reaching confluence, cells were treated with various concentrations of compound **5i** (10, 20, 30, 40, and 50  $\mu$ M) as well as a DMSO control, followed by a 48-hour incubation period. Subsequently, equal numbers of cells from both control and treated wells were transferred to 10 cm dishes to develop into colonies over a period of 3 to 5 days. After colony formation, the media was aspirated, and 100% methanol was incorporated into the cells, which were then kept in an incubator for 20 minutes at room temperature. Following methanol removal, cells underwent mild rinsing with tap water and covered with a crystal violet solution, incubating for five minutes at room temperature. Excess color was eliminated by rinsing the cells with water. The plates were inverted and air-dried overnight on tissue paper. Cell counting was performed using ImageJ software. The trial was conducted three times in triplicates, and statistical analysis was carried out using t-tests and the Kruskal-Wallis test in GraphPad Prism 8.0. Significance was attributed to P values below 0.05.

#### **5.2.3.3 Wound Healing Assay**

C4-2 cells were cultivated in a monolayer within 6-well plates. When the monolayer reached 70-80% confluency, the culture medium was removed, and a sterile 200  $\mu$ l pipette tip was employed to gently create a linear scratch across the middle of the monolayer. After rinsing the isolated cells with PBS, new RPMI medium augmented with 1% PenStrep, 1% L-glutamine,

and 10% FBS was added to the scratched wells. Bright field images capturing the cellular gap were taken using an LMI inverted microscope before the introduction of compound 5i. Subsequently, 5i was applied to the cells at a concentration of 16.50  $\mu$ M, with DMSO serving as the vehicle control. Following treatment, the well plates were placed in an incubator with 5% CO<sub>2</sub> at 37°C, and the gap width of the scratch was monitored by periodically capturing bright field images after 0, 24, and 48 hours. The ImageJ programme (<http://rsb.info.nih.gov/ij/download.html>) was utilized for the quantitative assessment of the scratch wound diameter. Using GraphPad Prism 8.0, the cellular gap distance was quantitatively analyzed as a proportion of the wound area. Significance was determined at \*P < 0.05.

#### **5.2.3.4 RNA Isolation, PCR amplification, and quantitative Real-Time expression analysis (RT-PCR)**

C4-2 cells were cultured in 10 cm dishes for a duration of two days. Cells at 70-80% confluency were subjected to treatment with either 16.50  $\mu$ M of compound 5i or DMSO and were then incubated for 24 hours. Total cellular RNA was extracted from the C4-2 cancer cell line using Trizol (Thermo Scientific), adhering to the manufacturer's guidelines. The isolated RNA underwent gel electrophoresis for quality assessment, and cDNA was synthesized using MMLV reverse transcriptase (Gibco). The success of cDNA synthesis was confirmed using GAPDH primers. RT-PCR (Biorad) was employed to evaluate the relative expression of various genes, including vimentin, COX-2, Il8, Il1- $\alpha$ , Il1- $\beta$ , Il6, and TNF- $\alpha$ , in the C4-2 cancer cell line. SYBR® qPCR mixture (Kapa) and specific primers designed for C4-2 cells, with GAPDH serving as the normalizing control, were used in the PCR reaction.

#### **5.2.3.5 Molecular Docking study**

The study focused on investigating how synthesized compounds interacted with the androgen receptor (AR). The AutoDock 4 tool was employed to identify the AR as the target protein. A scoring function based on energy was utilized to evaluate the binding affinity of the ligands to the androgen receptor (PDB ID: 2PNU), derived from the Protein Data Bank ([www.rcsb.org](http://www.rcsb.org)). AutoGrid was utilized to create a grid map representing docking sites for the proteins, with a grid size of 60x60x60 points in each dimension. The grid points' spacing was set at 0.375, and Gasteiger charges were calculated using AutoDock tools. Following the docking procedure, RMSD clustering maps were created using thresholds of 0.25, 0.5, and 1 to identify the optimal



cluster with the highest population and the lowest energy score. Molecular docking studies were subsequently conducted using tools in Discovery Studio v2.5 to analyze receptor-ligand interactions.

#### **5.2.3.6 ADME and drug likeness property**

The Lipinski Rules, also known as the Rule of Five (ROF), provide a practical framework for assessing the drug likeness of any compound and determining its potential efficacy as an orally-administered drug based on key pharmacokinetic properties such as absorption, distribution, metabolism, and excretion (ADME). These rules consider specific physicochemical attributes, including a molecular weight (MW) of no more than 500 Da, a logarithm of the partition coefficient (logP) of no more than 5, a limit of five hydrogen bond donors (HBD), and ten hydrogen bond acceptors (HBA). The SwissADME software was employed to evaluate the ADME properties of constituents, and compounds were classified as active if their oral bioavailability (OB) was equal to or greater than 30. Constituents meeting fewer than three criteria were categorized as inactive.

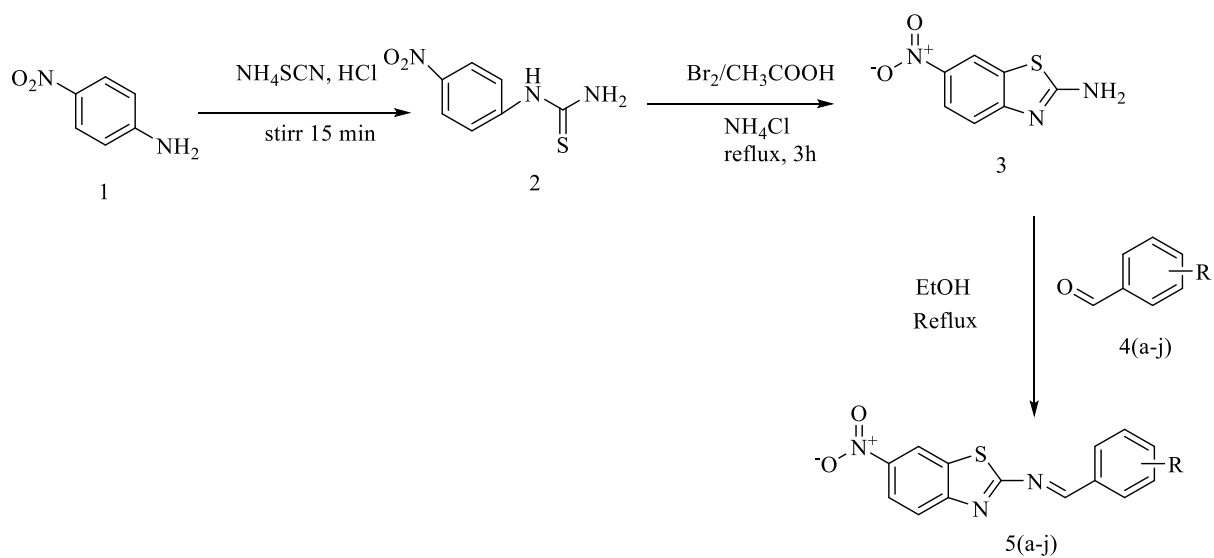
#### **5.2.3.7 Statistical analysis**

ImageJ software was utilized to quantify colony-forming units (CFU) and conduct wound healing assays. Graphical representation as well as statistical analysis were conducted using Graphpad prism 8.0 (Graphpad Software, Inc.). The data were presented as mean  $\pm$  SEM, and statistical significance was assessed using One-way ANOVA or the student t-test, as deemed appropriate. A significance threshold of \*P < 0.05 was contemplated. The assessment of colony-forming units and wound healing assays involved the application of ImageJ software.

### **5.3 Results & Discussion**

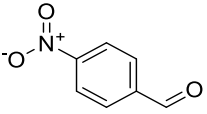
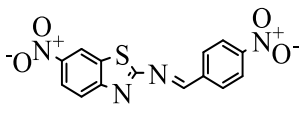
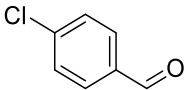
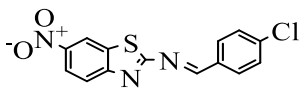
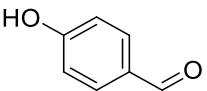
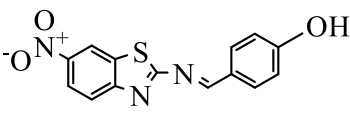
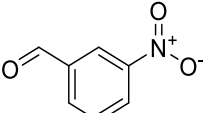
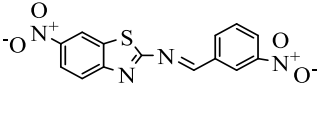
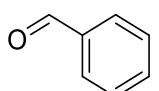
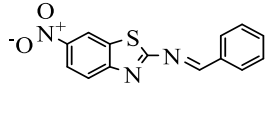
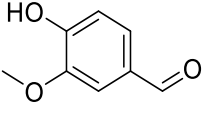
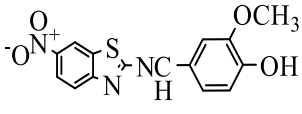
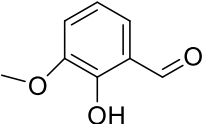
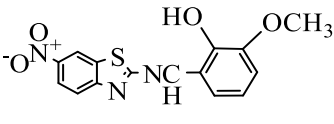
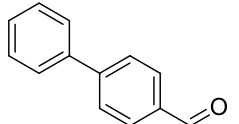
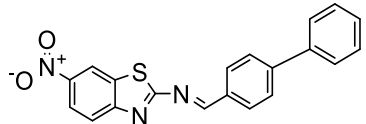
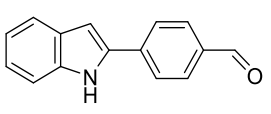
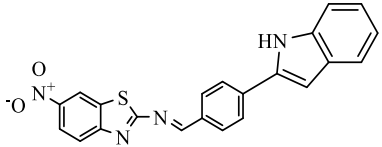
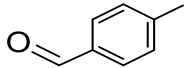
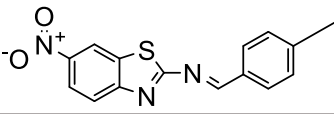
#### **5.3.1 Synthesis and characterization**

The title compounds **5a-5j** were synthesized using the procedure outlined in **Scheme 5.1**. The structures of these compounds (**Table 5.1**) were confirmed through Fourier transform infrared spectroscopy FT-IR,  $^1\text{H}$  NMR, and  $^{13}\text{C}$  NMR analyses.



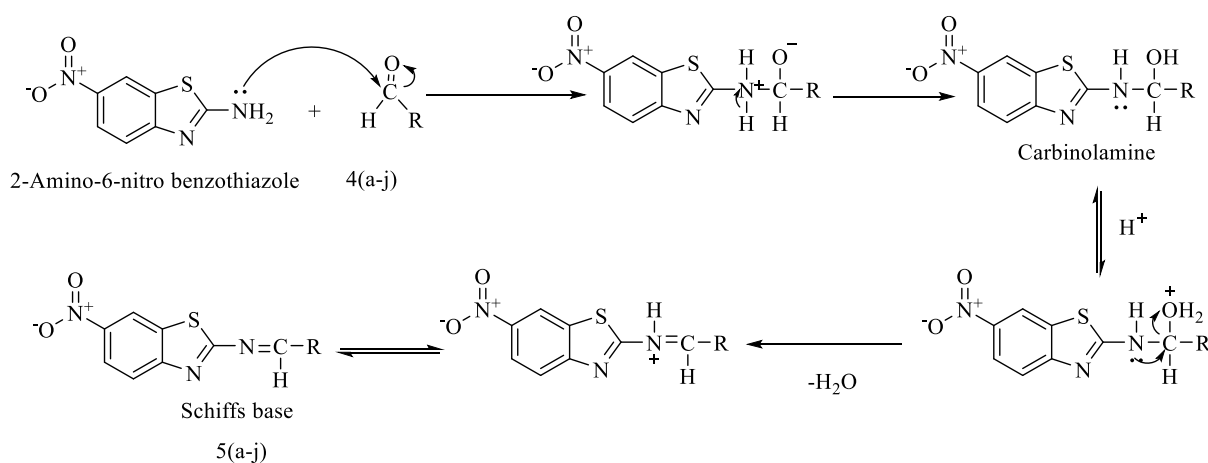
**Scheme 5.1. Synthesis of benzothiazole fused schiff bases (5a-5j)**

**Table 5.1. List of synthesized benzothiazole-schiff bases**

S.No.	Compound 4(a-j)	Product 5(a-j)	m.p.	Yield(%)
1.			175-178°C	85%
2.			188-190°C	88%
3.			190-193°C	92%
4.			198-200°C	85%
5.			190-193°C	80%
6.			198-200°C	85%
7.			195-198°C	86%
8.			181-185°C	85%
9.			176-180°C	87%
10.			110-113°C	79%

### 5.3.1.1 Reaction Mechanism

The process of imine formation is a reversible sequence initiated by nucleophilic addition to carbonyl group of either an aldehyde or a ketone by primary amine. Following this, a proton transfer occurs, resulting in the formation of a neutral amino alcohol called carbinolamine. The carbinolamine undergoes acid protonation at its oxygen atom, leading to the conversion of the oxygen into a more effective leaving group. This leaving group is then eliminated as water, leading to the formation of an iminium ion. The final step involves deprotonation of the nitrogen atom, ultimately yielding the desired imine product (**Scheme 5.2**). The entire process is reversible, and the imine can potentially revert back to the starting materials under appropriate conditions.

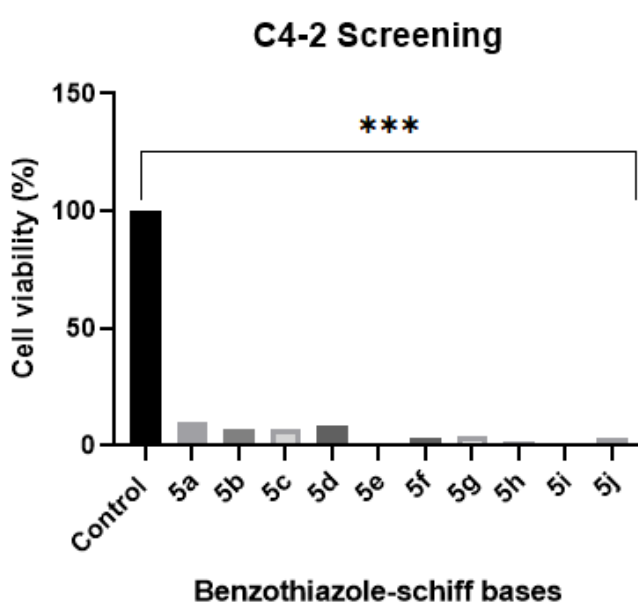


**Scheme 5.2. Mechanism of benzothiazole schiff base (5a-5j) formation**

### 5.3.2 MTT assay demonstrates pronounced cytotoxic effects of the synthesized compounds on various cell lines.

In the cytotoxicity assessment, A-549 and C4-2 cancer cells were subjected to testing with a range of synthesized substituted benzothiazole derivatives at various concentrations using DMSO as control. The cytotoxicity results revealed that all compounds exhibited moderate to substantial inhibitory effects on prostate cancer cells. Notably, compound 5i demonstrated comparatively higher cytotoxicity against C4-2 cell lines, as highlighted in **Figure 5.1**. Analyzing the SAR of these compounds provides insights into how modifications to the molecular structure can enhance their anticancer properties. This SAR analysis is crucial for comprehending the mechanisms underlying the anticancer effects of thiazole. Firstly, the

thiazole skeleton was identified as vital for anticancer efficacy and introduction of pharmacophores like indole further enhanced the activity. Presence of a benzyl or an alkyl group enhances the activity, whereas groups like OH and Cl generally exert a slightly diminishing effect. Similar reports wherein the anticancer activity was affected by the existence of an alkyl group at the C-6 position of benzothiazole ring, substitutions at meta and para positions with electron-withdrawing atoms such as fluorine were reported leading to an enhancement in the inhibitory potency of benzothiazole moiety [260, 261].



Moreover, compound 5i exhibited no adverse effects on HEK293T normal cells (**Figure 5.2**), suggesting its specific targeting of cancerous cells without affecting normal cell lines. Among the tested compounds, 5i emerged as the most potent agent, displaying significant cytotoxicity against C4-2 cancer cells while causing minimal harm to normal cells. Consequently, it was chosen for further evaluation.

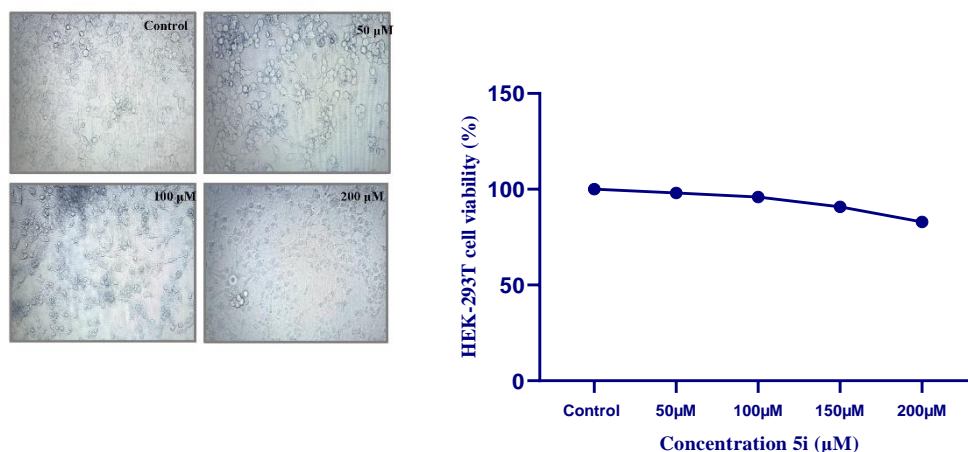


**Fig. 5.2.** Cytotoxicity test of 5i by MTT assay against HEK293T cell line

### 5.3.3 The Colony Formation Unit assay reveals a dose dependent reduction in cellular growth in vitro

The colony formation experiment was conducted using five concentrations (10, 20, 30, 40, 50 μM) to investigate the impact of 5i on suppressing growth and cellular progression in lung cancer cells. DMSO served as the vehicle control. C4-2 prostate cancer cells exhibited a decrease in colony-forming capacity in a dose-dependent manner in response to **5i** (**Figure 5.3a, b**). As the concentration increased, cell proliferation significantly decreased, reaching 50% inhibition at 16.50 μM in C4-2 cells.

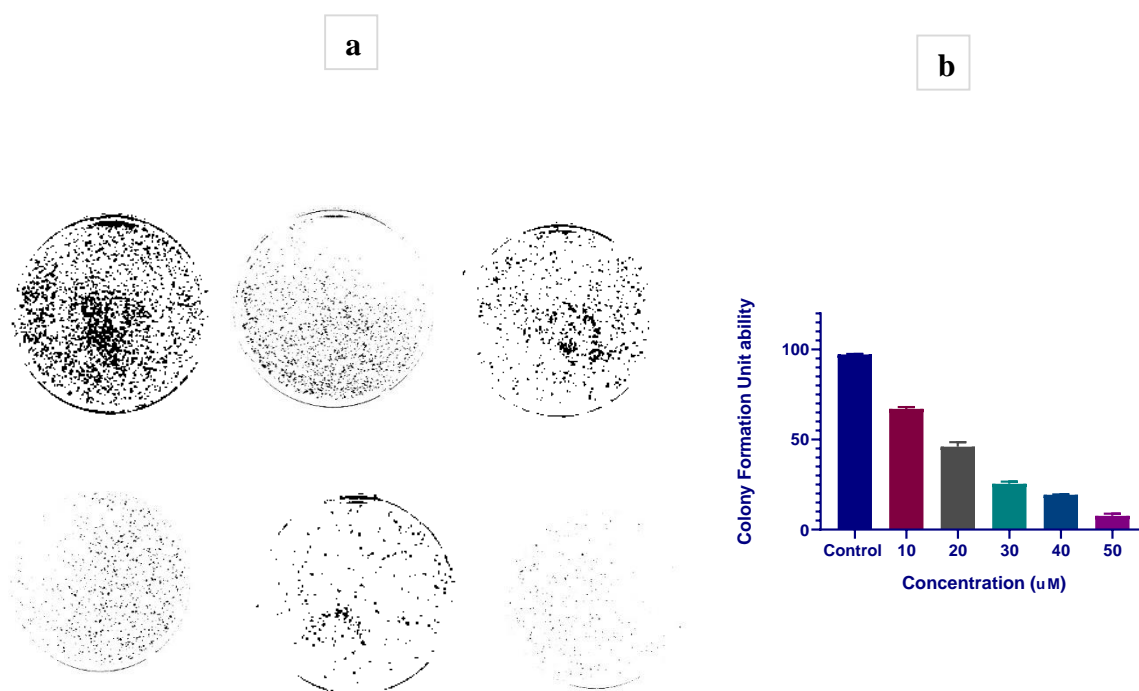


**Fig. 5.3.** Inhibition of colony formation by compound 5i in a dose dependent manner

- (a) Impact of 3c on the ability of C4-2 cancer cells to form colonies after exposure to 5i at various doses (10, 20, 30, 40 and 50 μM)
- (b) Graphical visualization of dose dependent suppression of CFU in C4-2 cells *in vitro*. The experiment was performed in triplicates and quantification and imaging was conducted using ImageJ software and Graphpad prism 8.0 and \*P < 0.0001 was taken as significant. Visualization of the dose-dependent suppression of CFU in A549 cells *in vitro*. The experiment was performed in triplicate, and \*P < 0.0001 was regarded significant.

### 5.3.4 Compound 5i suppresses wound healing/ cell migration *in vitro*

The assay results demonstrated that the compound effectively reduced the migration of C4-2 cells in a time dependent manner. The width of the cell gap was assessed at various time intervals (0, 24, and 48 hours post treatment) using ImageJ software (NIH) (**Fig. 5.4(a)**). Quantification of the wound area (**Fig. 5.4(b)**) and the closure of the wound gap (**Fig. 5.4(c)**) was carried out using ImageJ software, with the experiment conducted in triplicate. GraphPad Prism 8.0 was used for data analysis, and statistical significance was indicated by \*P < 0.0001. These results suggest a significant inhibitory impact of compound 5i on the processes of wound healing and cellular migration in the C4-2 cell line over the observed time period.

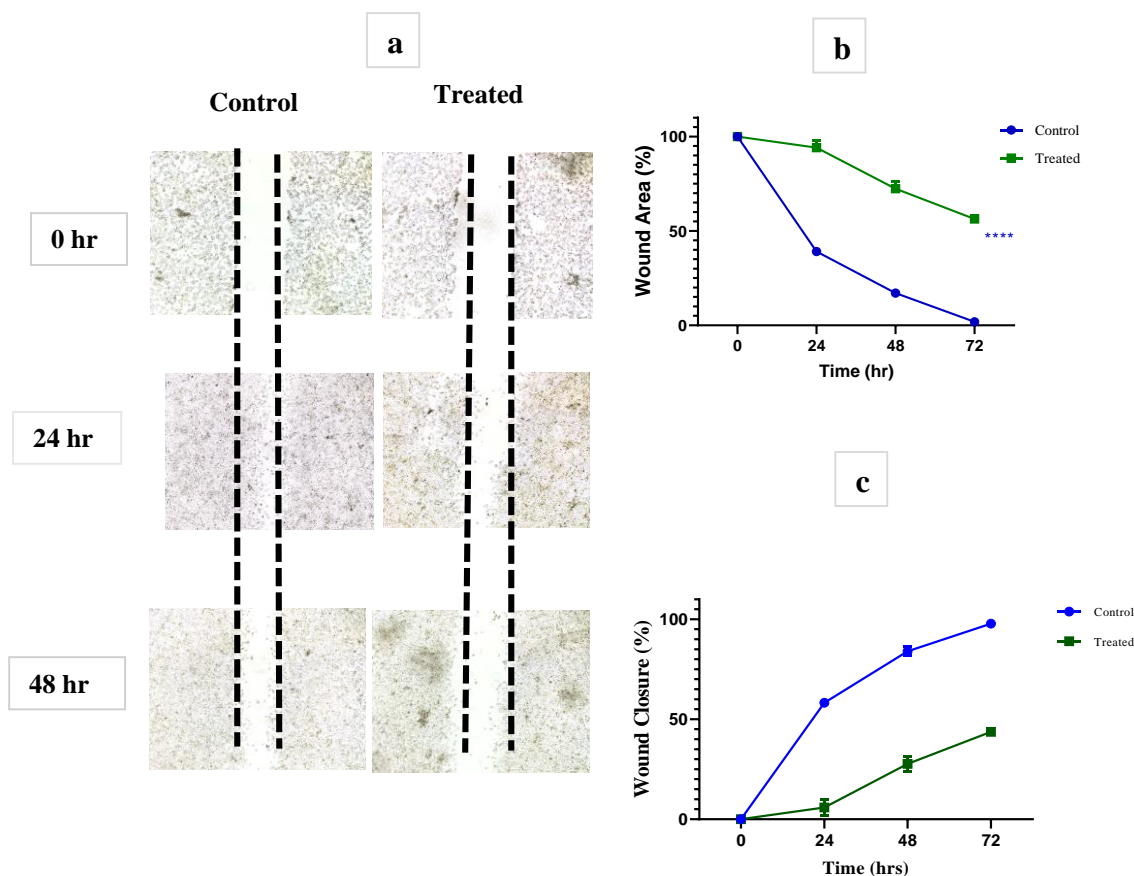


**Fig. 5.4.** Suppression of cellular migration in C4-2 cancer cells upon treatment with compound 5i in a time dependent manner

- (a) Confluent C4-2 cells upon treatment with 5i (16.50  $\mu$ M) after 48 hrs of wounding the cell monolayer using a sterilized pipette tip. Gap widths were evaluated after imaging cells at 0, 24, and 48 hours following treatment.
- (b) Representative images demonstrated suppression of wound healing in C4-2 cells upon treatment with 5i as compared to control DMSO.
- (c) Representative image showing wound closure in 5i treated C4-2 cells

Gap closure was evaluated using ImageJ software and the test was carried out in triplicates and quantified utilising Graphpad prism 8.0 software. \*P < 0.0001 was deemed to be significant.

### 5.3.5 Compound 5i reduces expression of androgen responsive genes

Androgens are well-established contributors to the growth and progression of prostate cancer, with the androgen-responsive pathway serving as a key indicator for monitoring prostate cancer advancement in humans. This study focused on examining the impact of the compound (E)-1-(4-(1H-indol-2-yl)phenyl)-N-(6-nitrobenzo[d]thiazol-2-yl)methanimine on the expression of androgen receptor (AR) target genes in C4-2 cancer cell line through RT-PCR. The study's outcomes revealed that the tested compound effectively lessened the expression of PSA and AR in C4-2 cells in vitro. These findings suggest that the compound may possess the ability to



impede the basal transcriptional activity of AR (**Figure 5.5**). The gene expression data were normalized using GAPDH (glyceraldehyde-3-phosphate dehydrogenase), and statistical examination was conducted using Graphpad Prism 8.0, with significance denoted as \*P < 0.0001.

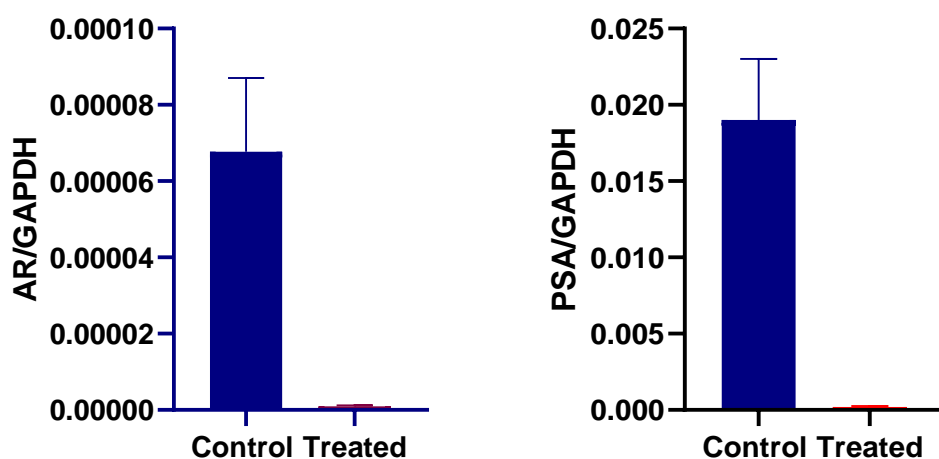


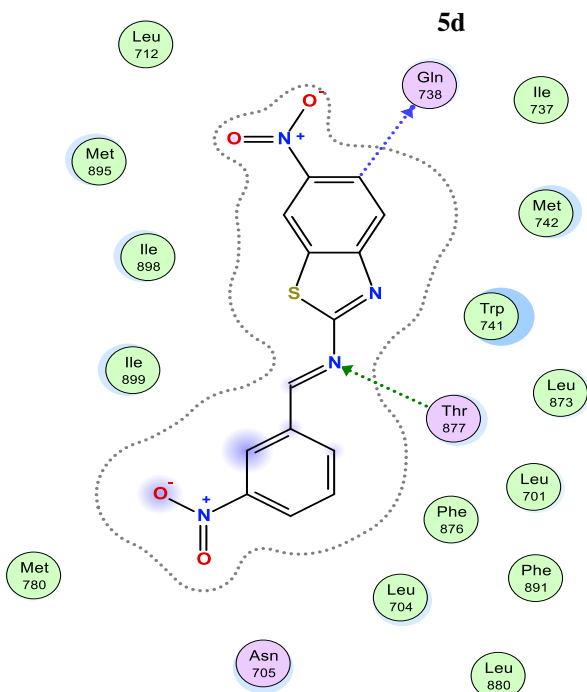
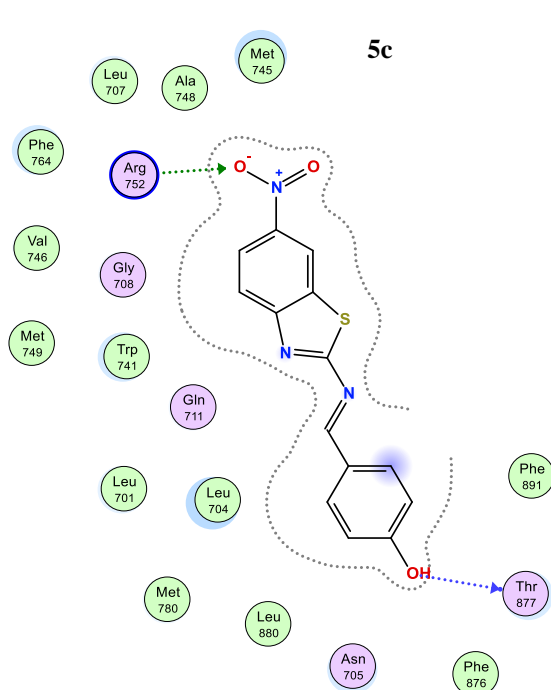
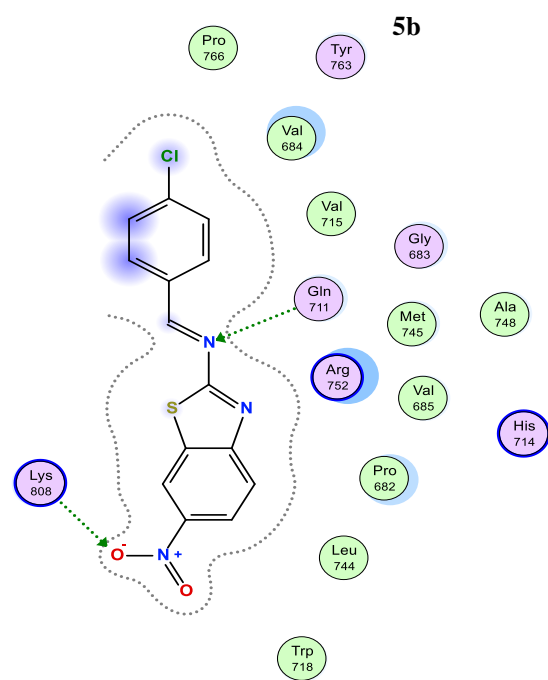
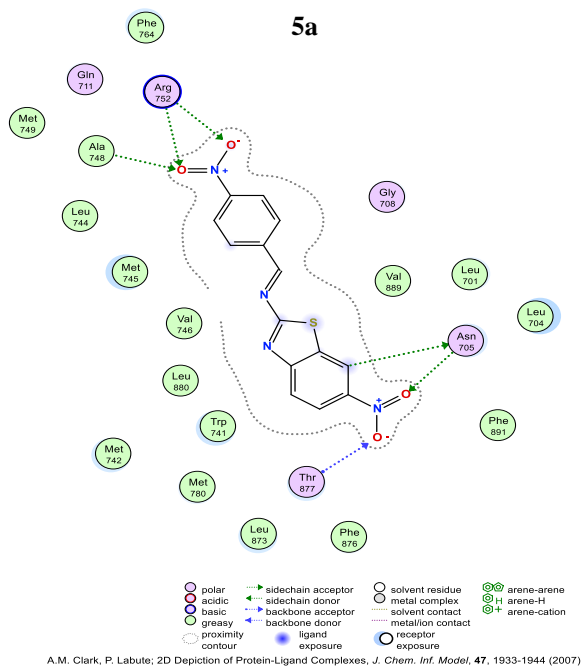
**Fig. 5.5.** Realtime gene expression of AR responsive genes following treatment with 5i (16.50  $\mu$ M) and DMSO as vehicle control

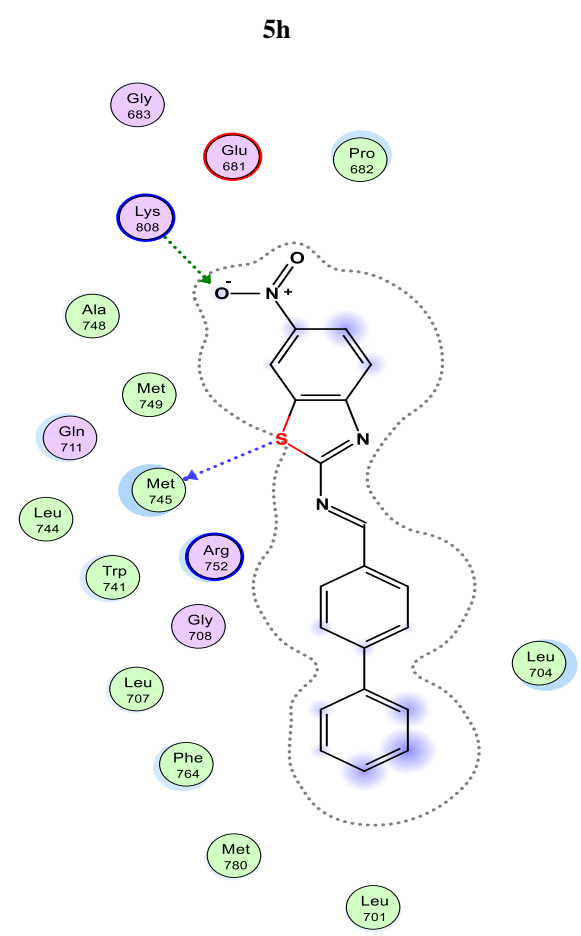
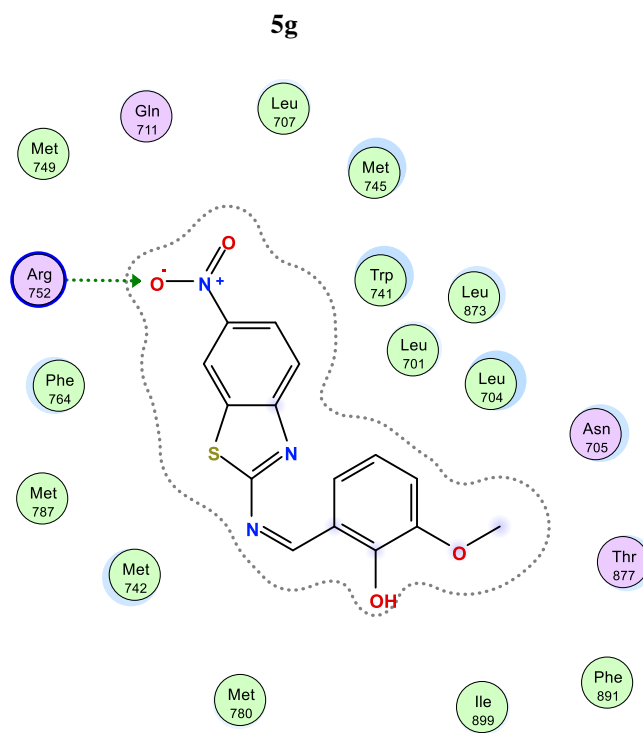
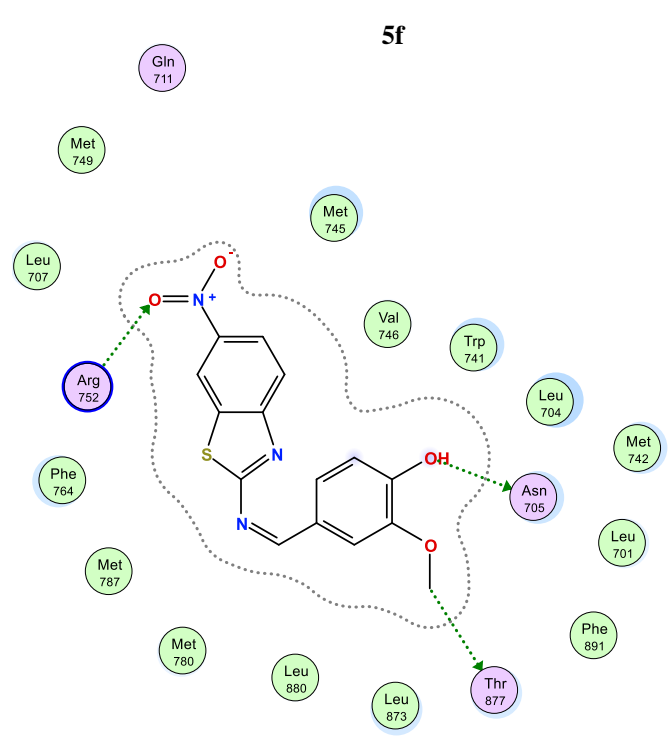
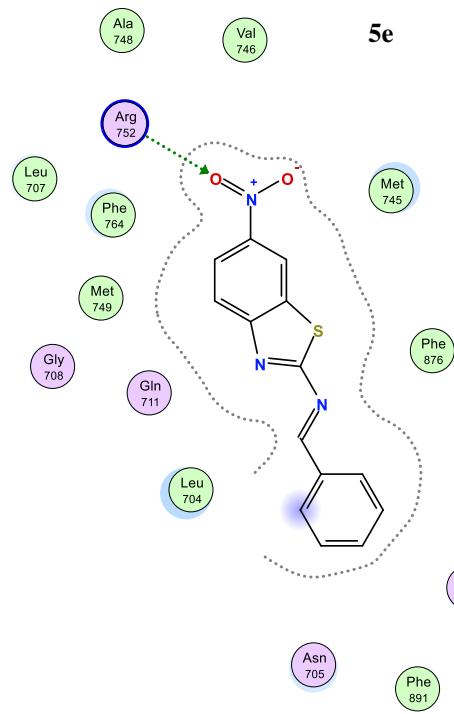
### 5.3.6 Analysis of Molecular Docking

AutoDock was used to evaluate the binding energy of compound 3g in the active site of the AR protein target. The interaction between the protein and 5i was reinforced by the establishment of several hydrogen bonds and stacking interactions with crucial residues of the protein. The docking analysis revealed that the affinity between AR and 5i was the most substantial, registering a score of -10.59 kcal/mol. 2D representations illustrating the intermolecular interactions between the docked compounds (**5a-5j**) and the target protein were generated (**Figure 5.6**). Notably, specific amino acid residues, including *GLU(681)*, *LYS(804)*, *PRO(682)*, *ALA(748)*, *LEU(744)*, *GLN(711)*, *PHE(784)*, *MET(745)*, *MET(749)*, *TRP(741)*, *MET(742)*, *LEU(873)*, *MET(780)*, *PHE(876)*, *LEU(701)*, *GLY(708)*, *SLEU(704)*, *ARG(752)* (**Table 5.2**), played a crucial role in facilitating the docking of compound 5i to the AR target protein.

**Table 5.2.** Energy binding score of the compound **5i** (kcal/mol) against various protein targets

<b>Compound</b>	<b>Amino acid residues</b>	<b>Energy binding score (kcal/mol)</b>
<b>5a</b>	<i>PHE(764), ARG(752), ALA(748), LEU(744), MET(745), VAL(746), LEU(880), TRP(741), MET(742), MET(780), THR(877), LEU(873), LEU(873), PHE(876), ASN(705), LEU(701), VAL(889), GLY(708), PHE(891), MET(749), LEU(704), GLN(711)</i>	-9.32
<b>5b</b>	<i>PRO(766), TYR(763), VAL(684), VAL(715), GLY(683), GLN(711), MET(745), ALA(748), ARG(752), VAL(685), HIS(714), PRO(682), LEU(744), TRP(718), LYS(808)</i>	-9.76
<b>5c</b>	<i>MET(745), ALA(748), LEU(707), PHE(764), ARG(752), VAL(746), GLY(708), MET(749), TRP(741)GLN(711), LEU(701), LEU(704), MET(780), LEU(880), ASN(705), PHE(705), THR(877), PHE(891)</i>	-9.74
<b>5d</b>	<i>LEU(712), MET(895), ILE(898), ILE(899), LEU(704), LEU(880), PHE(876), PHE(891), THR(877), LEU(701), LEU(873), MET(742), ILE(737)GLN(738), ASN(705), TRP(741)</i>	-9.91
<b>5e</b>	<i>ALA(748), VAL(746), ARG(752), LEU(707), PHE(764), MET(749)GLY(708), GLN(711), LEU(704), ASN(705), PHE(891), THR(877), LEU(880), MET(780), VAL(746), MET(745), LEU(701)</i>	-10.08
<b>5f</b>	<i>GLN(711), MET(749), LEU(707), ARG(752), MET(780), LEU(880), LEU(873), THR(877), PHE(891), LEU(701), ASN(705), MET(742), LEU(704), TRP(741), VAL(746), MET(745), MET(787), PHE(764)</i>	-9.97
<b>5g</b>	<i>GLN(711), MET(749), ARG(752), PHE(764), MET(787), MET(742), MET(780), ILE(899), PHE(891), THR(877), LEU(704), LEU(701), LEU(873), ASN(705), TRP(741), MET(745), LEU(707)</i>	-9.45
<b>5h</b>	<i>GLY(683), PRO(682), GLU(681), LYS(808), ALA(748), MET(745), GLN(711), LEU(744), ARG(752), GLY(708), LEU(707)PHE(764), MET(780), LEU(701), LEU(9704), PRO(682)</i>	-10.02
<b>5i</b>	<b><i>GLU(681), LYS(804), PRO(682), ALA(748), LEU(744), GLN(711), PHE(784), MET(745), MET(749), TRP(741), MET(742), MET(780), PHE(876), LEU(701), GLY(708), LEU(704), ARG(752), LEU(9873)</i></b>	<b>-10.59</b>
<b>5j</b>	<i>VAL(684), TYR(763), ALA(748), VAL(685), GLY(683), PRO(682), ARG(752), MET(745), GLU(681), LEU(744), TRP(718), HIS(714), VAL(715), GLN(711), LYS(808)</i>	-9.85





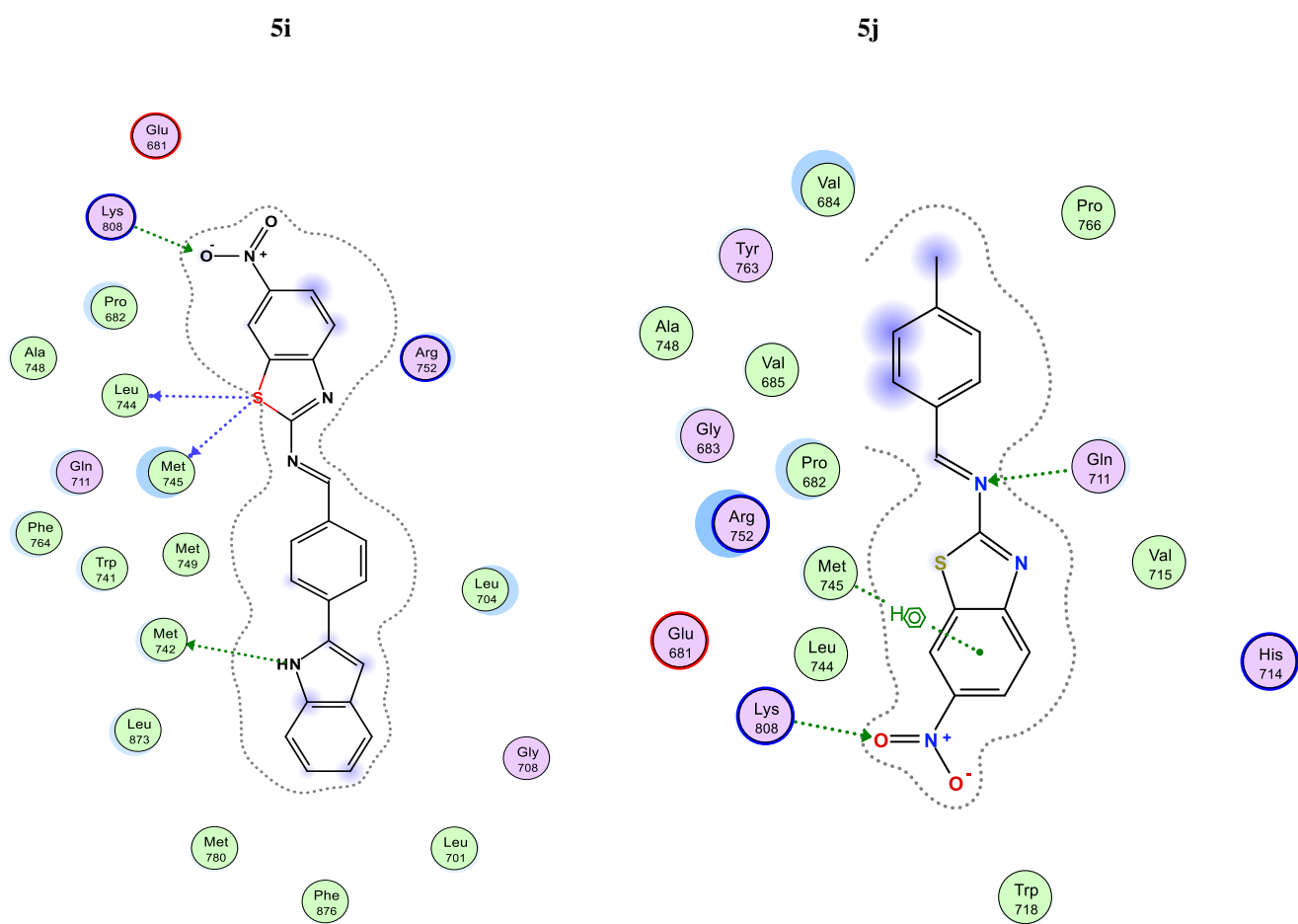


**Fig. 5.6.** 2D representation involving binding interactions between synthesized compounds (**5a-5j**) and AR protein binding site.

### 5.3.7 ADME and drug-likeness analysis

The active compounds underwent an assessment of their ADME properties using SwissADME. This tool predicts various physicochemical attributes, including molecular weight, solubility, and the count of hydrogen bonds donated and/or accepted to water molecules in the medium. These parameters, constituting the Lipinski Rule of Five, serve as criteria for evaluating a molecule's drug-like characteristics and predicting its pharmacokinetics in living organisms. The findings indicated that each compound demonstrated promising potential as a candidate for medication, aligning with the acceptable values stipulated by Lipinski's rule (Table 5.3).

Table 5.3: ADME characteristics and drug likeness properties of the screened molecules

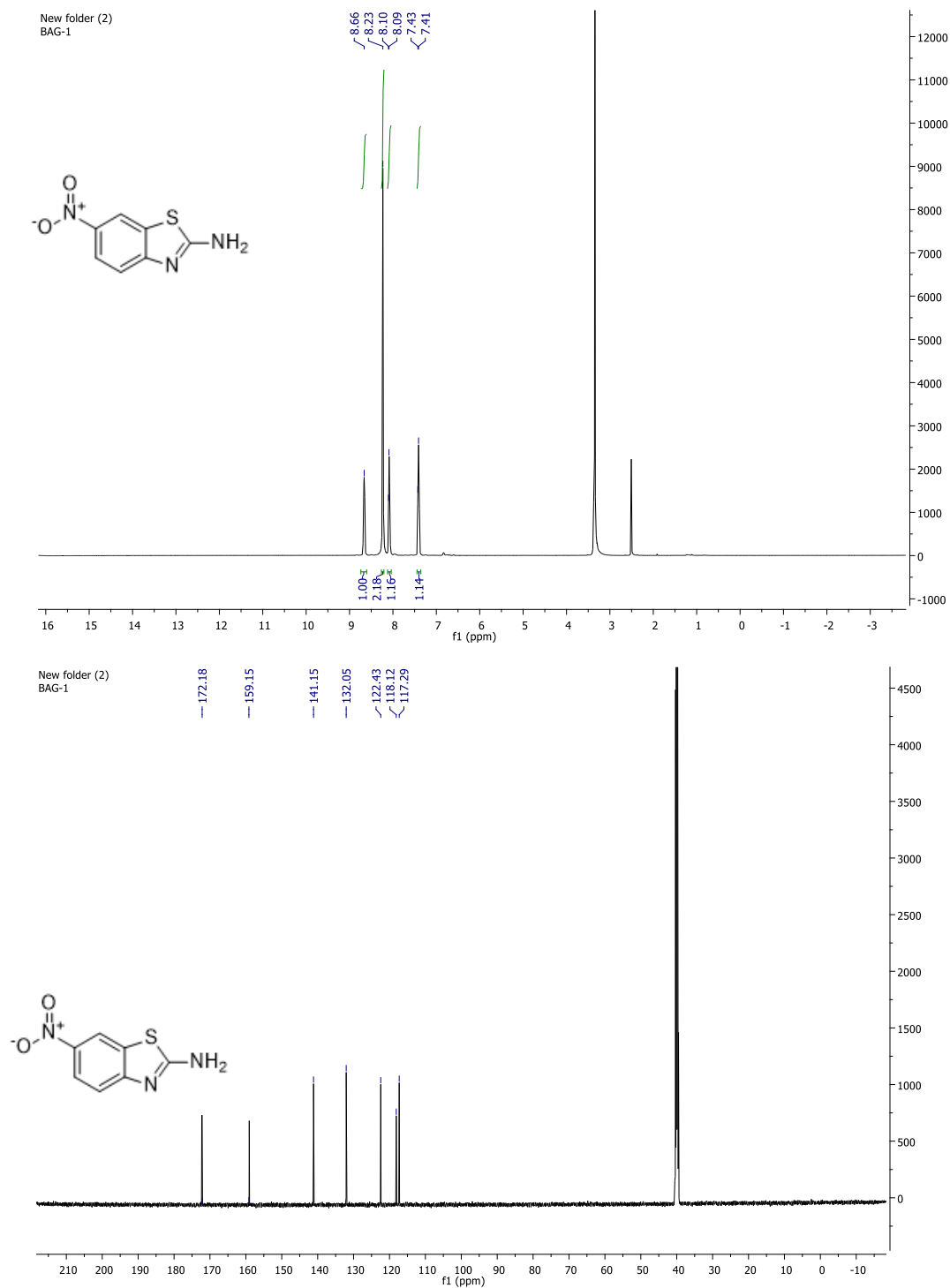
Compound	Molecular formula	Molecular weight	Number of rotatable bonds	Number of hydrogen bond acceptors	Number of hydrogen bond donors	Lipinski's rule
5a	C <sub>14</sub> H <sub>8</sub> N <sub>4</sub> O <sub>4</sub> S	328.3	4	6	0	YES
5b	C <sub>14</sub> H <sub>8</sub> ClN <sub>3</sub> O <sub>2</sub> S	317.5	3	4	0	YES
5c	C <sub>14</sub> H <sub>9</sub> N <sub>3</sub> O <sub>3</sub> S	299.3	3	5	1	YES
5d	C <sub>14</sub> H <sub>8</sub> N <sub>4</sub> O <sub>4</sub> S	328.3	4	6	0	YES
5e	C <sub>14</sub> H <sub>9</sub> N <sub>3</sub> O <sub>2</sub> S	283.3	3	4	0	YES
5f	C <sub>15</sub> H <sub>11</sub> N <sub>3</sub> O <sub>4</sub> S	329.3	4	6	1	YES
5g	C <sub>15</sub> H <sub>11</sub> N <sub>3</sub> O <sub>4</sub> S	329.3	4	6	1	YES
5h	C <sub>20</sub> H <sub>13</sub> N <sub>3</sub> O <sub>2</sub> S	359.4	4	4	0	YES
5i	C <sub>22</sub> H <sub>14</sub> N <sub>4</sub> O <sub>2</sub> S	398.4	4	4	1	YES
5j	C <sub>15</sub> H <sub>11</sub> N <sub>3</sub> O <sub>2</sub> S	297.3	3	4	0	YES

## 5.4 Conclusion

Benzothiazoles constitute a diverse class of synthetic compounds renowned for their broad spectrum of pharmacological effects. Some derivatives incorporating various phenyl/heterocyclic moieties with an imine linkage linkage this class have exhibited promising anti-cancer properties across various stages of cancer development. Notably, a synthesized derivative, (E)-1-(4-(1H-indol-2-yl) phenyl)-N-(6-nitrobenzo[d]thiazol-2-yl)methanimine, has demonstrated remarkable efficacy against the C4-2 cancer cell line, fueling enthusiasm for the exploration of small molecules in cancer therapy. Additionally, this derivative has effectively downregulated the expression of key genes associated with androgen response in castration-resistant prostate cancer cells in laboratory experiments. In the computational realm, analyses have identified compound (E)-1-(4-(1H-indol-2-yl) phenyl)-N-(6-nitrobenzo[d]thiazol-2-yl)methanimine as exhibiting the highest binding affinity for the AR protein, marking it as a potential lead candidate with favorable pharmacokinetic properties.

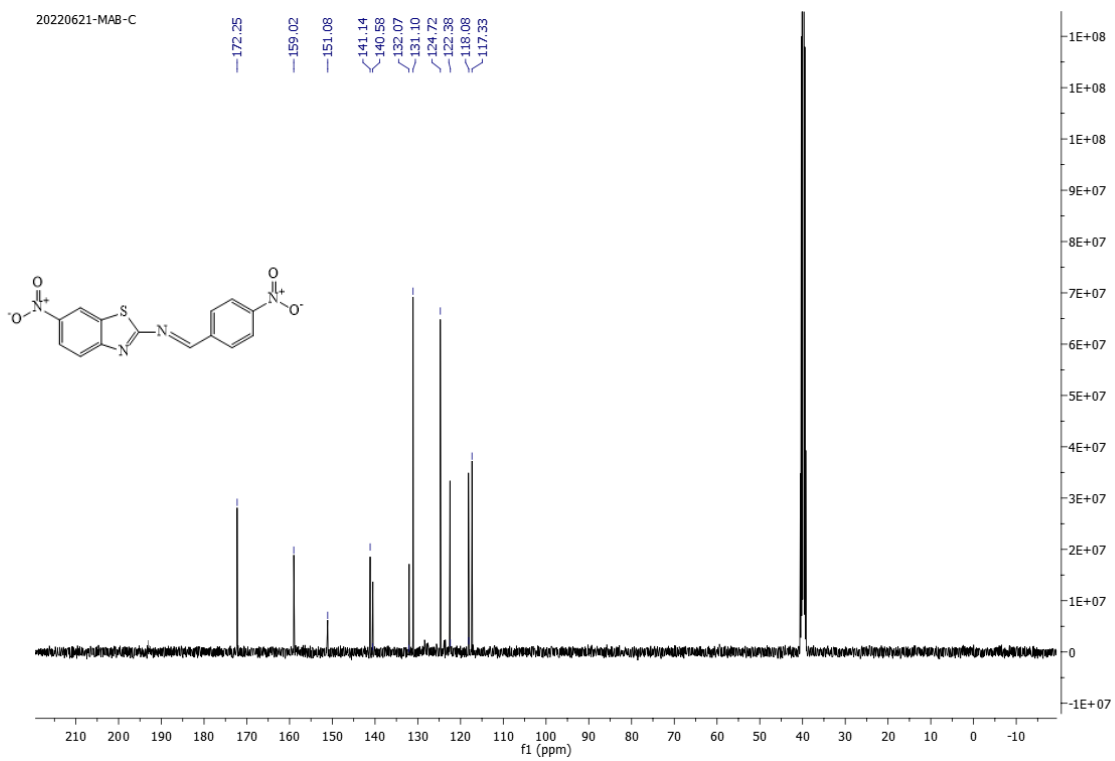
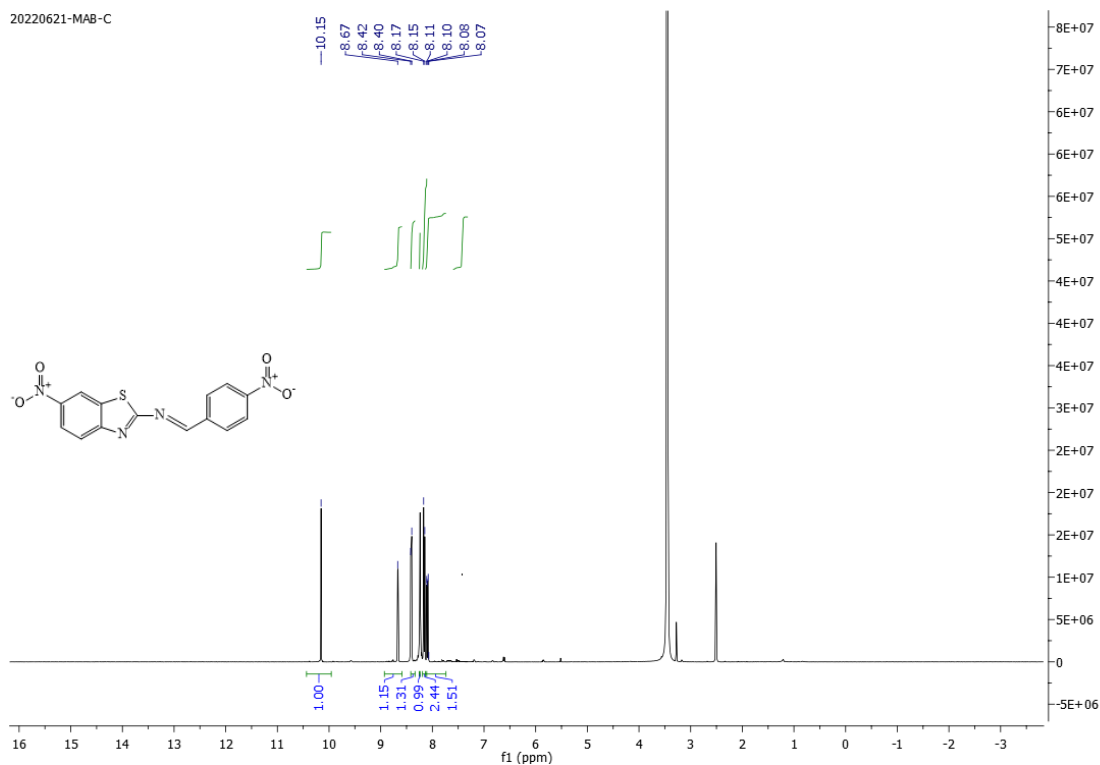
## REPRESENTATIVE SPECTRA

○ (3)

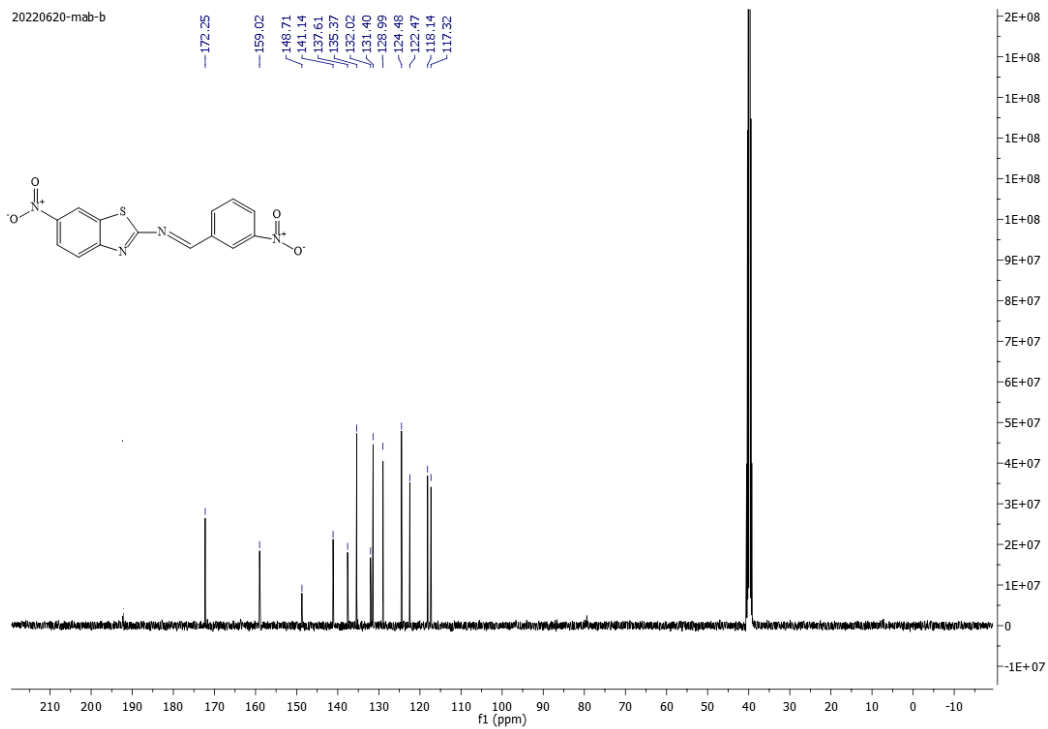
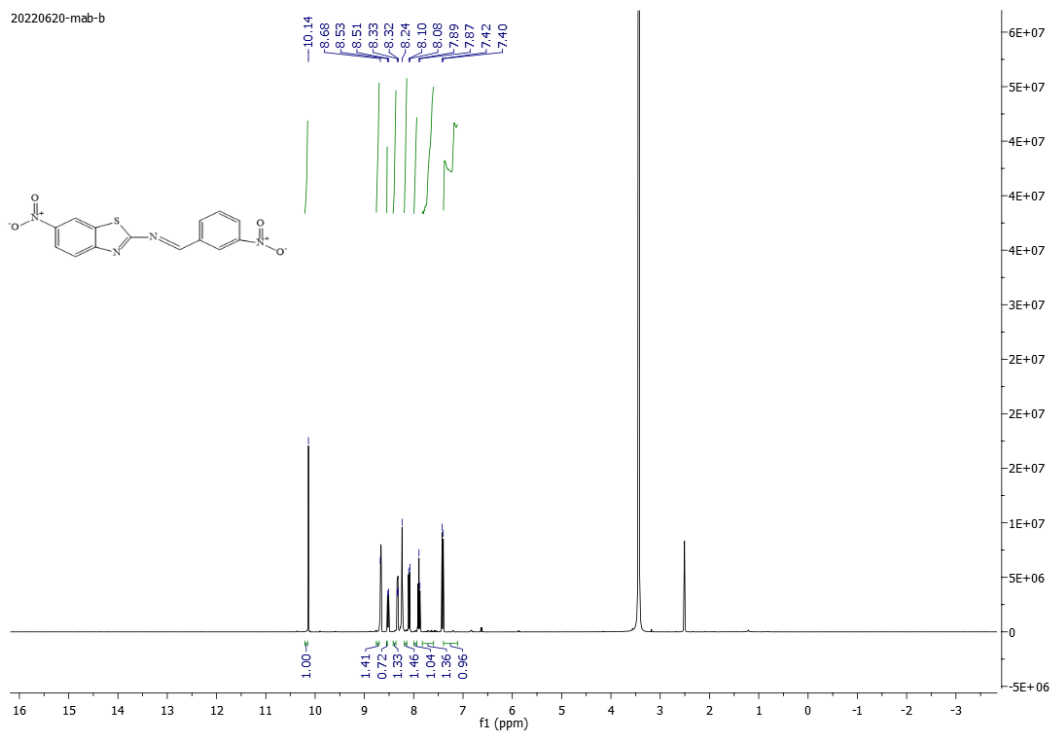




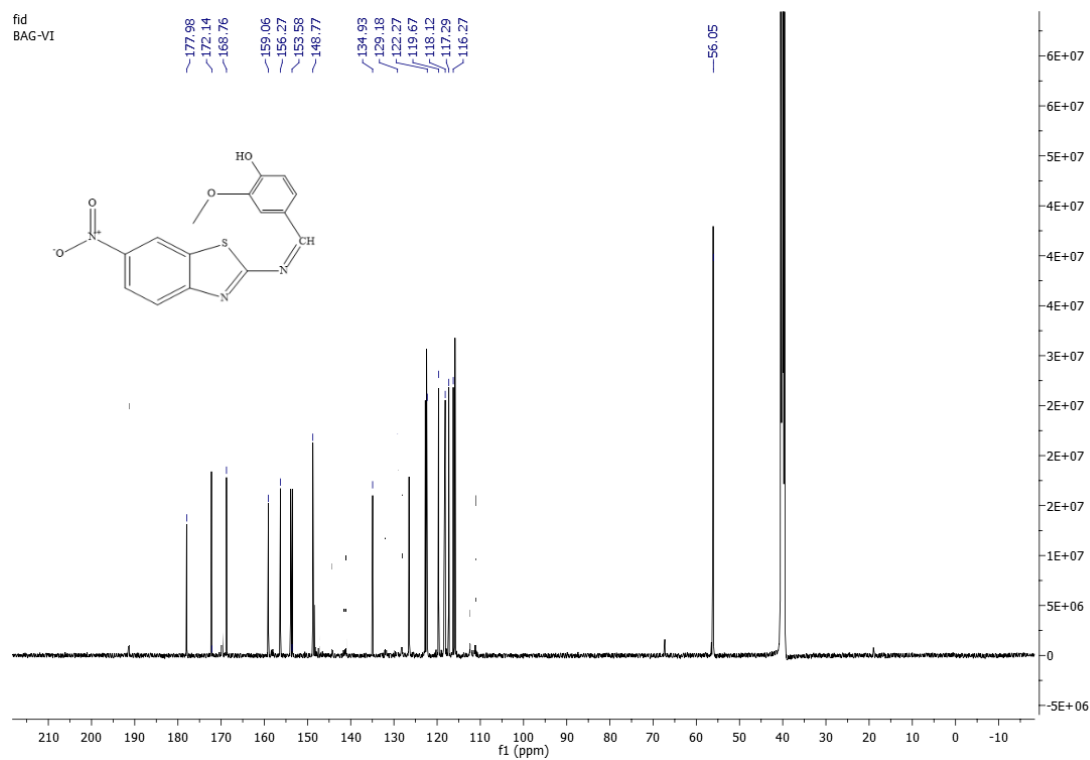
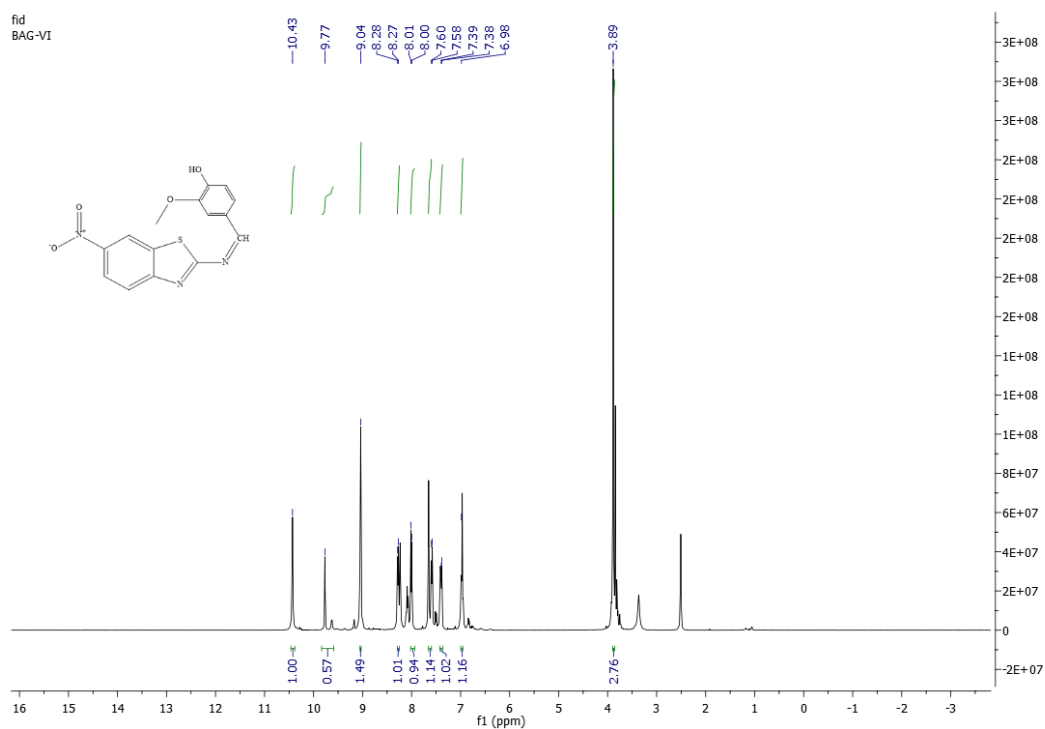
○ (5a)



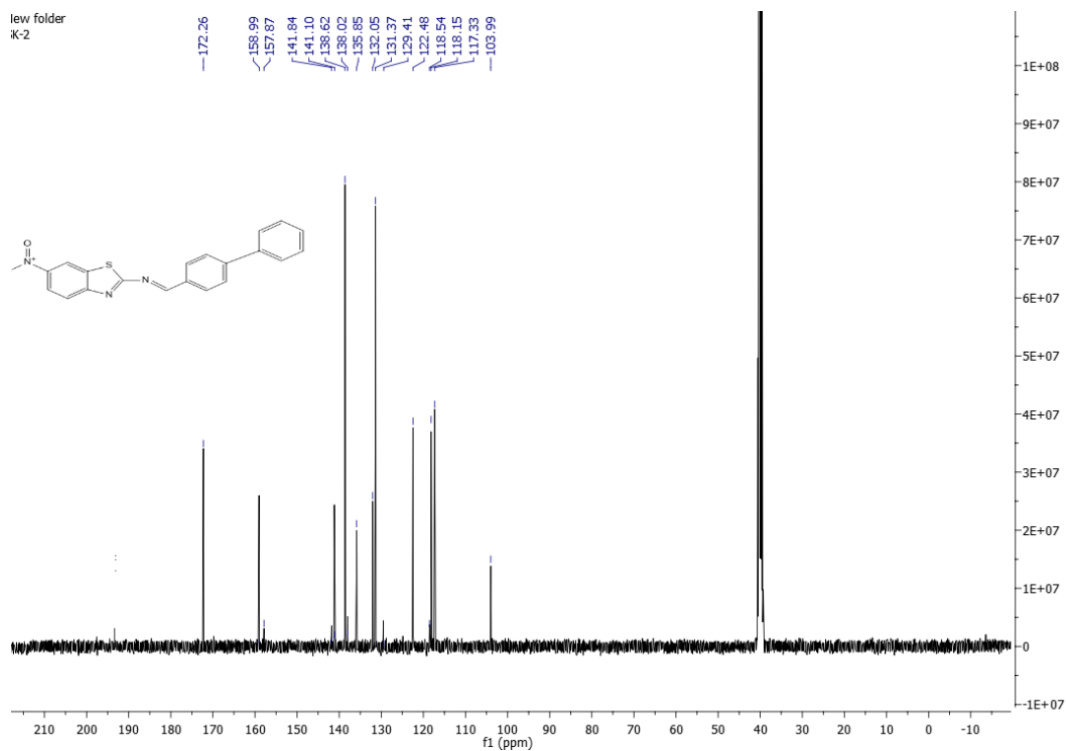
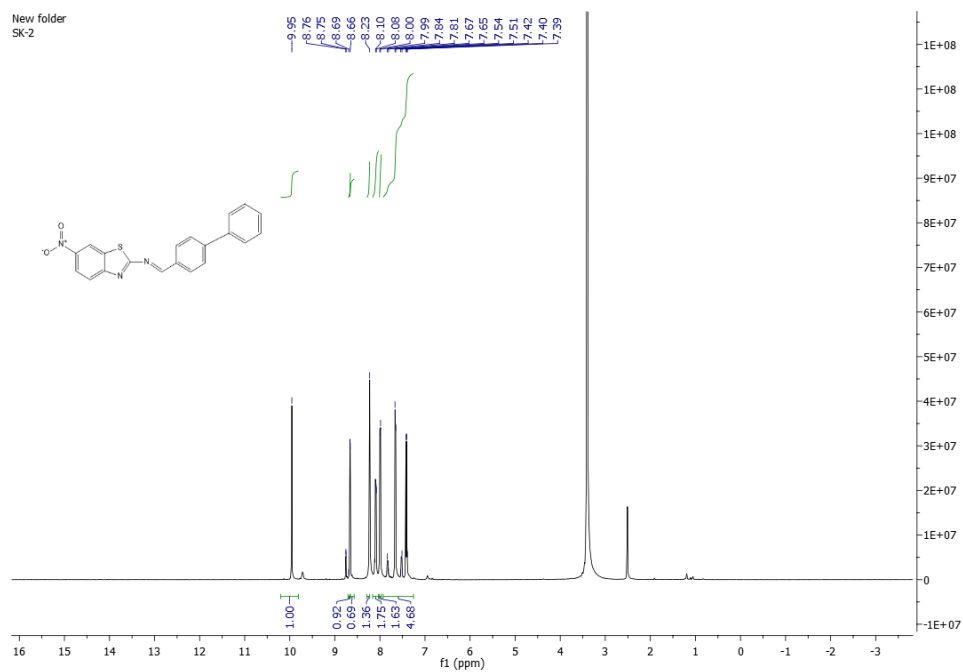
○ (5d)



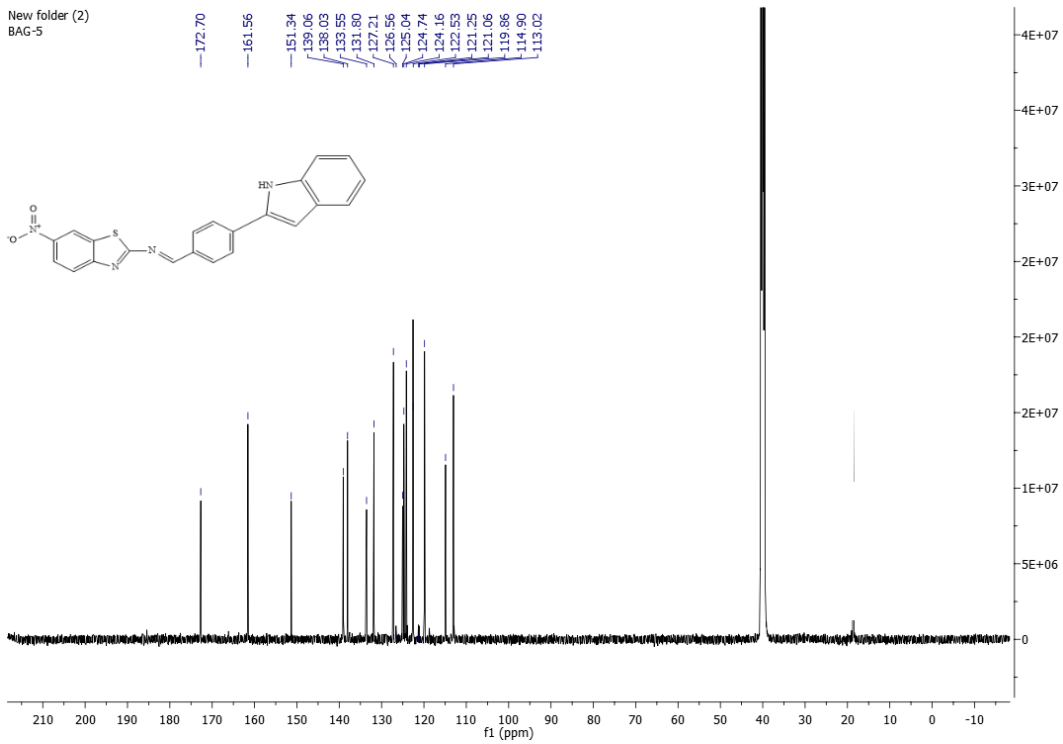
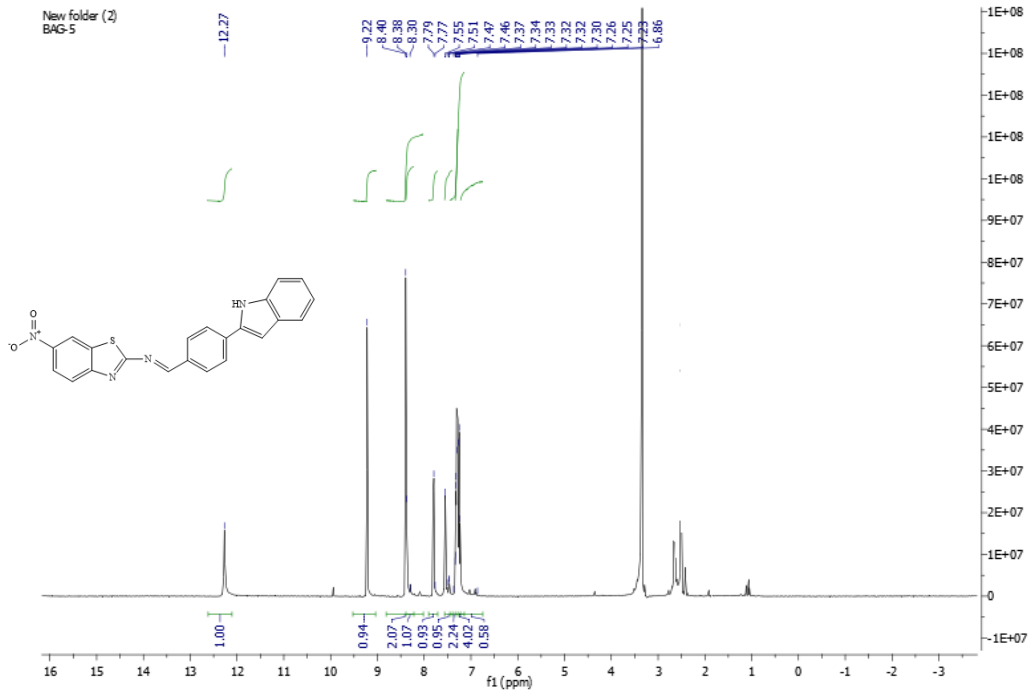
○ (5f)



○ (5h)



○ (5i)



*Chapter 6:*  
**Future Scope**

## 6.1 Introduction

The thiazole group plays a significant role in drug design due to its frequent presence in the chemical structures of numerous natural substances and bioactive compounds (**Figure 6.1**). Examples include thiamine, certain antibiotic drugs such as penicillin and micrococcin, as well as various metabolic products derived from fungi and primitive marine animals. Piperzinyl-thiazole scaffolds hold significance in various medical and pharmaceutical contexts, demonstrating efficacy as potent antiviral and anti-inflammatory agents, AChE inhibitors, antimicrobials, and EP1 receptor antagonists [262, 263]. Building upon these insights and our ongoing research on diverse five-membered heterocycles and structural studies, we have developed novel derivatives incorporating piperazinyl-thiazole moieties. Similarly, the inclusion of the 2,3-dihydro-1,3- thiazine ring within cephalosporin piques interest in the synthesis and subsequent biological assessment of the thiazine system.

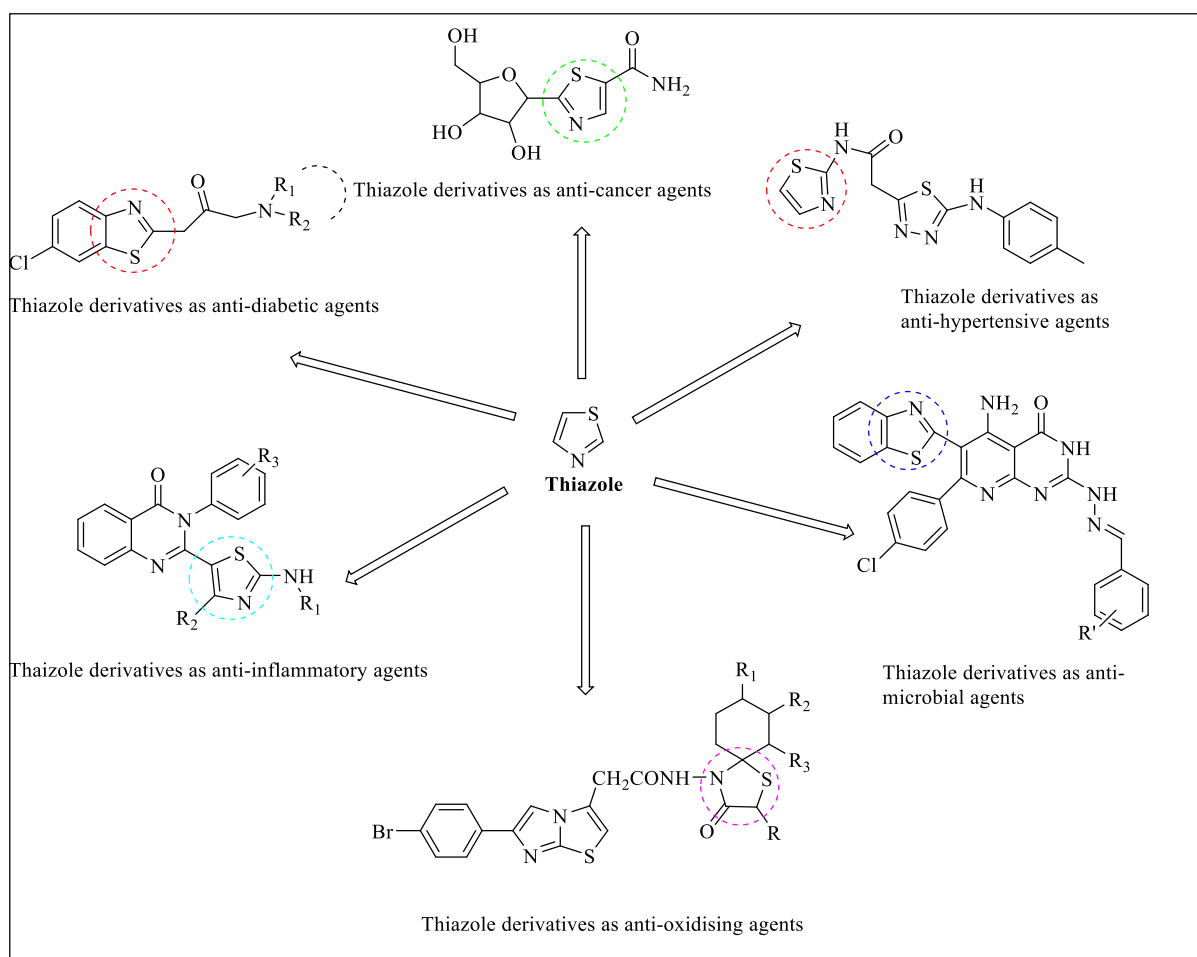


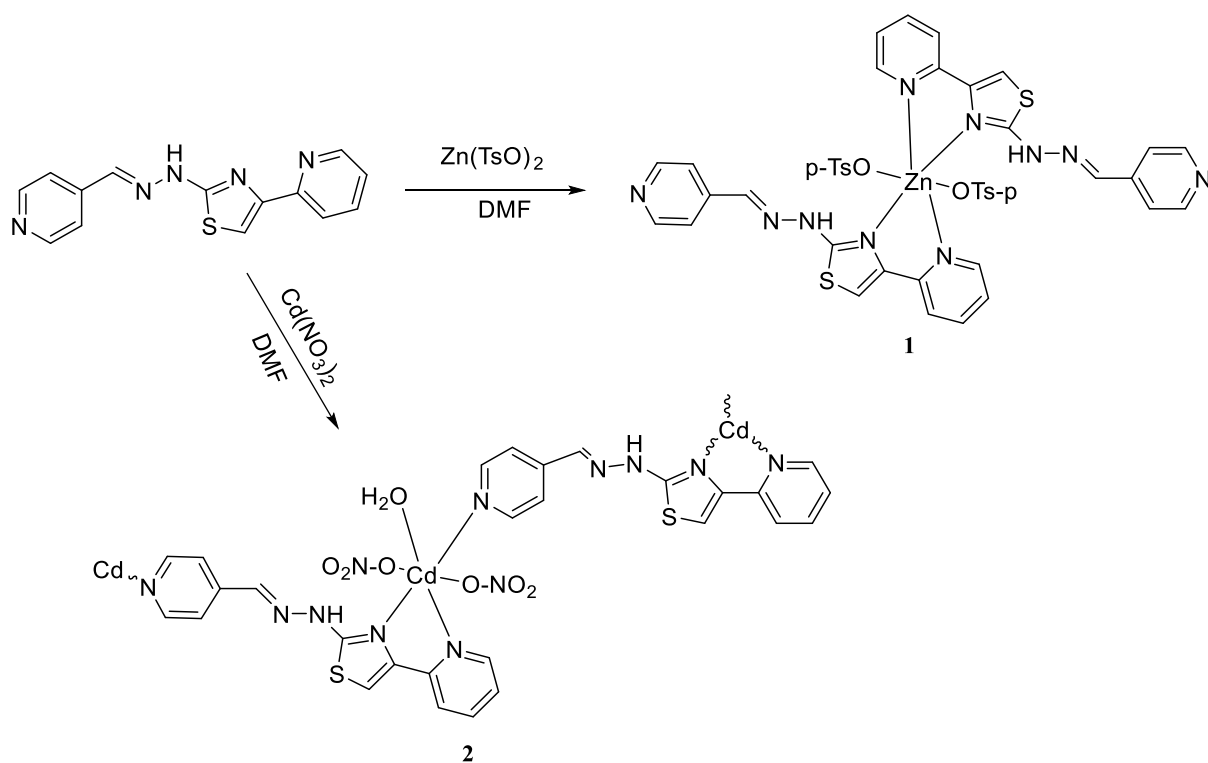
Figure 6.1: An overview of diverse pharmacological properties of thiazole ring

The future of research in heterocyclic chemistry, particularly focusing on benzothiazole and benzothiazine derivatives, holds significant promise and potential. Building on the insights gained from the current study, several avenues for future research can be envisioned:

### **6.2 Development of metal complexes containing thiazole/thiazines as chelating agents**

A novel pyridine thiazole derivative, 4-(pyridin-4-yl)-2-(2-(pyridin-2-yl-methylene)hydrazinyl) thiazole, was synthesized through cyclization has been reported. Subsequently, complexes  $[Zn(L)_2(TsO)_2] \cdot 2DMF$  **1** and  $\{[Cd(L)(NO_3)_2 \cdot 2H_2O]DMF\}_n$  **2** were formed by coordinating the ligand with  $Zn(TsO)_2$  and  $Cd(NO_3)_2$ , respectively. The resulting compounds were characterized using various techniques such as NMR, elemental analysis, IR spectroscopy, and single-crystal X-ray diffraction [264]. The study suggests promising applications for these complexes in the pharmaceutical field, building on the positive outcomes observed with similar pyridine thiazole derivatives in previous research. Similar approach can be used for metal complexation processes involving piperziny-thiazole entities as ligands. Further exploration involving different coordination sites or metal salts is deemed interesting in this context.

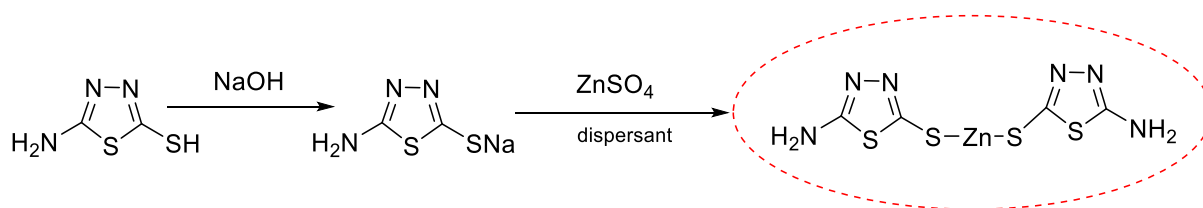




**Scheme 6.1:** Synthesis of complexes of 4-(pyridin-4-yl)-2-(2-(pyridin-2-ylmethylene) hydrazinyl) thiazole

### 6.3 Development of versatile nanoparticles of thiazole/thiazines as drug delivery systems

Nanotechnology has introduced a new method for developing a secure and highly efficient pesticide formulation. Thiazole-Zn, a commonly used bactericide, was effectively produced at the nanoscale through an innovative control approach during the final synthetic procedure. The likely formation mechanism, involving restricted particle aggregation within a nano-reactor, was explained. Subsequently, to evaluate the practical performance of thiazole-Zn nanoparticles, an NPF was conveniently created. Remarkably, the physicochemical characteristics of the NPF exhibited superior characteristics compared to the commercial pesticide formulation (CPF), specifically in terms of dispersibility, spreadability, wettability, and stability [265].



**Scheme 6.2:** Synthetic procedure for zn-thiazole nanoparticle

A synthone, specifically 3-(4-amino-phenyl)-2,3-dihydro-benzo<sup>2</sup>[1,3]thiazine derivative was employed in the synthesis of various Schiff bases. The characterization of the synthesized compounds was conducted using IR, NMR, and other spectrophotometric methods. Additionally, silver nanoparticles were produced through chemical reduction and characterized through X-Ray diffraction (XRD), FT-IR, atomic force microscope (AFM), and scanning electron microscope (SEM). These silver nanoparticles served as a foundational nano metal for the preparation of Schiff bases-Ag NPs derivatives. Similar approach can be devised for the synthesis of synthesized N-(6-nitrobenzo<sup>2</sup>thiazol-2-yl)methanimine based Schiff bases [266].

The future of thiazine and thiazole-based derivatives in medicine is highly promising. Ongoing research into their pharmacological properties, combined with innovative drug design and development techniques, positions these compounds as vital candidates for new therapies in treating various diseases, including infections, cancers, neurological disorders, and metabolic syndromes.

*Chapter 7:*  
**Summary & Conclusion**

This study highlights notable frameworks within organic chemistry, specifically focusing on benzothiazoles and benzothiazines. These compounds serve as important scaffolds, offering diverse opportunities for chemical exploration and synthesis. The research aims to provide a comprehensive understanding of the structural and functional characteristics of benzothiazoles and benzothiazines, shedding light on their potential application in anticancer research. Through detailed analysis and elucidation, the study aims to uncover the intrinsic properties and synthetic pathways of these compounds, thereby contributing to the advancement of organic chemistry knowledge and the development of novel molecules with valuable properties.

The study provides comprehensive insights into various aspects of the synthesis, biological activities, molecular interactions, and pharmacokinetic profiles of 1,4-benzothiazine derivatives, highlighting their potential as promising candidates for further development as anti-cancer agents. The synthesis of 1,4-benzothiazines was achieved through a two-step approach involving the oxidation of 2-aminobenzenethiols to disulfide, followed by cyclocondensation with 1,3-dicarbonyls. This method was optimized to enhance product yields, reaching up to 80-85%. Tested benzothiazine derivatives exhibited significant cytotoxic effects against A 549 lung cancer cells, with some compounds showing higher potency, notably compound 3c (Table 7.1). Compound 3c demonstrated dose-dependent inhibition of colony formation in A 549 cells with  $IC_{50}$  value of 25  $\mu$ M. Compound 3c effectively suppressed the migration of A 549 cells time-dependently. It also reduced the expression of pro-inflammatory genes in A 549 cells, indicating its potential anti-inflammatory effects. Molecular docking studies revealed strong binding affinities of compound 3c with various protein targets implicated in inflammation and cancer, such as COX-2, IL-8, IL-1 $\beta$ , and TNF- $\alpha$ . Assessment of pharmacokinetic attributes using SwissADME indicated that the synthesized compounds met Lipinski's rule of five criteria, suggesting their potential suitability as drug candidates.

**Table 7.1. The inhibition rates for A-549 and C4-2 in vitro (3a-3g)**

Compound	Inhibition rate of A-549% ( $\mu\text{M}$ )					Inhibition rate of C4-2(%) ( $\mu\text{M}$ )				
	10	20	30	40	50	10	20	30	40	50
<b>3a</b>	66.52	51.78	37.45	21.19	10.15	78.85	66.51	54.97	32.28	21.22
<b>3b</b>	60.10	49.27	33.95	17.38	3.42	74.60	58.30	49.75	25.04	10.08
<b>3c</b>	<b>50.88</b>	<b>40.01</b>	<b>20.64</b>	<b>10.83</b>	<b>1.02</b>	<b>68.79</b>	<b>53.11</b>	<b>40.08</b>	<b>19.86</b>	<b>5.33</b>
<b>3d</b>	71.29	61.28	51.30	30.21	13.75	81.42	73.51	65.02	40.05	24.02
<b>3f</b>	77.38	65.73	54.36	36.75	18.31	89.76	78.63	67.39	42.11	28.95
<b>3e</b>	62.31	53.71	40.66	20.41	2.67	78.33	61.98	51.02	29.92	8.91
<b>3g</b>	57.08	43.89	27.31	13.95	1.85	70.81	54.02	45.84	22.75	7.04
<b>EF24</b>	11.41	9.40	6.68	2.17	0.65	69.88	56.89	42.91	30.50	9.21
<b>Enzalutamide</b>	59.78	51.37	44.82	22.86	4.77	15.34	11.06	6.05	2.06	1.20

The study also presents a novel method for synthesizing 2-substituted thiazoles via C-N coupling, aiming for economic viability and environmental friendliness. This method eliminates drawbacks associated with previous synthesis methods, such as non-recyclability, toxicity, and high reaction temperatures. The investigation found that the desired product can be achieved through the combination of 2-chlorobenzothiazole with a secondary amine at room temperature and water as a solvent. Bioassay results indicate significant cytotoxic effects of synthesized benzothiazole derivatives against prostate cancer cells (Table 7.2). Compound 3g' exhibited the highest cytotoxicity and was chosen for further evaluation. Structure-activity relationship analysis revealed that electron-donating groups and fusion with biologically significant entities enhanced cytotoxic activity. CFU assay demonstrated dose-dependent inhibition of cellular growth by compound 3g' with an  $\text{IC}_{50}$  value of 19.45  $\mu\text{M}$ , while wound healing assay showed its ability to reduce cell migration over time. In vitro gene expression analysis revealed that compound 3g' reduced the expression of androgen receptor (AR) target genes in prostate cancer cells, suggesting its potential to inhibit the androgen-responsive pathway. Molecular docking analysis indicated strong binding affinity of compound 3g' with the AR protein target, supported by molecular dynamics simulation showing stable protein-ligand interactions. MM-GBSA calculations further validated the stability of the 2PNU+3g' complex, with the ligand demonstrating high binding affinity to the protein. Principal component analysis of MD trajectories provided insights into the stochastic atomic motion

within the protein-ligand complex. ADMET analysis showed that the synthesized compounds adhere to Lipinski's Rule of Five, indicating favorable drug-like properties for further development as potential drugs.

**Table 7.2. The inhibition rates for A-549 and C4-2 in vitro (3a'-3j')**

Compound	Inhibition rate of C4-2(%) ( $\mu$ M)					Inhibition rate of A-549(%) ( $\mu$ M)				
	10	20	30	40	50	10	20	30	40	50
3a'	50.12	35.98	28.05	16.19	7.15	68.95	55.51	42.97	32.98	19.22
3b'	54.23	40.97	34.95	22.98	10.42	70.60	58.30	46.75	35.04	26.08
3c'	50.58	36.01	27.65	17.83	7.62	62.99	51.11	40.08	29.86	17.39
3d'	55.29	41.18	34.30	21.26	10.75	65.92	54.11	45.80	30.15	19.31
3e'	45.78	34.64	24.06	15.75	6.37	59.76	48.63	37.39	22.11	9.95
3f'	59.31	49.78	38.86	27.49	13.68	71.33	59.98	49.02	39.92	29.31
<b>3g'</b>	<b>39.11</b>	<b>22.89</b>	<b>15.31</b>	<b>7.95</b>	<b>0.98</b>	<b>49.81</b>	<b>34.10</b>	<b>25.97</b>	<b>13.75</b>	<b>5.04</b>
3h'	50.65	35.67	29.66	15.71	7.89	67.41	52.37	41.98	39.60	15.88
3i'	50.88	37.01	28.64	15.83	6.92	60.79	53.11	42.08	29.86	17.33
3j'	52.90	39.95	30.29	20.79	9.50	64.19	54.30	45.08	32.90	18.92
Enzalutamide	11.41	8.40	5.68	1.17	0.65	69.88	56.89	42.91	30.50	9.21
EF24	59.78	51.37	44.82	22.86	4.77	15.34	11.06	6.05	2.06	1.20

Further, the studies outline the synthesis and characterization of various benzothiazole-based compounds (5a-5j) and their evaluation for anticancer potential through cytotoxicity assays, colony formation assays, and wound healing assays. The compounds were synthesized following a well-defined procedure and characterized using FT-IR,  $^1\text{H-NMR}$ , and  $^{13}\text{C-NMR}$  analyses. The synthesis yielded compounds with satisfactory purity and yields ranging from 79% to 92%. The synthesized compounds were evaluated for their cytotoxic effects on cancer cell lines (A549 and C4-2) and a normal cell line (HEK293T) using the MTT assay. Among the tested compounds, 5i exhibited the most promising cytotoxic effects against C4-2 cancer cells with minimal toxicity towards HEK293T normal cells (Table 7.3). This indicates its potential as a selective anticancer agent. The colony formation assay further confirmed the cytotoxic effects of compound 5i on C4-2 cells in a dose-dependent manner with an  $\text{IC}_{50}$  value

of 18.50  $\mu\text{M}$ . Treatment with 5i led to a significant reduction in colony formation ability, suggesting its inhibitory effect on cancer cell proliferation. Compound 5i demonstrated inhibition of cell migration in the wound healing assay. The compound effectively decreased the closure of the wound gap in C4-2 cells over time, indicating its potential to impede cancer cell migration and invasion. Molecular docking studies further elucidated its potential mechanism of action through binding interactions with the androgen receptor. These findings suggest that the synthesized benzothiazole-schiff base compounds may serve as a promising lead compound for the development of novel anti-cancer agents for the treatment of prostate cancer.

**Table 7.3. The inhibition rates for C4-2 and A-549 cell lines in vitro (5a-5i)**

Compound	Inhibition rate of C4-2(%) ( $\mu\text{M}$ )					Inhibition rate of A-549(%) ( $\mu\text{M}$ )				
	10	20	30	40	50	10	20	30	40	50
5a	55.52	40.78	32.45	20.19	10.15	68.85	56.51	44.97	32.28	19.22
5b	52.10	40.27	29.95	17.38	7.42	64.60	55.30	44.75	32.04	19.08
5c	50.88	40.01	20.64	10.83	7.02	62.79	53.11	40.08	29.86	15.33
5d	51.29	41.28	33.30	20.21	8.75	65.42	54.51	45.02	30.05	19.02
5e	45.38	35.73	24.36	6.75	1.31	59.76	48.63	37.39	22.11	9.95
5f	46.31	39.71	28.66	11.41	3.67	60.33	51.98	41.02	29.92	10.91
5g	47.08	39.89	29.31	13.95	3.85	59.81	44.02	35.84	22.75	10.04
5h	40.65	30.67	19.66	3.70	1.89	55.41	40.37	31.98	19.60	7.88
<b>5i</b>	<b>38.88</b>	<b>29.01</b>	<b>18.64</b>	<b>3.83</b>	<b>0.92</b>	<b>48.79</b>	<b>35.11</b>	<b>22.08</b>	<b>11.86</b>	<b>4.33</b>
5j	46.90	39.91	28.29	10.78	3.54	59.09	44.31	35.06	22.90	11.02
Enzalutamide	11.41	8.40	5.68	1.17	0.65	69.88	56.89	42.91	30.50	9.21
EF24	59.78	51.37	44.82	22.86	4.77	15.34	11.06	6.05	2.06	1.20

Overall, the biological significance of benzothiazoles and benzothiazines lies in their multifaceted pharmacological activities, which make them valuable compounds for drug discovery and development across various therapeutic areas. Further research into their mechanisms of action and optimization of their pharmacokinetic properties could unlock their full therapeutic potential.

## REFERENCES

1. Alvarez-Builla, J. and J. Barluenga, *Heterocyclic compounds: an introduction*. Modern Heterocyclic Chemistry, 2011: p. 1-9.
2. Yang, L., et al., *SAR analysis of heterocyclic compounds with monocyclic and bicyclic structures as antifungal agents*. ChemMedChem, 2022. **17**(12): p. e202200221.
3. Kalaria, P.N., S.C. Karad, and D.K. Raval, *A review on diverse heterocyclic compounds as the privileged scaffolds in antimalarial drug discovery*. European journal of medicinal chemistry, 2018. **158**: p. 917-936.
4. Al-Mulla, A., *A review: biological importance of heterocyclic compounds*. Der Pharma Chemica, 2017. **9**(13): p. 141-147.
5. Clark, J.S., *Heterocyclic chemistry*. Organic ChemistryII, 2010: p. 136-155.
6. Kabir, E. and M. Uzzaman, *A review on biological and medicinal impact of heterocyclic compounds*. Results in Chemistry, 2022: p. 100606.
7. Baumann, M., I.R. Baxendale, and S.V. Ley, *The flow synthesis of heterocycles for natural product and medicinal chemistry applications*. Molecular diversity, 2011. **15**: p. 613-630.
8. Wu, Y.-J., *Heterocycles and medicine: A survey of the heterocyclic drugs approved by the US FDA from 2000 to present*, in *Progress in Heterocyclic Chemistry*. 2012, Elsevier. p. 1-53.
9. Vitaku, E., D.T. Smith, and J.T. Njardarson, *Analysis of the structural diversity, substitution patterns, and frequency of nitrogen heterocycles among US FDA approved pharmaceuticals: miniperspective*. Journal of medicinal chemistry, 2014. **57**(24): p. 10257-10274.
10. Ali, I., et al., *Heterocyclic scaffolds: centrality in anticancer drug development*. Current drug targets, 2015. **16**(7): p. 711-734.
11. Henary, M., et al., *Benefits and applications of microwave-assisted synthesis of nitrogen containing heterocycles in medicinal chemistry*. RSC advances, 2020. **10**(24): p. 14170-14197.
12. Petri, G.L., et al., *Bioactive pyrrole-based compounds with target selectivity*. European journal of medicinal chemistry, 2020. **208**: p. 112783.
13. Sravanthi, T. and S. Manju, *Indoles—A promising scaffold for drug development*. European Journal of Pharmaceutical Sciences, 2016. **91**: p. 1-10.



14. Suliphuldevara Mathada, B., N. Gunavanthrao Yernale, and J.N. Basha, *The Multi-Pharmacological Targeted Role of Indole and its Derivatives: A review*. ChemistrySelect, 2023. **8**(1): p. e202204181.
15. Brüggemann, R.J., et al., *Clinical relevance of the pharmacokinetic interactions of azole antifungal drugs with other coadministered agents*. Clinical Infectious Diseases, 2009. **48**(10): p. 1441-1458.
16. Lacey, E., *The role of the cytoskeletal protein, tubulin, in the mode of action and mechanism of drug resistance to benzimidazoles*. International journal for parasitology, 1988. **18**(7): p. 885-936.
17. Briguglio, I., et al., *Benzotriazole: An overview on its versatile biological behavior*. European Journal of Medicinal Chemistry, 2015. **97**: p. 612-648.
18. Cao, Y., et al., *Indazole scaffold: A generalist for marketed and clinical drugs*. Medicinal Chemistry Research, 2021. **30**: p. 501-518.
19. Foley, M. and L. Tilley, *Quinoline antimalarials: mechanisms of action and resistance*. International journal for parasitology, 1997. **27**(2): p. 231-240.
20. Bhadra, K. and G.S. Kumar, *Therapeutic potential of nucleic acid-binding isoquinoline alkaloids: Binding aspects and implications for drug design*. Medicinal research reviews, 2011. **31**(6): p. 821-862.
21. Selvam, T.P. and P.V. Kumar, *Quinazoline marketed drugs*. Research in Pharmacy, 2015. **1**(1).
22. Ajani, O.O., *Present status of quinoxaline motifs: Excellent pathfinders in therapeutic medicine*. European journal of medicinal chemistry, 2014. **85**: p. 688-715.
23. Kawase, M., S. Saito, and N. Motohashi, *Chemistry and biological activity of new 3-benzazepines*. International Journal of Antimicrobial Agents, 2000. **14**(3): p. 193-201.
24. Duval, D., et al., *Stereochemical Study of a Bradicardisant Benzazepine-Type Drug. X-Ray Structure of the Chloride Salt and High-Field NMR Study of the Stereochemistry in Solution*. Magnetic resonance in chemistry, 1997. **35**(3): p. 175-183.
25. Shaheen, S., K.P. Rao, and M.S. Rao, *Effect of nitroxazepine on bone marrow cells of mice*. Toxicology letters, 1988. **44**(1-2): p. 215-217.
26. Saha, D., G. Jain, and A. Sharma, *Benzothiazepines: Chemistry of a privileged scaffold*. RSC advances, 2015. **5**(86): p. 70619-70639.
27. Donnelly, K., et al., *Benzodiazepines, Z-drugs and the risk of hip fracture: A systematic review and meta-analysis*. PloS one, 2017. **12**(4): p. e0174730.

28. Osler, M. and M.B. Jørgensen, *Associations of benzodiazepines, Z-drugs, and other anxiolytics with subsequent dementia in patients with affective disorders: a nationwide cohort and nested case-control study*. American Journal of Psychiatry, 2020. **177**(6): p. 497-505.
29. Carmona-Martínez, V., et al., *Therapeutic potential of pteridine derivatives: A comprehensive review*. Medicinal Research Reviews, 2019. **39**(2): p. 461-516.
30. Kumar, R., et al., *Triazines—A comprehensive review of their synthesis and diverse biological importance*. Curr. Med. Drug Res, 2017. **1**(1): p. 173.
31. Dorie, M.J. and J.M. Brown, *Modification of the antitumor activity of chemotherapeutic drugs by the hypoxic cytotoxic agent tirapazamine*. Cancer chemotherapy and pharmacology, 1997. **39**: p. 361-366.
32. Sachdeva, H., et al., *Oxygen-and sulphur-containing heterocyclic compounds as potential anticancer agents*. Applied Biochemistry and Biotechnology, 2022. **194**(12): p. 6438-6467.
33. Brickl, R., J. Schmid, and F. Koss, *Clinical pharmacology of oral psoralen drugs*. Photo-dermatology, 1984. **1**(4): p. 174-186.
34. Araújo, A., et al., *Review of the biological properties and toxicity of usnic acid*. Natural product research, 2015. **29**(23): p. 2167-2180.
35. Zuma, N.H., J. Aucamp, and D.D. David, *An update on derivatisation and repurposing of clinical nitrofurans*. European Journal of Pharmaceutical Sciences, 2019. **140**: p. 105092.
36. Roberts, C., *Clinical pharmacokinetics of ranitidine*. Clinical pharmacokinetics, 1984. **9**(3): p. 211-221.
37. Kontogiorgis, C., A. Detsi, and D. Hadjipavlou-Litina, *Coumarin-based drugs: a patent review (2008–present)*. Expert opinion on therapeutic patents, 2012. **22**(4): p. 437-454.
38. Zhu, J.J. and J.G. Jiang, *Pharmacological and nutritional effects of natural coumarins and their structure–activity relationships*. Molecular nutrition & food research, 2018. **62**(14): p. 1701073.
39. Kostova, I., *Coumarins as inhibitors of HIV reverse transcriptase*. Current HIV research, 2006. **4**(3): p. 347-363.
40. Su, C.-R., et al., *Anti-HBV and cytotoxic activities of pyranocoumarin derivatives*. Bioorganic & medicinal chemistry, 2009. **17**(16): p. 6137-6143.
41. Heimark, L.D., et al., *The mechanism of the warfarin-rifampin drug interaction in humans*. Clinical Pharmacology & Therapeutics, 1987. **42**(4): p. 388-394.

42. Ponnusamy, T., M. Alagumuthu, and S. Thamaraiselvi, *Drug efficacy of novel 3-O-methoxy-4-halo disubstituted 5, 7-dimethoxy chromans; evaluated via DNA gyrase inhibition, bacterial cell wall lesion and antibacterial prospective*. *Bioorganic & Medicinal Chemistry*, 2018. **26**(12): p. 3438-3452.
43. Patil, S.A., et al., *Chromenes: potential new chemotherapeutic agents for cancer*. *Future medicinal chemistry*, 2013. **5**(14): p. 1647-1660.
44. Gebhardt, P., et al., *Quercinol, an anti-inflammatory chromene from the wood-rotting fungus Daedalea quercina (Oak Mazegill)*. *Bioorganic & medicinal chemistry letters*, 2007. **17**(9): p. 2558-2560.
45. Havsteen, B.H., *The biochemistry and medical significance of the flavonoids*. *Pharmacology & therapeutics*, 2002. **96**(2-3): p. 67-202.
46. Shahrajabian, M.H., W. Sun, and Q. Cheng, *The importance of flavonoids and phytochemicals of medicinal plants with antiviral activities*. *Mini-Reviews in Organic Chemistry*, 2022. **19**(3): p. 293-318.
47. Pietta, P.-G., *Flavonoids as antioxidants*. *Journal of natural products*, 2000. **63**(7): p. 1035-1042.
48. Li, B.Q., et al., *The flavonoid baicalin exhibits anti-inflammatory activity by binding to chemokines*. *Immunopharmacology*, 2000. **49**(3): p. 295-306.
49. Singh, A., et al., *Karanjin*. *Phytochemistry*, 2021. **183**: p. 112641.
50. Klein-Júnior, L.C., et al., *Xanthenes and cancer: from natural sources to mechanisms of action*. *Chemistry & Biodiversity*, 2020. **17**(2): p. e1900499.
51. Lum, P.T., et al., *Therapeutic potential of mangiferin against kidney disorders and its mechanism of action: A review*. *Saudi Journal of Biological Sciences*, 2022. **29**(3): p. 1530-1542.
52. Shahid, M., et al., *Bioactive compound identification and in vitro evaluation of antidiabetic and cytotoxic potential of Garcinia atroviridis fruit extract*. *Food Bioscience*, 2023. **51**: p. 102285.
53. Maia, M., et al., *Xanthenes in Medicinal Chemistry—Synthetic strategies and biological activities*. *European Journal of Medicinal Chemistry*, 2021. **210**: p. 113085.
54. Shabir, G., A. Saeed, and P. Ali Channar, *A review on the recent trends in synthetic strategies and applications of xanthene dyes*. *Mini-Reviews in Organic Chemistry*, 2018. **15**(3): p. 166-197.

55. Laxmikeshav, K., P. Kumari, and N. Shankaraiah, *Expedition of sulfur-containing heterocyclic derivatives as cytotoxic agents in medicinal chemistry: a decade update*. Medicinal Research Reviews, 2022. **42**(1): p. 513-575.
56. Gramec, D., L. Peterlin Mašič, and M. Sollner Dolenc, *Bioactivation potential of thiophene-containing drugs*. Chemical research in toxicology, 2014. **27**(8): p. 1344-1358.
57. Overk, C.R., et al., *Structure–activity relationships for a family of benzothiophene selective estrogen receptor modulators including raloxifene and arzoxifene*. ChemMedChem: Chemistry Enabling Drug Discovery, 2007. **2**(10): p. 1520-1526.
58. Yan, J., et al., *Synthesis of Dihydro-5H-Benzo [c]-Fluorenes, Dihydroindeno [c]-Chromenes and Thiochromenes via Intramolecular Cyclization and their Effect on Human Leukemia Cells*. Advanced Synthesis & Catalysis, 2022. **364**(9): p. 1613-1619.
59. Wu, Q., et al., *Carbene-Catalyzed Access to Thiochromene Derivatives: Control of Reaction Pathways via Slow Release of Thiols from Disulfides*. Organic Letters, 2023.
60. Foley, P., *Psychopharmacology: a brief overview of its history*. NeuroPsychopharmacotherapy, 2022: p. 621-660.
61. Kaatz, G.W., et al., *Phenothiazines and thioxanthenes inhibit multidrug efflux pump activity in Staphylococcus aureus*. Antimicrobial agents and chemotherapy, 2003. **47**(2): p. 719-726.
62. Zhang, H.-Z., Z.-L. Zhao, and C.-H. Zhou, *Recent advance in oxazole-based medicinal chemistry*. European journal of medicinal chemistry, 2018. **144**: p. 444-492.
63. Bonaccorso, C., et al., *Glutamate binding-site ligands of NMDA receptors*. Current medicinal chemistry, 2011. **18**(36): p. 5483-5506.
64. Schiff, M.H. and A. Whelton. *Renal toxicity associated with disease-modifying antirheumatic drugs used for the treatment of rheumatoid arthritis*. in *Seminars in arthritis and rheumatism*. 2000. Elsevier.
65. Ali Mohamed, H., et al., *In vitro antimicrobial evaluation, single-point resistance study, and radiosterilization of novel pyrazole incorporating thiazol-4-one/thiophene derivatives as dual DNA gyrase and DHFR inhibitors against MDR pathogens*. ACS omega, 2022. **7**(6): p. 4970-4990.
66. Niu, Z.-X., et al., *Application and synthesis of thiazole ring in clinically approved drugs*. European Journal of Medicinal Chemistry, 2023. **250**: p. 115172.

67. Tahghighi, A. and F. Babalouei, *Thiadiazoles: The appropriate pharmacological scaffolds with leishmanicidal and antimalarial activities: A review*. Iranian journal of basic medical sciences, 2017. **20**(6): p. 613.
68. Hendawy, O.M., *A comprehensive review of recent advances in the biological activities of 1, 2, 4-oxadiazoles*. Archiv der Pharmazie, 2022. **355**(7): p. 2200045.
69. Liu, X.-F., M.-Y. Wang, and L.-N. He, *Heterogeneous catalysis for oxazolidinone synthesis from aziridines and CO<sub>2</sub>*. Current Organic Chemistry, 2017. **21**(8): p. 698-707.
70. Lyons, A., et al., *Discovery and structure–activity relationships of a novel oxazolidinone class of bacterial type II topoisomerase inhibitors*. Bioorganic & Medicinal Chemistry Letters, 2022. **65**: p. 128648.
71. Barbachyn, M.R. and C.W. Ford, *Oxazolidinone structure–activity relationships leading to linezolid*. Angewandte Chemie International Edition, 2003. **42**(18): p. 2010-2023.
72. Zappia, G., et al., *The contribution of oxazolidinone frame to the biological activity of pharmaceutical drugs and natural products*. Mini reviews in medicinal chemistry, 2007. **7**(4): p. 389-409.
73. Breitung, E.M., C.-F. Shu, and R.J. McMahon, *Thiazole and thiophene analogues of donor– acceptor stilbenes: molecular hyperpolarizabilities and structure– property relationships*. Journal of the American Chemical Society, 2000. **122**(6): p. 1154-1160.
74. Singh, A., et al., *Thiazole derivatives in medicinal chemistry: Recent advancements in synthetic strategies, structure activity relationship and pharmacological outcomes*. Journal of Molecular Structure, 2022. **1266**: p. 133479.
75. Keri, R.S., et al., *A comprehensive review in current developments of benzothiazole-based molecules in medicinal chemistry*. European Journal of Medicinal Chemistry, 2015. **89**: p. 207-251.
76. Singh, M., et al., *Design, synthesis and mode of action of some benzothiazole derivatives bearing an amide moiety as antibacterial agents*. RSC advances, 2014. **4**(36): p. 19013-19023.
77. Azzam, R.A., R.R. Osman, and G.H. Elgemeie, *Efficient synthesis and docking studies of novel benzothiazole-based pyrimidinesulfonamide scaffolds as new antiviral agents and Hsp90 $\alpha$  inhibitors*. ACS omega, 2020. **5**(3): p. 1640-1655.

78. Soni, B., et al., *Synthesis and evaluation of some new benzothiazole derivatives as potential antimicrobial agents*. European Journal of Medicinal Chemistry, 2010. **45**(7): p. 2938-2942.
79. Pathak, N., et al., *A review on anticancer potentials of benzothiazole derivatives*. Mini reviews in medicinal chemistry, 2020. **20**(1): p. 12-23.
80. Kharbanda, C., et al., *Synthesis and evaluation of pyrazolines bearing benzothiazole as anti-inflammatory agents*. Bioorganic & Medicinal Chemistry, 2014. **22**(21): p. 5804-5812.
81. Netalkar, P.P., et al., *Synthesis, crystal structures and characterization of late first row transition metal complexes derived from benzothiazole core: Anti-tuberculosis activity and special emphasis on DNA binding and cleavage property*. European journal of medicinal chemistry, 2014. **79**: p. 47-56.
82. Morales-Garcia, J.A., et al., *Biological and pharmacological characterization of benzothiazole-based CK-1 $\delta$  inhibitors in models of Parkinson's disease*. ACS omega, 2017. **2**(8): p. 5215-5220.
83. Webster, R., *Centrally acting muscle relaxants in tetanus*. British Journal of Pharmacology and Chemotherapy, 1961. **17**(3): p. 507-518.
84. Korkmaz, A. and E. Bursal, *Benzothiazole sulfonate derivatives bearing azomethine: Synthesis, characterization, enzyme inhibition, and molecular docking study*. Journal of Molecular Structure, 2022. **1257**: p. 132641.
85. Qadir, T., et al., *Recent advances in the synthesis of benzothiazole and its derivatives*. Current Organic Chemistry, 2022. **26**(2): p. 189-214.
86. Prajapati, N.P., et al., *Recent advances in the synthesis of 2-substituted benzothiazoles: a review*. Rsc Advances, 2014. **4**(104): p. 60176-60208.
87. Evindar, G. and R.A. Batey, *Parallel synthesis of a library of benzoxazoles and benzothiazoles using ligand-accelerated copper-catalyzed cyclizations of ortho-halobenzanilides*. The Journal of Organic Chemistry, 2006. **71**(5): p. 1802-1808.
88. Ma, D., et al., *Domino Condensation/S-Arylation/Heterocyclization Reactions: Copper-Catalyzed Three-Component Synthesis of 2-N-Substituted Benzothiazoles*. Angewandte Chemie, 2011. **123**(5): p. 1150-1153.
89. Batista, R.M., S.P. Costa, and M.M.M. Raposo, *Synthesis of new fluorescent 2-(2', 2''-bithienyl)-1, 3-benzothiazoles*. Tetrahedron letters, 2004. **45**(13): p. 2825-2828.

90. Kumar, A., R.A. Maurya, and P. Ahmad, *Diversity oriented synthesis of benzimidazole and benzoxa/(thia) zole libraries through polymer-supported hypervalent iodine reagent*. Journal of Combinatorial Chemistry, 2009. **11**(2): p. 198-201.
91. Ye, L.-m., et al., *Visible-light-promoted synthesis of benzothiazoles from 2-aminothiophenols and aldehydes*. Tetrahedron Letters, 2017. **58**(9): p. 874-876.
92. Bhat, R., et al., *Acacia concinna pod catalyzed synthesis of 2-arylbenzothia/(oxa) zole derivatives*. Iranian Journal of Catalysis, 2019. **9**(2): p. 173-179.
93. Liao, Y., et al., *Efficient 2-aryl benzothiazole formation from aryl ketones and 2-aminobenzenethiols under metal-free conditions*. Organic letters, 2012. **14**(23): p. 6004-6007.
94. Mayo, M.S., et al., *Convenient synthesis of benzothiazoles and benzimidazoles through Brønsted acid catalyzed cyclization of 2-amino thiophenols/anilines with  $\beta$ -diketones*. Organic letters, 2014. **16**(3): p. 764-767.
95. Loukrakpam, D.C. and P. Phukan, *TsNBr<sub>2</sub> Mediated Synthesis of 2-Acylbenzothiazoles and Quinoxalines from Aryl Methyl Ketones under Metal Free Condition*. ChemistrySelect, 2019. **4**(11): p. 3180-3184.
96. Gupta, S.D., H.P. Singh, and N. Moorthy, *Iodine-catalyzed, one-pot, solid-phase synthesis of benzothiazole derivatives*. Synthetic Communications, 2007. **37**(24): p. 4327-4329.
97. Rauf, A., S. Gangal, and S. Sharma, *Solvent-free synthesis of 2-alkyl and 2-alkenylbenzothiazoles from fatty acids under microwave irradiation*. ChemInform, 2008. **47**: p. 601-605.
98. Coelho, F.L. and L.F. Campo, *Synthesis of 2-arylbenzothiazoles via direct condensation between in situ generated 2-aminothiophenol from disulfide cleavage and carboxylic acids*. Tetrahedron Letters, 2017. **58**(24): p. 2330-2333.
99. Nadaf, R., et al., *Room temperature ionic liquid promoted regioselective synthesis of 2-aryl benzimidazoles, benzoxazoles and benzthiazoles under ambient conditions*. Journal of Molecular Catalysis A: Chemical, 2004. **214**(1): p. 155-160.
100. Wu, C., et al., *Dibenzothiazoles as novel amyloid-imaging agents*. Bioorganic & medicinal chemistry, 2007. **15**(7): p. 2789-2796.
101. Luo, B., et al., *Synthesis, antifungal activities and molecular docking studies of benzoxazole and benzothiazole derivatives*. Molecules, 2018. **23**(10): p. 2457.

102. Bose, D.S. and M. Idrees, *Hypervalent iodine mediated intramolecular cyclization of thioformanilides: expeditious approach to 2-substituted benzothiazoles*. The Journal of Organic Chemistry, 2006. **71**(21): p. 8261-8263.
103. Downer-Riley, N.K. and Y.A. Jackson, *Conversion of thiobenzamides to benzothiazoles via intramolecular cyclization of the aryl radical cation*. Tetrahedron, 2008. **64**(33): p. 7741-7744.
105. Feng, E., et al., *Metal-free synthesis of 2-substituted (N, O, C) benzothiazoles via an intramolecular C–S bond formation*. Journal of Combinatorial Chemistry, 2010. **12**(4): p. 422-429.
106. Xu, Z.-M., et al., *Exogenous photosensitizer-, metal-, and base-free visible-light-promoted C–H thiolation via reverse hydrogen atom transfer*. Organic letters, 2018. **21**(1): p. 237-241.
107. Gao, X., et al., *Ionic liquid-catalyzed C–S bond construction using CO<sub>2</sub> as a C1 building block under mild conditions: A metal-free route to synthesis of benzothiazoles*. ACS Catalysis, 2015. **5**(11): p. 6648-6652.
108. Luzina, E.L. and A.V. Popov, *Synthesis and anticancer activity of N-bis (trifluoromethyl) alkyl-N'-thiazolyl and N-bis (trifluoromethyl) alkyl-N'-benzothiazolyl ureas*. European journal of medicinal chemistry, 2009. **44**(12): p. 4944-4953.
109. Willard, L., et al., *The cytotoxicity of chronic neuroinflammation upon basal forebrain cholinergic neurons of rats can be attenuated by glutamatergic antagonism or cyclooxygenase-2 inhibition*. Experimental brain research, 2000. **134**: p. 58-65.
110. Sarojini, B.K., et al., *Synthesis, characterization, in vitro and molecular docking studies of new 2, 5-dichloro thienyl substituted thiazole derivatives for antimicrobial properties*. European journal of medicinal chemistry, 2010. **45**(8): p. 3490-3496.
111. Kalkhambkar, R., et al., *Synthesis of novel triheterocyclic thiazoles as anti-inflammatory and analgesic agents*. European Journal of Medicinal Chemistry, 2007. **42**(10): p. 1272-1276.
112. Shiradkar, M.R., et al., *Synthesis of new S-derivatives of clubbed triazolyl thiazole as anti-Mycobacterium tuberculosis agents*. Bioorganic & medicinal chemistry, 2007. **15**(12): p. 3997-4008.
113. Shiradkar, M., et al., *Clubbed triazoles: a novel approach to antitubercular drugs*. European journal of medicinal chemistry, 2007. **42**(6): p. 807-816.
114. Malipeddi, H., et al., *Synthesis and antitubercular activity of some novel thiazolidinone derivatives*. Tropical Journal of Pharmaceutical Research, 2012. **11**(4): p. 611-620.



115. Prabhu, P.P., A. Pai, and R.S. Padmashree, *Analgesic and anti-Inflammatory activity studies of some new aryl 4-thiazolidinones in experimental mice*. Pharmacologyonline, 2010. **1**: p. 1132-1139.
116. Kouatly, O., et al., *Adamantane derivatives of thiazolyl-N-substituted amide, as possible non-steroidal anti-inflammatory agents*. European journal of medicinal chemistry, 2009. **44**(3): p. 1198-1204.
117. Singh, N., S.K. Bhati, and A. Kumar, *Thiazolyl/oxazolyl formazanyl indoles as potent anti-inflammatory agents*. European journal of medicinal chemistry, 2008. **43**(11): p. 2597-2609.
118. Gouda, M.A., et al., *A review: Synthesis and medicinal importance of coumarins and their analogues (Part II)*. Current Bioactive Compounds, 2020. **16**(7): p. 993-1008.
119. Navarrete-Vázquez, G., et al., *Synthesis of 2-{2-[(a/b-naphthalen-yl)] acetamides with 11b-hydroxysteroid dehydrogenase inhibition and in combo antidiabetic activities q*. European Journal of Medicinal Chemistry, 2014. **74**(17): p. 9e186.
120. Salar, U., et al., *Syntheses of new 3-thiazolyl coumarin derivatives, in vitro  $\alpha$ -glucosidase inhibitory activity, and molecular modeling studies*. European journal of medicinal chemistry, 2016. **122**: p. 196-204.
121. Ajani, O.O., *Functionalized 1, 4-Benzothiazine: A Versatile Scaffold with Diverse Biological Properties*. Archiv der Pharmazie, 2012. **345**(11): p. 841-851.
122. Chattopadhyay, S., *Recent advancement in the synthesis of 1, 2-and 2, 1-benzothiazines*. Synthetic Communications, 2018. **48**(24): p. 3033-3078.
123. Rai, A., et al., *1, 4-Benzothiazines-a biologically attractive scaffold*. Mini Reviews in Medicinal Chemistry, 2018. **18**(1): p. 42-57.
124. Sharifi, A., et al., *[Omim][NO<sub>3</sub>], a green and base-free medium for one-pot synthesis of benzothiazinones at room temperature*. Synthetic Communications, 2013. **43**(15): p. 2079-2089.
125. Pratap, U.R., et al., *Baker's yeast catalyzed synthesis of 1, 4-benzothiazines, performed under ultrasonication*. Journal of Molecular Catalysis B: Enzymatic, 2011. **68**(1): p. 94-97.
126. Ghiasi, M., M. Aghawerdi, and M.M. Heravi, *QM study on regioselectivity in the synthesis of pyrimido [4, 5-b][1, 4] benzothiazines: kinetic and thermodynamic point of view*. Journal of the Iranian Chemical Society, 2017. **14**: p. 743-754.
127. Dabholkar, V.V. and R.P. Gavande, *Synthesis and biological evaluation of oxadiazolyl-1, 4-benzothiazines*. Rasayan J. Chem, 2010. **3**(4): p. 655-659.

128. Londhe, B.S., et al., *Novel synthesis of 1, 4-benzothiazines in water accelerated by  $\beta$ -cyclodextrin*. Journal of the Iranian Chemical Society, 2016. **13**: p. 443-447.
129. Sharifi, A., et al., *Ionic liquid [bmim][NO<sub>3</sub>], an efficient medium for green and one-pot synthesis of benzothiazinones at room-temperature*. Scientia Iranica, 2013. **20**(3): p. 555-560.
130. Baghernejad, B., M.M. Heravi, and H.A. Oskooie, *Practical and Efficient Synthesis of 3-Aryl-2 H-benzo [1, 4] thiazine Derivatives Catalyzed by KHSO<sub>4</sub>*. Synthetic Communications, 2011. **41**(4): p. 589-593.
131. Dar, A.M., H. Khanam, and M.A. Gato, *Anticancer and antimicrobial evaluation of newly synthesized steroidal 5, 6 fused benzothiazines*. Arabian Journal of Chemistry, 2014. **7**(4): p. 461-468.
132. Jeleń, M., et al., *Synthesis and selected immunological properties of substituted quino [3, 2-b] benzo [1, 4] thiazines*. European Journal of Medicinal Chemistry, 2013. **63**: p. 444-456.
133. Hasegawa, K., et al., *Dihydro-1, 4-benzothiazine-6, 7-dione, the ultimate toxic metabolite of 4-S-cysteaminylphenol and 4-S-cysteaminylcatechol*. Biochemical pharmacology, 1997. **53**(10): p. 1435-1444.
134. Sebbar, N.K., et al., *Novel 1, 4-benzothiazine derivatives: synthesis, crystal structure, and anti-bacterial properties*. Research on Chemical Intermediates, 2016. **42**: p. 6845-6862.
135. Cecchetti, V., et al., *Quinolinecarboxylic acids. 3. Synthesis and antibacterial evaluation of 2-substituted 7-oxo-2, 3-dihydro-7H-pyrido [1, 2, 3-de][1, 4] benzothiazine-6-carboxylic acids related to rufloxacin*. Journal of medicinal chemistry, 1993. **36**(22): p. 3449-3454.
136. Junnarkar, A., et al., *Neuropsychopharmacological study of 2, 4-dihydro [1, 2, 4] triazolo [3, 4-C][1, 4] benzothiazine-1-one (IDPH-791)*. Pharmacological research, 1992. **26**(2): p. 131-141.
137. Bakavoli, M., et al., *SAR comparative studies on pyrimido [4, 5-b][1, 4] benzothiazine derivatives as 15-lipoxygenase inhibitors, using ab initio calculations*. Journal of molecular modeling, 2008. **14**: p. 471-478.
138. Moserle, L., A. Amadori, and S. Indraccolo, *The angiogenic switch: implications in the regulation of tumor dormancy*. Current molecular medicine, 2009. **9**(8): p. 935-941.

139. Khandelwal, N., et al., *An efficient synthesis and biological study of substituted 8-chloro-5-methoxy/8-chloro-4H-1, 4-benzothiazines, their sulphones and ribofuranosides*. Journal of Chemical sciences, 2013. **125**: p. 85-93.
140. Bakavoli, M., et al., *Design and synthesis of pyrimido [4, 5-b][1, 4] benzothiazine derivatives, as potent 15-lipoxygenase inhibitors*. Bioorganic & medicinal chemistry, 2007. **15**(5): p. 2120-2126.
141. Matysiak, J., *Synthesis, antiproliferative and antifungal activities of some 2-(2, 4-dihydroxyphenyl)-4H-3, 1-benzothiazines*. Bioorganic & Medicinal Chemistry, 2006. **14**(8): p. 2613-2619.
142. Ohlow, M.J. and B. Moosmann, *Phenothiazine: the seven lives of pharmacology's first lead structure*. Drug discovery today, 2011. **16**(3-4): p. 119-131.
143. Nosova, E.V., et al., *Synthesis and biological activity of 2-amino-and 2-aryl (heteryl) substituted 1, 3-benzothiazin-4-ones*. Mini Reviews in Medicinal Chemistry, 2019. **19**(12): p. 999-1014.
144. Gupta, S.S., et al., *Eco-friendly and sustainable synthetic approaches to biologically significant fused N-heterocycles*. Chemistry of Heterocyclic Compounds, 2020. **56**: p. 433-444.
145. Kaur, N., *Ionic liquid promoted eco-friendly and efficient synthesis of six-membered N-polyheterocycles*. Current Organic Synthesis, 2018. **15**(8): p. 1124-1146.
146. Karmakar, R. and C. Mukhopadhyay, *Green Synthetic Approach: A Well-organized Eco-friendly Tool for Synthesis of Bio-active Fused Heterocyclic Compounds*. Current Green Chemistry, 2023. **10**(1): p. 5-24.
147. Nasiriani, T., et al., *Isocyanide-Based Multicomponent Reactions in Water: Advanced Green Tools for the Synthesis of Heterocyclic Compounds*. Topics in Current Chemistry, 2022. **380**(6): p. 50.
148. Bougrin, K., A. Loupy, and M. Soufiaoui., *Microwave-assisted solvent-free heterocyclic synthesis*. Journal of Photochemistry and Photobiology C: Photochemistry Reviews, 2005. **6**(2-3): p. 139-167.
149. Hadda, T.B., et al., *Impact of geometric parameters, charge, and lipophilicity on bioactivity of armed quinoxaline, benzothiazole, and benzothiazine: pom analyses of antibacterial and antifungal activity*. Phosphorus, Sulfur, and Silicon and the Related Elements, 2014. **189**(6): p. 753-761.

150. Pluta, K., B. Morak-Młodawska, and M. Jeleń, *Recent progress in biological activities of synthesized phenothiazines*. European journal of medicinal chemistry, 2011. **46**(8): p. 3179-3189.
151. Felicetti, T., et al., *Searching for novel inhibitors of the S. aureus NorA efflux pump: synthesis and biological evaluation of the 3-phenyl-1, 4-benzothiazine analogues*. ChemMedChem, 2017. **12**(16): p. 1293-1302.
152. Chaucer, P. and P.K. Sharma, *Study of thiazines as potential anticancer agents*. Plant Arch, 2020. **20**(2): p. 3199-3202.
153. Lombardino, J.G. and E.H. Wiseman, *Antiinflammatory 3, 4-dihydro-2-alkyl-3-oxo-2H-1, 2-benzothiazine-4-carboxamide 1, 1-dioxides*. Journal of Medicinal Chemistry, 1971. **14**(10): p. 973-977.
154. Ukrainets, I., L. Petrushova, and S. Dzyubenko, *2, 1-Benzothiazine 2, 2-dioxides. 1. Synthesis, structure, and analgesic activity of 1-R-4-hydroxy-2, 2-dioxo-1 H-2λ 6, 1-benzothiazine-3-carboxylic acid esters*. Chemistry of Heterocyclic Compounds, 2013. **49**: p. 1378-1383.
155. K Prashanth, M. and H. D Revanasiddappa, *Synthesis and antioxidant activity of novel quinazolinones functionalized with urea/thiourea/thiazole derivatives as 5-lipoxygenase inhibitors*. Letters in Drug Design & Discovery, 2014. **11**(6): p. 712-720.
156. Tanaka, T., et al., *Discovery of benzothiazine derivatives as novel, orally-active anti-epileptic drug candidates with broad anticonvulsant effect*. Bioorganic & Medicinal Chemistry Letters, 2015. **25**(20): p. 4518-4521.
157. Tawada, H., et al., *Studies on antidiabetic agents. IX.: a new aldose reductase inhibitor, AD-5467, and related 1, 4-benzoxazine and 1, 4-benzothiazine derivatives: synthesis and biological activity*. Chemical and pharmaceutical bulletin, 1990. **38**(5): p. 1238-1245.
158. Amin, A., et al., *Pharmacological Significance of Synthetic Bioactive Thiazole Derivatives*. Current Bioactive Compounds, 2022. **18**(9): p. 77-89.
159. Qadir, T., et al., *A review on medicinally important heterocyclic compounds*. The Open Medicinal Chemistry Journal, 2022. **16**(1). DOI: 10.2174/18741045-v16-e2202280.
160. Qadir, T., et al., *Recent advances in the synthesis of benzothiazole and its derivatives*. Current Organic Chemistry, 2022. **26**(2): p. 189-214.
161. Ali, T.E.-S. and A.M. El-Kazak, *Synthesis and antimicrobial activity of some new 1, 3-thiazoles, 1, 3, 4-thiadiazoles, 1, 2, 4-triazoles and 1, 3-thiazines incorporating acridine*

- and 1, 2, 3, 4-tetrahydroacridine moieties. *European Journal of Chemistry*, 2010. **1**(1): p. 6-11.
162. Dandia, A., et al., *Microwave assisted green chemical synthesis of novel spiro [indole-pyrido thiazines]: a system reluctant to be formed under thermal conditions*. *Tetrahedron*, 2004. **60**(24): p. 5253-5258.
163. Sucharitha, E.R., et al., *Fused benzo [1, 3] thiazine-1, 2, 3-triazole hybrids: Microwave-assisted one-pot synthesis, in vitro antibacterial, antibiofilm, and in silico ADME studies*. *Bioorganic & Medicinal Chemistry Letters*, 2021. **47**: p. 128201.
164. Ahmad, N., et al., *Microwave assisted synthesis and structure–activity relationship of 4-hydroxy-N'-[1-phenylethylidene]-2H/2-methyl-1, 2-benzothiazine-3-carbohydrazide 1, 1-dioxides as anti-microbial agents*. *European journal of medicinal chemistry*, 2011. **46**(6): p. 2368-2377.
165. Pratap, U.R., et al., *Baker's yeast catalyzed synthesis of 1, 4-benzothiazines, performed under ultrasonication*. *Journal of Molecular Catalysis B: Enzymatic*, 2011. **68**(1): p. 94-97.
166. MALAGU, K., et al., *Synthesis and antiviral activity of new 1, 4-benzothiazines: sulphoxides and sulphone derivatives*. *Pharmacy and Pharmacology Communications*, 1998. **4**(1): p. 57-60.
167. Prakash, O., N. Sharma, and K. Pannu, *Synthesis of 2, 2'-Bi-2H-3, 3'-diaryl-1, 4-benzothiazines from  $\alpha$ ,  $\alpha$ -Dibromoacetophenones and o-Aminothiophenol*. *Synthetic communications*, 2007. **37**(12): p. 1995-1999.
168. Zhang, L. and S. Zhang, *Copper-catalyzed one-pot synthesis of 1, 4-benzothiazine-3-ones*. *Tetrahedron Letters*, 2023. **130**: p. 154761.
169. Chu, C.-M., et al., *Ceric ammonium nitrate (CAN) as a green and highly efficient promoter for the 1, 4-addition of thiols and benzeneselenol to  $\alpha$ ,  $\beta$ -unsaturated ketones*. *Tetrahedron*, 2007. **63**(8): p. 1863-1871.
170. Comin, M.J., E. Elhalem, and J.B. Rodriguez, *Cerium ammonium nitrate: a new catalyst for regioselective protection of glycols*. *Tetrahedron*, 2004. **60**(51): p. 11851-11860.
171. Shelke, K., S. Sapkal, and M. Shingare, *Ultrasound-assisted one-pot synthesis of 2, 4, 5-triarylimidazole derivatives catalyzed by ceric (IV) ammonium nitrate in aqueous media*. *Chinese Chemical Letters*, 2009. **20**(3): p. 283-287.

172. Verma, M., et al., *Antibacterial and antioxidant assay of novel heteroaryl-substituted methane derivatives synthesized via ceric ammonium nitrate (CAN) catalyzed one-pot green approach*. *Molecular Diversity*, 2023. **27**(2): p. 889-900.
173. Daina, A., O. Michielin, and V. Zoete, *SwissADME: a free web tool to evaluate pharmacokinetics, drug-likeness and medicinal chemistry friendliness of small molecules*. *Scientific reports*, 2017. **7**(1): p. 42717.
174. Lipinski, C.A., *Lead-and drug-like compounds: the rule-of-five revolution*. *Drug discovery today: Technologies*, 2004. **1**(4): p. 337-341.
175. Majumdar, K. and D. Ghosh, *An efficient ligand-free ferric chloride catalyzed synthesis of annulated 1, 4-thiazine-3-one derivatives*. *Tetrahedron Letters*, 2014. **55**(19): p. 3108-3110.
176. Raslan, R.R., et al., *Synthesis and antitumor evaluation of some new thiazolopyridine, nicotinonitrile, pyrazolopyridine, and polyhydroquinoline derivatives using ceric ammonium nitrate as a green catalyst*. *Journal of Heterocyclic Chemistry*, 2022. **59**(5): p. 832-846.
177. Nagendra Prasad, T., et al., *Design, synthesis and biological evaluation of substituted 2-amino-1, 3-thiazine derivatives as antituberculosis and anti-cancer agents*. *Synthetic Communications*, 2019. **49**(10): p. 1277-1285.
178. Caetano, M.S., et al., *IL6 Blockade Reprograms the Lung Tumor Microenvironment to Limit the Development and Progression of K-ras–Mutant Lung Cancer*. *Cancer research*, 2016. **76**(11): p. 3189-3199.
179. Rani, D., V. Garg, and R. Dutt, *Anticancer Potential of Azole Containing Marine Natural Products: Current and Future Perspectives*. *Anti-Cancer Agents in Medicinal Chemistry (Formerly Current Medicinal Chemistry-Anti-Cancer Agents)*, 2021. **21**(15): p. 1957-1976.
180. Glyn, R.J. and G. Pattison, *Effects of replacing oxygenated functionality with fluorine on lipophilicity*. *Journal of Medicinal Chemistry*, 2021. **64**(14): p. 10246-10259.
181. Noolvi, M.N., H.M. Patel, and M. Kaur, *Benzothiazoles: Search for anticancer agents*. *European journal of medicinal chemistry*, 2012. **54**: p. 447-462.
182. Huang, S.-T., I.-J. Hsei, and C. Chen, *Synthesis and anticancer evaluation of bis (benzimidazoles), bis (benzoxazoles), and benzothiazoles*. *Bioorganic & medicinal chemistry*, 2006. **14**(17): p. 6106-6119.
183. Dhadda, S., et al., *Benzothiazoles: From recent advances in green synthesis to anti-cancer potential*. *Sustainable Chemistry and Pharmacy*, 2021. **24**: p. 100521.

184. Gomtsyan, A., *Heterocycles in drugs and drug discovery*. Chemistry of heterocyclic compounds, 2012. **48**: p. 7-10.
185. Zhang, T.Y., *The evolving landscape of heterocycles in drugs and drug candidates*, in *Advances in Heterocyclic Chemistry*. 2017, Elsevier. p. 1-12.
186. Kumar, A. and A.K. Mishra, *Advancement in pharmacological activities of benzothiazole and its derivatives: An up to date review*. Mini Reviews in Medicinal Chemistry, 2021. **21**(3): p. 314-335.
187. Casas-Ferreira, A.M., et al., *Non-separative mass spectrometry methods for non-invasive medical diagnostics based on volatile organic compounds: A review*. Analytica Chimica Acta, 2019. **1045**: p. 10-22.
188. Mishra, V.R., et al., *Design, synthesis, antimicrobial activity and computational studies of novel azo linked substituted benzimidazole, benzoxazole and benzothiazole derivatives*. Computational biology and chemistry, 2019. **78**: p. 330-337.
189. Mortimer, C.G., et al., *Antitumor benzothiazoles. 26. 2-(3, 4-Dimethoxyphenyl)-5-fluorobenzothiazole (GW 610, NSC 721648), a simple fluorinated 2-arylbenzothiazole, shows potent and selective inhibitory activity against lung, colon, and breast cancer cell lines*. Journal of medicinal chemistry, 2006. **49**(1): p. 179-185.
190. Bellina, F., et al., *Imidazole analogues of resveratrol: synthesis and cancer cell growth evaluation*. Tetrahedron, 2015. **71**(15): p. 2298-2305.
191. Yan, X., et al., *Current scenario of 1, 3-oxazole derivatives for anticancer activity*. Current Topics in Medicinal Chemistry, 2020. **20**(21): p. 1916-1937.
192. El-Nezhawy, A.O., et al., *Synthesis and Molecular Docking Studies of Novel 2-Phenyl-4-Substituted Oxazole Derivatives as Potential Anti-cancer Agents*. Journal of Heterocyclic Chemistry, 2016. **53**(1): p. 271-279.
193. Padmaja, R.D., M.M. Balamurali, and K. Chanda, *One-Pot, Telescopic Approach for the Chemoselective Synthesis of Substituted Benzo [e] pyrido/pyrazino/pyridazino [1, 2-b][1, 2, 4] thiadiazine dioxides and Their Significance in Biological Systems*. The Journal of Organic Chemistry, 2019. **84**(18): p. 11382-11390.
194. Lindgren, E.B., et al., *Synthesis and anticancer activity of (E)-2-benzothiazole hydrazones*. European journal of medicinal chemistry, 2014. **86**: p. 12-16.
195. Soltan, O.M., et al., *Molecular hybrids: A five-year survey on structures of multiple targeted hybrids of protein kinase inhibitors for cancer therapy*. European Journal of Medicinal Chemistry, 2021. **225**: p. 113768.

196. Rane, R.A. and V.N. Telvekar, *Synthesis and evaluation of novel chloropyrrole molecules designed by molecular hybridization of common pharmacophores as potential antimicrobial agents*. Bioorganic & medicinal chemistry letters, 2010. **20**(19): p. 5681-5685.
197. Manjula, S., et al., *Synthesis and antitumor activity of optically active thiourea and their 2-aminobenzothiazole derivatives: A novel class of anticancer agents*. European Journal of Medicinal Chemistry, 2009. **44**(7): p. 2923-2929.
198. Hallur, G., et al., *Benzoylphenylurea sulfur analogues with potent antitumor activity*. Journal of medicinal chemistry, 2006. **49**(7): p. 2357-2360.
199. Esteves-Souza, A., et al., *Synthesis, cytotoxicity, and DNA-topoisomerase inhibitory activity of new asymmetric ureas and thioureas*. Bioorganic & medicinal chemistry, 2006. **14**(2): p. 492-499.
200. Choi, S.-J., et al., *Solid phase combinatorial synthesis of benzothiazoles and evaluation of topoisomerase II inhibitory activity*. Bioorganic & medicinal chemistry, 2006. **14**(4): p. 1229-1235.
201. Saeed, S., et al., *Synthesis, characterization and biological evaluation of some thiourea derivatives bearing benzothiazole moiety as potential antimicrobial and anticancer agents*. European journal of medicinal chemistry, 2010. **45**(4): p. 1323-1331.
202. Lesyk, R. and B. Zimenkovsky, *4-Thiazolidones: centenarian history, current status and perspectives for modern organic and medicinal chemistry*. Current Organic Chemistry, 2004. **8**(16): p. 1547-1577.
203. Havrylyuk, D., et al., *Synthesis of novel thiazolone-based compounds containing pyrazoline moiety and evaluation of their anticancer activity*. European journal of medicinal chemistry, 2009. **44**(4): p. 1396-1404.
204. Geronikaki, A., et al., *2-Thiazolylimino/heteroarylimino-5-arylidene-4-thiazolidinones as new agents with SHP-2 inhibitory action*. Journal of medicinal chemistry, 2008. **51**(17): p. 5221-5228.
205. Havrylyuk, D., et al., *Synthesis and anticancer activity evaluation of 4-thiazolidinones containing benzothiazole moiety*. European Journal of Medicinal Chemistry, 2010. **45**(11): p. 5012-5021.
206. Rathi, A.K., et al., *Piperazine derivatives for therapeutic use: a patent review (2010-present)*. Expert opinion on therapeutic patents, 2016. **26**(7): p. 777-797.



207. Boumendjel, A., et al., *Piperazinobenzopyranones and phenalkylaminobenzopyranones: potent inhibitors of breast cancer resistance protein (ABCG2)*. Journal of medicinal chemistry, 2005. **48**(23): p. 7275-7281.
208. Frydrych, J., et al., *Nucleotide analogues containing a pyrrolidine, piperidine or piperazine ring: Synthesis and evaluation of inhibition of plasmodial and human 6-oxopurine phosphoribosyltransferases and in vitro antimalarial activity*. European Journal of Medicinal Chemistry, 2021. **219**: p. 113416.
209. Ammazalorso, A., et al., *2-substituted benzothiazoles as antiproliferative agents: Novel insights on structure-activity relationships*. European Journal of Medicinal Chemistry, 2020. **207**: p. 112762.
210. Al-Masoudi, N.A., B. Salih, and Y.A. Al-Soud, *Quantitative Structure-Activity Relationship (QSAR) on New Benzothiazoles Derived Substituted Piperazine Derivatives*. Journal of Computational and Theoretical Nanoscience, 2011. **8**(10): p. 1945-1949.
211. Trott, O. and A.J. Olson, *AutoDock Vina: improving the speed and accuracy of docking with a new scoring function, efficient optimization, and multithreading*. Journal of computational chemistry, 2010. **31**(2): p. 455-461.
212. Berman, H.M., et al., *The protein data bank*. Nucleic acids research, 2000. **28**(1): p. 235-242.
213. Shaw, D.E., et al., *Atomic-level characterization of the structural dynamics of proteins*. Science, 2010. **330**(6002): p. 341-346.
214. Chow, E., et al., *Desmond performance on a cluster of multicore processors*. DE Shaw Research Technical Report DESRES/TR--2008-01, 2008.
215. Shivakumar, D., et al., *Prediction of absolute solvation free energies using molecular dynamics free energy perturbation and the OPLS force field*. Journal of chemical theory and computation, 2010. **6**(5): p. 1509-1519.
216. Jorgensen, W.L., J. Chandrasekhar, and J.D. Madura, *Impey, RW; Klein, ML*. J. Chem. Phys, 1983. **79**: p. 926.
217. Martyna, G.J., D.J. Tobias, and M.L. Klein, *Constant pressure molecular dynamics algorithms*. The Journal of chemical physics, 1994. **101**(5): p. 4177-4189.
218. Kagami, L.P., et al., *Geo-Measures: A PyMOL plugin for protein structure ensembles analysis*. Computational Biology and Chemistry, 2020. **87**: p. 107322.

219. Daina, A., O. Michielin, and V. Zoete, *SwissADME: a free web tool to evaluate pharmacokinetics, drug-likeness and medicinal chemistry friendliness of small molecules*. Scientific reports, 2017. **7**(1): p. 42717.
220. Lipinski, C.A., *Lead-and drug-like compounds: the rule-of-five revolution*. Drug discovery today: Technologies, 2004. **1**(4): p. 337-341.
221. Cordes E, Jencks W., *On the mechanism of Schiff base formation and hydrolysis*. Journal of the American Chemical Society, 1962. **84**(5): p. 832-7.
222. Hameed A, Al-Rashida M, Uroos M, Abid Ali S, Khan KM., *Schiff bases in medicinal chemistry: a patent review (2010-2015)*. Expert opinion on therapeutic patents, 2017. **27**(1): p. 63-79.
223. Jia Y, Li J., *Molecular assembly of Schiff base interactions: construction and application*. Chemical reviews, 2015. **115**(3): p. 1597-621.
224. Kaczmarek MT, Zabiszak M, Nowak M, Jastrzab R., *Lanthanides: Schiff base complexes, applications in cancer diagnosis, therapy, and antibacterial activity*. Coordination Chemistry Reviews, 2018. **370**: p. 42-54.
225. Garnovskii AD, Nivorozhkin AL, Minkin VI., *Ligand environment and the structure of Schiff base adducts and tetracoordinated metal-chelates*. Coordination chemistry reviews, 1993. **126**(1-2): p. 1-69.
226. Yu T, Su W, Li W, Hong Z, Hua R, Li M., *Synthesis, crystal structure and electroluminescent properties of a Schiff base zinc complex*. Inorganica Chimica Acta, 2006. **359**(7): p. 2246-51.
227. Zhong X, Yi J, Sun J, Wei H-L, Liu W-S, Yu K-B., *Synthesis and crystal structure of some transition metal complexes with a novel bis-Schiff base ligand and their antitumor activities*. European journal of medicinal chemistry, 2006. **41**(9): p. 1090-2.
228. Yeğiner G, Gülcan M, Işık S, Ürüt GÖ, Özdemir S, Kurtoğlu M., *Transition metal (II) complexes with a novel azo-azomethine Schiff base ligand: Synthesis, structural and spectroscopic characterization, thermal properties and biological applications*. Journal of fluorescence, 2017. **27**: p. 2239-51.
229. Burlov A, Vlasenko V, Koshchienko YV, Makarova N, Zubenko A, Drobin YD., *Synthesis, characterization, luminescent properties and biological activities of zinc complexes with bidentate azomethine Schiff-base ligands*. Polyhedron, 2018. **154**: p. 65-76.
230. Wang K, Yang H, Liao Z, Li S, Hambsch M, Fu G., *Monolayer-assisted surface-initiated schiff-base-mediated aldol polycondensation for the synthesis of crystalline*

- sp<sup>2</sup> carbon-conjugated covalent organic framework thin films*. Journal of the American Chemical Society, 2023. **145**(9): p. 5203-10.
231. Gupta KC, Sutar AK., *Catalytic activities of Schiff base transition metal complexes*. Coordination Chemistry Reviews, 2008. **252**(12-14): p. 1420-50.
232. Lehweß-Litzmann A, Neumann P, Parthier C, Lüdtke S, Golbik R, Ficner R., *Twisted Schiff base intermediates and substrate locale revise transaldolase mechanism*. Nature Chemical Biology, 2011. **7**(10): p. 678-84.
233. Safin DA, Babashkina MG, Bolte M, Ptaszek AL, Kukułka M, Mitoraj MP., *Novel sterically demanding Schiff base dyes: An insight from experimental and theoretical calculations*. Journal of Luminescence, 2021. **238**: p. 118264.
234. Muthamma K, Sunil D, Shetty P, Kulkarni SD, Anand P, Kekuda D., *Eco-friendly flexographic ink from fluorene-based Schiff base pigment for anti-counterfeiting and printed electronics applications*. Progress in Organic Coatings, 2021. **161**: p. 106463.
235. Sabaa MW, Mohamed RR, Oraby EH., *Vanillin–Schiff's bases as organic thermal stabilizers and co-stabilizers for rigid poly (vinyl chloride)*. European polymer journal, 2009. **45**(11): p. 3072-80.
236. Verma C, Quraishi M., *Recent progresses in Schiff bases as aqueous phase corrosion inhibitors: Design and applications*. Coordination Chemistry Reviews, 2021. **446**: p. 214105.
237. Liao C, Kim U-J, Kannan K., *A review of environmental occurrence, fate, exposure, and toxicity of benzothiazoles*. Environmental science & technology, 2018. **52**(9): p. 5007-26.
238. Wakamatsu K, Ohtara K, Ito S., *Chemical analysis of late stages of pheomelanogenesis: conversion of dihydrobenzothiazine to a benzothiazole structure*. Pigment Cell & Melanoma Research, 2009. **22**(4):p. 474-86.
239. Etaiw SEH, Abd El-Aziz DM, Abd El-Zaher EH, Ali EA., *Synthesis, spectral, antimicrobial and antitumor assessment of Schiff base derived from 2-aminobenzothiazole and its transition metal complexes*. Spectrochimica Acta Part A: Molecular and Biomolecular Spectroscopy, 2011. **79**(5): p. 1331-7.
240. Pathak N, Rathi E, Kumar N, Kini SG, Rao CM., *A review on anticancer potentials of benzothiazole derivatives*. Mini reviews in medicinal chemistry, 2020. **20**(1): p. 12-23.
241. Bhoi P, Thorat SG, Alasmay FA, Wabaidur SM, Islam MA., *Design, synthesis, molecular modelling and antiproliferative evaluation of novel benzothiazole trihybrids*. Biophysical Chemistry, 2021. **278**: p. 106664.

242. Ammazalorso A, De Lellis L, Florio R, Laghezza A, De Filippis B, Fantacuzzi M., *Synthesis of novel benzothiazole amides: Evaluation of PPAR activity and anti-proliferative effects in paraganglioma, pancreatic and colorectal cancer cell lines*. Bioorganic & Medicinal Chemistry Letters, 2019. **29**(16): p. 2302-6.
243. Rao NN, Gopichand K, Nagaraju R, Ganai AM, Rao PV., *Design, synthesis, spectral characterization, DNA binding, photo cleavage and antibacterial studies of transition metal complexes of benzothiazole Schiff base*. Chemical Data Collections, 2020. **27**: p. 100368.
244. Kiran T, Pathak M, Chanda K, Balamurali M., *DNA and Protein Interaction Studies of Heteroleptic Copper (II) Derivatives of Benzothiazole-Based Schiff Base and N, N-Donor Ligands*. ChemistrySelect, 2020. **5**(22): p. 6792-9.
245. Ahlawat A, Singh V, Asija S., *Synthesis, characterization, antimicrobial evaluation and QSAR studies of organotin (IV) complexes of Schiff base ligands of 2-amino-6-substituted benzothiazole derivatives*. Chemical Papers, 2017. **71**(11): p. 2195-208.
246. Gupta K, Sirbaiya AK, Kumar V, Rahman MA., *Current perspective of synthesis of medicinally relevant benzothiazole based molecules: Potential for antimicrobial and anti-inflammatory activities*. Mini Reviews in Medicinal Chemistry, 2022. **22**(14): p. 1895-935.
247. Gabr MT, El-Gohary NS, El-Bendary ER, El-Kerdawy MM, Ni N., *Synthesis, in vitro antitumor activity and molecular modeling studies of a new series of benzothiazole Schiff bases*. Chinese Chemical Letters, 2016. **27**(3): p. 380-6.
248. Shaik TB, Hussaini SA, Nayak VL, Sucharitha ML, Malik MS, Kamal A., *Rational design and synthesis of 2-anilinopyridinyl-benzothiazole Schiff bases as antimetabolic agents*. Bioorganic & Medicinal Chemistry Letters, 2017. **27**(11): p. 2549-58.
249. Vamsikrishna N, Kumar MP, Ramesh G, Ganji N, Daravath S, Shivaraj., *DNA interactions and biocidal activity of metal complexes of benzothiazole Schiff bases: Synthesis, characterization and validation*. Journal of Chemical Sciences, 2017. **129**: p. 609-22.
250. Broughton HB, Watson IA., *Selection of heterocycles for drug design*. Journal of Molecular Graphics and Modelling, 2004. **23**(1): p. 51-8.
251. Heravi MM, Zadsirjan V., *Prescribed drugs containing nitrogen heterocycles: an overview*. RSC advances, 2020. **10**(72): p. 44247-311.
252. Eicher T, Hauptmann S, Speicher A. *The chemistry of heterocycles: structures, reactions, synthesis, and applications: John Wiley & Sons*; 2013.

253. Kim SJ, Lin C-C, Pan C-M, Rananaware DP, Ramsey DM, McAlpine SR., *A structure–activity relationship study on multi-heterocyclic molecules: two linked thiazoles are required for cytotoxic activity*. *MedChemComm*, 2013. **4**(2): p. 406-10.
254. Jemal A, Bray F, Center MM, Ferlay J, Ward E, Forman D., *Global cancer statistics*. *CA: a cancer journal for clinicians*, 2011. **61**(2): p. 69-90.
255. Carradori S, Guglielmi P, Luisi G, Secci D., *Nitrogen-and Sulfur-Containing Heterocycles as Dual Anti-oxidant and Anti-cancer Agents*, *Handbook of Oxidative Stress in Cancer: Mechanistic Aspects*: Springer; 2022. p. 2571-88.
256. Koli P, Singh RK., *Progress Nitrogen and Sulphur-based Heterocyclic Compounds for their Anticancer Activity*. *Key Heterocyclic Cores for Smart Anticancer Drug–Design Part II*. 2022:79.
257. T Chhabria M, Patel S, Modi P, S Brahmksatriya P., *Thiazole: A review on chemistry, synthesis and therapeutic importance of its derivatives*. *Current topics in medicinal chemistry*, 2016. **16**(26): p. 2841-62.
258. Rouf A, Tanyeli C., *Bioactive thiazole and benzothiazole derivatives*. *European journal of medicinal chemistry*, 2015. **97**: p. 911-27.
259. Singh IP, Gupta S, Kumar S., *Thiazole compounds as antiviral agents: An update*. *Medicinal Chemistry*, 2020. **16**(1):p. 4-23.
260. Singh M, Singh SK, Gangwar M, Nath G, Singh SK., *Design, synthesis and mode of action of some benzothiazole derivatives bearing an amide moiety as antibacterial agents*. *RSC advances*, 2014. **4**(36): p. 19013-23.
261. Ma J, Chen D, Lu K, Wang L, Han X, Zhao Y., *Design, synthesis, and structure–activity relationships of novel benzothiazole derivatives bearing the ortho-hydroxy N-carbamoylhydrazone moiety as potent antitumor agents*. *European journal of medicinal chemistry*, 2014. **86**: p. 257-69.
262. Sharma, R. N.; Xavier, F. P.; Vasu, K. K.; Chaturvedi, S. C.; Pancholi, S. S. *Synthesis of 4-benzyl-1, 3-thiazole derivatives as potential anti-inflammatory agents: an analogue-based drug design approach*. *Journal of enzyme inhibition and medicinal chemistry*, 2009. **24** (3), p. 890-897.
263. Ayati, A.; Emami, S.; Asadipour, A.; Shafiee, A.; Foroumadi, A. *Recent applications of 1, 3-thiazole core structure in the identification of new lead compounds and drug discovery*. *European Journal of Medicinal Chemistry*, 2015. **97**, p. 699-718.

264. Zou, X.; Shi, P.; Feng, A.; Mei, M.; Li, Y. Two metal complex derivatives of pyridine thiazole ligand: synthesis, characterization and biological activity. *Transition Metal Chemistry*, 2021, **46**, p. 263-272.
265. Xiao, D.; Cheng, J.; Liang, W.; Cheng, C.; Wang, Q.; Chai, R.; Yan, Z.; Du, Y.; Zhao, J. Innovative approach to nano thiazole-Zn with promising physicochemical and bioactive properties by nanoreactor construction. *Journal of agricultural and food chemistry*, 2019, **67** (42), p. 11577-11583.
266. Asha, S.; Hentry, C.; Bindhu, M.; Al-Mohaimed, A. M.; AbdelGawwad, M. R.; Elshikh, M. S. Improved photocatalytic activity for degradation of textile dyeing waste water and thiazine dyes using PbWO<sub>4</sub> nanoparticles synthesized by co-precipitation method. *Environmental Research*, 2021, **200**, p. 111721

## LIST OF PUBLICATIONS

1. **Amin A.**, Khazir Z., Arfa J., Dar M., Hurrah A., Bhat I., Parveen S., Nisar S., Sharma P.K., 2024. Anti-lung Cancer Activity of Synthesized Substituted 1,4-Benzothiazines: An insight from Molecular Docking and Experimental Studies, *Anti-cancer Agents in Medicinal Chemistry*, 24(5), pp. 385-371.
2. **Amin, A.**, Qadir, T., Sharma, P.K., Jeelani, I. and Abe, H., 2022. A Review on the Medicinal and Industrial Applications of N-Containing Heterocycles. *The Open Medicinal Chemistry Journal*, 16(1), DOI: 10.2174/18741045-v16-e2209010.
3. **Amin, A.**, Qadir, T., Salhotra, A., Sharma, P.K., Jeelani, I. and Abe, H., 2022. Pharmacological Significance of Synthetic Bioactive Thiazole Derivatives. *Current Bioactive Compounds*, 18(9), pp.77-89.
4. Qadir, T., **Amin, A.**, Salhotra, A., Sharma, P.K., Jeelani, I. and Abe, H., 2022. Recent advances in the synthesis of benzothiazole and its derivatives. *Current Organic Chemistry*, 26(2), pp.189-214.
5. Qadir, T., **Amin, A.**, Sharma, P.K., Jeelani, I. and Abe, H., 2022. A review on medicinally important heterocyclic compounds. *The Open Medicinal Chemistry Journal*, 16(1). DOI: 10.2174/18741045-v16-e2202280.
6. Qadir, T., **Amin, A.**, Sarkar, D. and Sharma, P.K., 2021. A review on recent advances in the synthesis of aziridines and their applications in organic synthesis. *Current Organic Chemistry*, 25(16), pp.1868-1893.
7. Jeelani, I., Qadir, T., Bhosale, M., Sharma, P.K., & **Amin, A.**, 2023. Pongamia Pinnata: An Heirloom Herbal Medicine. *The Open Medicinal Chemistry Journal*, 17, pp. 1-14.
8. Sharma, P.K., **Amin A.**, Kumar M., 2020. Synthetic Methods of Medicinally Important Heterocycles-thiazines: A Review. *The Open Medicinal Chemistry Journal*, 14(1), pp.71-82.
9. Sharma, P.K., **Amin A.**, Kumar M., 2020. A Review: Medicinally Important Nitrogen Sulphur Containing Heterocycles. *The Open Medicinal Chemistry Journal*, 14(1), pp.49-64.
10. **Amin A.**, Khazir Z., Bhat B., Hurrah A., Bhat I., Masoodi K.Z., Sharma P.K., 2024. Benzothiazole-piperazine Hybrids effectively target C4-2 castration resistant C4-2 cells in vitro implicated through Computational studies. *ChemistrySelect*, 9, e202401401.

## **LIST OF CONFERENCES**

- A Amin, P.K. Sharma, Phamacological Significance of Synthetic Thiazole Derivatives. 3<sup>rd</sup> International Conference on Recent Advances in Fundamental and Applied Sciences (25<sup>th</sup>& 26<sup>th</sup> June 2021 | Lovely Professional University, Punjab).
- A Amin, P.K. Sharma, Schiff base clubbed Benzothiazole: Synthesis, Potent Anti-bacterial and C4-2 Anticancer Activity, and Docking Study. 2nd International Conference on Advances in Biopolymers-2021 and Workshop on Fermented Foods & Gut Health (8<sup>th</sup> & 9<sup>th</sup> November 2021 | University of Kashmir, Hazratbal, Srinagar, Jammu and Kashmir, India)
- A Amin, P.K. Sharma, Synthesis, Characterization and anti-proliferative activity of (3-methyl-4H-benzo[b][1,4]thiazine-2-yl)(4phenlypiperazin-1-yl)mrthanone. Conference on Recent Advances in Biomedical Sciences and Regenerative Medicine (RABSRM) (6<sup>th</sup> and 7<sup>th</sup> May, 2022, SKUAST-Kashmir and UOK-Hazratbal)